Mechanistische Untersuchungen zur Physiologie der CO_2 Toleranz bei Cephalopoden

Mechanistic studies on the physiology of CO_2 tolerance in cephalopods

Dissertation

Zur Erlangung des akademischen Grades

Dr. rer. nat.

Mathematisch Naturwissenschaftliche Fakultät der Christian-Albrechts-Universität zu Kiel

Vorgelegt von

Marian Yong-An Hu

Kiel 2011

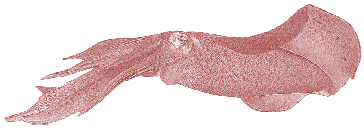

Gutachter:

1. Gutachter: Prof. Dr. Frank Melzner
2. Gutachter: Prof. Dr. Markus Bleich

Mündliche Prüfung abgelegt am 21.04.2011

Zum Druck genehmigt: 21.04.2011

Table of contents

Summary

Elevated environmental CO_2 concentrations (hypercapnia) are a stressor that has lately received considerable attention: anthropogenic CO_2 emissions are predicted to lead to a rise in surface ocean pCO_2 from 0.04 kPa up to 0.08 - 0.14 kPa within this century. The increased hydration of CO_2 changes seawater chemistry, causing a drop in ocean pH. This phenomenon has been termed "ocean acidification" (OA). Changes in aquatic CO_2 partial pressure affect the physiology of all water breathing animals as the CO_2 concentration in body fluids will increase as well in order to maintain a substantial outward directed diffusion gradient for CO_2. Among the aquatic taxa some have been identified as rather sensitive species (e.g. less active calcifying species such as corals or echinoderms) whereas others (many active species such as adult fish and cephalopods) can tolerate high CO_2 concentrations over long exposure times. It was shown that more tolerant organisms share the ability to compensate for a hypercapnia induced acidosis by actively accumulating bicarbonate and eliminating protons from their body fluids. This process requires the presence of an acid-base regulating machinery consisting of a variety of ion transporters and channels.

Using *in situ* hybridization and immuno histochemical methods, the present work demonstrates that Na^+/K^+-ATPase (*NKA*), a V-type-H^+-ATPase (*V-HA*), and Na^+/HCO_3^- cotransporter (*NBC*) are co-localized in NKA-rich cells in the gills of cephalopods. Furthermore, mRNA expression patterns of these transporters and selected metabolic genes were examined in response to moderately elevated seawater pCO_2 (0.16 and 0.35 kPa) over a time-course of six weeks in different ontogenetic stages. Our findings support the hypothesis that the energy budget of adult cephalopods is not significantly compromised during long-term exposure to moderate environmental hypercapnia. However, the down regulation of ion-regulatory and metabolic genes in late stage embryos, taken together with a significant reduction in somatic growth, indicates that in contrast to adult cephalopods early life stages are challenged more severely by elevated seawater pCO_2. This increased sensitivity of cephalopod early life stages could be due to two primary reasons. The first is related to gill development: similar to the situation in fish and decapod crustaceans, the cephalopod gill is the most important site for ion-regulatory processes. During larval development, rudimentary gill structures occur at stage 20, and differentiate over the course of embryonic development as well as after hatching. This differentiation indicates that gas exchange and ion regulatory capacity might be fully activated only after leaving the protective egg capsule. This could partially explain the higher susceptibility of embryonic stages to environmental hypercapnia.

The second reason for a higher sensitivity is due to the oviparous type of development in cephalopods. Cephalopod embryos are exposed to very low egg fluid pO_2 values (<6 kPa, ca. 28% air saturation) and high pCO_2 values (>0.3 kPa) under control conditions during the final phase of embryonic development. This is due to increasing metabolic rates and the egg casing acting as a diffusion barrier for dissolved gases. The present work demonstrates that environmental pCO_2 is additive to the natural accumulation of CO_2 in the perivitelline fluid (PVF). This almost linear increase of PVF pCO_2 is necessary in order to conserve the CO_2 diffusion gradient across the egg capsule that drives excretion of metabolic CO_2 to the seawater. Thus, alterations in environmental pCO_2 create a greater challenge to the developing embryo in comparison to juveniles or adults.

Despite the lack of adult-like high capacity ion regulatory epithelia (e.g. gills or kidneys) the present work demonstrates for the first time that cephalopod embryonic stages exhibit convergent acid-base regulatory features compared to teleosts. Epidermal ionocytes scattered on skin and yolk sac appear to be responsible for ionic and acid-base regulation before gill epithelia become functionable. Acid-base regulatory capacities are important for fish and cephalopod embryos, due to the beforehand mentioned, challenging abiotic conditions inside the protecting egg capsule. These epidermal ionocytes were characterized via immunohistochemistry, *in situ* hybridization and vital dye staining techniques. Similar to findings obtained in teleosts NHE3-rich cells take up sodium in exchange for protons, illustrating the energetic advantage of NHE based proton excretion in marine organisms. Using *in vivo* electrophysiological techniques, it was proven that acid equivalents are secreted by the yolk and skin integument.

The findings of the present work add significant knowledge to our mechanistic understanding of hypercapnia tolerance in marine organisms, as it demonstrates that cephalopods which were identified as powerful acid-base regulators in the context of ocean acidification already need to exhibit strong acid-base regulatory abilities during all phases of their life cycle. The convergence of key acid-base regulatory proteins in cephalopods and fish suggest that in a variety of marine ectothermic animals extracellular pH regulation mechanisms may follow common evolutionary principles.

Zusammenfassung

Aufgrung der stetig steigenden CO_2 Konzentrationen in der Atmosphäre hat Hyperkapnie als abiotischer Stressor in aquatischen Systemen in den letzten Jahren mehr und mehr an Aufmerksamkeit gewonnen. Modellberechnungen zufolge könnte, verursacht durch durch die anthropogenen CO_2 Emmissionen, noch innerhalb dieses Jahrhunderts der pCO_2 im Oberflächenwasser der Ozeane von derzeit 0.04 auf etwa 0.08 - 0.14 kPa ansteigen. Dies beeinflusst die Karbonatchemie des Meerwassers und hat zur Folge, dass der pH im Oberflächenwasser der Ozeane sinken wird. Dieses Phänomen wurde als Ozeanversauerung bezeichnet.

Der Anstieg im CO_2 Partialdruck beinflusst alle aquatischen Organismen, da der Anstieg des pCO_2 im Wasser ebenfalls zu einer Erhöhung des Blut pCO_2 führt. Die Aufrechterhaltung eines ausreichenden pCO_2 Gradienten ist essentiell, um die diffundive Exkretion von CO_2 vom Körper an das Wasser zu gewährleisten. Unter den marinen Organismen wurden einige taxonomischen Gruppen als besonders sensibel eingestuft (in der Regel weniger aktive, kalzifizierende Spezies wie z.B. Korallen und Echinodermaten), wohingegen aktive Taxa wie adulte Cephalopoden und Fische relativ tolerant erscheinen. Frühere Studien haben gezeigt, dass adulte Cephalopoden und Fische hohe CO_2 Konzentrationen über lange Zeiträume tolerieren können, ohne ihr Wachstum oder Kalzifizierungsraten zu verringern. Es hat sich gezeigt, dass diese Toleranz mit der Fähigkeit zusammen hängt, eine Hyperkapnie-induzierte Azidose durch die aktive Akkumulation von Bikarbonat im und / oder durch die Sekretion von Protonen aus dem Blut zu kompensieren. Diese Fähigkeit ist abhängig von einem ionenregulatorischen Apparat, der aus einer Vielzahl von Säure-Base relevanten Transportproteinen besteht.

Mit Hilfe von *in situ* Hybridisierung und immunohistologischen Methoden konnte diese Arbeit zeigen, dass wichtige Transportproteine wie z.B. Na^+/K^+-ATPase (*NKA*), H^+-ATPase (*V-HA*), und Na^+/HCO_3^- Kotransporter (*NBC*) in spezialisierten Epithelien in der Cephalopodenkieme kolokalisiert sind. Darüber hinaus wurden Expressionsmuster dieser Transporter und weiterer ausgewählter metabolischer Gene in Bezug auf erhöhte Seewasser pCO_2 (0,16 und 0,35 kPa) über eine Dauer von sechs Wochen in unterschiedlichen ontogenetischen Stadien untersucht. Ausserdem wurde das Wachstum der verschiedenen Stadien bestimmt und O_2- und pCO_2-Konzentration in der Eihülle wurden gemessen.

Die Ergebnisse unterstützen die Hypothese, dass Energiebudgets bei adulten Cephalopoden nicht signifikant durch chronisch erhöhten Seewasser pCO_2 beeinflusst werden. Allerdings

zeigte sich eine höhere Sensitivität bei frühen Entwicklungsstadien in Form einer verringerten Expression von ionenregulatorischen und metabolischen Genen begleitet durch eine signifikante Verzögerung in Wachstum und Entwicklung. Diese erhöhte Sensitivität bei frühen Entwicklungsstadien kann durch zwei Hauptgründe erklärt werden. Der Erste steht im Zusammenhang mit der Entwicklung ionenregulatorischer Epithelien. Ähnlich wie bei Fischen und Crustaceen ist auch bei Cephalopoden die Kieme eines der wichtigsten ionenregulatorischen Organe. Während der Larvalentwicklung entstehen rudimentäre Kiemenanlagen im 20. Entwicklungsstadium und differenzieren sich im Laufe der weiteren Ontogenese bis hin zum Schlüpfling. Diese späte Differenzierung legt nahe, dass die Fähigkeit zum Gasaustausch und die volle ionenregulatorische Kapazität erst nach dem Verlassen der schützenden Eikapsel erreicht werden. Das Fehlen ionenregulatorischer Strukturen wie man sie in adulten Tieren vorfindet, kann ein möglicher Grund für eine erhöhte Sensitivität bei frühen Entwicklungsstadien sein. Der Zweite Grund für eine höhere Empfindlichkeit bei Embyonalstadien kann durch die ovipare Entwicklung bei Cephalopoden erklärt werden. In der finalen Entwicklungsphase im Ei sind Cephalopodenembryos bereits unter Kontrollbedingungen sehr geringen O_2 Konzentrationen (<6 kPa, ca. 28% Luftsättigung) und hohen pCO_2 Werten (>0,3 kPa) ausgesetzt. Dies liegt an den steigenden metabolischen Raten und der Eischale, die eine Diffusionsbarriere für gelöste Gase darstellt. Diese Arbeit zeigt ferner, dass Anstiege des pCO_2 im Seewasser additiv zum bereits hohen pCO_2 in der Perivittellinflüssigkeit (PVF) sind. Der fast lineare Anstieg des PVF pCO_2 ist notwendig, um den Diffusionsgradienten von respiratorischem CO_2 aus dem Ei aufrecht zu erhalten. Aufgrund dieser Erkenntnis kann geschlossen werden, dass Anstiege des Umgebungs-pCO_2 einen größeren Stressor für Embryonalstadien (im Ei) darstellen als für Juvenile oder Adulte.

Trotz fehlender adult-typischer ionenregulatorischer Organe (Kiemen, Nieren und Darm) bei frühen Entwicklungsstadien zeigt diese Arbeit zum ersten Mal, dass Cephalopodenembryos konvergente Säure-Base regulatorische Strukturen zu Fischen entwickelt haben. Ionocyten auf der Haut und dem Dottersack sind für den Säure-Base-relevanten Ionentransport verantwortlich bevor die Kiemenepithelien voll differenziert und funktional sind. Säure-Base Regulation ist bereits für die frühen Entwicklungsstadien aufgrund der zuvor genannten extremen hypercapnischen Bedingungen in der Eikapsel von großer Wichtigkeit. Epidermale Ionocyten wurden anhand von *in situ* Hybridisierung, immunohistochemischen und „vital dye“-Färbungen charakterisiert. Ähnlich wie bei Fischen scheinen Zellen, die reich an NHE3 sind, Natrium im Austausch gegen Protonen

aufzunehmen. Der Einsatz von NHE-Proteinen kann als energetisch günstigere Variante der Protonenexkretion in marinen Organismen verstanden werden. Darüber hinaus zeigen *in vivo* elektrophysiologische Techniken, dass die Sekretion von Säureequivalenten tatsächlich über den Dottersack und die Haut stattfindet.

Diese Arbeit trägt signifikant zu unserem mechanistischen Verständnis der Hyperkapnietoleranz bei marinen Organismen bei. Sie zeigt, dass Cephalopoden, die im Kontext der Ozeanversauerung als tolerant identifiziert wurden, Mechanismen besitzen, um aktiv ihren Säure-Base Haushalt zu regulieren. Ferner besitzen Cephalopoden in allen Phasen ihrer Ontogenie signifikante Säure-Base regulatorische Kapazitäten und spezialisierte Organe, die auf eine konvergente Evolution mit Teleosteern hindeuten.

1. Introduction

1.1. Ocean acidification

The oceans cover over two-thirds of the Earth's surface and play a central role in global climate and biogeochemical cycles. The ocean surface waters are in permanent exchange with the atmosphere, absorbing carbon dioxide (CO_2), which affects the seawater carbonate chemistry. The hydration of one CO_2 molecule in water generates one bicarbonate ion (HCO_3^-) and one proton, and in a second step a carbonate ion (CO_3^{2-}) and another proton (equation 1.1.). This is why the increase of atmospheric CO_2 is shifting the equilibrium towards higher pCO_2 and lower carbonate ion concentration, generating more protons, and thus, making seawater more acidic.

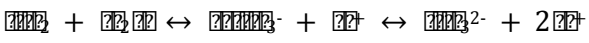

(Eq. 1.1.)

This equilibrium is highly pH dependent and can be represented in a Bjerrum plot (figure 1.1.A) with the concentrations of the three carbonate species given as a function of pH. In today`s oceans, carbonate ions account for 9% of total dissolved inorganic carbon (C_T), whereas the majority is present in the form of bicarbonate ions.

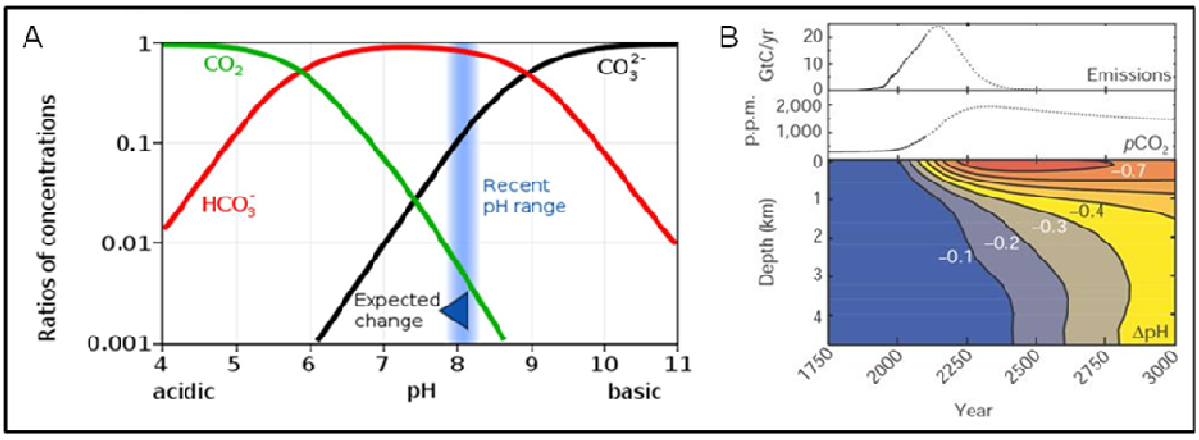

Figure 1.1. Bjerrum plot, showing the concentration of the three carbon species in relation to seawater pH (modified after Raven et al. 2005) (A). Release of CO_2 to the atmosphere from the anthropogenic burning of fossil fuels causes a marked increase in ocean acidity. Atmospheric CO_2 concentrations and changes in ocean pH are plotted against historical atmospheric CO_2 levels and predicted CO_2 emissions scenarios (adopted from Caldeira and Wickett 2003) (B).

In the past 200 years the oceans have absorbed approximately half of the CO_2 produced by fossil fuel combustion (Sabine et al. 2004). Long-term oceanic pCO_2 and pH changes

observed at the BATS (Bermuda Atlantic Time-series Study; 32°10'N, 64°30'W/Hydrostation S 32°50'N, 64°10'W) and calculations based on measurements of the surface oceans and known parameters of ocean chemistry indicate that this uptake of CO_2 has led to a reduction of surface seawater pH by ca. 0.1 units since industrialization (Caldeira and Wickett 2003; Orr et al. 2009). Furthermore, based on various stabilization scenarios for atmospheric pCO_2 provided by the Intergovernmental Panel on Climate Change Special Report on Emissions (SRES) (IPCC 2001), different possibilities were modeled with respect to changes in ocean surface pH and carbonate chemistry (Caldeira and Wickett 2005). In the "business-as-usual" scenario, which assume rising CO_2 emissions at current rates, the average pH of the oceans could decrease by 0.5 units by the year 2100 and by 0.8 to 1.4 pH units by the year 2300 (figure 1.1.B) (Caldeira and Wickett 2003; Caldeira and Wickett 2005). Probably these ocean surface pH reductions are greater than during the last 420,000 years, without considering biological feedback mechanisms in these simulations (Petit et al. 1999). This decline in ocean surface pH affects the distribution of carbonate species (e.g. HCO_3^- and CO_3^{2-}) as depicted in figure 1.1.A.

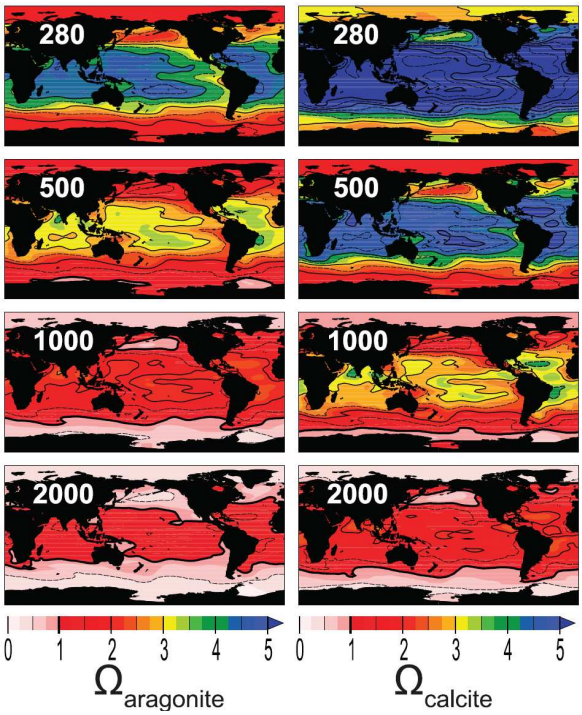

Figure 1.2. Saturation state of aragonite and calcite. Saturation state of aragonite ($\Omega_{aragonite}$) and calcite ($\Omega_{calcite}$) for different atmospheric CO_2 stabilization levels (ppm). By 500 ppm, aragonite will dissolve in parts of the near-surface Southern Ocean; by 1000 ppm, calcite will dissolve in most of the high latitude oceans. Results are obtained by adding model-predicted perturbations in geochemical fields to modern observations, except for the Arctic Ocean where results are directly from modelsimulations due to lacking of observations (Cao and Caldeira 2008).

As a consequence the saturation states of calcite (Ω_{Cal}) and aragonite (Ω_{Arg}), which are the products of $[Ca^{2+}]$ and $[CO_3^{2-}]$ divided by the respecting stoichiometric solubility product (see equation 1.2.), decrease with lowered pH. The concentration of these most important $CaCO_3$ polymorphs expressed by the Ω_{Cal} and Ω_{Arg}, respectively, determine the $CaCO_3$ saturation state (Feely et al. 2004). Under conditions of $\Omega < 1$, $CaCO_3$ starts to dissolve. Although biogenic carbonates are organic-inorganic compound materials, sub-saturating conditions eventually lead to dissolution and threaten calcifying organisms. Saturation states were modeled for different scenarios, demonstrating that ocean`s temperate and polar regions are the most vulnerable in

$$\Omega_{sp} = [Ca^{2+}] * [CO_3^{2-}]/K_{sp}^* \qquad \text{(Eq. 1.2.)}$$

respect to increasing atmospheric pCO_2 (figure 1.2.).

Finally, it has been described that local wind-driven upwelling effects can cause highly acidified conditions in coastal waters, such as the northern American continental shelf and the Kiel Fjord, with seasonal pCO_2 values of 0.12 kPa over a period of several weeks to months (Feely et al. 2008; Thomsen et al. 2010). It can be expected that global effects of OA will add on top of such local events leading to temporal pCO_2 values up to 0.3 kPa CO_2 or more (Melzner et al. submitted-b).

1.2. Biological impacts

Some marine organisms combine calcium with carbonate ions in the process of biomineralization in order to build tests, shells or skeletons. The produced calcium carbonates may be either in the form of calcite or aragonite of which latter is the more soluble form. After death of the organism these calcium carbonate compounds sink to deeper waters where they dissolve, and the carbon is again released to the water or they are buried in sediments in which case the carbon is removed from the carbon cycle. This process is often referred to as the “biological pump”. Planktonic calcifying organisms such as coccolitophores, molluscs or crustaceans were described as major compounds of this biological pump (Lalli and Parsons 2004). Several studies demonstrated that some of these planktonic calcifying organisms are particularly sensitive to ocean acidification due to the dissolution of their external shells in upper water layers, and thus may represent a negative feedback to increasing atmospheric CO_2 concentrations (Riebesell et al. 2000). Negative impacts on calcification, or the maintenance of calcareous structures were not only observed in planktonic organisms but also for benthic species, including snails, mussels and echinoderms (summarized by Ishimatsu and Dissanayake 2010). Several studies conducted experiments in naturally high pCO_2 habitats (e.g. upwelling regions or underwater volcanoes), showing that calcification is negatively impacted under acidified conditions (Hall-Spencer et al. 2008; Tunnicliffe et al. 2009). However, acidification born shell dissolution can not be considered as the only factor that impairs the success of calcifying organisms (Thomsen et al. 2010). Recently, it was suggested that the energy demanding process of shell formation and maintenance may be negatively impacted by a higher fraction of energy spent on compensatory processes such as metabolism and acid-base regulation (Cummings et al. 2010; Lanning et al. 2010; Lischka et al. 2010; Thomsen and Melzner 2010; Stumpp et al. submitted).

Water breathing animals exchange CO_2 across respiratory epithelia such as gills or skin by maintaining a substantial diffusion gradient with high pCO_2 values in tissues compared to the surrounding water (Evans et al. 2005; Melzner et al. 2009b). In order to maintain this diffusion gradient, the increase of seawater pCO_2 will result in an increase of pCO_2 in body tissues and fluids. Such hypercapnic conditions would cause an extracellular acidosis if not actively compensated (Heisler 1989). This acidification of body fluids of marine animals in response to increasing external pCO_2 occurs rapidly, within hours (Pörtner et al. 2004). However, it was observed that some animal groups can be considered more tolerant against CO_2-induced acid-base disturbances whereas others are more sensitive. Less mobile calcifying groups such as pteropods (Orr et al. 2005), echinoderms (Kurihara & Shirayama 2004) and bivalves (Kurihara et al. 2007) seem to be more sensitive to hypercapnia than active swimmers with high energy turnover rates, such as fish, crustaceans and cephalopods (Ishimatsu et al. 2005; Spicer et al. 2007; Gutowska et al. 2008; Melzner et al. 2009a; Ries et al. 2009; Small et al. 2010). Generally, sensitivity towards acidification is reflected in several features, such as long term reduction of growth, survival and reproduction in sea urchins, gastropods and copepods exposed to elevated pCO_2 (Shirayama & Thornton 2005). Especially, corals were suggested to suffer under the synergistic effects of acidification and warming due to an decreased carbonate accretion and the loss of their symbiontic algae (Hoegh-Guldberg et al. 2007).

Active organisms like teleost fish and cephalopod molluscs have a higher ability to compensate for acid-base disturbances due to their high and highly fluctuating metabolic rates (Melzner et al. 2009b). The flip side of such high metabolic rates is the accumulation of respiratory CO_2 in body fluids which reaches values of approximately 0.2 to 0.4 kPa (Larsen et al. 1997; Gutowska et al. 2009). During excessive exercise pCO_2 in body fluids increases, causing an extracellular acidosis with maximum pCO_2 values between 0.4 kPa (cephalopods) and up to 1.0 kPa (teleost fish) (Pörtner et al. 1991; Brauner et al. 2000). In general, fish and crustaceans can be characterized by high Na^+/K^+-ATPase (NKA) activity in their gill tissues. NKA provides the driving force in order to counter for acid-base disturbances, and, thus represents a key enzyme to compensate for pH shifts in body fluids caused by a respiratory acidosis (Seidelin et al. 2001; Choe and Evans 2004). Based on this knowledge, Melzner et al. (2009b) suggested that these features can be regarded as a pre-adaptation of active organisms in order to cope with elevated environmental hypercapnia, at least during short-term exposure. This hypothesis appears to hold true for the cephalopod *Sepia officinalis*. Under acidified conditions, this active cephalopod mollusc can tolerate high pCO_2 over long exposure times

(Gutowska et al. 2009). During a period of six weeks, juvenile *S. officinalis* maintained calcification rates under 0.4 and 0.6 kPa water pCO_2, and somatic growth compared to control animals (figure 1.3.). Calcification rates even increased, and led to a higher density of the chambered aragonitic cuttlebone in CO_2 treated animals (Gutowska et al. 2010b).

This hypercalcification might be due to pH compensatory mechanisms, which involve active HCO_3^- accumulation in body fluids. Hypercalcification may not be adaptive, but rather negatively influence swimming behavior and prey capture, as it must increase the density of the cuttlebone (Checkley et al. 2009; Gutowska et al. 2010b). Moreover, on the long run the maintenance of high blood bicarbonate levels may represent a severe energetic challenge to the animal and could result in a higher fraction of energy spent on acid-base regulation. Increased energy allocation towards intracellular acid-base regulatory processes during hypercapnic exposure were discussed as parsimonious explanations for a retarded growth and development in less powerful acid-base regulators (Thomsen and Melzner 2010; Stumpp et al. submitted). The hypothesis of energy allocation in response to environmental hypercapnia is discussed in greater detail in the first paragraph of section 4.

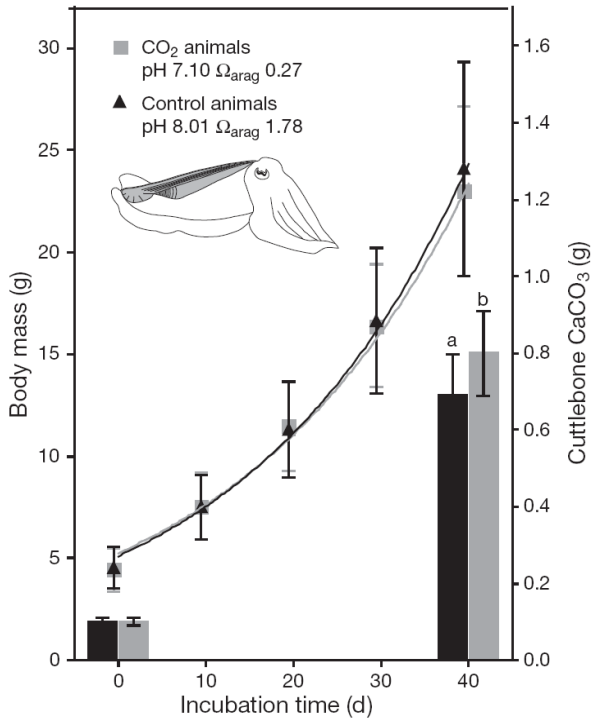

Figure 1.3. *Sepia officinalis* growth (left axis) and calcification (right axis) in the cuttlefish incubated under ~0.6 kPa CO_2 (grey) and control conditions (black). For $CaCO_3$ accretion, means not sharing the same letter above bars are significantly different. Data are mean ± SD (n = 20) (Gutowska et al. 2008).

1.3. Acid-base regulation

It was shown, that the predominant mechanism to counter acidosis is the active accumulation of bicarbonate in body fluids in order to buffer the excess of protons (Lloyd and White 1967; Heisler 1984; Heisler 1986; Ishimatsu et al. 2005). Active marine organisms like fish, crustaceans and cephalopods were identified as good regulators in response to environmental hypercapnia and their acid–base regulatory abilities have been well documented and the compensatory capacities nicely summarized (Whiteley et al. 2001; Claiborne and Edwards 2002). In general the effects of extracellular acid-base disturbances and the associated variations in extracellular pH

(pH_e), pCO_2 and [HCO_3^-] of body fluids can be illustrated in a Davenport diagram (figure 1.4.). In organisms that do not compensate pH_e fluctuations, the increased hydration of CO_2 in body fluids will lead to a passive increase of bicarbonate ions, along the non-bicarbonate buffer line (figure 1.4. dashed lines). In the case where an organism fully compensates its blood pH during hypercapnia, the increased concentration of protons that derive from the hydration of CO_2 are buffered by the actively increased concentration of bicarbonate ions in bodyfluids (figure 1.4. green time series). However, elevated environmental pCO_2 is always accompanied with increases in blood pCO_2 in order to maintain a sufficient outward directed diffusion gradient.

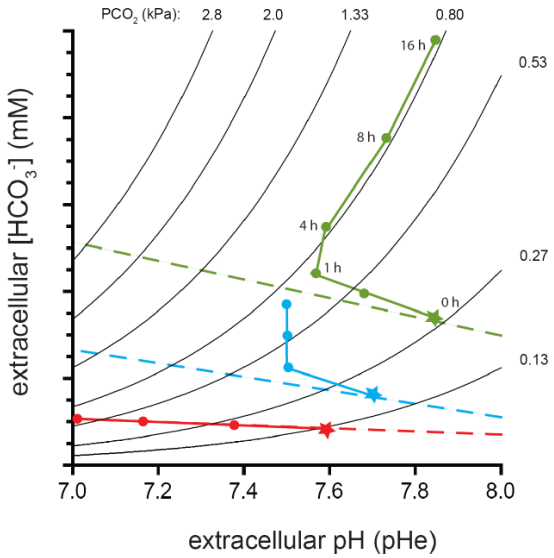

Figure 1.4. pH-bicarbonate (Davenport) diagram showing the schematic illustration of non-bicarbonate buffer lines, (dashed lines). Three different hypothetical organisms subjected to 0.5 kPa environmental hypercapnia. Red symbols: No active accumulation of bicarbonate in the extracellular space to compensate pH, pH follows the non-bicarbonate buffer line. Blue symbols, green symbols: partial/full pH compensation through active bicarbonate accumulation. Stars indicate control parameters, numbers indicate time (h) exposed to elevated pCO_2 (hypothetical time course!). Adopted from Melzner et al. (2009b).

For example, in response to 1 kPa CO_2 cod *Gadus morhua* and the eel *Conger conger* initially compensated the extracellular acidosis by actively increasing blood bicarbonate levels from 10 to 30 mM within 25 h (cod) and from 5 to 22 mM (eel), respectively (Toews et al. 1983; Larsen et al. 1997). However, studies that examined long-term tolerance to hypercapnia in marine invertebrate species together with acid-base regulation abilities are still limited (Michaelidis et al. 2005; Miles et al. 2007; Pane and Barry 2007; Spicer et al. 2007; Thomsen et al. 2010). Several studies conducted on decapod crustaceans demonstrated that these invertebrates fully compensate hypercapnia induced pH_e disturbances through active bicarbonate accumulation in body fluids. For example, in response to 1 kPa water pCO_2 *Cancer magister* increased its blood [HCO_3^-] by 12 mM within 24 h to fully compensate pH_e (Pane and Barry 2007). Studies on *Carcinus maenas* and *Callinectes sapidus* also indicated comparable high acid–base regulatory abilities (Henry and Cameron 1983; Truchot 1984; Cameron and Iwama 1987). A recent study by Gutowska et al. (2009) demonstrated that adult

cuttlefish *S. officinalis* can partially compensate blood pH when exposed to elevated environmental pCO_2 (0.6 kPa CO_2) by increasing blood [HCO_3^-] levels from 3.4 to 10.4 mM within 48 hours (schematically depicted in figure 1.4.). In this study it was concluded that the accumulation of blood bicarbonate is most probably achieved by active transport mechanisms involving the sodium pump as the main driving force for other secondary active transporters such as bicarbonate transporters, which are probably located in the cephalopod gill. Unfortunately, the mechanistic basis of acid-base regulation and its response towards hypercapnic stress in cephalopods is an almost completely unexplored field.

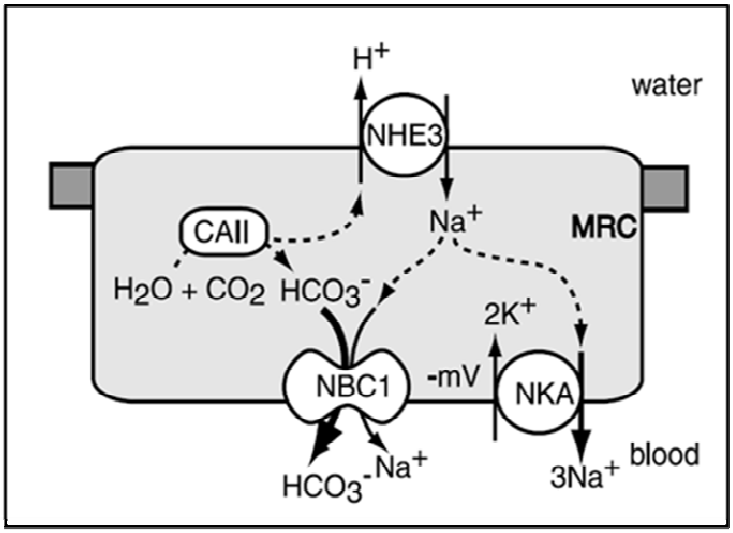

Figure 1.5. Model of acid secretion and Na^+ absorptive mechanisms in gill mitochondria-rich cells (MRCs) of FW Osorezan dace (adopted from Evans et al. (2005)). In the model, acid secretion and Na^+ absorption are initiated by Na^+-K^+-ATPase, which produces a low intracellular [Na^+] and a negative membrane potential. These conditions then favor Na^+ absorption, in exchange for acid secretion through an apical NHE3, which increases the intracellular pH. The higher pH increases intracellular [HCO_3^-] via CO_2 hydration by carbonic anhydrase isoform 2. Finally, the increased intracellular [HCO_3^-] and negative potential drive electrogenic efflux of Na^+ and HCO_3^- across the basolateral membrane through NBC1. Electrogenic transport is indicated with unequal arrow weights. Solid arrows indicate facilitated transport, and broken arrows indicate diffusion.

In adult fish and crustaceans, it is well established that the gill is the predominant site of acid-base relevant ion transport (Wheatly & Henry 1992, Claiborne & Edwards 2002, Evans et al. 2005, Hwang and Lee, 2007). The acid-base regulating machinery of this tissue (depicted in figure 1.5.) has been extensively investigated for various species of marine teleost fish such as salmon, trout, cod, eelpout (Seidelin et al. 2001; Evans et al. 2005; Hwang and Lee 2007; Deigweiher et al. 2008; Melzner et al. 2009a). The current model describes that the ubiquitous sodium potassium pump (Na^+/K^+-ATPase, NKA) is present in high concentrations in gill epithelia located mainly in basolateral membranes that provide an electrochemical gradient: in an ATP dependent process, $3Na^+$ are pumped out of the cell in exchange for $2K^+$ ions. This leads to low intracellular [Na^+]. This gradient is thought to be the main motor that can be used by secondary active transporters. Besides the direct ATP dependent extrusion of protons via V-type-H^+-ATPases these current models suggest an import of bicarbonate and an export of protons is achieved by secondary active transporters. These transporters mainly include apical

Na^+/H^+ exchangers (NHE) and Na^+ dependent Cl^-/HCO_3^- exchangers of the SLC4 solute transporter family that depend on the electro-chemical gradient created by the NKA (Boron 2004; Evans et al. 2005; Perry and Gilmour 2006; Horng et al. 2007). For example, an increased expression of NBC in the gill of the eelpout *Zoarces viviparous* was described in response to elevated water pCO_2 indicating an interaction of the NKA and Na^+/HCO_3^- cotransporter (NBC) in order to actively compensate for acid-base disturbances in body fluids and tissues (Deigweiher et al. 2008). Nevertheless, information on the mechanistic response towards moderately elevated pCO_2 is still very limited, especially for non model organisms (Fabry et al. 2008).

1.4. Cephalopods

In the aquatic environment fish can be considered the group of animals that reached the highest degree of complexity, in terms of sensory and locomotive ability. Among all invertebrates there is no phylum that has reached a comparable complexity except for cephalopods. Cephalopods have a highly developed neural system with very efficient sensory organs such as lens eyes, chemo-receptors, balance receptors and the ability to detect under water sound (Budelmann et al. 1997; Hu et al. 2009). Furthermore, cephalopods, especially the pelagic squids, are characterized by a high degree of mobility. It is believed that these features are derived from the competition of cephalopods and fish since the so called "Cambrian explosion" around 500 million years ago (O`Dor and Webber 1986; Smith and Caron 2010). Although many features (e.g. vision, activity and metabolism) of these two groups have been described as convergent, several anatomical and physiological features of cephalopods constrain their competition with fish. For example, the typical way of locomotion in cephalopods, jet propulsion, enables a high degree of mobility but at high energetic costs compared to undulatory swimming movements of fish (Wells and O`Dor 1991; O`Dor 2002). Moreover, although a considerable evolutionary refinement of hemocyanin-oxygen transport has occurred within the cephalopoda, this respiratory pigment is only able to carry about half the oxygen of the cellular hemoglobin of vertebrates (Brix et al. 1989). In order to optimize the transport efficiency of this pigment, cephalopod hemocyanins are characterized by a large Bohr-effect making them highly pH sensitive (Pörtner 1990). The fact that cephalopod hemocyanins are highly pH sensitive requires tightly regulated blood pH homeostasis in these organisms that have strong metabolic rate

fluctuations (Pörtner 1994; Pörtner and Zielinski 1998). However, information on a mechanistic basis regarding how cephalopods control their acid-base homeostasis are still poorly investigated. In fish both the gill and gut are the main sites of ion and acid-base regulation (Evans et al. 2005; Grosell 2006; Hwang and Lee 2007; Perry et al. 2010), while gut epithelia are mainly important for the secretion of HCO_3^- and $CaCO_3$ precipitation (Grosell 2006; Grosell et al. 2009a). For example during exposure to hypercapnic conditions (5 kPa CO_2), the aglomerular teleost *Porichthys notatus* drastically increases blood bicarbonate levels up to almost 40 mmol l^{-1} accompanied with significantly increased rectal fluid HCO_3^- levels (Perry et al. 2010). These results indicate that the gut system of marine teleosts is a major player in the maintenance of acid-base homeostasis. However, in gill tissues specialized cells, so called mitochondrion rich cells (MRCs), were identified as the main sites of ionic regulation in teleost (Hwang and Perry 2010). Using fish as a guide it can be hypothesized that also in cephalopods the gill or kidneys may be the primary sites for ion-regulation.

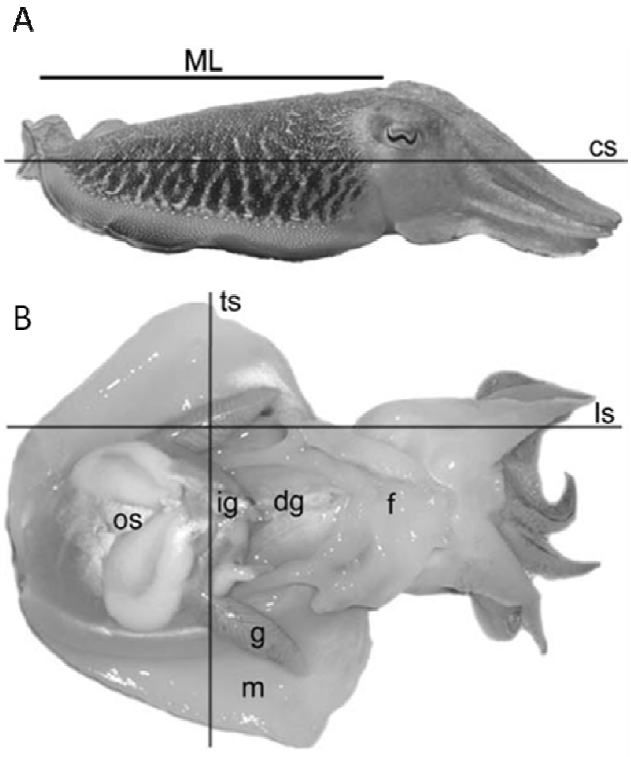

Figure 1.6. General anatomy of the cuttlefish *Sepia officinalis* (cs coronal section plane, ML dorsal mantle length) (A). Dissected specimen (ts transverse section plane, ls longitudinal section plane) with an opened mantle cavity revealing the orientation of organs such as digestive gland (dg), funnel (f), gills (g), ink gland (ig), and mantle (m) (B).

1.5. The cephalopod gill

The gills of decapod cephalopods such as *Sepia officinalis* (figure 1.6.A) are paired organs with bilateral symmetry, located on the ventral side inside the mantle cavity in a lateral position to the renal sac (figure 1.6.B). During inspiration the collar flaps and siphon of the funnel function as valves, which collapse inwardly when the mantle expands and water enters the mantle cavity through the opened collar flaps. Water is exhaled via the siphon by contraction of the mantle and closing of the collar flaps (Bone et al. 1994). By exhibiting a large surface, that is directly exposed to the water stream inside the mantle cavity, gills are the primary site for respiratory gas exchange as well as a major means of eliminating nitrogenous

(NH_4^+) wastes (Schipp et al. 1979; Donaubauer 1981; Wells 1990; Boucher-Rodoni and Mangold 1994). The blood is moved through the gills with the aid of the branchial hearts, contractile blood vessels and muscular movements of the gills (Wells and Wells 1982; Wells 1990; King et al. 2005). Oxygenated blood leaving the gills passes to the systemic heart and is then distributed via the arterial system to the rest of the animal. Inside the gill, the blood enters the primary (1°) afferent vessel bringing deoxygenated blood to the gill which is then sent to the secondary (2°) afferent vessel which is located inside the first order (1°) lamellae and finally distributed to the tertiary (3°) afferent vessels located in the 2° lamellae. Oxygenation takes place in the blood sinus of the 3° lamellae, and oxygen-rich blood is then transported back to the systemic heart via 3° to 1° efferent vessels (Figure 1.7.A). As mentioned above, the gill is divided into three different orders of lamellae. The primary lamella is folded in a fanlike pattern to form secondary (2°) lamellae that are aligned at right angles to the axis of the 1° lamella. Each 2° lamella, in turn, is folded in a fanlike pattern to form tertiary (3°) lamellae aligned at right angles to the axis of the 2° lamella (Young and Vecchione 2004).

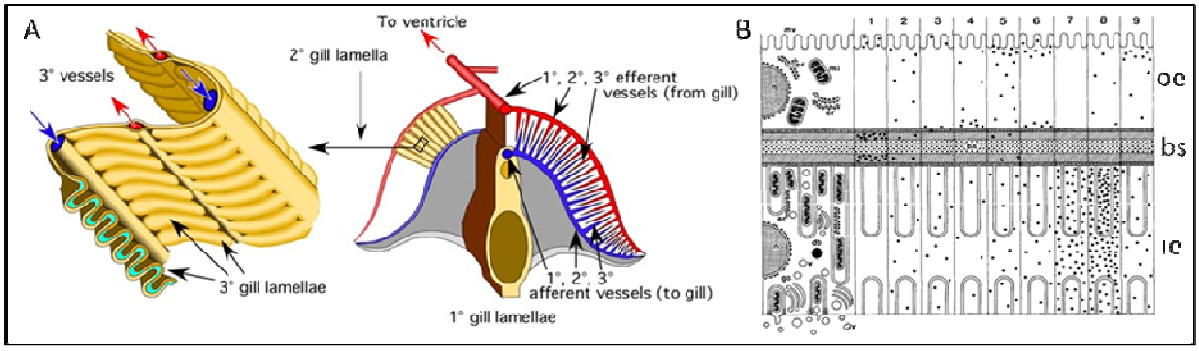

Figure 1.7. Diagram of the gill morphology of *Sepia officinalis* (A), indicating the direction of the blood flow and the arrangement of first to second order lamellae, showing the twice folded lamella of the gill of *S. officinalis*. The concave inner epithelium (green) of the third order gill lamellae belongs to the transport active epithelium, whereas the outer epithelium is exclusively involved in respiratory processes. Drawings adopted and modified after Young and Vecchione (2004). (B) Schematic presentation of the transport active inner epithelium (ie, green in part A) and the respiratory outer epithelium of the third order lamellae divided by a blood sinus (bs), summarizing the histochemical localization of enzymes: alkaline phosphatase (1), acid phosphatase (2), carbonic anhydrase (3), Mg^{2+}- triphosphatase (4), β-glucuronidase (5), glucose-6-phosphate dehydrogenase (6), malate dehydrogenase (7), succino-dehydrogenase (8), monoamine oxidase (9) (modified after Schipp et al. 1979)

Furthermore, the 3° gill lamellae can be divided into two epithelia consisting of one cell layer each, lining a blood sinus (figure 1.7.A, B). The inner, concave epithelium of the 3° lamellae (figure 1.7.A green color) is rich in mitochondria and various enzymes (e.g. alkaline phosphatase, acid phosphatase, carbonic anhydrase, Mg^{2+}-triphosphatase, β-glucuronidase, glucose-6-phosphate dehydrogenase, malate dehydrogenase, succino-dehydrogenase, monoamine oxidase) indicating active transport processes, whereas the outer epithelium, with its short diffusion distances (<7 µm) from the epithelial surface to the blood sinus, is

exclusively involved in respiratory processes (Schipp et al. 1979) (figure 1.7.B). These observations suggest that similar to the fish gill, the cephalopod gill has a dual function as gas exchange and ion-regulation organ.

1.6. Ontogeny-dependent sensitivities towards hypercapnia?

Previous studies demonstrated that adult fish as well as cephalopods can tolerate high CO_2 concentrations over long exposure times without being significantly affected in their performance and, thus, ecological fitness (Gutowska et al. 2008; Melzner et al. 2009a). On the other hand, embryos and larvae of marine organisms are often more vulnerable to environmental stress than adults. For example, fish eggs and larvae are known to be particularly sensitive to low water pH (Munday et al. 2009b; Munday et al. 2009c; Ishimatsu and Dissanayake 2010). As a consequence, even if elevated CO_2 is tolerable for adults, fish populations may still be affected due to the decreased survival of eggs and larvae. In this respect, the lack of functional osmo- and ion-regulatory organs in embryonic and larval stages can be hypothesized to be a key reason for an increased susceptibility towards hypercapnia induced acid-base disturbances.

The embryonic development of most marine fish, crustaceans and cephalopods takes place inside a protective egg capsule that is directly exposed to the surrounding water. The egg capsule creates a barrier between the developing embryo and the external medium and protects the embryo from biotic (e.g. predation) and abiotic stressors (e.g osmo-protection) (Charmantier and Charmantier-Daures 2001). The flip side of this protecting envelope is a limited permeability for diffusion of gases such as O_2 and CO_2. It has been observed that among many molluscan taxa, the eggs undergo a swelling process during development, leading to an enlarged egg surface area and a reduced capsule thickness in order to maintain sufficient gas (e.g. O_2 and CO_2) fluxes by diffusion (Seymour and Bradford 1994). It has been shown that also late embryos of the cuttlefish *Sepia officinalis* are exposed to high respiratory CO_2 concentrations in the egg capsule due to their high metabolic activity and the egg capsule wall serving as a diffusion barrier. For example, pCO_2 in the perivitelline fluid (PVF) during the final embryonic phase increased from 0.13 to 0.41 kPa causing a pH drop in the PVF from 7.7 to 7.2 (Gutowska and Melzner 2009). These hypercapnic conditions within the PVF may lead to acid-base disturbances that can constitute additional abiotic stressors to the developing embryo. On the other hand hypoxic conditions develop in order to maintain high fluxes of

oxygen into the PVF (Cronin and Seymour 2000; Gutowska and Melzner 2009). Towards hatching PVF pO_2 declined from >12 kPa to less than 5 kPa, in the common cuttlefish *S. officinalis* (Gutowska and Melzner 2009). Similar observations were obtained for the giant cuttlefish *Sepia apama*, with PVF oxygen partial pressures starting at 12 kPa and decreasing towards hatching to 5 kPa (Cronin and Seymour 2000).

In the light of the abiotic features inside the cephalopod egg, elevated environmental CO_2 could be considered an extraordinary stressor to the developing embryo: in order to maintain a sufficiently high diffusion gradient of CO_2 (approximately 0.2 kPa) out of the egg, the increase of external pCO_2 should be additive to the already high PVF pCO_2. Thus, hypercapnia induced acid-base disturbances may be even more pronounced in embryos of marine species with an oviparous type of development. The PVF pCO_2 in response to elevated sea water pCO_2 can be hypothesized to increase in a linear fashion according the following equation:

$$\text{PVF } pCO_{2\,\text{hypercap}} = \text{PVF } pCO_{2\,\text{control}} + \Delta \text{ water } pCO_2 \qquad \text{(Eq. 1.3.)}$$

In fish early stages that also have an embryonic development inside a protecting egg capsule, the skin and the yolk sac membrane was discovered to be a central organ of ion-regulation. When gill epithelia are not yet completely developed, epidermal ionocytes are precociously scattered on the skin to mediate ion and acid-base balance (Hsiao et al., 2007; Hwang and Lee, 2007). Based on vital dye binding and immunocytochemical studies, distinct types of epidermal ionocytes have been characterized in fish. Functional studies also provide evidence that different types of zebra fish ionocytes, such as NaR (Na^+/K^+ ATPase-rich) cells, HR (H^+-ATPase-rich) cells, and NCC (thiazide-sensitive Na^+/Cl^- cotransporter expressing) cells, mediate an equivalent function as their counterparts in the kidneys of terrestrial vertebrates (Lin et al., 2006; Horng et al., 2007; Hwang and Lee, 2007; Yan et al., 2007; Lin et al., 2008). This feature might be the reason for relative tolerance against acid-base disturbances during embryonic development of teleosts compared to most marine invertebrates studied so far.

In cephalopods, epidermal ionocytes had not been discovered prior to this thesis. During cephalopod organogenesis, before systemic and branchial hearts are developed, muscle cells on the yolk sac are responsible for convective circulation of the hemolymph: peristaltic movements propel hemolymph around the yolk syncytium and into the extensive lacunar blood system of the embryo. Prior to differentiation of blood vessels, these blood sinuses are occupying large volumes of the embryonic body, particulary in the (metabolically)

active head region (see von Boletzky 1987a; von Boletzky 1987b). Thus, the integument must be the main respiratory organ in cephalopods prior to gill development. Well perfused and metabolically active regions such as the head and the 'yolk sac heart' are prime candidate tissues for the occurrence of ionocytes, analogous to the situation in fish.

Similar to fish and crustaceans, cephalopod gills are probably also the most important ion-regulatory organs in juveniles and adults. During larval development, rudimentary gill structures occur at stage 20 and become complete after hatching (Arnold 1965, Schipp et al. 1979). Furthermore, Schipp et al. (1979) showed that the cephalopod gill changes morphogenetically shortly after hatching, transforming into a highly folded epithelium with deep lateral interdigitations and brush border. It also has a high density of vesicles, mitochondria and carbonic anhydrase located in the cells of the inner branchial epithelium (Schipp et al. 1979). This formation and proliferation of the gill after hatching indicates that the gas exchange, and the ion regulatory capacity might be fully activated only post-hatch. Bearing this metamorphosis of the cephalopod gill in mind, the impacts of acidification through elevated pCO_2 can be expected to be more dramatic in early life stages (late embryonic stages).

1.7. Questions and research hypotheses

a) What are the sites of ion regulation in cephalopods?

A first aim of this work is dedicated to the identification of ion regulatory epithelia in cephalopods and the comparison with those described in other marine organisms such as teleost fish and decapod crustaceans. Using fish and crustaceans as a guide we hypothesize that, also in cephalopods, the gill constitutes the major site for acid-base relevant transport in adults.

An additional objective was to gain first insights into the ontogeny of ion regulatory epithelia in late embryos, hatchlings and adult cephalopods. The transition from embryo to hatchling can be seen as an event where biotic and abiotic environmental conditions change dramatically for the animal and, thus, special focus is dedicated to the organization and distribution of ion-regulatory epithelia in early life stages. In order to provide answers to these questions classical- and immunohistological staining methods were applied and maximum Na^+/K^+- ATPase activity was determined for tissues which are believed to be involved in ion regulatory processes.

b) Do cephalopod early stages exhibit alternative sites of acid-base regulation?

It is hypothesized that in order to cope with respiratory acidosis inside the egg capsule, early developmental stages of cephalopods need to secrete protons from their (extra) cellular compartments. The anatomical and morphological features of cephalopod embryos led to the hypothesis that in convergence with fish, the yolk epithelium of cephalopod embryos may constitute a major site of acid-base regulation, as it is well perfused from in and outside and has a large surface area. In order to address this question, cuttlefish (*Sepia officinalis*) and squid (*Sepioteuthis lessoniana*) early life stages were used as experimental animals in order to demonstrate the presence of alternative sites of ion regulation via immunohistochemical, *in situ* hybridization, vital dye and electrophysiological methods.

c) What are major components of the acid-base regulatory machinery in cephalopods?

The acid-base regulating machinery has been extensively investigated for various species of marine teleost fish (Seidelin et al. 2001; Evans et al. 2005; Hwang and Lee 2007; Deigweiher et al. 2008; Melzner et al. 2009a). (Un)fortunately, only little information exists for cephalopods. Thus, this study proposes that similar to teleost fish, active acid-base homeostasis in body fluids of cephalopods is achieved via a convergent ion-regulatory machinery as described for teleost fish and decapods crustaceans. Generally, this would include the presence of Na^+/K^+-ATPase located in basolateral membranes of the transport active gill epithelium that provides the primary driving force for other secondary active transporters, such as bicarbonate transporters (SLC4 family) or sodium proton exchangers (NHE). Furthermore, it is hypothesized that acid base relevant enzymes such as the carbonic anhydrase or V-type-H^+-ATPase may also play an important role in the acid-base regulating machinery of cephalopods.

d) Are there ontogeny-dependent sensitivities/responses?

Embryos and larvae are often more vulnerable to environmental stress than adults. For example, fish eggs and larvae are known to be particularly sensitive to low water pH (Munday et al. 2009b; Ishimatsu and Dissanayake 2010; Tseng et al. in prep.). The lack of high power ion-regulatory organs such as gills, kidneys and gut in embryonic and larval stages may be a

key reason for an increased susceptibility towards ocean acidification. Furthermore, the final stage of embryonic development in oviparous animals is often characterized by extremely low O_2 and high CO_2 concentrations inside the egg. Consequently, environmental pCO_2 may constitute a stronger stressor for the developing embryo, as increases of environmental pCO_2 must be additive to the PVF pCO_2 in order to maintain a substantial diffusion gradient of CO_2 directed out of the egg.

e) Can we make predictions about the sensitivity of cephalopods to ocean acidification?

The overall goal of the present work is dedicated to the question, in how far cephalopods might be affected by the ongoing increase of atmospheric CO_2 during the upcoming centuries. In this respect it can be hypothesized that species sensitivity might be very different among different ontogenetic stages. Juveniles or adults may be more tolerant due to their high acid-base regulatory capacities. Nevertheless, in response to chronically elevated blood [HCO_3^-] levels a hypercalcification of the cuttlebone was described for the cuttlefish *S. officinalis* (Gutowska et al. 2010b). This hypercalcification might still have negative long-term effects on buoyancy control, and thus, behavior of cuttlefish.

On the other hand it can be hypothesized that embryos may react very differently to elevated water pCO_2, as major acid-base regulatory organs (e.g. gills) are not yet fully developed. It can be expected that the sensitivity threshold of embryonic stages is decreased in comparison to juveniles or adults.

2. Methods

2.1. Animals and experimental design

Sepia officinalis egg clusters were collected in Zeeland, Netherlands, in May 2008, 2009 and in Luc sur mer, France in 2010, and transported to the Leibniz-Institute of Marine Sciences (IFM-GEOMAR), Kiel at stage 17-20 (stages according to Lemaire (1970)). After hatch, cuttlefish were raised in a closed recirculating system (1200 l total volume, protein skimmer, nitrification filter, UV disinfection unit, salinity 31-32, NH_4^+ <0.1 mg l^{-1}, NO_2^- <0.1 mg l^{-1}, NO_3^- <10 mg l^{-1}, temperature 15°C and constant 12 h dark 12 h light cycle). Cuttlefish hatchlings were initially fed with live mysids and progressively transitioned to feed on *Paleamonetes varians.* The animals showed normal development and behavior.

Loligo vulgaris egg clusters were collected in Zeeland, Netherlands, in May 2009 and transported to the Leibniz-Institute of Marine Sciences (IFM-GEOMAR), Kiel, at stage 12-15 (stages according to Lemaire (1970)). The egg masses were immediately transferred to the experimental setup and used for growth and perivitelline fluid (PVF) analysis (see section 2.2. below).

Sepiteuthis lessoniana egg clusters (stage 8-15) were collected in Aodi, Taiwan (R.O.C.) in July 2010 by SCUBA diving and reared in a closed recirculating system (600 l total volume, UV disinfection unit, salinity 32-34, NH_4^+ <0.1 mg l^{-1}, temperature 28°C and constant 12 h dark 12 h light cycle) at the Institute of Cellular and Organismic Biology, Academia Sinica. Table 2.1. summarizes the animals and experimental treatments used for the present work.

Table 2.1. Animals and experiments used in the present dissertation

year	date	origin	species	stage used	CO_2 experiment	parameters measured	publication
2008	May	Oostershelde, NL	*S. officinalis*	juv.	control; 0.14 kPa; 0.40 kPa	NAK activity, gene expression, immunohistology, *in situ* hybridization	discussion, 1, 3
2009	June	Oostershelde, NL	*S. officinalis*	emb.	control; 0.14 kPa; 0.40 kPa	growth, gene expression, PVF parameters (O2, pH, DIC, pCO2),	discussion, 1
2009	June	Oostershelde, NL	*L. vulgaris*	emb.	control; 0.14 kPa; 0.40 kPa	PVF parameters, (O_2, pH, DIC, $p\,CO_2$) growth	discussion
2010	May	Luc sur Mer, FR	*S. officinalis*	embr./hat.	control; 0.14 kPa; 0.40 kPa	growth, yolk consuption, metabolic rates, immunohistology, *in situ* hybridization	discussion
2010	July	Aodi, TW	*S. lessoniana*	embr./hat.	control	SIET, immuno/vital dye staining, SEM, *in situ* hybridization	discussion, 2

Stages: juveniles (juv.); hatchlings (hat.); embryos (embr.)
Species: *Sepia officinalis*, *Loligo vulgaris*, *Sepioteuthis lessoniana*

2.1.1. General experimental setup

Embryos and Hatchlings

Sepia officinalis egg clusters were separated and then incubated in nine aquariums (25 l volume) equipped with 25 to 30 eggs inside a 15°C climate chamber for approximately eight weeks. The aquariums were continuously equilibrated with the appropriate gas mixtures (0.04 kPa, 0.14 kPa and 0.4 kPa CO_2 in pressurized air) supplied by a central automatic gas mixing-facility (Linde Gas, HTK Hamburg, Germany). The nine tanks with three replicates for each pCO_2 level were randomly distributed. A light regime with a 12 h/12 h light/dark-cycle was chosen. Artificial seawater (SEEQUASAL, Münster, Germany) was prepared in three 400 l reservoir tank and pre-equilibrated with the respective pCO_2. Two thirds of the water in the experimental tanks was exchanged daily with water from the reservoir tanks to maintain high water quality within the system (ammonia levels < 0.3 mg l^{-1}). For sampling of gill tissues, late stage embryos (stage 30 (Lemaire 1970)) and hatchlings (2 days post hatching) were dissected by opening of the ventral mantle cavity. The two gills, which were approximately 1.5 mm in length were sampled with two sharp forceps and then quickly shock-frozen in liquid nitrogen and stored at -80°C for gene expression analysis.

Juveniles

48 *Sepia officinalis* specimens (dorsal mantle length (DML) 3-4 cm) were maintained in a flow through system consisting of 16 PVC basins (30 × 30 × 35 cm) in a 15 °C climate chamber at the IFM-GEOMAR, Kiel. A light regime with a 12 h/12 h light/dark-cycle was chosen. Artificial seawater (SEEQUASAL, Germany) was prepared daily in a 400 l reservoir tank. From this reservoir tank the water passed through a 12 W UV sterilizer before being distributed to the experimental tanks. From these experimental tanks water was drained out through an overflow at a rate of approximately 20 ml min^{-1}. Before the start of the experiments the animals were maintained under control conditions for 14 days. Eight experimental tanks were equipped with three individuals each, and continuously equilibrated with the appropriate gas mixture (0.3 kPa CO_2) supplied by a central automatic gas mixing-facility (Linde Gas, HTK Hamburg, Germany). The remaining eight were also equipped with three individuals and equilibrated with pressurized air. Throughout the duration of the experiment, cuttlefish were fed daily with live *P. varians* The eight tanks simulating elevated CO_2-conditions and control tanks were randomly distributed and water ammonia levels were maintained <0.3 mg l^{-1}. During the experiment (42 days) tissue samples were taken at three time points, 2 days, 10 days and 42 days. At each time point, eight specimens from each

treatment (total of 16 animals) were anaesthesized in 2.5% EtOH in seawater. Afterwards the animals were sacrificed by decapitation and the mantle cavity was opened on the ventral side. The gills were immediately dissected using microscissors and forceps. The tip of the left gill was fixed with 4% paraformaldehyde (PFA) in seawater at 4°C overnight, and then washed several times with phosphate-buffered saline (PBS). These gills for in situ hybridization were stored in 100% MeOH at -80°C. The remaining right and the left gill were quickly shock-frozen in liquid nitrogen and stored at -80°C for enzyme assays and gene expression analysis.

The investigations comply with the German animal welfare principles No. V 31 and the animal use protocols were approved by the animal care committee of the Christian-Albrechts-University, Kiel.

2.1.2. Determination of the seawater carbonate system

The pH was measured with a WTW 340i meter and WTW SenTix 81 electrode calibrated daily with Radiometer IUPAC precision pH buffers 7.00 and 10.00 (S11M44, S11 M007).

Total dissolved inorganic carbon (C_T) was measured coulometrically according to Dickson et al. (2007) using a SOMMA (Single-Operator Multi-Metabolic Analyzer) auto analyzer (Marianda, Kiel, Germany). Total alkalinity (A_T) was determined by using the methods of Dickson et al. (2007) and Gran (1952) by means of a potentiometric open-cell titration with hydrochloric acid. The measurement was performed using a VINDTA (Versatile Instrument for the Determination of Titration Alkalinity) auto analyzer (Marianda, Kiel, Germany). As reference material for both types of analysis (C_T as well as A_T) Dickson seawater standard was used (Dickson et al. 2003). Seawater carbonate chemistry parameters were calculated from C_T and A_T with the software CO2SYS (Lewis &Wallace 1998) using the dissociation constants of Mehrbach et al. (1973) as refitted by Dickson & Millero (1987).

2.2. Determination of PVF abiotic parameters

The sampling and characterization of the PVF eggs was performed according to Gutowska and Melzner (2009). At the final stage of development (stage 30 (Lemaire 1970)) eggs were carefully lifted out of the water and immediately sampled for PVF. To measure pO_2, a 1 ml plastic syringe with integrated fiber optic sensors (optodes, tip diameter 0.1 mm, Presens GmbH, Regensburg, Germany) was used. During the measurement period for pH and pO_2,

the PVF sample and sensors were placed in a thermostatted water bath at 15°C. The oxygen optode was calibrated according to the manufacturer's instructions with water vapor saturated air and a Na_2SO_3 solution.

A pH electrode (WTW sentix81 and pH340i pH meter, WTW, Weilheim, Germany), calibrated with seawater buffers, was used to measure pH in 0.5 ml Eppendorf tubes. Another 500 µl of PVF was sampled with a gas-tight glas syringe for the determination of total dissolved inorganic carbon (DIC). DIC was measured in triplicate (100 µl each) using a Corning 965 carbon dioxide analyzer (Olympic Analytical Service (OAS), England). The carbonate system speciation was calculated from DIC and pH_{NBS} using CO2SYS.

Following PVF sampling, eggs were dissected and biometric parameters of the embryos were determined. Dimensions were measured using a Leica MZ95 stereo microscope equipped with the Image-Pro Plus software and animal wet mass was determined using a balance (Sartorius TE64).

2.3. Oxygen consumption measurements

Oxygen consumption of individual eggs and hatchlings was determined by closed-bottle respirometry. Animals were collected directly from the incubation tanks and gently placed into 18 ml (stage 26–28 embryos), 44 ml (stage 29–30 embryos) or 130 ml (1-3 day old hatchlings) glass vessels filled with 0.2 µm filtered seawater from the respective tanks. Respiration chambers containing eggs were closed air-free with glass slides and placed into a temperature controlled water bath at 16.00 ± 0.02 °C (Lauda Proline RP855, Lauda-Königshofen, Germany). After an equilibration time of 15 min (for embryos) and 30 min (for hatchlings), chambers were carefully inverted (2x) without disturbing the animal to ensure equal oxygen distribution. Chambers were slightly opened and the pO_2 at the beginning of the measurement was determined by inserting a needle type fibre optic oxygen sensor (optodes, PreSens GmbH, Regensburg, Germany) connected to a fibre optic oxygen meter (Oxy-4 Micro, PreSens GmbH). The chambers were closed, avoiding air bubbles inside the chamber and incubated in the water bath for 2-3 h. Prior to the determination of oxygen concentrations at the end of the incubation chambers were carefully inverted (5x) in order guarantee an equal oxygen distribution. Oxygen saturation never decreased below a critical value of 70%. Three chambers not containing animals served as controls. Due to bacteria and small metazoans that live on the egg capsule (Cronin and Seymour 2000) embryonic MO_2 was determined as the

difference between whole egg and capsule respiration. Oxygen consumption by the capsule was measured in the same manner as described above. Measurements were recorded on a personal computer using software provided by the manufacturer (OXY 4 v2.11 Micro) and stable values were obtained after 2–3 min. Calibration of the oxygen sensors was performed at 16°C using water vapor saturated air (100% oxygen saturation) and a 1% w/v Na_2SO_3 solution (0% oxygen saturation) at the respective ambient air pressure.

After respiration measurements eggs were dried on paper tissues and egg wet mass was determined using a precision balance (Sartorius BA110S, Göttingen, Germany). Eggs were dissected and embryos were checked for vitality. Measurements were omitted when animals were dead or ink was observed in the perivitelline fluid, indicating a stress response during handling especially in late stage (stage 29/30) embryos. Yolk and animal were carefully wiped on tissue paper and wet masses were determined.

2.4. Biochemical and molecular techniques

2.4.1. Enzyme activity and protein levels

Na^+/K^+-ATPase activity was measured in whole animal and tissue crude extracts in a coupled enzyme assay with pyruvate kinase (PK) and lactate dehydrogenase (LDH) using the method of Allen and Schwarz (1969) as described by Melzner et al. (2009a). Crude extracts were obtained by quickly homogenizing the tissue samples in a conical tissue grinder in 10 volumes of ice-cold buffer (50mM imidazole, pH 7.8, 250 mM sucrose, 1mM EDTA, 5 mM β-mercaptoethanol, 0.1% (w/v) deoxycholate, proteinase inhibitor cocktail from Sigma-Aldrich (Taufkirchen, Germany, Cat. No. P8340) followed by Ultra Turrax treatment (3 x 5s) on ice. For *S. officinalis* whole animal homogenates the ink gland was quickly removed before homogenization, as the ink would absorb light during the photometric test. Cell debris was removed by centrifugation for 10 min at 1000 g and 4°C. The supernatant was used as crude extract. The reaction was started by adding 10 µl of the sample homogenate to the reaction buffer containing 100 mM imidazole, pH 7.8, 80 mM NaCl, 20 mM KCl, 5 mM $MgCl_2$, 5 mM ATP, 0.24 mM Na-($NADH_2$), 2 mM phosphoenolpyruvate, about 12 U/ml PK and 17 U/ml LDH, using a PK/LDH enzyme mix (Sigma-Aldrich). The oxidation of NADH coupled to the hydrolysis of ATP was followed photometrically at 15°C in a DU 650 spectrophotometer (Beckman Coulter, USA) over a period of 10 min, measuring the decrease

of extinction at λ = 339 nm. The fraction of Na^+/K^+-ATPase activity in total ATPase (TA) activity was determined by the addition of 17 µl of 5 mM ouabain to the assay. Each sample was measured in sextuples. Enzyme activity was calculated using an extinction coefficient for NADH of ε = 6.31 mM^{-1} cm^{-1} and given as micromoles ATP consumed per gram tissue fresh mass per hour.

For immunoblotting, 25 µl of crude extracts for Na^+/K^+-ATPase were used. Proteins were fractionated by SDS-PAGE on 10% polyacrylamide gels, according to Lämmli (1970), and transferred to PVDF membranes (Bio-Rad, Munich, Germany), using a tank blotting system (Bio-Rad). Blots were preincubated for 1 h at room temperature in TBS-Tween buffer (TBS-T, 50 mM Tris -HCl, pH 7.4, 0.9% (wt/vol) NaCl, 0.1% (vol/vol) Tween20) containing 5% (wt/vol) non-fat skimmed milk powder. The primary antibody for the Na^+/K^+-ATPase was the polyclonal antibody α (H-300). Blots were incubated with primary antibodies at 4°C overnight. After washing with TBS-T, blots were incubated for 1 h with horseradish conjugated goat anti-rabbit IgG antibody (Santa Cruz Biotechnology, INC.) diluted 1:2000 in TBS-T containing 5% non-fat skimmed milk powder. Protein signals were visualized by using the ECL Western Blotting Detection Reagents (GE Healthcare, Munich, Germany) and recorded by a LAS-1000 CCD camera (Fuji, Tokyo, Japan).

2.4.2. Molecular cloning

Fragments of the *Sepia* Na^+/K^+-ATPase (*NKA*), Na^+/HCO_3^- co-transporter (*NBC*), Na^+-dependent Cl^-/HCO_3^- exchanger (*NDCBE*), cytoplasmatic carbonic anhydrase (*CA*) and V-type-ATPase (*V-HA*) genes were isolated from gill tissue by means of reverse transcription followed by PCR (RT–PCR). Degenerate primers were designed using Mac-Vector® 10.0.2 (Symantec Corporation) software, using highly conserved regions of sequences of cephalopods, bivalves and fish obtained from GenBank. Reverse transcription was performed with Superscript RT (Invitrogen, Karlsruhe, Germany) and gene specific primers according to the manufacturer's instructions with mRNA as templates (see next section for RNA extraction protocol). In the following PCR, primer pair 5´-AAGTCGTGCCAATGTGTTGTA-3´ and 5´-TACTTYCCACGWGGACTTTCTTAG-3´ resulted in a 268 bp fragment of the *NKA* (GQ153672.1), the primer pair 5´-GCGGAAGGAGGTGTAGAAGAAGT-3´ and 5´-CATAGTCHAGTGTCGTAAGTAGGC-3´ resulted in a 582 bp fragment of *NBC* (bankit1344341), the primer pair 5´-GCCAGRTGGATWAAGTTTGA-3´ and 5´-GGTWGGSACRGGRACCTCTG-3´ resulted in a 693 bp fragment of the *NDCBE*

(bankit1344354), the primer pair 5´-CTACARYTAYCCYCTRACCGC-3´ and 5´-AAAGTRAARGTGACCCCKAG-3´ resulted in a 215 bp fragment of cytosolic *CAII* (bankit1344380) and the primer pair 5´- GARTAYTTYMGNGAYATGGGN -3´ and 5´-RTTYTGYTGNARRAARTCRTCYTT -3´ resulted in a 556 bp fragment of *VHA* subunit a (bankit1370003). The sequences obtained for cytosolic CAII and the NBCe of cuttlefish show high similarities compared to teleosts and mammals (publication 1, supplementary figure 2S).

cDNA was amplified using Taq-Polymerase (Invitrogen, Karlsruhe, Germany) in the presence of 1.5 mM $MgCl_2$ (PCR conditions: 4 min denaturation at 94°C, 45 sec annealing at 53°C and 45 sec elongation at 72°C, 35 cycles followed by a final amplification step of 8 min at 72°C). PCR fragments were separated after electrophoresis in 1% agarose gels. Extraction and purification of the PCR fragments from the gel was accomplished using the QIAquick® gel extraction kit (QIAGEN, Hilden, Germany). Cloning and isolation of plasmids was performed using the pGEM®-T Easy Vector Systems and JM 109 competent *E. coli* cells (Promega, Madison, WI, USA). Plasmids were extracted using the Qiaprep Spin Miniprep Kit (QIAGEN, Hilden, Germany) and sequenced at the sequencing platform of the Institute for Clinical Molecular Biology (IKMB), Christian-Albrechts- University of Kiel (Kiel, Germany).

2.4.3. Quantitative real time PCR

For RNA extraction, whole gills were homogenized under liquid nitrogen, using pestle and mortar. 25 mg homogenates were used for further extraction. RNA extraction was performed according to the QIAgen RNeasy Mini Handbook (Qiagen, Hilden, Germany) with an additional cleaning step using the QIAshredder column (Qiagen, Hilden, Germany) performed after homogenization in RLT-buffer. RNA was eluted and stored in 100 µl RNase-free water at -80°C. DNA was removed by DNase digestion with the DNA-free kit (Applied Biosystems, Darmstadt, Germany). Concentration of the isolated RNA was determined photometrically using a NanoDrop ND-1000 spectrophotometer (PEQLAB, Erlangen, Germany).

Primers for qRT-PCR were designed using the primer analysis software Primer Express v. 2.0 (Applied Biosystems) with the default parameters of the TaqMan MGB Probe and Primer design procedure. We selected PCR amplicons to range from 50 to 100 bp in size.

qRT-PCR was performed on ABI StepOne plus Sequence Detection System (Applied Biosystems) using the Power SYBR® Green QPCR Master Mix (Applied Biosystems). The PCR reaction consisted of 10 µl SYBR Green PCR Master Mix, 2 µM forward and reverse primers, 2.0 µl 1:10-diluted template cDNA and 2.0 µl water in a total reaction volume of 20

µL. Thermocycling was performed using the following conditions: 10 min at 95°C, 45 cycles of 15 s at 95°C, and 1 min at 62°C. To verify that the reaction yielded only a single product, a dissociation protocol after thermocycling revealed the melting curve of the PCR amplicon from 65 to 95°C. Data were recorded as fractional cycle at an arbitrary *C*T-value during the exponential phase of the reaction. All the data from one gene were recorded in triplicates at the same time. The average of each triplicate was calculated and then served as input for comparing the different time points and treatments.

To determine the amplification efficiency of each primer pair, a standard curve of 4 serial dilution points (insteps of 2-fold) of a cDNA mixture was analyzed using linear regression. The amplification efficiency of an individual reaction was determined by the ABI StepOne plus Sequence Detection System. PCR efficiencies of single genes ranged from 1.84 to 2.0. A control with mRNA was used in order to test for DNA contaminations in the samples.

NormFinder, a Microsoft Excel add-in (available at http://www.mdl.dk/ publicationsnormfinder.htm) was used to identify housekeeping gene candidates. The genes cleavage and polyadenylation specificity factor (CPSF) and ubiquitin conjugated protein (UCP) were identified as the best housekeeping genes between treatments and incubation times. For the normalization factor (NF_n) a geometric mean of the best fitting housekeepers (REF_{1-n}) was calculated using the following equation:

$$NFn = \sqrt[n]{REF1 * REF2 * \ldots * REFn} \qquad \text{(Eq. 2.1.)}$$

2.5. Histological methods

2.5.1. Classical histology and immunocytochemistry

Whole animals or isolated gills from *Sepia officinalis*, *Loligo vulgaris*, *Sepioteuthis lessoniana* and *Octopus vulgaris* were fixed by direct immersion for 24 h in Bouin's fixative followed by rinsing in 70% ethanol. Samples were fully dehydrated in graded ethanol series and embedded in Paraplast (Paraplast Plus, Sigma, P3683). Sections of 4 µm were cut on a Leitz Wetzlar microtome, collected on poly-L-lysine-coated slides, and stored at 37°C for 48 hours. One series was used for classical light microscopy using the Masson`s trichome method for tissular topography. The other series was used for immunohistology. The slides

were deparafinized in Histochoice Tissue fixative (Sigma, H2904) for ten minutes, washed in Butanol and passed through a descending alcohol series (100%, 95%, 90%, 70% and 50% for 5 min each). Slides were washed in PBS (pH 7.3) and exposed to a heat shock inside the PBS bath using a microwave (80% of power for 2x3 min) Afterwards samples were transferred to a PBS bath containing 150 mM NaCL and Tween 20 (conc. 0.2 µl/ml) for ten minutes, and a PBS bath containing 5% skimmed milk for 20 min to block non-specific bindings. The primary antibody, a rabbit polyclonal antibody raised against an internal region of Na^+/K^+-ATPase α1 of human origin (Na^+/K^+-ATPase α (H-300), Santa Cruz Biotechnology, INC.) was diluted in PBS to 10 µg ml^{-1}, placed in small droplets of 100 µl on the sections, and incubated for 2 h at room temperature in a wet chamber. To remove unbound antibodies, the sections were then washed (3x5 min) in PBS and incubated for 1 h with small droplets (100 µl) of secondary antibody, tetramethyl rhodamine isothiocyanate-labeled goat anti rabbit IgG (Santa Cruz Biotechnology, INC.). After rinsing in PBS (3x5 min), sections were covered with a mounting medium and examined with a fluorescent microscope (Leitz Diaplan coupled to a Ploemopak 1-Lambda lamp) with an appropriate filter set (577 nm band-pass excitation filter) and a phase contrast device. For higher magnification, an Axiovert 200M microscope equipped with an ApoTome for optical sectioning using the Axio Vision 4.6 software (Carl Zeiss, Jena, Germany) was used. Negative controls were performed several times for every antibody and every species by omitting the primary antibody. To observe the sections we used a filter set (450–490 nm band-pass excitation filter) and a phase contrast device.

For whole mount immunocytochemistry whole animals were fixed by direct immersion for 12 h in 4% PFA followed by rinsing in 70% ethanol. Samples were fully dehydrated in graded ethanol series and stored in 100% ethanol. For immocytochemistry samples were transferred to a PBS bath containing containing 10% bovine serum albumin (BSA) for 30 min to block non-specific bindings. The primary antibodies used were a rabbit polyclonal antibody raised against an internal region of Na^+/K^+-ATPase α1 of human origin (diluted 1:50; Na^+/K^+-ATPase α (H-300), Santa Cruz Biotechnology, INC.) and a polyclonal antibody raised in rabbit against a synthetic peptide corresponding to a C-terminal region of tilapia NHE3 (diluted 1:100; generously provided by Dr. Toyoji Kaneko). Samples were incubated over night at 4°C on an orbital shaker. To remove unbound antibodies, the samples were then washed (3x5 min) in PBS and incubated over night at 4°C with secondary antibody, goat anti rabbit IgG Alexa-Flour 488 and 568 (dilution 1:100). To allow double-color immunofluorescence staining for NKA and NHE3, one of the polyclonal antibodies (e.g. NKA) was directly labeled with Alexa Fluor dyes using Zenon antibody labeling kits

(Molecular Probes, Eugene, OR, USA). After rinsing in PBS (3x5 min), samples were examined with a fluorescent microscope (Zeiss Imager 1M) with an appropriate filter set and a phase contrast device.

2.5.2. *In situ* hybridization

The partial sequence of the Na^+/K^+-ATPase cDNA was obtained by PCR (forward 5´-TGAAGAAGATGTGGAVGAAGGCG-3´ and reverse 5´-CGGATGAATGCTGTGAHCTGATAC-3´) amplification and inserted into the pGEM-T easy vector (Promega, Madison, WI, USA) for the synthesis of antisense and sense RNA probes. After the PCR with the T7 and SP6 primers, the products were, respectively, subjected to *in vitro* transcription with T7 and SP6 RNA polymerase (Roche, Penzberg, Germany), in the presence of digoxigenin (dig)-UTP. Dig-labeled RNA probes were examined with RNA gels and dot-blot assays to confirm quality and concentration. For dot-blot assays, synthesized probes and standard RNA probes were spotted on nitrocellulose membrane according to the manufacturer's instructions. After cross-linking and blocking, the membrane was incubated with an alkaline phosphatase (AP)-conjugated anti-dig antibody and stained with nitro blue tetrazolium (NBT) and 5-bromo-4-chloro-3-indolyl phosphate (BCIP).
Fixed samples were immersed in PBS containing 30% sucrose overnight, and then embedded in tissue freezing medium (Jung Leica, Nussloch, Germany) at -20°C. Cryosections at 10 µm were made with a cryostat (Leica, Heidelberg, Germany) and were transferred to poly-L-lysine-coated slides. After washing with PBS-Tween (PBST), slides were incubated with hybridization buffer (HyB) containing 60% formamide, 5 x SSC, and 0.1% Tween-20 H_2O for 5 min at 70°C. Prehybridization was performed in HyB^+, which is the hybridization buffer supplemented with 200 µg ml^{-1} yeast tRNA and 100 µg ml^{-1} heparin for 2 h at 57°C. After prehybridization, samples were incubated in the RNA probe diluted 1:2000 in HyB^+ at 57°C overnight for hybridization. Samples were then washed at 65°C for 10min in 100% HyB, 75% HyB and 25% 2xSSC, 10min in 50% HyB and 50% 2xSSC, 10min in 25% HyB and 75% 2xSSC, and twice for 30 min in 2xSSC and incubated at 65°C. Samples were washed twice for 10 min in PBST at room temperature. After serial washings, slides were incubated for 1h in pre-blocking solution containing 1% BSA and 20 % sheep serum diluted in PBST for 2h. Samples were then incubated in 1:2000 AP-conjugated anti-dig antibody in blocking solution overnight. Finally, staining reactions were conducted with NBT and BCIP in staining buffer (1M Tris, pH 9.5; 1M $MgCl_2$, 5M NaCl; 0.1 % Tween 20) (1:100) at 37°C until the signal was

sufficiently strong. The staining reaction was terminated by several washings methanol and slides were stored in PBS.

For immunocytochemical staining, mRNA probe hybridized slides were washed in PBS (pH 7.3) and treated according to the immunocytochemical protocol described in section 2.5.1..

2.5.3. Vital dye staining

Embryos were carefully removed from the egg capsule and incubated in the perivitelline fluid (PVF) for vital dye staining. A Na^+-dependent fluorescent reagent (Sodium Green tetra-acetate cell permeant; Invitrogen), was diluted in DMSO to a 10-mM stock solution. Sodium Green is well established as a reagent to detect intracellular Na^+ accumulation (Winslow et al. 2002; Esaki et al. 2007). Living stage 26-28 embryos were incubated in 10 µM Sodium Green diluted in 0.2 µm filtered natural SW for 40 min.

Mitochondrial-staining reagent, MitoTracker Green FM (Invitrogen, M-7514), was used to detect mitochondria rich cells on the skin of cephalopod embryos. For staining with MitoTracker, embryos were incubated for 30 min in 500 nM MitoTracker for 30 min. In double stains of Sodium Green and MitoTracker with concavalin A (Con A; a lectin protein capable of selectively binding α-mannopyranosyl and α-glucopyranosyl residues), embryos were first incubated in 10 µM Sodium Green or 500 nM MitoTracker for 40 min and subsequently transferred to a solution of 50 µg/ml of Alexa Fluor 594-conjugated ConA (Invitrogen) diluted in filtered seawater and incubated for 40 min.

Embryos were washed briefly with filtered seawater and anesthetized with 0.2-0.5% $MgCl_2$ which is a widely used non-toxic anaesthetic for cephalopods (Messenger et al. 1985). Pictures were taken using a fluorescent microscope (Imager M1, Zeiss). Sodium Green was excited by a mercury vapor light source through an excitation filter with maximum transmission at 485 nm and a 20-nm bandwidth. The fluorescence was collected using a 515 to 565 nm band-pass emission filter. We confirmed that the anaesthetic $MgCl_2$ did not affect illumination of Sodium Green and additionally performed negative controls with untreated embryos. Single focused images were created from a series of partially focused images using software from Helicon Focus (Helicon, Ukraine).

2.5.4. Scanning electron microscopy

For observations by electron microscope living squid embryos were removed from the egg capsule and immediately fixed in 4% paraformaldehyde with 5% glutaraldehyde diluted in PBS for 10 h. Afterwards the samples were transferred to a 0.1 M sodium cacodylate buffer solution (CACO) and washed three times. The membrane fixation was performed with 1% OsO_4 in 0.1M PB for 30 min under a fume hood. After fixation the samples were washed in 0.1 M sodium cacodylate buffer. For dehydration the samples passed an ascending concentration of ethanol (50%, 70%, 80%, 95% and 100%). The samples were dried in a critical point drier (Hitachi HCP-2 CPD), gold coated (Cressington Sputter Coater 108), and observed using a scanning electron microscope (ESEM, FEI Quanta 200).

2.6. Scanning ion-selective electrode technique

The scanning ion selective electrode technique (SIET) was used to measure H^+ fluxes at the surface of *Sepioteuthis lessoniana* embryos (stage 28). Glass capillary tubes (no. TW 150–4, World Precision Instruments, Sarasota, FL) were pulled on a Sutter P-97 Flaming Brown pipette puller (Sutter Instruments, San Rafael, CA) into micropipettes with tip diameters of 3-4 µm. These were then baked at 120°C overnight and vapor-sianized with dimethyl chlorosilane (Sigma- Aldrich) for 30 min. The micropipettes were backfilled with a 1 cm column of electrolytes and frontloaded with a 20 to 30 µm column of liquid ion exchanger cocktail (Sigma-Aldrich) to create an ionselective microelectrode (probe). The following ionophore cocktail (and electrolytes) was used: H^+ ionophore I cocktail B (40 mM KH_2PO_4 and 15 mM K_2HPO_4; pH 7). The details of the system were described in a previous report (Lin et al. 2006). To calibrate the ion-selective probe, the Nernstian property of each microelectrode was measured by placing the microelectrode in a series of standard solutions (pH 6, 7, and 8). By plotting the voltage output of the probe against log [H^+] values, a linear regression yielded a Nernstian slope of 58.6 ± 0.6 (n = 10) for H^+.

2.6.1. Measurement of surface H^+ gradients

The SIETwas performed at room temperature (26–28°C) in a small plastic recording chamber filled with 2 ml “recording medium” that contained 0.5 mM NaCl, 0.2 mM $CaSO_4$, 0.2 mM $MgSO_4$, 300 µM MOPS buffer, and 0.3 mg l^{-1} ethyl 3-aminobenzoate methanesulfonate

(Tricaine, Sigma-Aldrich). The pH of the recording media was adjusted to 7.0 by adding NaOH or HCl solutions. Before the measurement, embryos were slightly anaesthetized with 0.2–0.5% $MgCl_2$ which is a widely used non-toxic anaesthetic for cephalopods (Messenger et al. 1985) and positioned in the center of the chamber with its dorsal side contacting the base of the chamber. The ion-selective probe was moved to the target position (10–20 µm away from the larval surface) to record the ionic activities, then the probe was moved away (10 mm) to record the background. In this study, $[H^+]$ were used to represent the measured H^+ gradients between the targets (at the surface of larval skin) and background.

2.6.2. Measurement of apparent H^+ fluxes

An anesthetized embryo was laid dorsally in the chamber for SIET measurements. A "line-scan recording" was made by probing a series of spots along a line (with seven spots) across the lateral surface of the entire embryo. At every spot, the voltage difference in microvolts was measured by probing orthogonally to the surface at a 10 µm distance.

The calculation of ionic flux was performed analogous to previous reports (Smith et al. 1999; Donini and O´Donnell 2005; Shih et al. 2008). Voltage differences obtained from the ASET software were converted into a concentration (activity) gradient using the following equation:

$$\Delta C = C_b \text{ X } 10^{(\Delta V/S)} - C_b \qquad \text{(Eq. 2.2.)}$$

where ΔC (µmol l^{-1} cm^{-3}) is the concentration gradient between the two points, C_b (µmol l^{-1}) is the background ion concentration, ΔV (µV) is the voltage gradient obtained from ASET, and S is the Nernst slope of the electrode. The concentration gradient was subsequently converted into ionic flux using Fick's law of diffusion in the following equation:

$$J = D(\Delta C)/\Delta X \qquad \text{(Eq. 2.3.)}$$

where J (pmol cm^{-2} s^{-1}) is the net flux of the ion, D is the diffusion coefficient of the ion (9.37 X 10^{-5} cm^2 s^{-1} for H^+; ΔC (pmol l^{-1} cm^{-3}) is the concentration gradient; and ΔX (cm) is the distance between the two points.

When probing H^+ flux in a buffered medium, several reports adjusted the H^+ flux for the buffering capacity of the medium (Faszewski and Kunkel 2001; Donini and O´Donnell 2005). However, it is difficult to know the true buffering capacity, which is determined not only by additional buffers but also by other factors such as NH_3, CO_2, and HCO_3^- in the

medium. Therefore, we did not calculate the buffering capacity but present the data as "apparent H^+ flux" in this study.

3. Publications

List of publications and declaration of my contributions to them. All experiments were designed and conducted by myself, or with support of the coauthors. All manuscripts were written by myself, and revised together with the coauthors.

1. Marian Y. Hu, Yung-Che Tseng, Meike Stumpp, Magdalena A. Gutowska, Rainer Kiko, Magnus Lucassen, Frank Melzner (2011) *Elevated seawater pCO_2 differentially affects branchial acid-base transporters over the course of development in the cephalopod* Sepia officinalis. American Journal of Physiology, Regulatory, Integrative and Comparative Physiology (in press)

2. Marian Y. Hu, Yung-Che Tseng, Li-Yih Lin, Mireille Charmantier-Daures, Pung-Pung Hwang and Frank Melzner *New insights into ion regulation of cephalopod molluscs: a role of epidermal ionocytes in acid-base regulation during embryogenesis.* American Journal of Physiology, Regulatory, Integrative and Comparative Physiology (under review)

3. Marian Y. Hu, Elliott Sucré, Mireille Charmantier-Daures, Guy Charmantier, Magnus Lucassen, Nina Himmerkus and Frank Melzner (2010) *Localization of ion-regulatory epithelia in embryos and hatchlings of two cephalopods.* Cell and Tissue Research 339:571-583

Publication 1

Elevated seawater pCO_2 differentially affects branchial acid-base transporters over the course of development in the cephalopod *Sepia officinalis*

Elevated seawater pCO_2 differentially affects branchial acid-base transporters over the course of development in the cephalopod *Sepia officinalis*

Marian Y. Hu[1], Yung-Che Tseng[2], Meike Stumpp[1], Magdalena A. Gutowska[3], Rainer Kiko[1], Magnus Lucassen[4], Frank Melzner[1]

[1]Biological Oceanography, Leibniz-Institute of Marine Sciences (IFM-GEOMAR), Kiel 24105, Germany

[2]Institute of Cellular and Organismic Biology, Academia Sinica, Nankang, Taipei, Taiwan, Republic of China (ROC)

[3] Institute of Physiology, Christian-Albrechts-University, Kiel 24118, Germany

[4]Alfred Wegener Institute for Polar and Marine Research, Bremerhaven 27568, Germany

*To whom correspondence should be addressed:

e-Mail: mhu@ifm-geomar.de

tel: +49 (0)431-600 4275

fax: +49 (0)431-600 4446

Keywords: Acid-base regulation, Na^+/K^+-ATPase, SLC4 family, embryonic development, ocean acidification

Abstract

The specific transporters involved in maintenance of blood pH homeostasis in cephalopod molluscs have not been identified to date. Using *in situ* hybridization and immuno histochemical methods, we demonstrate that Na^+/K^+-ATPase (*soNKA*), a V-type-H^+-ATPase (*soV-HA*), and Na^+/HCO_3^- cotransporter (*soNBC*) are co-localized in NKA-rich cells in the gills of *Sepia officinalis*. mRNA expression patterns of these transporters and selected metabolic genes were examined in response to moderately elevated seawater pCO_2 (0.16 and 0.35 kPa) over a time-course of six weeks in different ontogenetic stages. The applied CO_2 concentrations are relevant for ocean acidification scenarios projected for the coming decades. We determined strong expression changes in late stage embryos and hatchlings, with one to three log2-fold reductions in *soNKA*, *soNBCe*, *socAII* and *COX*. In contrast, no hypercapnia induced changes in mRNA expression were observed in juveniles during both short- and long-term exposure. However a transiently increased demand of ion regulatory demand was evident during the initial acclimation reaction to elevated seawater pCO_2. Gill Na^+/K^+-ATPase activity and protein concentration were increased by approximately 15% in during short (2-11 day), but not long term (42 day) exposure. Our findings support the hypothesis that the energy budget of adult cephalopods is not significantly compromised during long-term exposure to moderate environmental hypercapnia. However, the down regulation of ion-regulatory and metabolic genes in late stage embryos, taken together with a significant reduction in somatic growth, indicates that cephalopod early life stages are challenged by elevated seawater pCO_2.

Introduction

Water breathing ectothermic animals maintain a diffusion gradient of CO_2 across respiratory epithelia in order to excrete this metabolic endproduct. Increases in seawater pCO_2 (hypercapnia) lead to an increased pCO_2 of body fluids in order to maintain the diffusive flux of CO_2 out of the animal (Melzner et al. 2009a). Environmental hypercapnia is a stressor that has lately received considerable attention: anthropogenic CO_2 emissions are expected to lead to increases in surface ocean pCO_2 from 0.04 kPa up to 0.14 kPa (ocean acidification) within this century (Caldeira and Wickett 2003). However, a high variability of abiotic factors is the rule in many coastal habitats already now (Hoppema 1993), and hypercapnia is a characteristic of many marine systems, e.g. in upwelling regions along the continental shelfs (Feely et al. 2008) and seasonally hypoxic systems (80). It can be expected that effects of ocean acidification will increase pCO_2 in a non-linear fashion in coastal CO_2 -enriched habitats, probably leading to pCO_2 values around 0.2-0.4 kPa within the next decades (Thomsen et al. 2010).

Physiological tolerance to elevated seawater pCO_2 is hypothesized to be connected to the ability of an organism to regulate extracellular acid-base status during exposure to hypercania, especially in organisms that rely on pH sensitive respiratory pigments (Pörtner et al. 2004). Accordingly, active marine ectotherms (i.e. teleosts, crustaceans, cephalopods) have been found to be the most tolerant to environmental hypercapnia as their high metabolic rates are supported by efficient acid-base regulation (Melzner et al. 2009b). This compensatory reaction has been studied in great detail in teleost fish (e.g. Toews et al. 1983; Claiborne and Heisler 1984; Claiborne and Evans 1992; Hyashi et al. 2004), where extracellular pH (pH_e) is fully compensated during hypercapnia by net accumulation of bicarbonate (HCO_3^-) via ion transporting cells of the gill epithelium. For example, in response to a pCO_2 of 1 kPa, cod *Gadus morhua* compensate extra cellular acidosis by actively increasing blood [HCO_3^-] from 10 to 30 mM accompanied by an equimolar reduction in plasma chloride concentrations (Toews et al. 1983; Larsen et al. 1997). Only decapod crustaceans have been shown to posses comparable acid-base regulatory abilities (Cameron and Iwama 1987; Pane and Barry 2007; Spicer et al. 2007). Recently, Gutowska et al. (2009) demonstrated that a cephalopod, *Sepia officinalis*, can also efficiently maintain high pH_e when exposed to hypercapnia (0.6 kPa) by increasing blood [HCO_3^-] from 3.4 to 10.4 mM.

However, the mechanisms that contribute to extracellular pH regulation in cephalopods are unexplored at present.

Acid-base regulating epithelia and organs have been extensively investigated in a number of marine fish species (Seidelin et al. 2001; Evans et al. 2005; Grosell 2006; Hwang and Lee 2007; Deigweiher et al. 2008; Melzner et al. 2009a). These studies proposed models of acid-base regulation in specialized, mitochondria-rich cells (MRC) localized in skin or gill epithelia. Besides the direct ATP dependent extrusion of protons via V-type-H^+-ATPases, these models suggest an import of bicarbonate and an export of protons by secondary active transporters, e.g. apical Na^+/H^+ exchangers (NHE) and Na^+ dependent Cl^-/HCO_3^- exchangers of the SLC4 solute transporter family that depend on the electro chemical gradient created by the Na^+/K^+-ATPase (NKA) located in basolateral membranes (Boron 2004; Evans et al. 2005; Perry and Gilmour 2006; Horng et al. 2007). In cephalopods, little is known on the specific transporters involved in branchial acid base regulation. Earlier studies have demonstrated that NKA also occurs in basolateral membranes of cephalopod gills with maximum activity levels comparable to those described for shallow water teleost fish (Schipp et al. 1979; Gibbs and Somero 1990; Turner et al. 2004; Hu et al. 2010a). In contrast to the fish gill, the gill of the decapod cephalopod *S. officinalis* (cuttlefish) is a highly folded epithelium consisting of two epithelial layers that line a blood sinus. The thin peripheral layer has been hypothesized to be primarily involved in respiration whereas the inner epithelium is responsible for ion regulation and, probably, nitrogen excretion (Schipp et al. 1979; Donaubauer 1981). Immunohistochemical and cytochemical findings suggest an analogy between cells of this inner epithelium and ionocytes of teleosts and their capacity for active ion transport (Schipp et al. 1979; Hu et al. 2010a). In this inner, mitochondria-rich epithelium, Schipp et al. (1979) demonstrated the presence of cytoplasmatic carbonic anhydrase (cCA), as well as several dehydrogenases (malate-, succinate-, and glucose-6-phosphate dehydrogenase) that are involved in aerobic metabolism. Furthermore, Schipp et al. (1979) described that the gill epithelium is not fully developed in late-stage embryos, with significant differentiation occurring post-hatching. This could imply that cuttlefish embryos and young hatchlings have significantly weaker ion regulatory capacities than juveniles or adults, especially if no alternative sites, such as skin integument or yolk epithelium cover these functions.

Yet, late-stage cephalopod embryos are exposed to stressful abiotic conditions inside the egg capsule: pO_2 can be as low as 5 kPa, pCO_2 can reach values of up to 0.4 kPa (Cronin and

Seymour 2000; Gutowska and Melzner 2009). This is due to the egg capsule wall acting as a diffusion barrier to dissolved gases. The transition phase from the hypoxic and hypercapnic environment of the egg fluid to seawater is an extraordinary event in the life history of cephalopods. Not only do abiotic conditions dramatically change, but the metabolic rates of the hatchlings also steeply increases (e.g. Cronin and Seymour 2000). Both significantly challenge the maintenance of acid-base homeostasis and require potent acid-base regulatory machinery.

This is the first study to examine mechanisms of hypercapnia induced acid-base regulation in cephalopods on the molecular level. In a first step we used information on acid-base regulation in fish as a guide in order to clone putative acid-base regulation genes of the cuttlefish gill, encoding for Na^+/K^+-ATPase (so*NKA*), cytoplasmatic carbonic anhydrase (soc*CAII*), V-type-H^+-ATPase (*soV-HA*) and two bicarbonate transporters, electrogenic Na^+/HCO_3^- cotransporter (*soNBCe*) and Na^+ dependent Cl^-/HCO_3^- exchanger (*soNDCBE*). We then studied transcriptional responses of acid-base and selected metabolic genes (soNKA, soCAII, soNBCe, soNDCBE, ATP-synthase, octopine dehydrogenase, cytochrome-c-oxydase and cytochrome-P450) in different life stages of the cuttlefish *S. officinalis*. We hypothesized that in response to hypercapnia, acid-base regulatory gene candidate transcripts would show specific up regulations in order to support an increased demand of the acid-base regulating machinery and that the elevated metabolic requirements for acid-base regulation would be reflected in an upregulation of marker genes for key metabolic pathways. Functional capacities of Na^+/K^+-ATPase were determined as this enzyme is believed to be the major driving force for most energy-dependent ion transport. We further hypothesized that increases in environmental pCO_2 as projected by ocean acidification scenarios must be additive to the pCO_2 inside the egg in order to maintain a sufficient diffusion gradient of CO_2 from the egg to the seawater. This extreme egg environment and the incompletely developed ion regulatory epithelia of embryos would then lead to a higher sensitivity of embryonic life stages towards acid-base disturbances.

Material and Methods

Experimental Animals

Sepia officinalis egg clusters were collected in Zeeland, Netherlands, in May 2008 and 2009 and transported to the Leibniz-Institute of Marine Sciences (IFM-GEOMAR), Kiel, at stage 17-20 (stages according to Lemaire (1970)). After hatch, cuttlefish were raised in a closed recirculating system (1200 l total volume, protein skimmer, nitrification filter, UV disinfection unit, salinity 31-32, NH_4^+ <0.1 mg L^{-1}, NO_2^- <0.1 mg L^{-1}, NO_3^- <10 mg L^{-1}, temperature 15°C and constant 12 h dark 12 h light cycle). Cuttlefish hatchlings were initially fed with live mysids and progressively transitioned to feed on *Paleamonetes varians.* The animals showed normal development and behavior.

CO_2 Pertubation Experiments

Experiment 1: embryos and hatchlings

Sepia officinalis egg clusters and *Loligo vulgaris* egg masses were collected in May 2009. 25 to 30 individual eggs containing embryos (stage 17-18 (60)) were incubated in nine PVC aquaria (25 L volume) inside a 15 °C climate chamber for eight weeks. The aquaria were continuously equilibrated with the appropriate gas mixtures (0.04 kPa, 0.14 kPa and 0.4 kPa CO_2 in pressurized air) supplied by a central automatic gas mixing-facility (Linde Gas, HTK Hamburg, Germany). The nine tanks, with three replicate tanks for each treatment were randomly distributed in a water bath. A light regime with a 12 h : 12 h light/dark-cycle was chosen. Artificial seawater (SEEQUASAL, Münster, Germany) was prepared in three 400 L reservoir tanks and pre equilibrated with the respective pCO_2. Two thirds of the water in the experimental tanks was exchanged daily with CO_2 pre-equilibrated water from the reservoir tanks to maintain high water quality within the system. For sampling of gill tissues, late stage embryos (stage 30 (Lemaire 1970)) and hatchlings (2 days post hatching) were dissected by opening of the ventral mantle cavity. The two gills, which were approximately 1.5 mm in length, were quickly dissected with two sharp forceps, shock-frozen in liquid nitrogen, and stored at -80°C for gene expression analysis.

Determination of perivitelline fluid (PVF) abiotic parameters

At the final stage of development (stage 30 (Lemaire 1970)) eggs were carefully lifted out of the water and the PVF immediately sampled from the egg using a syringe. A pH electrode (WTW Mic and pH340i pH meter, WTW, Weilheim, Germany), calibrated with seawater AMP and TRIS buffers (Dickson et al. 2007), was used to measure PVF pH in 0.5 mL Eppendorf tubes. Another 500 µL of PVF was sampled with a gas-tight glass syringe for the determination of total dissolved inorganic carbon (C_T). C_T was measured in triplicate (100 µL each) using a Corning 965 carbon dioxide analyzer (Olympic Analytical Service (OAS), Malvern, U.K.). The carbonate system speciation was calculated from C_T and pH_{NBS} with the CO2SYS software and using the dissociation constants of Mehrbach et al. (1973) as refitted by Dickson & Millero (1987). During the measurement period for pH and pO_2, the PVF sample and sensors were placed in a thermostatted water bath at 15°C. The oxygen optode was calibrated according to the manufacturer's instructions with water vapor saturated air and a Na_2SO_3 solution. Following PVF sampling, eggs were dissected and biometric parameters were determined. Body dimensions, including dorsal mantle length (DML) and body mass (BM) were determined using a Leica MZ95 stereo microscope equipped with a CCD camera and using Image-Pro Plus software (Media Cybernetics, Bethesda, USA). Animal wet mass was determined using a precision balance (Sartorius TE64). In total, 15 eggs were sampled for each treatment.

Experiment 2: juveniles

48 *Sepia officinalis* specimen (dorsal mantle length (DML) 3-4 cm) were maintained in a flow through seawater system consisting of 16 PVC aquaria (25 L volume) in a 15 °C climate chamber at the IFM-GEOMAR, Kiel. A light regime with a 12 h : 12 h light/dark-cycle was chosen. Artificial seawater was prepared daily in a 400 L reservoir tank. From this reservoir tank the water passed through a 12 W UV sterilizer before being distributed to the experimental aquaria via gravity feed at a rate of 20 mL min^{-1}. Before the start of the experiments the animals were maintained under control conditions for 14 days. The experimental tanks contained three individuals. Tanks were continuously equilibrated with the appropriate gas mixture (0.3 kPa CO_2) supplied by the central automatic gas mixing-facility or pressurize air (0.04 kPa), and randomly arranged with respect to CO_2 level.

Throughout the duration of the experiment, cuttlefish were fed daily with one live *P. varians* each (approximately 10-15% of cuttlefish body mass). It needs to be noted that juveniles were not fed *ad libitum* but food supply was high enough to produce growth rates of 1.5% per day, which relate to maximum growth rates of 4% observed for animals of comparable size and at the same temperature (e.g. Forsythe et al. 2002; Grigoriou and Richardson 2004). Tissue samples were taken 2 days, 11 days and 42 days after the start of the experiment. At each time point, eight specimen from each treatment (total of 16 animals, one from each of n = 8 replicate aquaria) were anaesthetized in 2.5% EtOH in seawater for ca. 2-3 minutes. Afterwards the animals were sacrificed by decapitation and the mantle cavity was opened on the ventral side. The gills were immediately dissected using micro scissors and forceps. The tip of the left gill was fixed with 4% paraformaldehyde (PFA) in seawater at 4°C overnight, and then washed several times with phosphate-buffered saline (PBS). These gills were stored in 100% MeOH at -80°C for *in situ* hybridization. The remaining right and the left gill were quickly shock-frozen in liquid nitrogen and stored at -80°C for enzyme assays and gene expression analysis. The investigations comply with the German animal welfare principles No. V 31 and the animal use protocols were approved by the animal care committee of the Christian-Albrechts-University, Kiel.

Determination of seawater abiotic parameters

Specific seawater conditions for the various incubations are given in Table 1. Temperature, pH (NBS scale) and salinity were determined daily. pH_{NBS} was measured with a WTW 340i meter and WTW SenTix 81 electrode calibrated daily with Radiometer IUPAC precision pH_{NBS} buffers 7.00 and 10.00 (S11M44, S11 M007). Additionally, water ammonia concentrations were determined every two to three days and levels were maintained <0.3 mg L^{-1}.
Total dissolved inorganic carbon (C_T) was measured coulometrically according to Dickson et al. (Dickson et al. 2007) using a SOMMA (Single-Operator Multi-Metabolic Analyzer) auto analyzer (Marianda, Kiel, Germany). Total alkalinity (A_T) was determined by using the methods of Dickson et al. (Dickson et al. 2007) by means of a potentiometric open-cell titration with hydrochloric acid. The measurement was performed using a VINDTA (Versatile Instrument for the Determination of Titration Alkalinity) auto analyzer (Marianda, Kiel, Germany). As reference material for both types of analysis (C_T as well as A_T) certified

reference material was used (Dickson et al. 2003). Seawater carbonate chemistry speciation was calculated from C_T and A_T with the software CO2SYS (Lewis and Wallace 1998) using the dissociation constants of Mehrbach et al. (1973) as refitted by Dickson & Millero (1987).

Cloning of soNKA, soNBCe, soNDCBE, socCAII and soV-AH Fragments

Fragments of the *Sepia* Na^+/K^+-ATPase (*NKA*), Na^+/HCO_3^- co-transporter (*NBC*), Na^+-dependent Cl^-/HCO_3^- exchanger (*NDCBE*), cytoplasmatic carbonic anhydrase (*CA*) and V-type-ATPase (*V-HA*) genes were isolated from gill tissue by means of reverse transcription followed by PCR (RT–PCR). Degenerate primers were designed using Mac-Vector® 10.0.2 (Symantec Corporation) software, using highly conserved regions of sequences of cephalopods, bivalves and fish obtained from GenBank. Reverse transcription was performed with Superscript RT (Invitrogen, Karlsruhe, Germany) and gene specific primers according to the manufacturer's instructions with mRNA as templates (see next section for RNA extraction protocol). In the following PCR, primer pair 5´-AAGTCGTGCCAATGTGTTGTA-3´ and 5´-TACTTYCCACGWGGACTTTCTTAG-3´ resulted in a 268 bp fragment of the *NKA* (GQ153672.1), the primer pair 5´-GCGGAAGGAGGTGTAGAAGAAGT-3´ and 5´-CATAGTCHAGTGTCGTAAGTAGGC-3´ resulted in a 582 bp fragment of *NBC* (bankit1344341), the primer pair 5´-GCCAGRTGGATWAAGTTTGA-3´ and 5´-GGTWGGSACRGGRACCTCTG-3´ resulted in a 693 bp fragment of the *NDCBE* (bankit1344354), the primer pair 5´-CTACARYTAYCCYCTRACCGC-3´ and 5´-AAAGTRAARGTGACCCCKAG-3´ resulted in a 215 bp fragment of cytosolic *CAII* (bankit1344380) and the primer pair 5´-GARTAYTTYMGNGAYATGGGN -3´ and 5´- RTTYTGYTGNARRAARTCRTCYTT -3´ resulted in a 556 bp fragment of *VHA* subunit a (bankit1370003). The sequences obtained for cytosolic CAII and NBCe of cuttlefish show high similarities when compared to teleosts and mammals (supplementary figure 2S).

cDNA was amplified using Taq-Polymerase (Invitrogen, Karlsruhe, Germany) in the presence of 1.5 mM $MgCl_2$ (PCR conditions: 4 min denaturation at 94 °C, 45 sec annealing at 53 °C and 45 sec elongation at 72 °C, 35 cycles followed by a final amplification step of 8 min at 72 °C). PCR fragments were separated after electrophoresis in 1% agarose gels. Extraction and purification of the PCR fragments from the gel was accomplished using the QIAquick® gel extraction kit (QIAGEN, Hilden, Germany). Cloning and isolation of plasmids was performed

using the pGEM®-T Easy Vector Systems and JM 109 competent *E. coli* cells (Promega, Madison, WI, USA). Plasmids were extracted using the Qiaprep Spin Miniprep Kit (QIAGEN, Hilden, Germany) and sequenced by the sequencing platform of the Institute for Clinical Molecular Biology (IKMB), Christian-Albrechts- University of Kiel (Kiel, Germany).

Real-Time Quantitative PCR (qRT-PCR)

For RNA extraction, whole gills from embryos, hatchlings and juveniles were homogenized under liquid nitrogen, using pestle and mortar. 25 mg homogenates were used for further extraction. RNA extraction was performed according to the manufacturer's instructions with an additional cleaning step using the QIAshredder column (Qiagen, Hilden, Germany) performed after homogenization in RLT-buffer. RNA was eluted and stored in 100 µL RNase-free water at -80°C. DNA contaminations were removed by DNase digestion with the DNA-free kit (Applied Biosystems, Darmstadt, Germany). Concentration and integrity of the isolated RNA was determined photometrically using a NanoDrop ND-1000 spectrophotometer (PeqlabEQLAB, Erlangen, Germany) and via electrophoresis using the Experion electrophoresis system (Bio-Rad, Munich, Germany).

Primers for qRT-PCR were designed using the primer analysis software Primer Express v. 2.0 (Applied Biosystems) with the default parameters of the TaqMan MGB Probe and Primer design procedure. We selected PCR amplicons to range from 50 to 100 bp in size. Selected genes and primer sequences are given in Table 2. ATP-Synthase, cytochrome p450, ubiquitin-conjugated enzyme and cleavage and polyadenylation specificity factor sequences were obtained from a *S. officinalis* gill cDNA library (Melzner, Kiko, Lucassen, unpublished).. qRT-PCR was performed on an ABI StepOne plus Sequence Detection System (Applied Biosystems) using the Power SYBR Green QPCR Master Mix (Applied Biosystems). The PCR reaction consisted of 10 µL SYBR green PCR master mix, 3 µL (2 pmol μL^{-1}) forward and reverse primers, 2.0 µL 1:10-diluted template cDNA and 2.0 µL water in a total reaction volume of 20 µL. Thermocycling was performed using the following conditions: 10 min at 95°C, 45 cycles of 15 s at 95°C, and 1 min at 62°C. Melting curve analysis demonstrated a single PCR amplicon for each reaction. Data were recorded as fractional cycle at an arbitrary C_T-value in triplicate during the exponential phase of the reaction. To determine the amplification efficiency of each primer pair, a standard curve of 4 serial dilution points (in

steps of 2-fold) of a cDNA mixture was analyzed using linear regression. The amplification efficiency of an individual reaction was determined using the ABI StepOne plus Sequence Detection System. PCR efficiencies of investigated genes ranged from 1.84 to 2.0.

NormFinder, a Microsoft Excel add-in (available at http://www.mdl.dk/publicationsnormfinder.htm) was used to identify housekeeping gene candidates. The genes cleavage and polyadenylation specificity factor (*CPSF*) and ubiquitin conjugated protein (*UBC*) were identified as the best housekeeping genes between treatments and incubation times. For the normalization factor (NF_n) the geometric mean of the best fitting housekeepers (REF_{1-n}) was calculated.

Na^+/K^+-ATPase Activity Assay

Na^+/K^+-ATPase activity was measured in gill tissue crude extracts of juvenile specimens in a coupled enzyme assay with pyruvate kinase (PK) and lactate dehydrogenase (LDH) using the method of Allen and Schwarz (Schwartz et al. 1969) as described by Melzner et al. (2009a). Crude extracts were obtained by quickly homogenizing the tissue samples in a conical tissue grinder in 10 volumes of ice-cold buffer (50mM imidazole, pH 7.8, 250 mM sucrose, 1 mM EDTA, 5 mM β-mercaptoethanol, 0.1% (w/v) deoxycholate, proteinase inhibitor cocktail from Sigma-Aldrich (Taufkirchen, Germany, Cat. No. P8340)) followed by Ultra Turrax treatment (3 x 5s) on ice. Cell debris was removed by centrifugation for 10 min at 1000g and 4°C. The supernatant was used as crude extract. The reaction was started by adding 10 µl of the sample homogenate to the reaction buffer containing 100 mM imidazole, pH 7.8, 80 mM NaCl, 20 mM KCl, 5 mM $MgCl_2$, 5 mM ATP, 0.24 mM Na-($NADH_2$), 2 mM phosphoenolpyruvate, about 12 U mL^{-1} PK and 17 U mL^{-1} LDH, using a PK/LDH enzyme mix (Sigma-Aldrich). The oxidation of NADH coupled to the hydrolysis of ATP was followed photometrically at 15°C in a DU 650 spectrophotometer (Beckman Coulter, USA) over a period of 10 min, measuring the decrease of extinction at λ = 339 nm. The fraction of Na^+/K^+-ATPase activity in total ATPase activity was determined by the addition of 17 µL of 5 mM ouabain to the assay. Each sample (n = 8) was measured in sextuple. Enzyme activity was calculated using an extinction coefficient for NADH of ε = 6.31 $mM^{-1} \cdot cm^{-1}$ and given as µmol ATP g^{-1} h^{-1}.

Immunoblotting

For immunoblotting, 20 µL of crude extracts from the Na^+/K^+-ATPase activity measurement were used. Proteins were fractionated by SDS-PAGE on 10% polyacrylamide gels, according to Lämmli (1970), and transferred to PVDF membranes (Bio-Rad, Munich, Germany), using a tank blotting system (Bio-Rad). Blots were pre-incubated for 1 h at room temperature in TBS-Tween buffer (TBS-T, 50 mM Tris -HCl, pH 7.4, 0.9% (wt/vol) NaCl, 0.1% (vol/vol) Tween20) containing 5% (wt/vol) nonfat skimmed milk powder. The primary antibody for the Na^+/K^+-ATPase was the polyclonal antibody α (H-300) (Santa Cruz Biotechnology, Heidelberg, Germany) specific to the *S. officinalis* α-subunit of the Na^+/K^+-ATPase (Hu et al. 2010a). Blots were incubated with primary antibodies with a concentration of 2 µg mL^{-1} at 4°C overnight. After washing with TBS-T, blots were incubated for 1 h with horseradish conjugated goat anti-rabbit IgG antibody (Santa Cruz Biotechnology, INC.) diluted 1:2000 in TBS-T containing 5% non-fat skimmed milk powder. Protein signals were visualized by using the ECL Western Blotting Detection Reagents (GE Healthcare, Munich, Germany) and recorded using a LAS-1000 CCD camera (Fuji, Tokyo, Japan). Signal intensity was calculated using the AIDA Image Analyzer software (ver. 3.52, Raytest, Straubenhardt, Germany).

In situ hybridization

Isolated plasmids from the generated clones were used for the synthesis of antisense and sense RNA probes. Following PCR with T7 and SP6 primers, the products were subjected to *in vitro* transcription with T7 or SP6 RNA polymerase (Roche, Penzberg, Germany), in the presence of digoxigenin (dig)-UTP. Dig-labeled RNA probes were examined with RNA gels and dot-blot assays to confirm quality and concentration. For dot-blot assays, synthesized probes and standard RNA probes were spotted on nitrocellulose membrane according to the manufacturer's instructions. After cross-linking and blocking, the membrane was incubated with an alkaline phosphatase (AP)-conjugated anti-dig antibody and stained with nitro blue tetrazolium (NBT) and 5-bromo-4-chloro-3-indolyl phosphate (BCIP). Fixed samples were immersed in PBS containing 30% sucrose overnight, and then embedded in tissue freezing medium (Jung Leica, Nussloch, Germany) at -20°C. 10 µm thick cryosections were generated with a cryotome (Leica, Heidelberg, Germany) and were transferred onto poly-L-lysine-coated slides. After washing with PBS-Tween (PBST; 0.1% Tween in phosphate buffered

saline), slides were incubated with hybridization buffer (HyB) containing 60% formamide, 5 x saline sodium citrate buffer (SSC), and 0.1% Tween-20 in H_2O for 5 min at 70°C. Pre - hybridization was performed in HyB^+, which is the hybridization buffer supplemented with 200 µg mL^{-1} yeast tRNA and 100 µg mL^{-1} heparin for 2 h at 57°C. Following pre - hybridization, samples were incubated with the RNA probe diluted 1:2000 in HyB^+ at 57°C overnight for hybridization. Samples were then washed at 65°C for 10 min in 100% HyB, 75% HyB and 25% 2xSSC, 10 min in 50% HyB and 50% 2xSSC, 10 min in 25% HyB and 75% 2xSSC, and twice for 30 min in 2xSSC and incubated at 65°C. Samples were washed twice for 10 min in PBST at room temperature. After serial washings, slides were incubated for 1h in pre-blocking solution containing 1% BSA and 20 % sheep serum diluted in PBST for 2h. Samples were then incubated in 1:2000 AP-conjugated anti-dig antibody in blocking solution overnight. Finally, samples were washed with PBST and staining reactions were conducted with NBT and BCIP in staining buffer (1M Tris, pH 9.5; 1M $MgCl_2$, 5M NaCl; 0.1 % Tween 20) (1:100) at 37°C until the signal was sufficiently strong. The staining reaction was terminated by several (2-3) washings with methanol and slides were stored in PBS for further immunohistochemical stanings.

For immunocytochemical staining, mRNA probe hybridized slides were washed in PBS (pH 7.3) and exposed to a heat shock inside the PBS bath using a microwave (600 Watts for 2x3 min). Afterwards, samples were transferred to a PBS bath containing 150 mM NaCl and Tween 20 (conc. 0.2 µL mL^{-1}) for ten minutes, and a PBS bath containing 5% skimmed milk for 20 min to block non-specific bindings. The primary antibody, a rabbit polyclonal antibody raised against an internal region of Na^+/K^+-ATPase α1 of human origin (Na^+/K^+180 -ATPase α (H-300), Santa Cruz Biotechnology, Heidelberg, Germany) was diluted in PBS to 10 µg mL^{-1}, placed in small droplets of 100 µL on the sections, and incubated for 2 h at room temperature in a wet chamber. To remove unbound antibody, the sections were then washed (3x5 min) in PBS and incubated for 1 h with small droplets (100 µL) of secondary antibody, FITC -labeled goat anti rabbit IgG (Santa Cruz Biotechnology, Heidelberg, Germany). After rinsing in PBS (3x5 min), sections were covered with a mounting medium and examined with a fluorescence microscope (Zeiss, Axio SCOPE. A1, Hamburg, Germany) with an appropriate filter set (488 nm band-pass excitation filter). Bright field and fluorescence images were aquired from *in situ* hybridized and immuno-histochemically stained sections and merged using Adobe® Photoshop® CS2.

Statistical analysis

Values are presented as means ± SE and compared using Student's *t*-test or one-way ANOVA followed by Tukey's Posthoc tests using Sigma Stat 10.0 (Systat Software INC.). Statistical analysis of qRT-PCR results was performed on mRNA quantities normalized to the geometric mean of the housekeeping genes *CPSF* and *UBC*.

Results

Growth and Perivitelline Fluid (PVF) Abiotic Conditions

At the time point of PVF and gill sampling for quantitative real-time PCR all *Sepia officinalis* eggs contained viable embryos (stage 30, (Lemaire 1970)) with fresh masses (FM) of 169.4 mg ± 8.8 mg (control, n = 15) and 161.9 ± 4.8 mg (0.37 kPa, n = 15) (Fig. 1A). All animals appeared normally developed and organogenesis was complete. The DML of *S. officinalis* late-stage embryos was significantly different between control (6.91 ± 0.19 mm) and 0.37 kPa CO_2 treated animals (6.33 ± 0.17 mm). Hatchlings (two days post - hatch) were characterized by a significantly reduced body mass of 13% and a reduced DML by 40% in response to 0.37 kPa (Fig 1B). Intermediate hypercapnia (0.16 kPa) did not cause growth delays in embryos and hatchlings. Juvenile growth rates were not significantly influenced during exposure to 0.37 kPa CO_2. Juvenile cuttlefish had an initial mass of 11.90 ± 2 g, and grew at rate of 0.13 ± 0.02 g d^{-1} under control and 0.20 ± 0.05 g d^{-1} under high CO_2 conditions, increasing body mass by approximately 50% during the 42 day trial.

The PVF was characterized by average pH values of 7.4 and a mean pCO_2 of 0.26 kPa under control conditions (Fig 2A, B). Under hypercapnia, PVF pH significantly decreased to 7.2 (seawater pCO_2: 0.16 kPa) and 7.0 (seawater pCO_2: 0.37 kPa). Hypercapnia led to additive increases in PVF pCO_2. This resulted in a PVF pCO_2 of 0.45 kPa and of 0.78 kPa when exposed to seawater pCO_2 of 0.16 kPa and 0.37 kPa, respectively. Thus, CO_2 diffusion gradients were maintained even under relatively high seawater pCO_2, suggesting maintained rates of metabolic CO_2 excretion.

Real-Time Quantitative-PCR

In late stage embryos and hatchlings, reduced somatic growth is accompanied with changes in mRNA expression of several genes. In gill tissues of late stage embryos (Fig. 3A) significant 0.8 to 2.1 log2-fold (40% to 75%) down regulation was observed in response to 0.37 kPa CO_2 for the transcripts of ion transporting proteins so*NKA*, so*NBCe* and soc*CAII.* so*NDCBE* showed no CO_2-dependent change in expression. At the intermediate pCO_2 of 0.16 kPa only two significant changes were observed in embryos: *NBCe* was 1.2 log2-fold down regulated and c*CAII* was up-regulated (0.5 log2-fold). In hatchlings (Fig. 3B), a similar general expression pattern was observed with strong down regulation (up to 3.0 log2-fold; 85%) of all acid-base regulatory candidate genes (e.g. *NKA*, *NBCe* and c*CAII*) in response to 0.37 kPa CO_2. In addition, ATP-synthase, cytochrome-c-oxidase subunit 1 (*COX*) and cytochrome P-450 (*CYP-450*) were significantly down regulated in hatchlings. At the intermediate pCO_2 of 0.16 kPa only two significant changes were observed: *NBCe* was 0.6 log2-fold down regulated and *COX* was 0.3 log2-fold up-regulated.

In juveniles, mRNA expression of all genes tested did not significantly differ between treatments after 2, 11 and 42 days of hypercapnia (Fig 3C and Fig. 4). Although no differences between CO_2 treatments were measured, a significant increase in expression has been observed with time for several genes. For example so*NKA* was 0.11 log2-fold (+12.93%), so*NBCe* 0.23 log2-fold (+29.53%), soc*CAII* 0.25 log2-fold (+33.64%) and *ODH* was 0.2 log2-fold (+25.39%) up regulated (Fig. 4). All genes related to ion-transport showed a significant increase in expression over the course of the experimental period.

Gill NKA activity and protein

Na^+/K^+-ATPase (NKA) maximum activities in gill tissues of juvenile cuttlefish steadily declined over the time course of the hypercapnia trial in the control and the CO_2 treatment (Fig. 5A). NKA maximum activity differed significantly between treatments after 48 h incubation with 94.8 ± 18.5 $\mu mol_{ATP}\ g_{FM}^{-1}\ h^{-1}$ at control pCO_2 and 112.5 ± 13.7 $\mu mol_{ATP}\ g_{FM}^{-1}\ h^{-1}$ at a seawater pCO_2 0.3 kPa. From 48 h to 11 days, maximum activity was significantly increased by ca. 15%

in CO_2 treated animals. At 42 days of incubation, no significant difference between control and CO_2 treated animals was observed.

NKA protein concentrations were determined by immunoblotting (Fig. 5B). Besides the strong immunoreactivity of a 100 kDa protein, further weaker bands were visible which may be explained by unspecific binding of the polyclonal antibody used (see supplemental Fig. 1S). NKA protein tended to follow the patterns of the activity measurements at least for the time points of 48 h and 11 days, with increases of 16% and 34%, respectively. Similar, significantly higher protein levels were found after 11 days, whereas long-term acclimated hypercapnic juveniles displayed the same NKA protein content as the controls. After 42 days, NKA protein concentrations increased by 30-40%, matching the increased *NKA* mRNA expression by 20-25% at this time point. However, no transcriptional response was detected for soNKA, during both short- and long-term exposure to elevated seawater pCO_2 (Fig. 5C).

Localization of ion transporters in gill tissues

To identify the cell types that specifically express *soNKA*, *soNBCe* and *soV-AH* mRNA, *in vitro* synthesized RNA probes were used to detect mRNA of these proteins in cryosections of gills of *S. officinalis* juveniles. Subsequent immunocytochemical labeling with an anti- Na^+/K^+-ATPase α subunit antibody was carried out (Fig. 6, 7B).

In gill tissues of *S. officinalis* the *NKA* mRNA was predominantly expressed in the concave part (third order lamellae) of the transport active epithelium of the entire second order lamellae (Fig. 6A, 7A). The cells of this transport active epithelium are higher and more voluminous compared to those of the outer respiratory epithelium (Fig. 6A). Furthermore, the localization of NKA by immunocytochemistry demonstrates *NKA* transcript and protein to be co-localized in ionocytes of the inner epithelium (Fig. 6A). The concentration of the enzyme was high in basolateral regions (close to the blood sinus) (Fig. 6A, B, C). Furthermore, so*NBCe* (Fig. 6B) and *soV-HA* (Fig. 6C) transcripts were also detected in cells of the inner transport active epithelium of third order gill lamellae. Merged images of NKA immunocytochemistry and *in situ* hybridization demonstrate that NKA protein and mRNA, *soNBCe* mRNA and *soV-HA* mRNA are co - localized in ion transporting cells of the inner epithelium of the third order gill lamellae.

Discussion

Effects of moderate hypercapnic stress on marine organisms recently moved into the focus of research due to rising atmospheric CO_2 levels in the atmosphere, which lead to an acidification of the oceans (Pörtner et al. 2004; Fabry et al. 2008; Melzner et al. 2009b). The present study investigated responses to environmental hypercapnia in different life stages of the cephalopod *Sepia officinalis*. On the organismic level, we observed reduced somatic growth under 0.37 kPa CO_2 in early developmental stages. On the protein level, the characterization of Na^+/K^+-ATPase in juveniles revealed an increased activity and protein concentration under elevated seawater pCO_2 (ca. 0.3 kPa) during short-term incubation. In order to address the response of the acid-base regulating machinery, we cloned genes that may play a key role in pH_e compensation under hypercapnic conditions, such as so*NKA*, so*NBCe*, so*NDCBE*, soc*CAII* and so*V-HA*. Dynamic changes in gene expression could be observed in late stage embryos and hatchlings, but no CO_2-related expression responses were observed in juveniles during short- and long-term incubation. Finally, immunohistology and *in situ* hybridization showed for the first time, that gills of cephalopods exhibit specialized cells in the inner, transport active epithelium that express so*NKA*, so*NBCe* and so*V-HA*.

Growth and perivitelline fluid (PVF) abiotic conditions

As adult fish (Fivelstad et al. 2003; Foss et al. 2003), juvenile cephalopods can tolerate high seawater pCO_2 of up to 0.6 kPa over long exposure times without suffering from decreased growth and calcification (Gutowska et al. 2008). However, the present study demonstrates that even if juveniles or adults tolerate high pCO_2, early life stages are more susceptible towards environmental hypercapnia. Hypercapnia induced reductions in larval and embryonic growth have also been observed in several other invertebrate species such as copepods, echinoderms, and bivalves (Kurihara et al. 2004; Kurihara and Shirayama 2004; Kurihara et al. 2007; Dupont et al. 2008; Dupont and Thorndyke 2009; Dupont et al. 2010).

The increased sensitivity of cephalopod early life stages could be due to two primary reasons. The first is related to gill development: similar to the situation in fish and decapod

crustaceans, the cephalopod gill is the most important site for ion-regulatory processes (Schipp et al. 1979; Hu et al. 2010a). During larval development, rudimentary gill structures occur at stage 20, and significantly differentiate over the course of embryonic development as well as after hatching (Arnold 1965; Schipp et al. 1979). Schipp et al. (1979) demonstrated that the cephalopod gill changes morphogenetically within several days after hatching to become a highly folded epithelium with a high density of vesicles, mitochondria and a high concentration of cCA and NKA. This differentiation indicates that gas exchange and ion regulatory capacity might be fully activated only after leaving the protective egg capsule. This could partially explain the higher susceptibility of embryonic stages to environmental hypercapnia.

Furthermore, the abiotic conditions in the perivitelline fluid (PVF) are directly influenced by the pCO_2 of the surrounding seawater (Fig. 2). Cephalopod embryos are exposed to very low pO_2 values (<6 kPa, ca. 28% air saturation) during the final phase of embryonic development. This is due to increasing metabolic rates and the egg casing acting as a diffusion barrier for dissolved gases (Cronin and Seymour 2000). On the flip side, this diffusion limitation not only decreases pO_2 inside the egg, but also results in PVF pCO_2 values >0.3 kPa and pH values <7.5 under control conditions (Gutowska and Melzner 2009). The present results indicate that environmental pCO_2 is additive to the natural accumulation of CO_2 in the perivitelline fluid (PVF) leading to very high PVF pCO_2 of up to 0.5 and 0.7 kPa inside the egg at a seawater pCO_2 of 0.16 or 0.37 kPa, respectively. This almost linear increase of PVF pCO_2 is necessary in order to conserve the CO_2 diffusion gradient across the egg capsule that drives excretion of metabolic CO_2 to the seawater. Thus, alterations in environmental pCO_2 create a greater challenge to the developing embryo in comparison to juveniles or adults. This is particularly striking, as cephalopod blood pCO_2 typically is 0.2-0.3 kPa higher than that of the surrounding medium (Pörtner et al. 1991; Gutowska et al. 2009). It is therefore reasonable to expect a blood pCO_2 in the 0.7-1.0 kPa range in the hypercapnic embryos of this study. These conditions may lead to metabolic depression, which has been suggested to be elicitated by extracellular acidosis in some marine invertebrates (73). However, adult cuttlefish have been shown to be able to accumulate millimolar concentrations of HCO_3^- in their blood in response to hypercapnia in order to stabilize pH_e (see below, Gutowska et al. 2009). If embryonic *S. officinalis* also respond with a similar pH_e compensatory reaction with respect to the high extracellular pCO_2 encountered during hypercapnia, this may represent a

severe energetic challenge and could result in a higher fraction of aerobic scope spent on acid-base regulation. Both, a (potential) hypercapnia induced metabolic depression and increased energy allocation towards ion regulatory processes would most likely have negative repercussions on embryonic growth. Future studies need to determine the extracellular acid-base regulatory capacity of embryonic cephalopods.

Gene Expression

Gene expression profiles revealed strong differences between early developmental stages (late embryos and hatchlings) compared to six month old juveniles. In late embryos and hatchlings exposed to 0.37 kPa CO_2 for 5 weeks, reduced somatic growth is accompanied by changes in the expression of several genes which are involved in ion regulatory (e.g. so*NKA*, so*NBCe*, soc*CAII*) and metabolic (e.g. *ATP-synthas*e, *COX, CYP450*) processes. Intriguingly, mRNA of all acid-base regulation gene candidates (so*NKA*, so*NBCe* and soc*CAII*), were down regulated by up to 80% in response to elevated seawater pCO_2.

The significant down regulation of the gene candidates is also likely causally linked to a developmental delay in the embryos. Large differences in mRNA expression profiles have been attributed to a hypercapnia induced developmental delay in sea urchin larvae (e.g. Stumpp, Dupont, Thorndyke, Melzner, unpublished). Thus, strong differences in mRNA expression could be indirect hypercapnia effects. For example, in larvae of *Strongylocentrotus purpuratus NKA*, mRNA levels peak during gastrulation (25 h post - fertilization) followed by an almost 100 % decline to trace levels at 60 h post-fertilization (Marsh et al. 2000). Thus, a slight difference in developmental rate would cause large changes in *NKA* mRNA expression. Delays in developmental rate of early life stages in response to hypercapnia have been found in several marine invertebrate species (Dupont and Thorndyke 2009; Dupont et al. 2010). Interestingly, when *S. officinalis* late stage embryos were exposed to 0.16 kPa CO_2 only so*cCAII* exhibited an increased expression. Accordingly, an upregulation of so*cCAII* in gills of late stage *S. officinalis* embryos subjected to seawater pCO_2 of 0.16 kPa (= 0.45 kPa PVF pCO_2) would support a role of this enzyme in active pH_e regulation. However, while no significantly reduced somatic growth was observed in 0.16 kPa embryos and hatchlings, a significant downregulation of ion-regulatory genes, especially so*NBC* was detected. A possible explanation for this phenomenon could be a slight

delay in gill differentiation and, thus, expression of ion-regulatory genes despite similar body dimensions. It is important to note that during the transition phase from embryo to hatchling, the cephalopod gill is subject to strong proliferation (Schipp et al. 1979; Hu et al. 2010a). More detailed histological studies are needed to resolve whether altered expression profiles under moderate hypercapnic stress are related to varying degrees of gill epithelia differentiation. The consistent strong down regulation of acid-base relevant genes (e.g. so*NKA*, so*NBC* and soc*CAII*) in response to 0.37 kPa water pCO_2 (0.75 kPa PVF pCO_2), suggests that the former transporters might be co - regulated as a functional unit. The location and function of acid-base relevant transporters are discussed in greater detail below.

The expression patterns of ATP-synthase, which is the key enzyme in ATP synthesis, correlates with those of the ion regulatory genes, which suggests a coupling of metabolic (e.g. energy providing) and ion-regulatory (energy consuming) processes. This observation is supported by a significant hypercapnia induced down regulation of *COX* mRNA levels, at least in hatchlings. In addition, CYP450, which is involved in the metabolism/oxidation of endogenous organic compounds such as lipids, steroidal hormones and exogenous xenobiotics (e.g. Meunier et al. 2004), was significantly down regulated in embryos and hatchlings. This indicates that the development of ion regulatory epithelia is tightly coupled to metabolic capacities. It has been previously shown that the proliferation of gill epithelia involves mitochondrial proliferation as well (1979).

In juveniles no significant hypercapnia-dependent responses in gene expression were found during the course of the experiment, which indicates that routine expression profiles are sufficient for the organism to cope with elevated pCO_2 up to 0.3 kPa. A CO_2 independent increase in mRNA expression along the experimental interval has been observed for all ion regulatory genes (except *soNDCBE*) studied (Fig. 4), which again supports the hypothesis that acid-base regulatory gene candidates in gill tissues are co-regulated. The observed increase in expression during the 42 day interval is probably closely related to growth and feeding rate, as the animals increased their body mass by approximately 50% during the experiment at a rate of 1.43% per day. Body mass, feeding and growth rates are directly related to differences in specific metabolic rate, enzyme activities and mRNA expression (Somero and

Childress 1980; Gibbs and Somero 1990; Yang and Somero 1996; Moyes and LeMoine 2005; Grigoriou and Richardson 2008).

Effects of hypercapnia on Na^+/K^+-ATPase

In juvenile *S. officinalis*, two distinct hypercapnia acclimation phases were observed with respect to so*NKA* mRNA expression, protein concentration and maximum activity. The first phase is a short-term response (<11 days), and the second is a long-term acclimation phase (42 days). After 11 days, NKA maximum activity was 15% higher under hypercapnia compared to control conditions, which was also reflected in a higher NKA protein concentration. This increase indicates a higher energetic demand to maintain the electrochemical gradient across the cell membrane and, thus, higher acid-base regulatory capacities in response to elevated water pCO_2. These findings correspond to the strong extracellular pH compensation reaction that was observed in the same species: *S. officinalis* elevates blood bicarbonate from 3.4 to 10.1 mmol [HCO_3^-] in response to acute hypercapnia (0.6 kPa CO_2) (Gutowska et al. 2010b). It is likely that the elevated gill NKA activity supports this pH regulatory response. Similar observations were made for Atlantic cod *Gadus morhua* and eelpout *Zoarces viviparus* exposed to 0.3 kPa and 1.0 kPa CO_2, respectively. NKA activities increased within the first days upon hypercapnic exposure in eelpout, and in both teleosts NKA activity almost doubled in response to long-term 0.6 kPa CO_2 exposure (Deigweiher et al. 2008; Melzner et al. 2009a). However, it can not be excluded that besides gill epithelia alternative sites (e.g. gut, kidneys) may also play a role in these compensatory processes. Long-term acclimation of 42 days revealed a decrease of NKA activity and protein concentration in *S. officinlis* gills back to control levels. One possible explanation for this effect could be the energetic favourable reorganization of physiological features in order to cope with this relatively moderate environmental stressor. In this respect, reversible phosporylation of the α-subunit by several protein kinases (PKA, PKC, PKG, tyrosine kinase) was reported to modulate Na^+/K^+-ATPase activity in vertebrates and invertebrates (Bertorello and Katz 1995; Chibalin et al. 1999; Ramnanan and Storey 2006). This post-translational modulation of NKA activity may also explain the seemingly inconsistent results of NKA enzyme activity, protein concentration and mRNA expression in response to acid-base disturbances (e.g. Feder and Walser 2005). Furthermore, the phospholipid composition

of biological membranes can be directely linked to ion permeability and enzyme (e.g. Na^+/K^+-ATPase) activity in gills of fish and crustaceans and might be a key element that undergoes modification during hypercapnia acclimation (Kimelberg and Papahadjopoulus 1972; Chapelle et al. 1976; Towle 1977; Palacios and Racotta 2007). Long-term maintenance of elevated NKA activity is an energetically expensive way to counter ionic disturbances (Febry and Lutz 1987; Gibbs and Somero 1990). The reduction of gill Na^+/K^+-ATPase activity after 42 days of hypercapnia suggests that long-term acclimation is probably accomplished without (a significant) re-arrangement of the energy budget. This is crucial for maintenance of control rates of somatic growth and calcification, as observed in a growth trial with juvenile *S. officinalis* exposed to a pCO_2 of 0.6 kPa for six weeks (Gutowska et al. 2008).

Acid-base regulation

Active organisms like fish and cephalopods exhibit a sophisticated ion regulatory machinery which is beneficial in coping with acid-base disturbances caused by respiratory acidosis, and might pre-adapt species to cope with future environmental hypercapnia through ocean acidification (Seidelin et al. 2001; Choe and Evans 2004; Melzner et al. 2009b). The present work demonstrates for the first time that gene transcripts essential for acid-base regulation in teleost fish (Tseng et al. 2006; Hwang and Lee 2007; Hwang 2009) are also found in the gill of the cephalopod mollusc *S. officinalis*. Earlier work by Schipp et al. (1979) already demonstrated a high concentrations of cCA in the transport active cells of the inner epithelium but only low concentrations in the outer, respiratory epithelium. Our findings demonstrate that NKA-rich cells in the cephalopod gill exhibit a set of enzymes that have been shown to be fundamental for pH_e homeostasis in vertebrates.

For the two bicarbonate transporters belonging to the SLC4 solute carrier family, sequence alignments show a maximum identity of 83% (so*NBCe*) and 100% (so*NDCBE*) when compared to the respective sequences from the squid *Loligo pealei*. Electrophysiological studies demonstrated that base equivalent transport by squid *NBCe* is electrogenic with a 1:2 stochiometry whereas *NDCBE* is electroneutral, achieving the exchange of one external Na^+ for one internal Cl^- and the inward flux of two base equivalents (Virkki et al. 2002; Piermarini et al. 2006). The relative expression of these two bicarbonate transporters in *S. officinalis* gill tissues revealed that *soNBCe* is expressed at least one order of magnitude higher than

soNDCBE in cuttlefish gill. This finding corresponds to studies that cloned and characterized *NBCe* and *NDCBE* orthologues in the squid *Loligo pealei* demonstrating their presence in giant fiber lobes, olfactory lobes, heart and gills (Virkki et al. 2002; Piermarini et al. 2006). On one hand, Northern blots revealed strong signals for *NDCBE* in olfactory and giant fibre lobes but only weak signals in gills and heart. On the other hand, a high expression of squid electrogenic *NBCe* was detected in gills and heart, but not in olfactory and giant fiber lobes (Piermarini et al. 2006). Piermarini et al. (71) suggested that *NBCe* in gills of squid could be involved in HCO_3^- uptake similar to the situation in the vertebrate kidney. In the renal proximal tubule, HCO_3^- reabsorption is achieved via electrogenic NBCe1-A, which is located basolaterally. The basolateral HCO_3^- efflux is also accompanied by a decrease in intracellular [Na^+], which may also enhance proton excretion via Na^+-dependent H^+ exchangers (NHE) across both, apical and basolateral membranes (Boron and Boulpaep 1983; Boron 2006). The majority of protons are excreted into the lumen of the tubule via different NHE isoforms located in the brush-border membrane of the proximal tubule (Wang et al. 1999; Goyal et al. 2003). Genetic knock-out demonstrated that among these NHE isoforms, NHE-3 mediates up to 50% of the total NHE activity in this epithelium (Wang et al. 1999). Moreover, up to 40% of the proximal tubule HCO_3^- reabsorption is Na^+ independent and is sensitive to bafilomycin inhibition, which supports the involvement of V-type-H^+-ATPase (Wagner et al. 2003). Following acidification of the lumen, secreted H^+ and filtered HCO_3^- form H_2O and CO_2 catalyzed by extracellular membrane-bound CAIV, and CO_2 diffuses into the tubule cells, where it reacts with H_2O to form HCO_3^- mediated by cCAII. The generated HCO_3^- is reabsorbed into the blood via basolateral electrogenic Na^+/HCO_3^- cotransportes (Wagner et al. 2003; Boron 2006).

We hypothesize that active HCO_3^- accumulation in body fluids and, thus, pH_e regulation in cephalopods is potentially achieved according to the hypothetical model depicted in Fig.7 C. In this model HCO_3^- is formed via CO_2 hydration in the cytosol by cCAII. The central role of cytosolic CAII in regulating acid-base balance was studied in great detail for both, fish and crustaceans (Henry and Cameron 1983; Henry 1988; Henry and Swenson 2000; Perry and Gilmour 2006; Gilmour and Perry 2009; Gilmour et al. 2009). For example Georgalis et al. (2006) provided direct evidence for a role of gill cCAII in regulating acid–base balance during exposure to 0.8 kPa CO_2 by demonstrating a 20% reduction in branchial acid efflux in trout subjected to CA inhibition. Subsequently, the increased intracellular [HCO_3^-] and negative

membrane potential created by the sodium pump could drive electrogenic efflux of Na^+ and HCO_3^- across the basolateral membrane through NBCe. Acid secretion on the apical membrane could be achieved by V-type-H^+- ATPase or a so far unidentified NHE-like protein.

Perspectives and significance

The present work corresponds with earlier findings (Gutowska et al. 2008; Gutowska et al. 2009) in demonstrating that juveniles of the cuttlefish *Sepia officinalis* can tolerate up to six week exposure to elevated seawater pCO_2 (0.3 kPa CO_2) without significantly altering mRNA expression profiles of potential key acid-base regulatory and metabolic enzymes. Although transient and moderate responses were found on the NKA protein level, routine expression of genes coding for important ion-regulatory proteins seem to be sufficient to cope with a CO_2 induced acidosis up to 0.3 kPa CO_2. Transcripts of key enzymes of metabolism, such as ATP-synthase, cytochrome-c-oxidase and octopine dehydrogenase did not respond to hypercapnia stress, indicating the possibility that energy demand is not greatly increased by the severity of abiotic stress applied. These observations support the hypothesis that active organisms like adult teleost fish and cephalopods can tolerate long-term exposure to elevated water pCO_2 comparatively well. The ability of such active ectothermic organisms to tolerate environmental hypercapnia is most likely linked to their high ion regulatory capacity. Nevertheless, several studies have demonstrated that a hypercapnia induced acid-base disturbance which is compensated via HCO_3^- accumulation in body fluids may lead to a hypercalcification of $CaCO_3$ structures such as fish otoliths, crustacean carapaces and cephalopod cuttlebones (Checkley et al. 2009; Gutowska et al. 2010b). In the long run, hypercalcification of structures responsible for buoyancy and balance control may negatively influence swimming behavior, active metabolism and prey capture.

This study also demonstrated that embryos may respond more sensitively to environmental stress than adults. As a consequence, even if elevated CO_2 levels are tolerable for juveniles or adults, cephalopod populations may still be affected due to the decreased fitness of embryos and hatchlings. The higher sensitivity in early life stages is most probably due to the fact that increases in environmental pCO_2 are additive to the naturally high pCO_2 (up to 0.4 kPa) of the PVF. This leads to extreme hypercapnic conditions (pCO_2 up to 0.7 kPa) inside the egg. Furthermore, an increased sensitivity may also be explained by the incomplete

development and functionality of ion-regulatory epithelia in early developmental stages (Schipp et al. 1979; Fioroni 1990). The characterization of these gill epithelia provided evidence that specialized cells contain a set of specific enzymes that are most likely involved in controlling extracellular pH homeostasis. The cephalopod gill acid-base regulatory machinery, consisting of NKA rich cells, equipped with proteins such as *soNBCe*, *socCAII* and *soV-HA,* shows a convergent evolution pattern to that of decapod crustaceans and teleost fish. Expression pattern of acid-base regulatory genes in early cephalopod life stages responded in an opposed manner as described for marine fish and crustaceans most likely due to a developmental delay, and, thus not due to direct action of elevated pCO_2. However, the present study provides a first mechanistic platform for future research on ion-regulation in a powerful acid-base regulating marine invertebrate. The application of non - invasive electrophysiological methods such as ion-selective electrodes in combination with specific inhibitors will be crucial in order to gain deeper insights into the function of putative transporters in cephalopod gill epithelia. Future comparative studies should focus on the detailed characterization of key acid-base regulatory proteins in a variety of marine ectothermic animals to contribute towards a general understanding of the evolution and common principles of extracellular pH regulation mechanisms.

Acknowledgements

The authors thank T. Reusch for use of his qRT-PCR machine and we are grateful to N. Bergmann, U. Panknin for valuable advice on (N.B.) and help with carrying out the qRT-PCR assays (U.P.). This study was partly funded by a DFG Excellence Cluster Future Ocean grant awarded to F.M. and a DAAD/NSC PPP grant (project ID 50128946) awarded to F.M. and P.P. Hwang (Institute of Cellular and Organismic Biology, Academia Sinica, Taiwan). This work is a contribution to the German Ministry of Education and Research (BMBF) funded project “Biological Impacts of Ocean ACIDification” (BIOACID) subproject 3.1.3 awarded to F.M., M.A.G. and M.L..

Literature

1. **Arnold JM.** Normal embryonic stages of the squid, *Loligo pealii* (Lesueur). *Biol Bull* 128: 24-32, 1965.
2. **Bertorello AM and Katz AI.** Regulation of Na^+-K^+-pump activity: Pathways between Receptors and effectors. *News Physiol Sci* 10: 253-259, 1995.
3. **Boron WF.** Acid-base transport by the renal proximal tubule. *J Am Soc Nephrol* 17: 2368-2382, 2006.
4. **Boron WF.** Regulation of intracellular pH. *Adv Physiol Educ* 28: 160-179, 2004.
5. **Boron WF and Boulpaep EL.** Intracellular pH regulation in the renal proximal tubule of the salamander: basolateral HCO_3^- transport. *J Gen Physiol* 81: 53-94, 1983.
6. **Caldeira K and Wickett ME.** Anthropogenic carbon and ocean pH. *Nature* 425: 365, 2003.
7. **Cameron JN and Iwama GK.** Compensation of progressive hypercapnia in channel catfish and blue crabs. *J Exp Biol* 133: 183-197, 1987.
8. **Chapelle S, Dandrifosse G, and Zwingelstein G.** Metabolism of phospholipids of anterior or posterior gills of the crab *Eriocheir sinensis* during the adaptation of this animal to media of various salinities. *J Biochem* 7: 343-351, 1976.
9. **Checkley J, David M, Dickson AG, Takahashi M, Radich JA, Eisenkolb N, and Asch R.** Elevated CO_2 enhances otolith growth in young fish. *Science* 324: 1683, 2009.
10. **Chibalin AV, Ogimoto G, Pedemonte CH, Pressley TA, Katz AI, Féraille E, Berggren P-O, and Bertorello AM.** Dopamine-induced endocytosis of Na^+/K^+-ATPase is initiated by phosphorylation of Ser-18 in the rat α subunit and is responsible for the decreased activity in epithelial cells. *J Biol Chem* 274: 1920-1927, 1999.
11. **Choe KP and Evans DH.** Compensation for hypercapnia by a euryhaline elasmobranch: Effect of salinity and roles of gills and kidneys in fresh water. *J Exp Zool A* 297A: 52-63, 2004.
12. **Claiborne JB and Evans DH.** Acid-base balance and ion transfers in the spiny dogfish (*Squalus acanthias*) during hypercapnia - a role for ammonia excretion. *J Exp Zool* 261: 9-17, 1992.
13. **Claiborne JB and Heisler N.** Acid-base regulation and ion transfers in the carp (*Cyprinus carpio*) during and after exposure to environmental hypercapnia. *J Exp Biol* 108: 25-43, 1984.
14. **Cronin ER and Seymour RS.** Respiration of the eggs of the giant cuttlefish *Sepia apama*. *Mar Biol* 136: 863-870, 2000.
15. **Deigweiher K, Koschnick N, Pörtner H-O, and Lucassen M.** Acclimation of ion regulatory capacities in gills of marine fish under environmental hypercapnia. *Am J Physiol* 295: R1660–R1670, 2008.
16. **Dickson A and Millero F.** A comparison of the equilibrium constants for the dissociation of carbonic acid in seawater media. *Deep Sea Res A* 34: 1733-1743, 1987.
17. **Dickson AG, Afghan JD, and Anderson GC.** Reference materials for oceanic CO_2 analysis: a method for the certification of total alkalinity. *Mar Chem* 80: 185-197, 2003.
18. **Dickson AG, L SC, and R CJ.** Guide to best practices for ocean CO_2 measurements. *PICES Special Publication* 3: 1-191, 2007.
19. **Donaubauer HH.** Sodium- and potassium-activated adenosine triphosphatase in the excretory organs of *Sepia officinalis* (Cephalopoda). *Mar Biol* 63: 143-150, 1981.

20. **Dupont S, Havenhand J, Thorndyke W, Peck L, and Thorndyke MC.** CO_2-driven ocean acidification radically affect larval survival and development in the brittlestar *Ophiothrix fragilis*. *Mar Ecol Prog Ser* 373: 285-294, 2008.
21. **Dupont S, Lundve B, and Thorndyke MC.** Near future ocean acidification increases growth rate of the lecithotrophic larvae and juveniles of the sea star *Crossaster papposus*. *J Exp Zool B* 314: DOI: 10.1002/jezmde.21342, 2010.
22. **Dupont S, Ortega-Martinez O, and Thorndyke MC.** Impact of near-future ocean acidification on echinoderms. *Ecotoxycology* 19: 449-462, 2010.
23. **Dupont S and Thorndyke MC.** Impact of CO_2-driven ocean acidification on invertebrates early life-history–what we know, what we need to know and what we can do (Discussion paper). *Biogeosci* 6: 3109-3131, 2009.
24. **Evans DH, Piermarini PM, and Choe KP.** The multifunctional fish gill: Dominant site of gas exchange, osmoregulation, acid-base regulation, and excretion of nitrogenous waste. *Physiol Rev* 85: 97-177, 2005.
25. **Fabry VJ, Seibel BA, Feely RA, and Orr JC.** Impacts of ocean acidification on marine fauna and ecosystem processes. *J Mar Sci* 65: 414-432, 2008.
26. **Febry R and Lutz P.** Energy partitioning in fish: the activity-related cost of osmoregulation in a euryhaline cichlid. *J Exp Biol* 128: 63-85, 1987.
27. **Feder ME and Walser J-C.** The biological limitations of transcriptomics in elucidating stress and stress responses. *J Evol Biol* 18: 901-910, 2005.
28. **Feely RA, Sabine CL, Hernandez-Ayon JM, Ianson D, and Hales B.** Evidence for upwelling of corrosive "acidified" water onto the continental shelf. *Science* 320: 1490-1492, 2008.
29. **Fioroni P.** Our recent knowledge of the development of the cuttlefish (*Sepia officinalis*). *Zool Anz* 224: 1-25, 1990.
30. **Fivelstad S, Olsen AB, Asgard T, Baeverfjord G, Rasmussen T, Vindheim T, and Staffanson S.** Long-term sublethal effects on carbon dioxide on Atlantic salmon smolts (*Salmo solar* L.): ion regulation, haematology, element composition, nephrocalcinosis and growth parameters. *Aquaculture* 215: 301-319, 2003.
31. **Forsythe J, Lee P, Walsh L, and Clark T.** The effects of crowding on growth of the European cuttlefish, *Sepia officinalis* Linnaeus, 1758 reared at two temperatures *J Exp Mar Biol Ecol* 269: 173-185, 2002.
32. **Foss A, Rosnes BA, and Oiestad V.** Graded environmental hypercapnia in juvenile spotted wolffish (*Anarhichas minor* Olafson): effects on growth, food conversion efficiency and nephrocalcinosis. *Aquaculture* 220: 607-617, 2003.
33. **Georgalis T, Perry SF, and Gilmour KM.** The role of branchial carbonic anhydrase in acid–base regulation in rainbow trout (*Oncorhynchus mykiss*). *J Exp Biol* 209: 518-530, 2006.
34. **Gibbs A and Somero GN.** Na^+-K^+-adenosine triphosphatase activities in gills of marine teleost fishes: changes with depth, size and locomotory activity level. *Mar Biol* 106: 315-321, 1990.
35. **Gilmour KM and Perry SF.** Carbonic anhydrase and acid-base regulation in fish. *J Exp Biol* 212: 1647-1661, 2009.
36. **Gilmour KM, Thomas K, Esbaugh AJ, and Perry SF.** Carbonic anhydrase expression and CO_2 excretion during early development in zebrafish *Danio rerio*. *J Exp Biol* 212: 3837-3845, 2009.
37. **Goyal S, Vanden Heuvel G, and Aronson PS.** Renal expression of novel Na/H exchanger isoform NHE8. *Am J Physiol Renal Physiol* 284: F467–F473, 2003.

38. **Grigoriou P and Richardson CA.** Aspects of the growth of cultured cuttlefish *Sepia officinalis* (Linnaeus 1758). *Aquacult Res* 35: 1141-1148, 2004.
39. **Grigoriou P and Richardson CA.** The effect of ration size, temperature and body weight on specific dynamic action of the common cuttlefish *Sepia officinalis*. *Mar Biol* 154: 1085-1095, 2008.
40. **Grosell M.** Intestinal anion exchange in marine fish osmoregulation *J Exp Biol* 209: 2813-2817, 2006.
41. **Gutowska MA and Melzner F.** Abiotic conditions in cephalopod (*Sepia officinalis*) eggs: embryonic development at low pH and high pCO_2. *Mar Biol* 156: 515-519, 2009.
42. **Gutowska MA, Melzner F, Langenbuch M, Bock C, Claireaux G, and Pörtner H-O.** Acid-base regulatory ability of the cephalopod (*Sepia officinalis*) in response to environmental hypercapnia. *J Comp Physiol B* in Press, 2009.
43. **Gutowska MA, Melzner F, Pörtner H-O, and Meier S.** Cuttlebone calcification increases during exposure to elevated seawater pCO_2 in the cephalopod *Sepia officinalis*. *Mar Biol* 157: 1653-1663, 2010.
44. **Gutowska MA, Pörtner H-O, and Melzner F.** Growth and calcification in the cephalopod *Sepia officinalis* under elevated seawater pCO_2. *Mar Ecol Prog Ser* 373: 303-309, 2008.
45. **Henry RP.** Multiple functions of carbonic anhydrase in the crustacean gill. *J Exp Zool* 248: 19-24, 1988.
46. **Henry RP and Cameron JN.** The role of carbonic anhydrase in respiration, ion regulation and acid-base balance in the aquatic crab *Callinectes sapidus* and the terrestrial crab *Gecarcinus lateralis*. *J Exp Biol* 103: 205-223, 1983.
47. **Henry RP and Swenson ER.** The distribution and physiological significance on carbonic anhydrase in vertebrate gas exchange organs. *Resp Physiol* 121: 1-12, 2000.
48. **Hoppema JMJ.** Carbon dioxide and oxygen disequilibrium in a tidal basin (Dutch wadden sea). *Neth J Sea Res* 31: 221-229, 1993.
49. **Horng JL, Lin LY, Huang JC, Katoh F, Kaneko T, and Hwang PP.** Knockdown of V-ATPase subunit A (atp6v1a) impairs acid secretion and ion balance in zebrafish (*Danio rerio*). *Am J Physiol Regul Integr Comp Physiol* 292: R2068-R2076, 2007.
50. **Hu MY, Sucré E, Charmantier-Daures M, Charmantier G, Lucassen M, and Melzner F.** Localization of ion regulatory epithelia in embryos and hatchlings of two cephalopods. *Cell Tiss Res* 441: 571-583, 2010.
51. **Hwang PP.** Ion uptake and acid secretion in zebrafish (*Danio rerio*). *J Exp Biol* 212: 1745-1752, 2009.
52. **Hwang PP and Lee TH.** New insights into fish ion regulation and mitochondrion-rich cells. *Comp Biochem Physiol A* 148: 479-497, 2007.
53. **Hyashi M, Kita J, and Ishimatsu A.** Comparison of the acid-base responses to CO_2 and acidification in Japanese flounder (*Paralichthys olivaceus*). *Mar Poll Bull* 49: 1062-1065, 2004.
54. **Kimelberg HK and Papahadjopoulus D.** Phospholipid requirements for $(Na^+ + K^+)$ATPase activity: head-group specificity and fatty acid fluidity. *Biochim Biophys Acta* 282: 277-292, 1972.
55. **Kurihara H, Kato S, and Ishimatsu A.** Effects of increased seawater pCO_2 on early development of the oyster *Crassostrea gigas*. *Aquat Biol* 1: 91-98, 2007.
56. **Kurihara H, Shimode S, and Shirayama Y.** Effects of raised CO_2 concentration on the egg production rate and early development of two marine copepods (*Acartia steueri* and *Acartia erythraea*). *Mar Poll Bull* 49: 721-727, 2004.

57. **Kurihara H and Shirayama Y.** Effects of increased atmospheric CO_2 on sea urchin early development. *Mar Ecol Prog Ser* 274: 161-169, 2004.
58. **Lämmli UK.** Cleavage of structural proteins during the assembly of the head of Bacteriophage T4. *Nature* 227: 680-685, 1970.
59. **Larsen BK, Pörtner H-O, and Jensen FB.** Extra- and intracellular acid-base balance and ionic regulation in cod (*Gadus morhua*) during combined and isolated exposures to hypercapnia and copper. *Mar Biol* 128: 337-346, 1997.
60. **Lemaire J.** Table de développement embryonaire de *Sepia officinalis* L. (Mollusque Céphalopode). *Bull Soc Zool Fr* 95: 773-782, 1970.
61. **Lewis E and Wallace DWR.** Program developed for CO2 system calculations. *Oak Ridge, Oak Ridge National Laboratory ORNL/ CDIAC-105*, 1998.
62. **Marsh AG, Leong PKK, and Manahan DT.** Gene expression and enzyme activities of the sodium pump during sea urchin development: implications for indices of physiological state. *Biol Bull* 199: 100-107, 2000.
63. **Mehrbach C, Culberso C, Hawley J, and Pytkowic R.** Measurement of apparent dissociation constants of carbonic acid in seawter at atmospheric pressure. *Limnol Oceanogr* 18: 897-907, 1973.
64. **Melzner F, Göbel S, Langenbuch M, Gutowska MA, Pörtner H-O, and Lucassen M.** Swimming performance in atlantic cod (*Gadus morhua*) following long-term (4-12 month) acclimation to elevated seawater pCO_2. *Aqua Toxicol* 92: 30-37, 2009.
65. **Melzner F, Gutowska MA, Langenbuch M, Dupont S, Lucassen M, Thorndyke MC, Bleich M, and Pörtner H-O.** Physiological basis for high CO_2 tolerance in marine ectothermic animals: pre-adaptation through lifestyle and ontogeny? *Biogeosciences* 6: 2313-2331, 2009.
66. **Meunier B, De Visser SP, and Shaik S.** Mechanism of oxidation reactions catalyzed by cytochrome P450 enzymes. *Chem Rev* 104: 3947-3980, 2004.
67. **Moyes CD and LeMoine CMR.** Control of muscle bioenergetic gene expression: implications for allometric scaling relationships of glycolytic and oxidative enzymes. *J Exp Biol* 208: 1601-1610, 2005.
68. **Palacios E and Racotta IS.** Salinity stress test and its relation to future performance and different physiological responses in shrimp postlarvae. *Aquaculture* 268: 123-135, 2007.
69. **Pane EF and Barry JP.** Extracellular acid-base regulation during short-term hypercapnia is effective in a shallow-water crab, but ineffective in a deep-sea crab. *Mar Ecol Prog Ser* 334: 1-9, 2007.
70. **Perry SF and Gilmour KM.** Acid–base balance and CO_2 excretion in fish: Unanswered questions and emerging models. *Resp Physiol Neurobiol* 154: 199-215, 2006.
71. **Piermarini PM, Choi I, and Boron WF.** Cloning and characterization of an electrogenic Na/HCO_3^- cotransporter from the squid giant fiber lobe. *Am J Physiol Cell Physiol* 292: C2023-C2045, 2006.
72. **Pörtner H-O, Webber DM, Boutilier RG, and O`Dor RK.** Acid-base regulation in exercising squid (*Illex illecebrosus*, *Loligo pealei*). *Am J Physiol Regul Integr Comp Physiol* 261: R239-R246, 1991.
73. **Pörtner HO, Langenbuch M, and Reipschläger A.** Biological impact of elevated ocean CO_2 concentrations: Lessons from animal physiology and earth history. *J Oceanograph* 60: 705-718, 2004.
74. **Ramnanan CJ and Storey KB.** Suppression of Na^+/K^+-ATPase activity during estivation in the land snail *Otala lactea*. *J Exp Biol* 209: 677-688, 2006.

75. **Schipp R, Mollenhauer S, and Boletzky S.** Electron microscopical and histochemical studies of differentiation and function of the cephalopod gill (*Sepia officinalis* L.). *Zoomorph* 93: 193-207, 1979.
76. **Schwartz AA, Allen JC, and Harigaya S.** Possible involvement of cardiac Na^+/K^+-adenosine triphosphatase in the mechanism of action of cardiac glycosides. *J Pharmacol Exp Ther* 168: 31-41, 1969.
77. **Seidelin M, Brauner CJ, Jensen FB, and Madsen SS.** Vacuolar-Type H^+-ATPase and Na^+,K^+-ATPase expression in gills of atlantic salmon (*Salmo salar*) during isolated and combined exposure to hypoxia and hypercapnia in fresh water. *Zool Sci* 18: 1199-1205, 2001.
78. **Somero GN and Childress JJ.** A violation of the metabolism-size scaling paradigm: activities of glycolytic enzymes in muscle increase in larger fish. *Physiol Zool* 53: 322-337, 1980.
79. **Spicer JI, Raffo A, and Widdicombe S.** Influence of CO_2-related seawater acidification on extracellular acid-base balance in the velvet swimming crab *Necora puber*. *Mar Biol* 151: 1117-1125, 2007.
80. **Thomsen J, Gutowska MA, Saphörster J, Heinemann A, Trübenbach K, Fietzke J, Hiebenthal C, Eisenhauer A, Körtzinger A, Wahl M, and Melzner F.** Calcifying invertebrates succeed in a naturally CO_2 enriched coastal habitat but are threatened by high levels of future acidification. *Biogeosciences Discussions (accepted)*: 5119-5156, 2010.
81. **Toews DP, Holeton GF, and Heisler N.** Regulation of the acid-base status during environmental hypercapnia in the marine teleost fish *Conger conger*. *J Exp Biol* 107: 9-20, 1983.
82. **Towle DW.** Sodium pump sites in teleost gill: unmasking by detergent. *Am Zool* 177: 877, 1977.
83. **Tseng Y-C, Huang C-J, Chang JC-H, Wen-Yuan Teng W-Y, Baba O, Fann M-J, and Hwang PP.** Glycogen phosphorylase in glycogen-rich cells is involved in the energy supply for ion regulation in fish gill epithelia. *Am J Physiol Regul Integr Comp Physiol* 293: R482-R491, 2006.
84. **Turner N, Hulbert AJ, and Else PL.** Sodium pump molecular activity and membrane lipid composition in two disparate ectotherms, and comparison with endotherms. *J Comp Physiol B* 175: 77-85, 2004.
85. **Virkki LV, Choi I, Davis BA, and Boron WF.** Cloning of a Na^+-driven Cl/HCO_3^- exchanger from squid giant fiber lobe. *Am J Physiol Cell Physiol* 285: C771-C780, 2002.
86. **Wagner CA, Finberg KE, Breton S, Marshanski V, Brown D, and Geibel JP.** Renal vacuolar H^+-ATPase. *Physiol Rev* 84: 1263-1314, 2003.
87. **Wang T, Yang CL, Abbiati T, Schultheis PJ, Shull GE, Giebisch G, and Aronson PS.** Mechanism of proximal tubule bicarbonate absorption in NHE3 null mice. *Am J Physiol Renal Physiol* 277: F298–F302, 1999.
88. **Yang T-H and Somero G.** Activity of lactate dehydrogenase but not its concentration of messenger RNA increases with body size in barred sand bass, *Paralabrax nebulifer* (Teleostei). *Biol Bull* 191: 155-158, 1996.
89. **Young RE and Vecchione M.** Cephalopod gills- Tree of Life Web Project: http://to/web.org. 2004.

Figures and tables

Fig. 1. Biometric information of embryos (A) and hatchlings (B) of *Sepia officinalis* reared under different CO_2 concentrations. The somatic growth is documented by the dorsal mantle length (DML) and their body mass (BM). Asterisks indicate significant differences between CO_2 treated and control animals. Bars represent standard errors (n = 15).

Fig. 2. Abiotic parameters determined in perivitelline fluid (PVF) of *Sepia officinalis* and in the experimental sea water. PVF CO_2 concentrations were calculated from pH and dissolved inorganic carbon (C_T) at different ambient pCO_2 (A). pH of the PVF at different ambient pCO_2 (B). Dotted and dashed lines inserted into the graph represent the ambient water pH and pCO_2, respectively. Values are given as means including percentiles of 5^{th} (bars) and 95^{th} (boxes) (n = 15).

Fig. 3. Expression profiles from selected genes determined for gill tissues of different ontogenetic stages of *Sepia officinalis*. Embryos (A) and hatchlings (B) were incubated at three different pCO_2 values (contol, 0.16 and 0.37 kPa) for four weeks until hatching whereas juveniles (C) were incubated for six weeks at a pCO_2 of 0.32 kPa. Expression of the gene candidates are normalized to the geometric mean of so*CPSF* and so*UBC*. Asterisks denote a significant change in gene expression (n = 8-10).

Fig. 4. Juvenile *Sepia officinalis* gill mRNA expression of gene candidates related to ion regulation (A-D), metabolism (E-G) and stress (F) during 48 h, 11 days and 42 days of exposure to 0.3 kPa hypercapnia. Expression of the gene candidates are normalized to the geometric mean of so*CPSF* and so*UBC* and given in % of the maximum expression of each gene tested. No significant differences were observed for the expression of genes between

treatments. Letters denote a significant difference between each time point and values are expressed as means ± SE (*n* = 8).

Fig. 5. Juvenile *Sepia officinalis* specific gill Na^+/K^+-ATPase activity (A), relative protein concentration (B) and relative mRNA expression (C) in control (0.04 kPa) and CO_2 treated (0.3 kPa) animals at the three time points 48 h, 11 d and 42 d. Activity is given in µmoles ATP g^{-1} fresh mass (FM) h^{-1}. Expression Na^+/K^+-ATPase is normalized to the geometric mean of so*CPSF* and so*UBC* and given in % of the maximum expression determined. Significant differences compared to the control group ($P < 0.05$*; $P < 0.01$**) are indicated by asterisks (t-test). Values are means ± SE (n = 6-8).

Fig. 6. . Expression of so*NKA*, so*NBC* and *soV-HA* in cells of the inner epithelium (ie) of the third order gill lamellae of juvenile *Sepia officinalis*, reared under control conditions, visualized by *in situ* hybridization. Large cells in the inner (ie), transport active epithelium of the gill lamellae are rich in *NKA* (indicated by arrows), while the outer (oe) is thin and exclusively involved in respiratory processes (A). Merged image demonstrates that NKA protein and so*NBC* mRNA are co-localized in ion transporting cells of the inner epithelium (B). Furthermore, so*V-HA* is co - expressed in NKA-rich cells of the transport active epithelium (C). The outer and the inner epithelium are lining a blood sinus (bs). Insertions, hybridization with a sense mRNA probe as the negative control.

Fig. 7. Diagram of the gill morphology of *Sepia officinalis* (A), indicating the arrangement of first to second order lamellae located on both lateral sides of the branchial gland (bg), showing the folded lamellae of the gill of *S. officinalis*. The concave inner epithelium (ie) of the third order gill lamellae belongs to the transport active epithelium, whereas the outer epithelium (oe) is exclusively involved in respiratory processes. Drawings adopted and modified from Young and Vecchione (2004). Immunohistochemical staning of a gill lamella,

demonstrating NKA to be exclusively located in the inner epithelium of the third order lamellae (B). Scale bar = 50µm. Hypothetical model of a cell in the transport active inner epithelium (rectangular sector in A) equipped with various transporters, which are involved in acid-base regulatory processes (C). CO_2 is hydrated by carbonic anhydrase (CA) after diffusive entry resulting in HCO_3^- and H^+. Net accumulation of extracellular HCO_3^- is supported by the basolateral NBC. Net proton extrusion is possibly achieved by apical NHEe-like protein powered by elevated Na^+/K^+-ATPase activity in the basolateral membrane.

Table 1. Seawater physiochemical conditions during six week hypercapnia experiment (juvenile *S. officinalis*); temperature, salinity, pH, pCO_2: partial pressures of CO_2; Ω_{Arag}: aragonite saturation state; A_T: total alkalinity. Values are presented as mean ± SD

Table 2. Primer sequences used for qRT-PCR

Figure 1

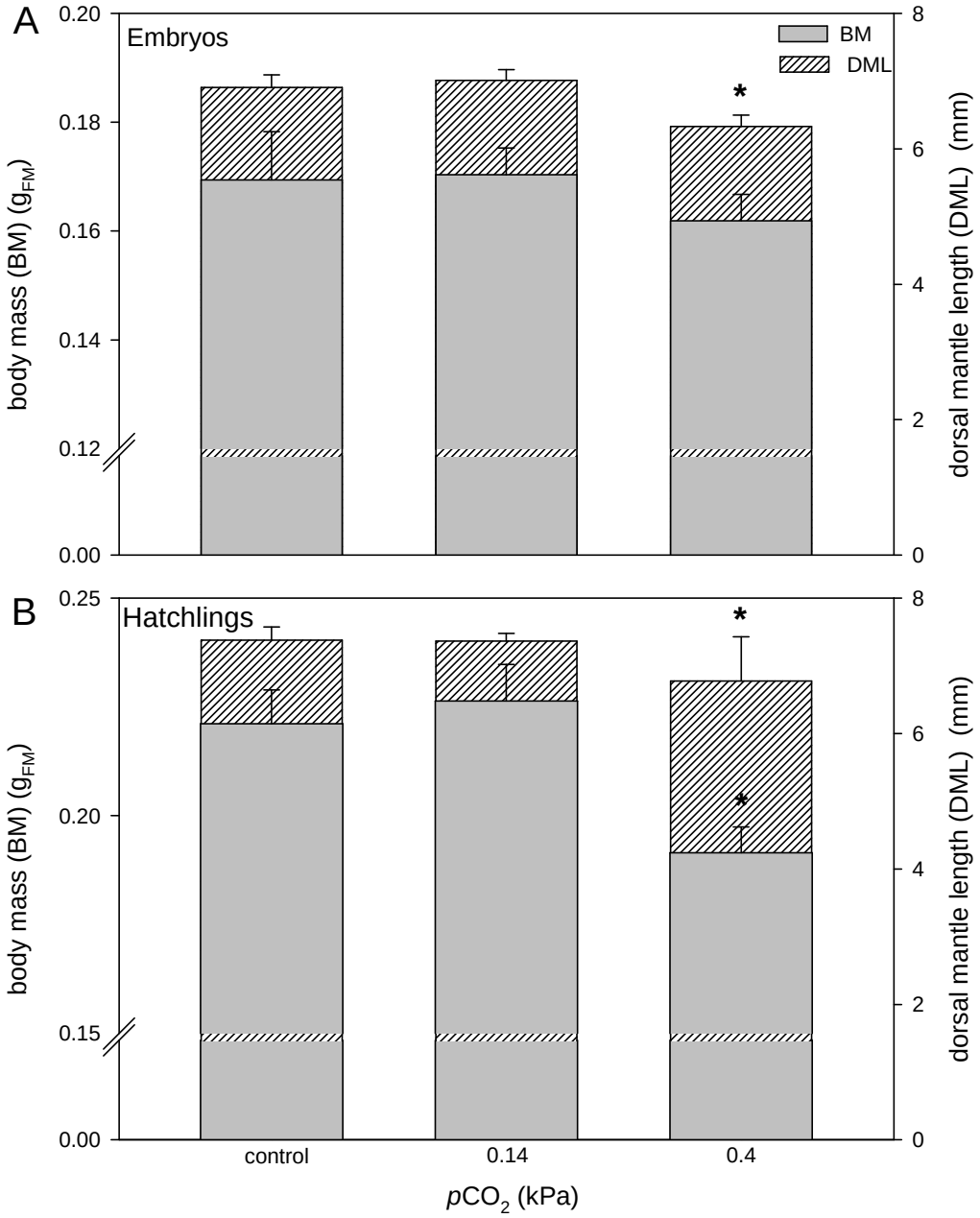
A
Embryos
BM
DML
body mass (BM) (g$_{FM}$)
dorsal mantle length (DML) (mm)
0.20
0.18
0.16
0.14
0.12
0.00
8
6
4
2
0
*
B
Hatchlings
0.25
0.20
0.15
0.00
control
0.14
0.4
pCO$_2$ (kPa)

Figure 2

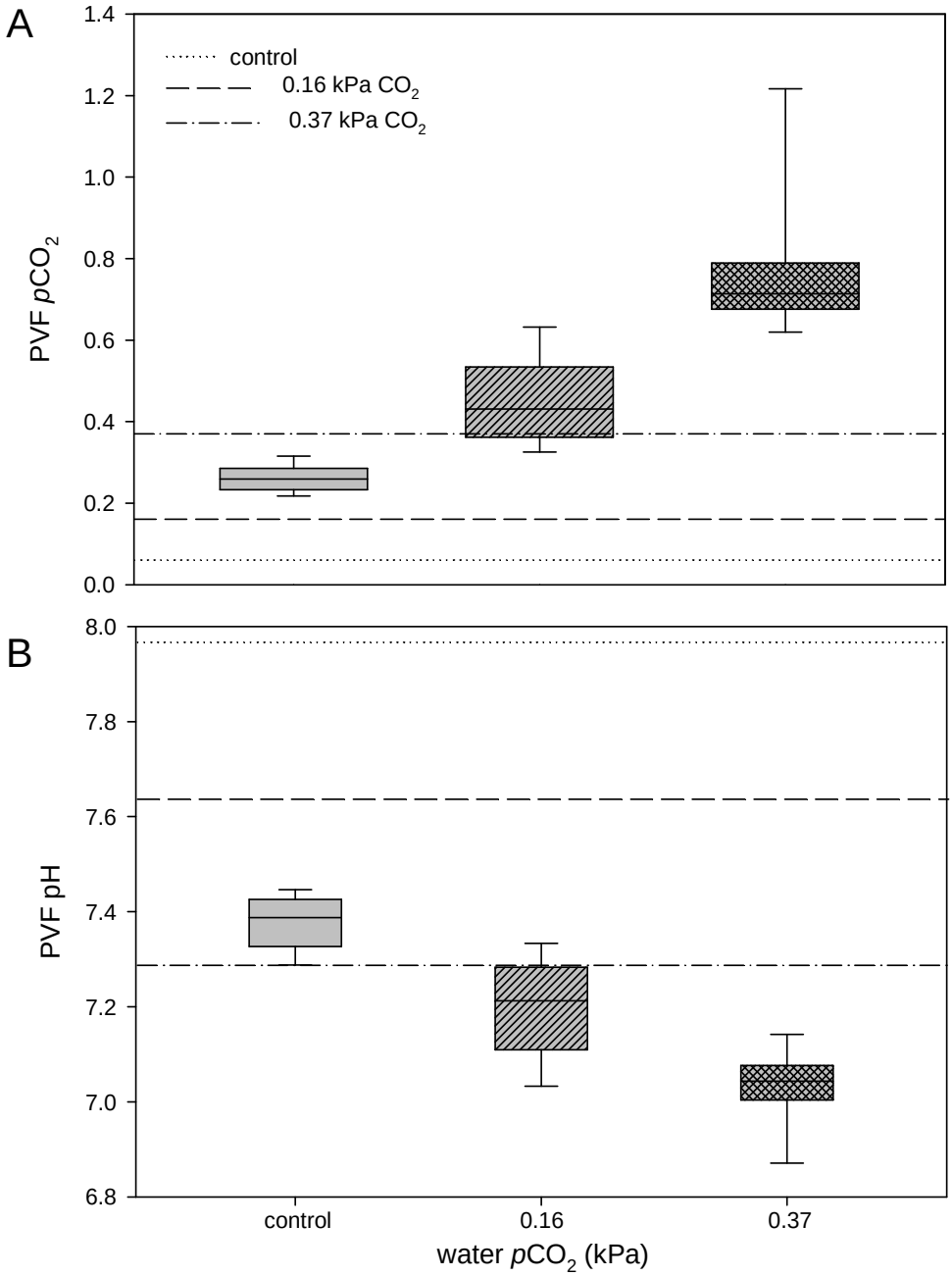
A
control
0.16 kPa CO2
0.37 kPa CO2
PVF pCO2
1.4
1.2
1.0
0.8
0.6
0.4
0.2
0.0
B
PVF pH
8.0
7.8
7.6
7.4
7.2
7.0
6.8
control
0.16
0.37
water pCO2 (kPa)

Figure 3

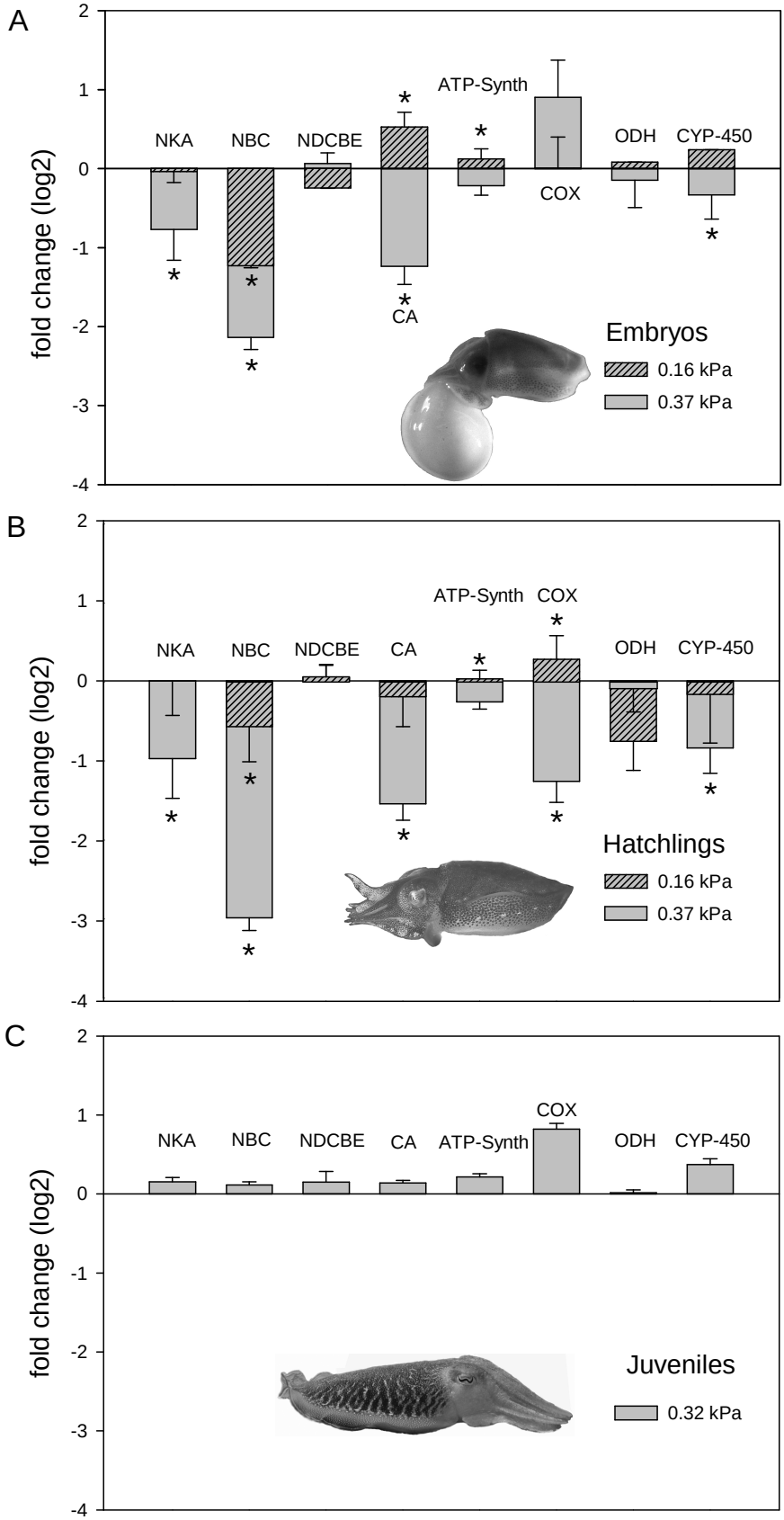
A
fold change (log2)
NKA
NBC
NDCBE
CA
ATP-Synth
COX
ODH
CYP-450
Embryos
0.16 kPa
0.37 kPa
B
fold change (log2)
NKA
NBC
NDCBE
CA
ATP-Synth
COX
ODH
CYP-450
Hatchlings
0.16 kPa
0.37 kPa
C
fold change (log2)
NKA
NBC
NDCBE
CA
ATP-Synth
COX
ODH
CYP-450
Juveniles
0.32 kPa

Figure 4

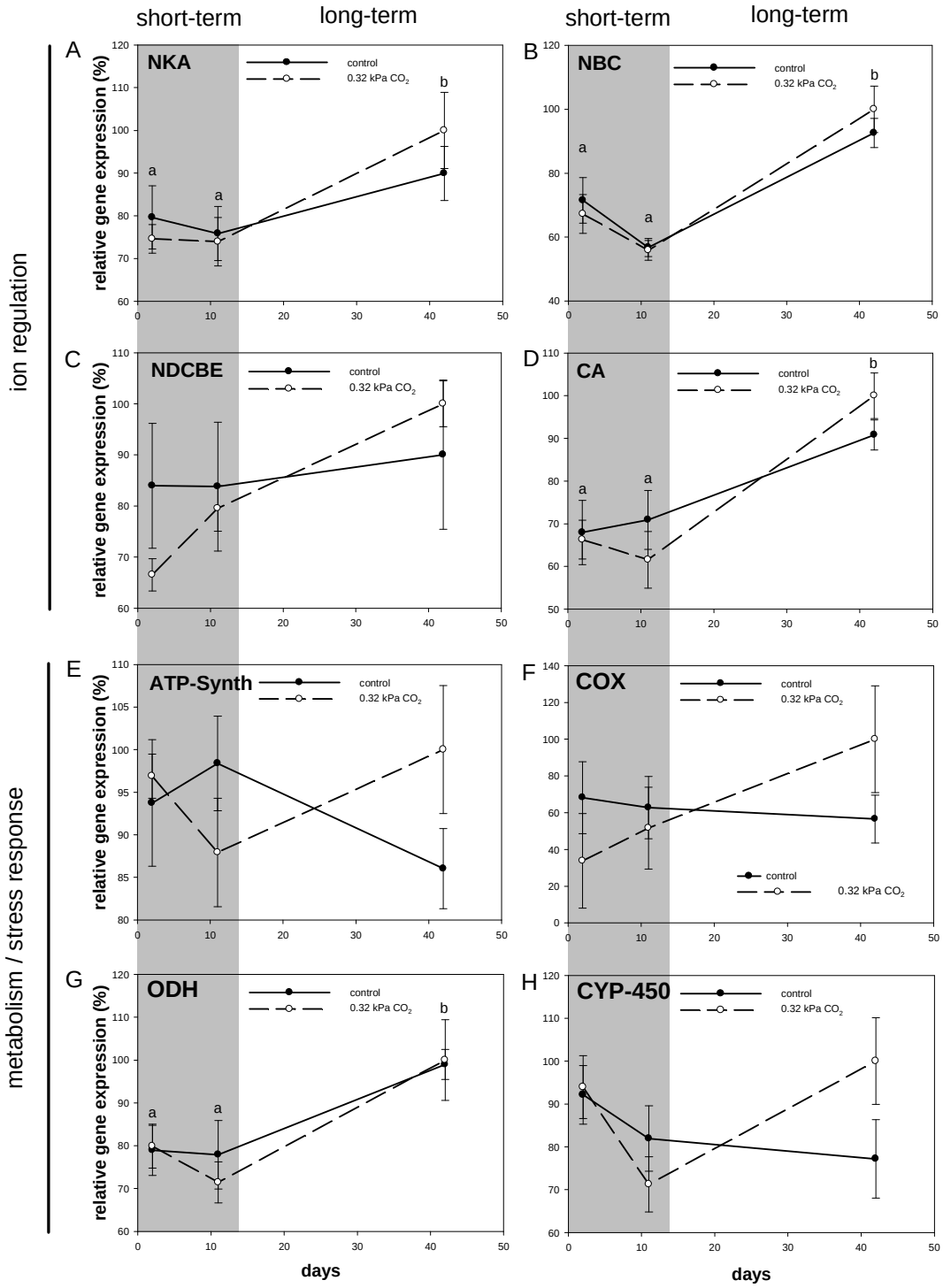
short-term
long-term
short-term
long-term
ion regulation
metabolism / stress response
A
NKA
B
NBC
C
NDCBE
D
CA
E
ATP-Synth
F
COX
G
ODH
H
CYP-450
control
0.32 kPa CO2
relative gene expression (%)
days
a
b

Figure 5

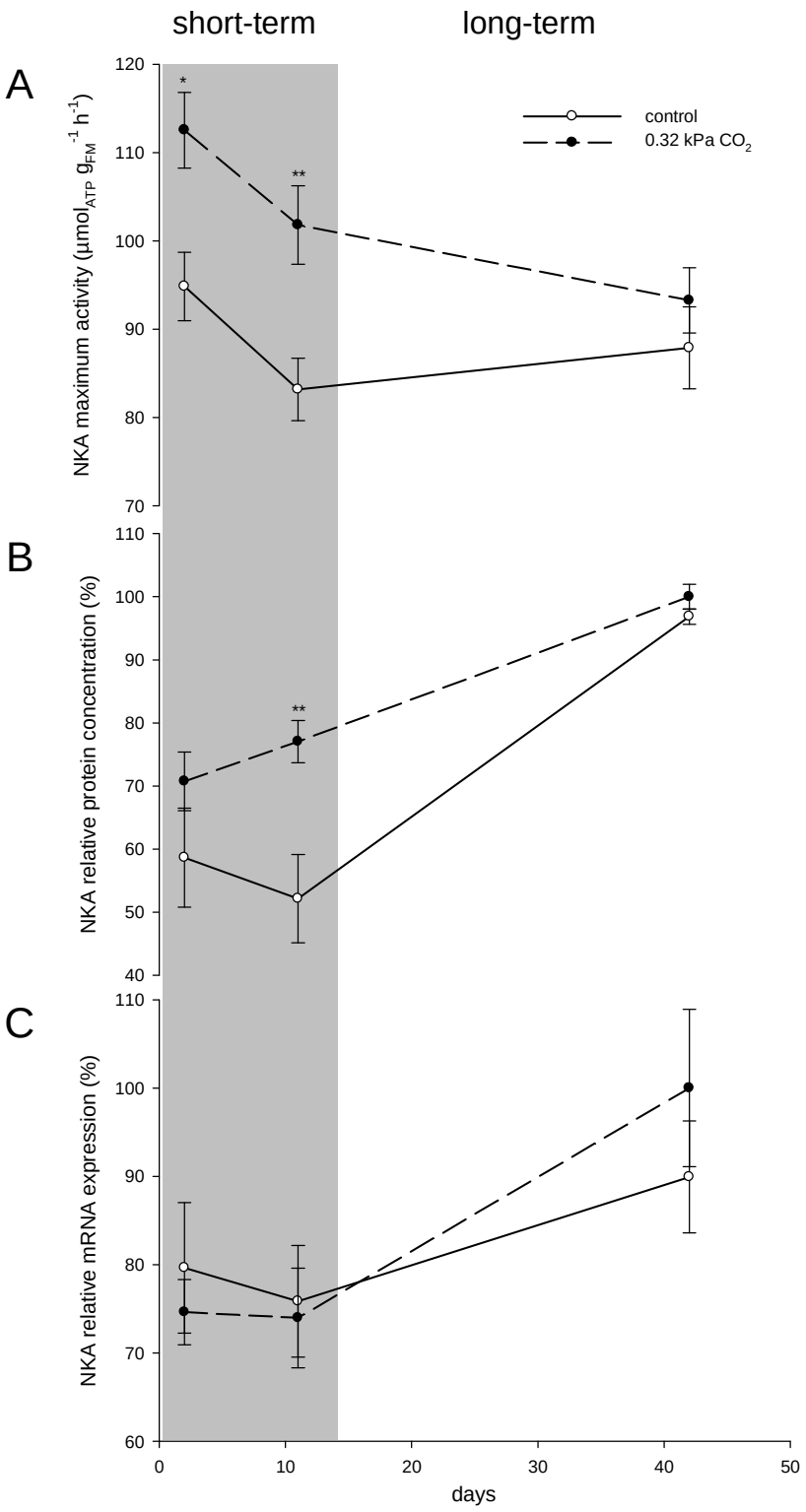
short-term
long-term
A
B
C
control
0.32 kPa CO2
NKA maximum activity (µmol ATP gFM -1 h-1)
NKA relative protein concentration (%)
NKA relative mRNA expression (%)
days
*
**
**
120
110
100
90
80
70
60
50
40
0
10
20
30
40
50

Figure 6

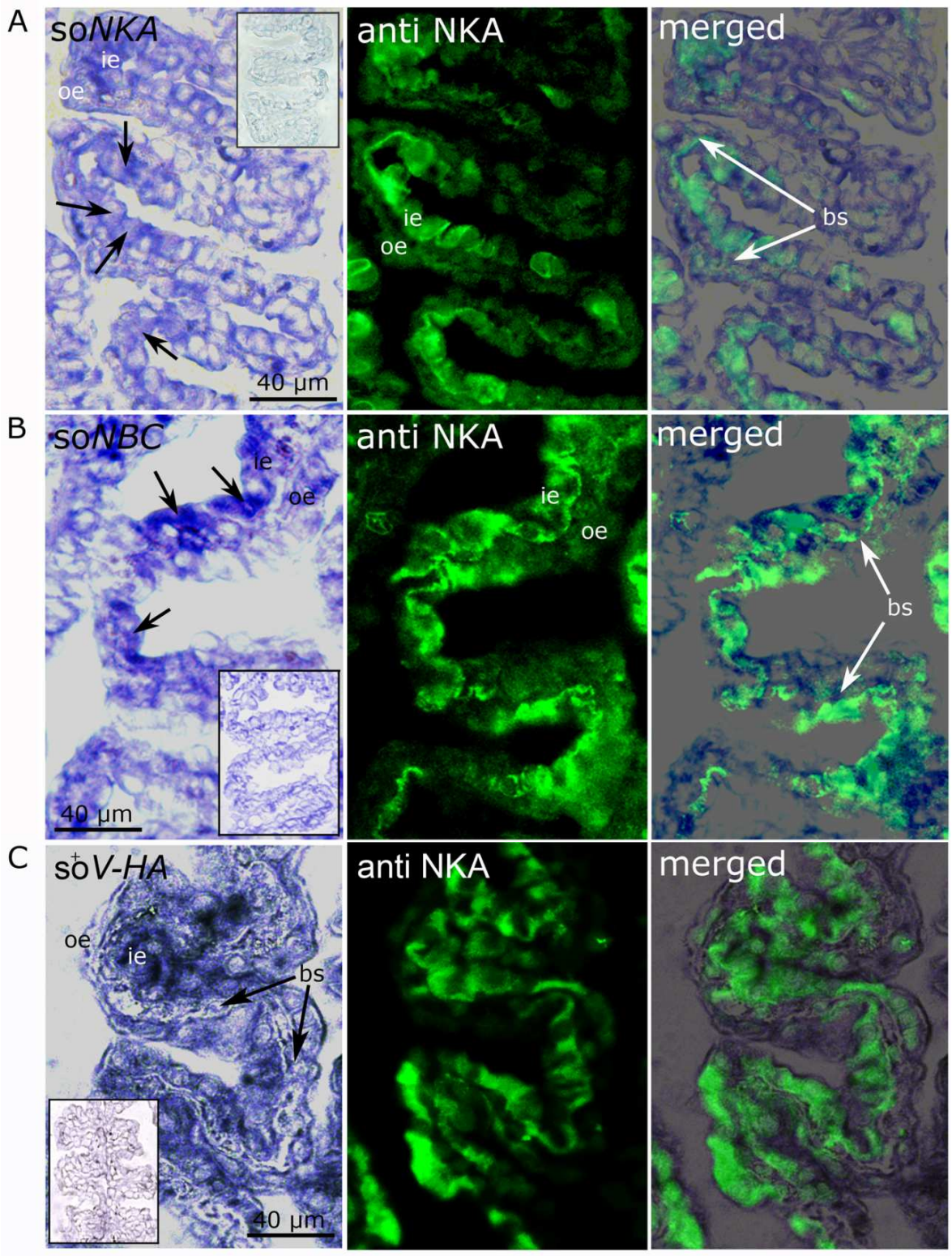
A
soNKA
ie
oe
40 µm
anti NKA
ie
oe
merged
bs
B
soNBC
ie
oe
40 µm
anti NKA
ie
oe
merged
bs
C
so+V-HA
oe
ie
bs
40 µm
anti NKA
merged

Figure 7

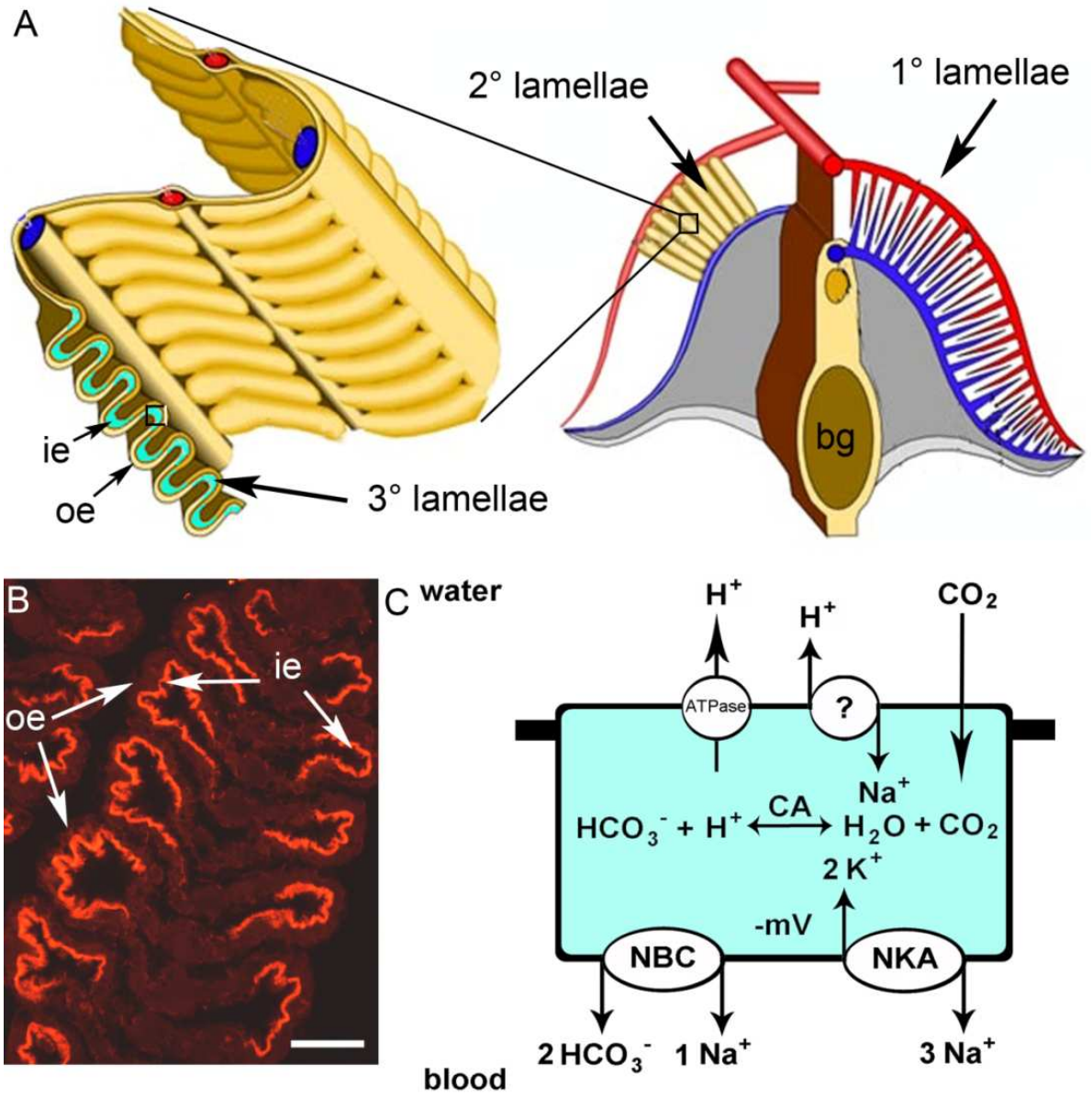
A
2° lamellae
1° lamellae
ie
oe
3° lamellae
bg
B
ie
oe
C
water
H+
H+
CO2
ATPase
?
Na+
HCO3- + H+
CA
H2O + CO2
2 K+
-mV
NBC
NKA
2 HCO3-
1 Na+
3 Na+
blood

Table 1

	Incubation group	Temperature [°C]	Salinity	pH	ΩAr	CO_2 [Pa]	A_T
Embryos and hatchlings	Control	14.60 ± 0.47	34.94 ± 0.10	7.96 ± 0.02	1.69 ± 0.06	70.97 ± 4.13	2413.81 ± 49.10
	CO_2 ~ 0.14 kPa	14.62 ± 0.47	34.92 ± 0.07	7.63 ± 0.02	0.84 ± 0.01	164.04 ± 24.48	2431.89 ± 56.12
	CO_2 ~ 0.4 kPa	14.62 ± 0.45	34.90 ± 0.05	7.28 ± 0.03	0.39 ± 0.02	371.35 ± 28.52	2415.16 ± 43.00
Juveniles	Control	14.81 ± 0.20	33.08 ± 0.20	8.21 ± 0.08	3.53 ± 0.53	50.255 ± 8.757	2827.00 ± 129.08
	CO_2 ~ 0.4 kPa	14.83 ± 0.21	33.09 ± 0.21	7.39 ± 0.09	0.75 ± 0.11	308.936 ± 37.401	3127.53 ± 141.91

Table 2

Gene name	Abbreviation	Function	Acc. No.	Primer sequence 5´-3´ (forward and reverse)	Amplicon length
test genes					
Na/K-ATPase	NKA	Electro/chemical gradient	GQ153672.1	CTGTCCTGAAAAGGGAATGCA TTTCCAATAGAAAGCTCAACACATTT	76
Na/HCO_3 cotransporter	NBC	Secondary active ion-transport	bankit1347543	GGAAGAATGCATGAAAGACACAAT TCGCTTCATGTGTTGATGGAA	70
Na-driven Cl/HCO_3 exchanger	NDCBE	Secondary active ion-transport	bankit1347548	AGGAGCTGAATCCGCCAAT AGCCGGTAGCTTGGTGGTT	65
Carbonic anhydrase	CA	Bicarbonate formation	bankit1347557	ACCTTTAGCCATCCGCTGAA TCCGTTGTTGGTGACTTCCA	66
ATP-synthase	ATP-Synth	Electron transport chain	bankit1347571	GGAGAGAGCTGCCAAGATGAA CCTGGGTCTCGATGACTGGTA	74
Cytochrome p450	CYP 450	Xenobiotic defence	bankit1347604	CCGGCGGTGCCAGTTA TGCGGGAATTTTGTAATCATCA	69
Cytochrome-c oxydase	COX	Electron transport chain	YP514795	TCCTCCTCCGCAGTTGAAAG GCCCGCATGTGATAAGTTACTAGA	81
Octopine dehydrogenase	ODH	Anaerobic metabolism	AY545135	GCCGAGTCAACCCGGTTT CGCTGGTTCGACCTCCAA	65
reference genes					
Cleavage and polyadenylation specificity factor	CPSF	mRNA polyadenylation	bankit1345716	CACACCAGCCCATGAAAAGA GGTGGTGTTGGCGAGTATGC	68
Ubiquitin-conjugated enzyme	UBC	Protein degradation	bankit1345727	CAATAATACCGTGAAAGTGGCAGAT TTTCCTGAGCTTCATATATTTCATCAG	74

Publication 2

New insights into ion regulation of cephalopod molluscs: a role of epidermal ionocytes in acid-base regulation during embryogenesis

New insights into ion regulation of cephalopod molluscs: a role of epidermal ionocytes in acid-base regulation during embryogenesis

Marian Y. Hu[1#], Yung-Che Tseng[2#], Li-Yih Lin[3], Mireille Charmantier-Daures[4], Pung-Pung Hwang[2*] and Frank Melzner[1]

[1] Leibniz-Institute of Marine Sciences (IFM-GEOMAR), Kiel 24105, Germany

[2] Institute of Cellular and Organismic Biology, Academia Sinica, Nangang, Taipei, Taiwan, Republic of China (ROC)

[3] Department of Life Science, National Taiwan Normal University, Taipei, Taiwan, Republic of China (ROC)

[4]Equipe Adaptation Ecophysiologique et Ontogenèse, UMR 5119 Ecolag, Université Montpellier 2, F-34095 cedex 05, France

*To whom correspondence should be addressed:

P. P. Hwang, Institute of Cellular and Organismic Biology, Academia Sinica, Nankang, Taipei, Taiwan 11529, R.O.C

TEL: +8862-2789-9521; FAX: +8862-2789-9576; E-mail: pphwang@gate.sinica.edu.tw

[#] These authors contributed equally to the present work

Abstract

The constraints of an active life in a pelagic habitat led to a numerous convergent morphological and physiological adaptations that enable cephalopod molluscs and teleost to compete for similar resources. Here we show for the first time that such convergent developments are also found in the ontogenetic progression of ion regulatory tissues: epidermal ionocytes scattered on skin and yolk sac appear to be responsible for ionic and acid-base regulation before gill epithelia become functionable. Acid-base regulatory capacities are important for fish and cephalopod embryos, due to challenging abiotic conditions (low pH, high pCO_2) inside the protecting egg capsule.

Epidermal ionocytes were characterized via immunohistochemistry, *in situ* hybridization and vital dye staining techniques. We found one group of cells that is recognized by Concavalin A and MitoTracker, which also expresses Na^+/H^+ exchangers (NHE) and Na^+/K^+-ATPase. Similar to findings obtained in teleost these NHE3-rich cells take up sodium in exchange for protons, illustrating the energetic superiority of NHE based proton excretion in marine systems. Novel *in vivo* electrophysiological techniques prove that acid equivalents are secreted by the yolk and skin integument. Intriguingly, epidermal ionocytes of cephalopod embryos are ciliated as demonstrated by scanning electron microscopy demonstrating a dual function of epithelial cells in water convection, and ion regulation. These findings add significant knowledge to our mechanistic understanding of hypercapnia tolerance in marine organisms, as it demonstrates that marine taxa which were identified as powerful acid-base regulators in the context of ocean acidification already need to exhibit strong acid-base regulatory abilities during embryogenesis.

Introduction

Cephalopods are exclusively marine invertebrates that have a high degree of mobility, high metabolic rates, well developed neuronal systems and efficient sensory organs (Hanlon and Messenger 1996; Budelmann et al. 1997; Seibel and Drazen 2007; Hu et al. 2009). It is believed that these features are derived from the evolutionary competition of cephalopods and fish in the marine environment (Packard 1972; O`Dor and Webber 1986). Owing to their active lifestyle, marine invertebrates such as cephalopods and crustaceans as well as marine vertebrates (e.g. fish) are also powerful acid-base regulators that actively maintain their blood pH within tight boundaries in order to protect their pH sensitive respiratory pigments from acidosis (Pörtner et al. 1991; Wheatly and Henry 1992; Claiborne and Edwards 2002; Evans et al. 2005; Gutowska et al. 2009).

In marine crustaceans the gill was identified as a major site for ionic regulation enabling the active secretion of acid/base equivalents into the surrounding sea water by involving primarily Na^+/H^+ and HCO_3^-/Cl^- exchange mechanisms in order to maintain extracellular pH homeostasis (Wheatly and Henry 1992; Charmantier and Charmantier-Daures 2001; Whiteley et al. 2001). These epithelia are rich in Na^+/K^+-ATPase (NKA) which provides the driving force for a variety of other secondary active transport processes such as apical Na^+/H^+ exchangers (NHE) and Na^+ dependent Cl^-/HCO_3^- exchangers (NBCs) that can extrude protons and import HCO_3^- (Boron 2004; Romero et al. 2004). Therefore, NKA is regarded an excellent marker for the ion-regulatory capacity of a given tissue (Gibbs and Somero 1990).

Recently it has been shown that gills of cephalopods also exhibit high NKA concentrations in basolateral membranes of the transport active gill epithelium. Furthermore, these NKA rich cells express acid-base regulatory proteins such as Na^+ dependent Cl^-/HCO_3^- exchangers (NBCs), carbonic anhydrase (CA) and V-type-H^+-ATPase (V-HA) (Hu et al. 2010a; Hu et al. 2010b).

Analogous to the situation in cephalopod molluscs and crustaceans, both gill and gut are also the main sites of ion and acid-base regulation in fish (Evans et al. 2005; Grosell 2006; Hwang and Lee 2007). While gut epithelia are mainly important for the secretion of HCO_3^- and $CaCO_3$ precipitation (Grosell et al. 2009a), specialized cells, so called mitochondrion rich cells (MRCs) were identified as the main sites of ionic regulation in teleost gill epithelia (for a review see Hwang and Lee 2007).

In contrast to adults, fish early life stages show ontogeny specific alternative sites for ion-regulation. Before gill epithelia are fully developed, scattered epidermal ionocytes on the skin mediate ion and acid-base balance (Pan et al. 2005; Lin et al. 2006; Hsiao et al. 2007; Hwang and Perry 2010). Recently, functional genomics and immunohistological studies revealed the embryonic yolk-sac epithelium to be the major site for osmoregulation in teleosts (see reviews by Hwang 2009; Hwang and Perry 2010). Such an ontogeny-dependent shift in the location of ion-regulatory epithelia has also been demonstrated in marine crustaceans (Charmantier and Charmantier-Daures 2001; Charmantier et al. 2001; Cieluch et al. 2005). For example, decapodit stages of the brown shrimp *Crangon crangon* exhibit NKA rich ionocytes in the branchiostegite epithelium. These disappear in juveniles and positive NKA immunoreactivity is found in cells of the gill lamellae (Cieluch et al. 2005).

In contrast to decapod crustaceans and teleost fish, the comparatively stenohaline cephalopod molluscs are weak osmoregulators. Their body fluids are slightly hypoosmotic (cuttlefish *Sepia officinalis*) or isoosmotic (squid *Lolliguncula brevis*) with respect to the environmental seawater (Robertson 1949; Schipp and Hevert 1980), a feature that is probably closely related to their comparatively thin (and ion permeable) skin, which serves as a respiratory organ (Madan and Wells 1996). Nevertheless, the ability to regulate extracellular pH must already be very important for the developing cephalopod embryo due to high metabolic rates at the end of development and the egg capsule acting as a diffusion barrier for respiratory gases (e.g. O_2 and CO_2) to the environment. High pCO_2 (up to 0.4 kPa) builds up in the egg perivitelline fluid (PVF) in order to drive excretory flux of metabolic CO_2. The consequence is a comparatively low PVF pH of <7.4 towards the end of embryonic development (Gutowska and Melzner 2009). It can be hypothesized from these findings that already the developing embryo needs a potent acid-base regulatory machinery to eliminate protons from body fluids in order to cope with hypercapnia induced acidosis.

This work addresses the question, whether early developmental stages of cephalopod mollusks secrete protons and in how far they are characterized by specific sites for ion and acid-base regulation. The anatomical and morphological features of cephalopod embryos prompted us to formulate the hypothesis that also in cephalopods, the yolk epithelium may constitute a major site of acid-base regulation, as it is well perfused from in and outside and has a large surface area.

We use cuttlefish (*Sepia officinalis*) and squid (*Sepioteuthis lessoniana*) early life stages in order to demonstrate alternative sites of ion regulation via immunohistochemical, *in situ* hybridization, vital dye and electrophysiological methods.

Material and methods

Experimental animals

Sepiteuthis lessoniana egg clusters were collected in Aodi, Taiwan (R.O.C.) in July 2010 by SCUBA diving and reared in a closed recirculating system at the Institute of Cellular and Organismic Biology, Academia Sinica. *Sepia officinalis* egg clusters were collected in Luc sur Mer, France, in May 2010. Cuttlefish eggs were raised at the Leibniz-Institute of Marine Sciences (IFM-GEOMAR), Kiel, Germany, in a closed recirculating system.

Na^+/K^+-ATPase activity assay

Na^+/K^+-ATPase activity was measured in whole animal crude extracts in a coupled enzyme assay with pyruvate kinase (PK) and lactate dehydrogenase (LDH) using the method of Allen and Schwarz (1969) as described by Melzner et al. (2009a). The oxidation of NADH coupled to the hydrolysis of ATP was followed photometrically at 15°C in a DU 650 spectrophotometer (Beckman Coulter, USA) over a period of 10 min, measuring the decrease of extinction at λ = 339 nm. The fraction of Na^+/K^+-ATPase activity in total ATPase activity was determined by the addition of 17 µl of 5 mM ouabain to the assay. Each sample was measured in sextuples. Enzyme activity was calculated using an extinction coefficient for NADH of ε = 6.31/mM·cm and given as micromoles ATP consumed per gram tissue fresh mass per hour.

In situ hybridization

Digoxigenin- or dinitrophenol-labeled (Roche, Penzberg, Germany) RNA probes were synthesized by in vitro transcription with T7 and SP6 RNA polymerase (Roche). Whole mount in situ hybridization was performed as previously described (Thisse et al. 2004).

Immunohistochemical staining

For immunocytochemistry on paraffine sections, whole animals were fixed by direct immersion for 24 h in Bouin's fixative followed by rinsing in 70 % ethanol. Samples were fully dehydrated in graded ethanol series and embedded in Paraplast (Paraplast Plus, Sigma, P3683). Sections of 4 µm were cut on a Leitz Wetzlar microtome, collected on poly-L-lysine-coated slides, and stored at 37°C for 48 h. The slides were deparafinized in Histochoice tissue fixative (Sigma, H2904) for ten minutes, washed in butanol and passed through a descending alcohol series.

For whole mount and sections samples were washed with PBS, and incubated with 3 % BSA for 30 min to block nonspecific binding. Samples were then incubated overnight at 4°C with a Na^+/K^+-ATPase α1 of human origin (diluted 1:50; Na^+/K^+-ATPase α (H-300), Santa Cruz Biotechnology, INC.) and a polyclonal antibody raised in rabbit against a synthetic peptide corresponding to a C-terminal region of tilapia NHE3 (diluted 1:100; generous provided by Dr. Toyoji Kaneko). After being rinsed with PBS for 20 min, samples were further incubated in goat anti rabbit IgG Alexa-Flour 488 and 568 (dilution 1:100). To allow double-color immunofluorescence staining for NKA and NHE3, one of the polyclonal antibodies (e.g. NKA) was directly labeled with Alexa Fluor dyes using Zenon antibody labeling kits (Molecular Probes, Eugene, OR, USA). After rinsing in PBS (3x5 min), samples were examined with a fluorescent microscope (Zeiss Imager 1M) with an appropriate filter set and a phase contrast device.

Vital dye staining

Embryos were carefully removed from the egg capsule and incubated in the perivitelline fluid (PVF) for vital dye staining. Na -dependent fluorescent reagent, Sodium Green tetra-acetate cell permeant (Invitrogen), was diluted in DMSO to a 10-mM stock solution. Sodium Green is well established as a reagent to detect intracellular Na^+ accumulation (Tseng et al.; Esaki et al. 2007). Living stage 26-28 embryos were incubated in 10 µM Sodium Green diluted in 0.2 µm filtered natural SW for 40 min.

Mitochondrial-staining reagent, MitoTracker Green FM (Invitrogen, M-7514), was used to detect mitochondria rich cells on the skin of cephalopod embryos. For staining with

MitoTracker, embryos were incubated for 30 min in 500 nM MitoTracker for 30 min. In double stains of Sodium Green and MitoTracker with concanavalin A (ConA; a lectin protein capable of selectively binding α-mannopyranosyl and α-glucopyranosyl residues), embryos were first incubated in 10 µM Sodium Green or 500 nM MitoTracker for 40 min and subsequently transferred to a solution of 50 µg/ml of Alexa Fluor 594-conjugated ConA (Invitrogen) diluted in filtered seawater and incubated for 40 min.

Embryos were washed briefly with filtered seawater and anesthetized with 0.2-0.5 % $MgCl_2$ which is a widely used non-toxic anaesthetic for cephalopods (Messenger et al. 1985). Pictures were taken using a fluorescent microscope (Imager M1, Zeiss). Sodium Green was excited by a mercury vapor light source through an excitation filter with maximum transmission at 485 nm and a 20-nm bandwidth. The fluorescence was collected using a 515- to 565-nm band-pass emission filter. We performed negative controls with untreated embryos (supplemental Fig.S2). Single focused images were created from a series of partially focused images using software from Helicon Focus (Helicon Soft, Kharkov, Ukraine).

Scanning electron microscopy

For observations by electron microscope living squid embryos were removed from the egg capsule and immediately fixed in 4 % paraformaldehyde with 5 % glutaraldehyde for 10 h. Afterwards the samples were transferred to a 0.1 M sodium cacodylate buffer solution (CACO) and washed three times. The membrane fixation was performed with 1 % OsO_4 in 0.1 M PB for 30 min under a fume hood. After fixation the samples were washed in 0.1 M sodium cacodylate buffer. For dehydration the samples passed an ascending concentration of ethanol. The samples were dried in a critical point drier (Hitachi HCP-2 CPD), gold coated (Cressington Sputter Coater 108), and observed using a scanning electron microscope (ESEM, FEI Quanta 200).

Scanning ion-selective electrode technique

The SIET was used to measure H^+ fluxes at the surface of *Sepioteuthis lessoniana* embryos (stage 28). Glass capillary tubes (no. TW 150–4, World Precision Instruments, Sarasota, FL)

were pulled on a Sutter P-97 Flaming Brown pipette puller (Sutter Instruments, San Rafael, CA) into micropipettes with tip diameters of 3–4 µm. These were then baked at 120°C overnight and vapor-sianized with dimethyl chlorosilane (Sigma- Aldrich) for 30 min. The micropipettes were backfilled with a 1 cm column of electrolytes and frontloaded with a 20 to 30 µm column of liquid ion exchanger cocktail (Sigma-Aldrich) to create an ionselective microelectrode (probe). The following ionophore cocktail (and electrolytes) was used: H^+ ionophore I cocktail B (40 mM KH_2PO_4 and 15 mM K_2HPO_4; pH 7). The details of the system were described in a previous report (Lin et al. 2006). To calibrate the ion-selective probe, the Nernstian property of each microelectrode was measured by placing the microelectrode in a series of standard solutions (pH 6, 7, and 8). By plotting the voltage output of the probe against log [H^+] values, a linear regression yielded a Nernstian slope of 58.6 ± 0.6 (*n* = 10) for H^+.

Measurement of surface H^+ gradients and determination of apparent H^+ fluxes

The SIET was performed at room temperature (26–28°C) in a small plastic recording chamber filled with 2 ml “recording medium” that contained 0.5 mM NaCl, 0.2 mM $CaSO_4$, 0.2 mM $MgSO_4$, 300 µM MOPS buffer, and 0.3 mg/l ethyl 3-aminobenzoate methanesulfonate (Tricaine, Sigma-Aldrich). The pH of the recording media was adjusted to 7.0 by adding NaOH or HCl solutions. Before the measurement, embryos were slightly anaesthetized with 0.2–0.5 % $MgCl_2$ and positioned in the center of the chamber with its dorsal side contacting the base of the chamber. The ion-selective probe was moved to the target position (10–20 µm away from the larval surface) to record the ionic activities, then the probe was moved away (10 mm) to record the background. In this study, [H^+] were used to represent the measured H^+ gradients between the targets (at the surface of larval skin) and background. The voltage outputs were converted to H^+ concentrations according to the 3-point calibration curve (described above), and Δ[H^+] was used to represent the measured H^+ gradients between the target point on the skin surface and the background.

Results

Ontogeny-dependent of Na^+/K^+-ATPase activity and localization in cephalopod

During embryonic development of *Sepia officinalis* ATPase activities in whole animal homogenates reached detectable levels in stage 26/27 embryos with a body mass of 30 to 60 mg_{FM} (Fig. 1A). Later, in stage 28 to 29 embryos enzyme activities increase rapidly, until activities stabilize towards hatching (200-300 mg body mass). After hatch animals increase their body mass, but do not show a further increase in specific Na^+/K^+-ATPase and total ATPase activity. Both, total ATPases and Na^+/K^+-ATPase increase in a similar fashion, following a sigmoid curve matching the increased concentration of this enzyme detected via immuno-histochemical methods. During this final phase of development from stage 27 until hatching embryos increase their body mass by approximately 400 % (from 100 to 400 mg wet mass).

In *Sepia officinalis* stage 24 embryos (ML=2-3 mm), the gills were 60-80 µm in length and not yet fully differentiated, missing the 2^{nd} and 3^{rd} order lamellae (Fig. 1B). During ontogeny the gills progressively differentiate with 1^{st} to 3^{rd} order vessels and lamellae visible in stage 30 embryos at a total gill length of approximately 900 µm and ML 8-10 mm (Fig. 1B). NKA is not detectable in gill tissues until stage 24 embryos, whereas in later stages (25 to 30) this enzyme begins to progressively occur in the developing gill (Fig. 1B). The increase of NKA staining correlates with the differentiation of gill lamellae towards hatching.

The pancreatic appendages (PA) in *S. officinalis* are part of the digestive tract and consist of alveolar/tubular shaped protrusions of the ductus hepatopancreas within the dorsal renal sac (Fig. 1C). In stage 30 embryos these protrusions had a diameter ranging from 15-25 µm to 100-200 µm (ML=6-7 mm). These appendages consist of an inner and an outer epithelium. The cells of both epithelia line a blood sinus with their basal lamina. Generally, the cells of the inner epithelium are two to three-fold higher than those from the outer epithelium (Fig. 1C). In late stage embryos (stage 27-30) the cells of the inner epithelium can be characterized by a very strong NKA immunoreactivity, whereas the outer epithelium shows little immunoreactivity in its membranes. In stage 23 embryos no or only very weak NKA immunoreactivity is detectable in the PA. With the differentiation of this organ during embryonic development, the occurrence of NKA increases towards hatching in a similar manner as described for the gill epithelium (Fig. 1C).

Whole mount *in situ* hybridization

Whole mount in situ hybridization with *S. officinalis* embryos revealed expression of NKA in the head region and on the yolk epithelium. In stage 27 embryos reaction precipitates were found in several areas of the head with highest densities below the eye (Fig. 2A), and on the ventral side of the head (Fig. 2A). Strong NKA expression was observed in sensory cells of the olfactory organ forming an oval shape on the embryo`s cheeks (Fig. 2A). In addition to sensory cells of the olfactory organ sensory cells of the head-line organ exhibited clearly visible expression of NKA. These sensory cells are forming longitudinal lines on the head of late stage embryos and belong to the head line system described for some decapod cephalopods (Arnold and Williams-Arnold 1980; Budelmann et al. 1997) (Fig. 2A).

Finally, single oval shaped cells scattered on the yolk sac epithelium showed expression of NKA in these late stage cuttlefish embryos (Fig. 2A).

Characterization and morphology of ionocytes on the yolk epithelium and skin

Whole mount immunohistochemical analysis demonstrates that particular cells which are scattered on the yolk sac epithelium of cephalopod embryos show a positive NKA immunoreactivity (Fig. 2B). These NKA-rich cells (NaRCs) are approximately 10 µm in diameter and occur in densities of 40-60 cells per 100 μm^2. Double staining of NKA and NHE3 demonstrates that NHE3 is co-localized with NaRCs on the yolk sac epithelium (Fig. 2B). Furthermore, high magnification images show that the distribution of NKA is mesh-like whereas NHE3 is distributed equally in membranes of NaRCs. Furthermore, no sodium-rich cells were found on the yolk sac epithelium. Instead, small vesicles located inside the pavement cells/accessory cells (Pisam and Rambourg 1991) of the entire yolk epithelium show positive sodium reactivity (Fig. 3).

Besides the yolk epithelium single cells scattered on mantle and head of squid and cuttlefish embryos showed a positive NKA immunoreactivity (Fig. 4). Double staining with Concavalin A (ConA) revealed that NKA rich cells are not co localized with ConA labeled cells. Instead ConA labeled cells on the entire skin of cephalopod embryos were characterized by high Na^+/H^+ exchanger (NHE3) concentrations and sodium accumulation (Fig. 4). The general distribution pattern of these sodium-rich cells on the skin of *Sepioteuthis*

lessoniana embryos reveals that sodium rich cells are located on the mantle, the head and the yolk epithelium of squid embryos. However, highest densities of sodium-rich cells are found on the lateral side of the head, arms and close to the olfactory organ (Fig. 4).

Using MitoTracker we were able to identify two types of mitochondrium rich cells including sensory cells exclusively located on the head of the embryo and the beforehand mentioned ConA labeled ionocytes (Fig. 4). By merging Sodium Green labeled cells with a bright field phase contrast image we were able to show that the sodium-rich, ConA labeled ionocytes are ciliated cells distributed over the entire skin of the cephalopod embryo which highest densities located in the head and arm region (Figs. 4, 5D).

Scanning electron microscopy analysis reveals the occurrence of different types of ciliated cells located on the mantle, head and yolk of the embryo as previously described by Arnold and Williams-Arnold (1980) (Fig. 5). Moreover, high resolution images demonstrate that underneath the cilia these cells seem to have mesh-like openings (Fig. 5C indicated by arrows) which resemble ionocyte openings described for the skin of fish larvae (Hsiao et al. 2007; Horng et al. 2009). The presence of these pores on the outer surface of skin ionocytes is further supported by the pattern of ConA labeling which consists of dots scattered over the entire surface of one ionocyte (Fig. 5E, the pattern is very similar to that observed in zebrafish by Horng et al. (2009)).

H^+ gradients on the surface of skin and yolk epithelia

Using ion selective electrodes we determined H^+ gradients, from which fluxes of H^+ were calculated at different locations on the entire surface of squid embryos (Fig. 6). On the yolk, smaller proton gradients were detected with a $\Delta[H^+]$ 1.0 to 1.5 µmol over the entire yolk epithelium (points 1 to 5). On the skin close to the eye (point 6) proton secretion shows peak $\Delta[H^+]$ with up to 2.5 µmol, whereas on the mantle (point 7) proton $\Delta[H^+]$ levels decrease again down to 1.9 µmol.

Discussion

The convergent evolution of morphological and physiological features enabling mobile cephalopods and fish to compete for similar resources in marine pelagic and bentho-pelagic habitats has been widely recognized (Packard 1972; O`Dor and Webber 1986). Here we show for the first time that such convergent development can be found in the lecithotrophic embryonic stages of decapod cephalopods: epidermal ionocytes on skin and yolk sac appear to be responsible for ionic regulation before gill epithelia become functionable. Furthermore, this is the first study that shows that *in vivo* acid equivalents are secreted by the yolk and skin integument of a marine invertebrate.

Marine animals that exhibit an oviparous mode of development such as most fish and cephalopods are exposed to very high pCO_2 values during their embryonic development. This is mainly due to the fact that egg capsules of most molluscs, amphibians and fish were shown to act as a diffusion barrier for respiratory O_2 and CO_2 (Diez and Davenport 1987; Cohen and Strathmann 1996; Cronin and Seymour 2000; Fernandez et al. 2000; Gutowska and Melzner 2009). In order to maintain a sufficiently high flux of oxygen in and carbon dioxide out of the egg capsule, hypoxic hypercapnic conditions develop inside the egg fluid of cephalopod (and, probably, fish) eggs, particularly towards the end of embryonic development, when metabolic rates are highest (Gutowska and Melzner 2009). A recent study demonstrated, that increases in environmental pCO_2 are additive to those of the perivitelline fluid (PVF) of cephalopod eggs, leading to pCO_2 values as high as 0.6 kPa at an environmental pCO_2 of 0.35 kPa (Hu et al. 2010b). Such high environmental pCO_2 values can be encountered by cephalopod and fish egg masses in seasonally hypoxic coastal habitats (Thomsen et al. 2010). Hypoxic hypercapnic conditions constitute a major abiotic stress to the developing embryo in terms of acid-base disturbances as they also lead to an increased pCO_2 of body fluids in order to maintain the diffusive flux of CO_2 out of the animal (Melzner et al. 2009b). As late stage embryonic fish and cephalopods rely on haemoglobin/haemocyanin driven oxygen transport as well, it can be assumed that these embryonic stages require an efficient acid-base regulatory machinery in order to protect their pH sensitive respiratory pigments from hypercapnia induced pH reductions. In order to accomplish this, both, cephalopods and fish have to manipulate their extracellular carbonate system: elevated blood [HCO_3^-] at the high surrounding pCO_2 values guarantee pH values

suitable for protein mediated gas transport (Larsen et al. 1997; Gutowska et al. 2009). However, maintenance of blood acid-base status requires continuous net H^+ excretion, thus, ion regulatory effort.

During larval development of fish and cephalopods, rudimentary gill structures progressively occur and become completed when the organism has reached an adult-type morphology (Arnold 1965; Schipp et al. 1979; Hwang 1990; Pan et al. 2005). Prior to the gills it has been demonstrated that the fish integument is responsible for respiratory gas exchange (Wells and Pinder 1996) and ionocytes on the yolk epithelium are involved in osmo- and acid-base regulation (Guggino 1980; Hwang et al. 1994; Lin et al. 2006; Hwang and Perry 2010). During cephalopod organogenesis, thus before systemic and branchial hearts are developed, muscle cells on the yolk sac are responsible for convective circulation of hamolymph: peristaltic movements propel hemolymph around the yolk syncytium and into the extensive lacunar blood system of the embryo. Prior to differentiation of blood vessels, these blood sinuses are occupying large volumes of the embryonic body, particularly in the (metabolically) active head region (see von Boletzky 1987a; von Boletzky 1987b). Thus, the integument must be the main respiratory organ in cephalopods prior to gill development, and well perfused and metabolically active regions such as the head and the 'yolk sac heart' are prime candidate tissues for the localization of ionocytes. With our study we can add prove that exactly these tissues are major sites of ionic exchange in the developing cephalopod embryo. The characterization of epidermal ionocytes, predominantly located on the skin in the head region of cephalopod embryos, demonstrated that one group of cells which were recognized by ConA and MitoTracker also express NHE3. These NHE3-rich cells are apparently responsible for sodium uptake. Further, our micro-electrode measurements demonstrated that these cells also mediate proton excretion. Another group of epithelial cells are exclusively labeled by the NKA antibody. It is unclear what the function of these cells is. In zebrafish (*Danio rerio*) embryos, at least three types of epidermal ionocytes were identified and classified into Na^+/Cl^- -cotransporter (NCC), Na^+/K^+-ATPase (NaR) and proton pump (HR) rich cells (for a review see Hwang and Perry 2010). The latter were further characterized by high sodium accumulation which was completely blocked in the presence of amiloride, a NHE inhibitor, supporting the role of apical NHE3 in sodium uptake (Esaki et al. 2007). Interestingly, epidermal ionocytes located in the head region of *S. lessoniana* embryos share many parallel features to fish HR cells, such as high sodium

concentrations, high mitochondrial densities, NHE3 protein, but no detectable NKA immunoreactivity. However, ionocytes located on the yolk sac epithelium are rich in NKA and NHE3. Another group of ConA-positive cells which are similar to accessory/pavement cells in appearance (supplemental Fig. S1) surprisingly can absorb sodium from the ambient medium.

While the skin, especially in the head and tentacle region, is characterized by a strong outward directed proton flux, the cephalopod yolk epithelium is characterized by a comparatively lower proton efflux. Although the yolk sac organ is characterized by a lower efflux of protons, it needs to be noted that this organ exhibits a relatively large surface area compared to the head and the mantle. Especially in earlier stages with a decreasing body surface to yolk surface ratio, the yolk can be considered an even more significant site for proton secretion, and thus, pH regulation.

In embryos of teleosts, the yolk epithelium was also identified as a major site of ionic regulation, indicated by the presence of four different subtypes of ionocytes equipped with transporters relevant for ion/acid-base regulation (see reviews by Hwang and Lee 2007; see reviews by Hwang and Perry 2010). Athough V-type-H^+-ATPases were identified to be key players of apical acid secretion pathways in fresh water fish (Evans et al. 2005; Perry and Gilmour 2006; Hwang and Lee 2007), new models for pH regulation are recently emerging for the marine environment (Wu et al. 2010). Immunohistochemical and electrophysiological methods demonstrated that epithelial ionocytes of *Oryzias latipes* larvae which are rich in NHE3 and Rhcg are actively involved in the secretion of protons (Wu et al. 2010). This involvement of NHE-like proteins in the secretion of protons and thus acid-base regulation is similar to their role in the renal proximal tubule of the mammalian kidney. Here, the majority of protons are excreted into the lumen of the tubule via different NHE isoforms, including NHE2, NHE3 and NHE8 located in the brush-border microvilli of the proximal tubule (Wang et al. 1999; Goyal et al. 2003; Wagner et al. 2003).

We hypothesize that active proton secretion from body fluids to the environment and, thus, pH_e regulation in cephalopod embryos is potentially achieved according to the hypothetical model depicted in Fig. 7. In this model, mitochondria-rich cells located on the skin of the embryo exhibit positive NHE3 immunoreactivity and high cytosolic sodium accumulation. Furthermore, the microenvironment in this area is characterized by increased

proton secretion and suggests, that also in cephalopod embryos NHE proteins may be major players of proton secretion in exchange for environmental sodium. The involvement of NHE in order secrete acid equivalent in the marine environment can be regarded thermodynamically favorable due to high external [Na^+] (approximately 460 mM) compared to low intracellular [Na^+] (approximately 30 mM in *Sepia officinalis*) which provide a natural driving force (Robertson 1949; Potts 1994). In the freshwater environment, where sodium gradients are opposed to those in marine habitats, V-type-H^+-ATPases were proposed to be responsible for the majority of H^+ secretion (Lin et al. 2006).

Intriguingly, the present work demonstrates that epidermal ionocytes of cephalopod embryos are ciliated. The primary role of these ciliated cells is to create a convective current inside the perivitelline fluid (PVF) in order to prevent the formation of gradients of dissolved respiratory gases and excretory products within PVF prior to full development of the ventilatory organs, the mantle and collar flap musculature (Arnold and Williams-Arnold 1980; Fioroni 1990; Bone et al. 1994). To our best knowledge this is the first report that shows that ciliated epidermal cells are involved in both, water transport, and are equipped with high concentrations of ion transporting molecules capable of proton secretion.

Further investigations are necessary to identify and characterize the full set of acid-base relevant proteins of these ionocytes. NHE and Rh proteins may be important candidate genes as they were proposed to have a dual NH_3/CO_2 transport function (Soupene et al. 2002; Soupene et al. 2004; Nawata et al. 2010), and thus, may represent another group of key transporters in embryonic acid-base regulation and gas exchange. Moreover, direct in vivo electrophysiological measurements demonstrate that acid equivalents are secreted by the yolk and skin integument of a marine organism, and that NHE may represent a major player in this process. Future investigations will apply ion selective electrode techniques on single ionocytes in combination with specific inhibitors, in order to demonstrate the importance of NHE proteins for proton secretion in embryonic stages of cephalopods and fish, and, thus utilize a comparative approach to derive fundamental mechanisms of acid-base regulation in these marine high-power taxa.

Acknowledgements

We are very grateful to J.P Robin and A. Fink who helped to obtain the cuttlefish eggs. This study was partly funded by a DFG Excellence Cluster Future Ocean grant awarded to F.M. and a DAAD/NSC PPP grant (project ID 50128946) awarded to F.M. and P-P. H.. This work is a contribution to the German Ministry of Education and Research (BMBF) funded project "Biological Impacts of Ocean ACIDification"(BIOACID) subproject 3.1.3 awarded to F.M..

References

1. Budelmann BU, Schipp R, von Boletzky S (1997) Cephalopoda. In: Harrison FW, Kohn AJ, editors. Microscopic anatomy of invertebrates. New-York: Wiley-Liss.

2. Hu MY, Yan HY, Chung WS, Shiao YC, Hwang PP (2009) Acoustically evoked potential in two cephalopods infered using the auditory brainstem response (ABR) approach. Comp Biochem Physiol 153: 278-283.

3. Hanlon RT, Messenger JB (1996) Cephalopod behaviour. Cambribge: Cambridge University Press. 232 p.

4. Seibel BA, Drazen JC (2007) The rate of metabolism in marine animals: environmental constraints, ecological demands and energetic opportunities. Phil Trans R Soc B doi: 10.1098/rstb2007.2101.

5. Packard A (1972) Cephalopods and fish: the limits of convergence. Biol Rev 47: 241-307.

6. O`Dor RK, Webber DM (1986) The constraints on cephalopods: why squid aren´t fish. Can J Zool 64: 1591-1605.

7. Gutowska MA, Melzner F, Langenbuch M, Bock C, Claireaux G, et al. (2009) Acid-base regulatory ability of the cephalopod (*Sepia officinalis*) in response to environmental hypercapnia. J Comp Physiol B in Press.

8. Pörtner H-O, Webber DM, Boutilier RG, O`Dor RK (1991) Acid-base regulation in exercising squid (*Illex illecebrosus*, *Loligo pealei*). Am J Physiol Regul Integr Comp Physiol 261: R239-R246.

9. Claiborne JB, Edwards SL (2002) Acid-base regulation in fishes: Cellular and molecular mechanisms. J Exp Zool 293: 302-319.

10. Evans DH, Piermarini PM, Choe KP (2005) The multifunctional fish gill: Dominant site of gas exchange, osmoregulation, acid-base regulation, and excretion of nitrogenous waste. Physiol Rev 85: 97-177.

11. Wheatly MG, Henry RP (1992) Extracellular and intracellular acid-base regulation in crustaceans. J Exp Zool 263: 127-142.

12. Charmantier G, Charmantier-Daures M (2001) Ontogeny of osmoregulation in crustaceans: The embryonic phase. Amer Zool 41: 1078-1089.

13. Whiteley NM, Scott JL, Breeze SJ, McCann L (2001) Effects of water salinity on acid-base balance in decapod crustaceans. J Exp Biol 204: 1003-1011.

14. Boron WF (2004) Regulation of intracellular pH. Adv Physiol Educ 28: 160-179.

15. Romero MF, Fulton CM, Boron WF (2004) The SLC4 family of HCO_3^- transporters. Eur J Physiol 447: 495-509.

16. Gibbs A, Somero GN (1990) Na^+-K^+-adenosine triphosphatase activities in gills of marine teleost fishes: changes with depth, size and locomotory activity level. Mar Biol 106: 315-321.

17. Hu MY, Sucré E, Charmantier-Daures M, Charmantier G, Lucassen M, et al. (2010) Localization of ion regulatory epithelia in embryos and hatchlings of two cephalopods. Cell Tiss Res 441: 571-583.

18. Hu MY, Tseng Y-C, Stumpp M, Gutowska MA, Kiko R, et al. (2010) Elevated seawater pCO_2 differentially affects branchial acid-base transporters over the course of development in the cephalopod *Sepia officinalis*. Am J Physiol Regul Integr Comp Physiol under review.

19. Grosell M (2006) Intestinal anion exchange in marine fish osmoregulation J Exp Biol 209: 2813-2817.

20. Hwang PP, Lee TH (2007) New insights into fish ion regulation and mitochondrion-rich cells. Comp Biochem Physiol A 148: 479-497.

21. Grosell M, Genz J, Taylor JR, Perry SF, Gilmour KM (2009) The involvement of H^+-ATPase and cerbonic anhydrase in intestinal HCO_3^- secretion in seawater-acclimated rainbow trout. J Exp Biol 212: 1940-1948.

22. Hsiao CD, You MS, Guh YJ, Ma M, Jiang YJ, et al. (2007) A positive regulatory loop between *foxi3a* and *foxi3b* is essential for specification and differentiation of zebrafish epidermal ionocytes. PLoS ONE 2: e302.

23. Lin LY, Horng JL, Kunkel JG, Hwang PP (2006) Proton pump-rich cell secretes acid in skin of zebrafish larvae. Am J Physiol Cell Physiol 290: C371-378.

24. Pan TC, Liao BK, Huang CJ, Lin LY, Hwang PP (2005) Epithelial Ca(2+) channel expression and Ca(2+) uptake in developing zebrafish. Am J Physiol Regul Integr Comp Physiol 289: R1202-1211.

25. Hwang PP, Perry SF (2010) Ionic and acid-base regulation. In: Perry SF, Ekker M, Farrel AP, Brauner CJ, editors. Zebrafish. London: Elsevier. pp. 311-344.

26. Hwang PP (2009) Ion uptake and acid secretion in zebrafish (*Danio rerio*). J Exp Biol 212: 1745-1752.

27. Cieluch U, Charmantier G, Grousset E, Charmantier-Daures M, Anger K (2005) Osmoregulation, immunolocalization of Na^+/K^+-ATPase, and ultrastructure of branchial epithelia in the developing brown shrimp, *Crangon crangon* (Decapoda, Caridea). Physiol Biochem Zool 78(6): 1017-1025.

28. Charmantier G, Haond C, Lignot J-H, Charmantier-Daures M (2001) Ecophysiological adaptation to salinity throughout a life cycle: A review in homarid lobsters. J Exp Biol 204: 967-977.

29. Robertson JD (1949) Ionic regulation in some marine invertebrates. J Exp Biol 26: 182-200.

30. Schipp R, Hevert F (1980) Ultrafiltration in the branchial heart appendage of dibranchiate cephalopods: a comparative ultrastructural and physiological study. J Exp Biol 92: 23-35.

31. Madan JJ, Wells MJ (1996) Cutaneous respiration in *Octopus vulgaris*. J Exp Biol 199: 2477-2483.

32. Gutowska MA, Melzner F (2009) Abiotic conditions in cephalopod (*Sepia officinalis*) eggs: embryonic development at low pH and high pCO_2. Mar Biol 156: 515-519.

33. Schwartz AA, Allen JC, Harigaya S (1969) Possible involvement of cardiac Na^+/K^+-adenosine triphosphatase in the mechanism of action of cardiac glycosides. J Pharmacol Exp Ther 168: 31-41.

34. Melzner F, Göbel S, Langenbuch M, Gutowska MA, Pörtner H-O, et al. (2009) Swimming performance in atlantic cod (*Gadus morhua*) following long-term (4-12 month) acclimation to elevated seawater pCO_2. Aqua Toxicol 92: 30-37.

35. Thisse B, Heyer V, Lux A, Alunni V, Degrave A, et al. (2004) Spatial and temporal expression of the zebrafish genome by large-scale in situ hybridization screening

Methods Cell Biol 77: 505-519.

36. Esaki M, Hoshijima K, Kobayashi S, Fukuda H, Kawakami K, et al. (2007) Visualization in zebrafish larvae of Na^+ uptake in mitochondria-rich cells whose differentiation is dependent on *foxi3a*. Am J Physiol Regul Integr Comp Physiol 292: R470-R480.

37. Tseng YC, Lee JR, Lee SJ, Hwang PP Functional analysis of the glucose transporters-1, -6, and -13.1 expressed by zebrafish epithelial cells. Am J Physiol Regul Integr Comp Physiol (in press).

38. Messenger JB, Nixon M, Ryan KP (1985) Magnesium chloride as an anaesthetic for cephalopods. Comp Biochem Physiol 82: 203-205.

39. Arnold JM, Williams-Arnold LD (1980) Development of the ciliature pattern on the embryo of the squid *Loligo pealei*: a scanning electron microscope study. Biol Bull 159: 102-116.

40. Pisam M, Rambourg A (1991) Mitochondria-rich cells in the gill epithelium of teleost fishes: an ultrastructural approach. Int Rev Cytol 130: 191-232.

41. Horng JL, Lin LY, Hwang PP (2009) Functional regulation of H^+-ATPase-rich cells in zebrafish embryos acclimated to an acidic environment. Am J Physiol Cell Physiol 296: c682-692.

42. Cronin ER, Seymour RS (2000) Respiration of the eggs of the giant cuttlefish *Sepia apama*. Mar Biol 136: 863-870.

43. Cohen CS, Strathmann RR (1996) Embryos at the edge of tolerance: Effects of environment and structure of egg masses on supply of oxygen to embryos. Biol Bull 190: 8-15.

44. Diez JM, Davenport J (1987) Embryonic respiration in the spiny dogfish (*Scyliorhinus canicula* L.). J Mar Biol Ass UK 67: 249-261.

45. Fernandez M, Bock C, Pörtner H-O (2000) The cost of being a caring mother: the ignored factor in the reproduction of marine invertebrates. Ecol Lett 3: 487-494.

46. Thomsen J, Gutowska MA, Saphörster J, Heinemann A, Trübenbach K, et al. (2010) Calcifying invertebrates succeed in a naturally CO_2 enriched coastal habitat but are threatened by high levels of future acidification. Biogeosciences Discussions (accepted): 5119-5156.

47. Melzner F, Gutowska MA, Langenbuch M, Dupont S, Lucassen M, et al. (2009) Physiological basis for high CO_2 tolerance in marine ectothermic animals: pre-adaptation through lifestyle and ontogeny? Biogeosciences 6: 2313-2331.

48. Larsen BK, Pörtner H-O, Jensen FB (1997) Extra- and intracellular acid-base balance and ionic regulation in cod (*Gadus morhua*) during combined and isolated exposures to hypercapnia and copper. Mar Biol 128: 337-346.

49. Arnold JM (1965) Normal embryonic stages of the squid, *Loligo pealii* (Lesueur). Biol Bull 128: 24-32.

50. Schipp R, Mollenhauer S, Boletzky S (1979) Electron microscopical and histochemical studies of differentiation and function of the cephalopod gill (*Sepia officinalis* L.). Zoomorph 93: 193-207.

51. Hwang PP (1990) Salinity effects on development of chloride cells in the larvae of ayu *Plecoglossus altivelis*. Mar Biol 107: 1-7.

52. Wells PR, Pinder AW (1996) The respiratory development of atlantic salmon. J Exp Biol 199: 2737-2744.

53. Hwang PP, Tsai YN, Tung YC (1994) Calcium balance in embryos and larvae of the freshwater-adapted teleost, *Oreochromis mossambicus*. Fish Physiol Biochem 13: 325-333.

54. Guggino WBT (1980) Salt balance in embryos of *Fundulus heteroclitus* and *F. bermudae* adapted to sea water. Am J Physiol 238R: 42-49.

55. von Boletzky S (1987) Embryonic phase. In: Boyle RP, editor. Cephalopod lifecycles. London: Academic Press. pp. 5-31.

56. von Boletzky S (1987) Ontogenetic and phylogenetic aspects of the cephalopod circulatory system. Experientia 43: 478-483.

57. Perry SF, Gilmour KM (2006) Acid–base balance and CO_2 excretion in fish: Unanswered questions and emerging models. Resp Physiol Neurobiol 154: 199-215.

58. Wu S-C, Horng J-L, Liu S-T, Hwang PP, Wen Z-H, et al. (2010) Ammonium-dependent sodium uptake in mitochondrion-rich cells of medaka (*Oryzias latipes*) larvae. Am J Physiol Cell Physiol 298: C2237-2250.

59. Goyal S, Vanden Heuvel G, Aronson PS (2003) Renal expression of novel Na/H exchanger isoform NHE8. Am J Physiol Renal Physiol 284: F467–F473.

60. Wang T, Yang CL, Abbiati T, Schultheis PJ, Shull GE, et al. (1999) Mechanism of proximal tubule bicarbonate absorption in NHE3 null mice. Am J Physiol Renal Physiol 277: F298–F302.

61. Wagner CA, Finberg KE, Breton S, Marshanski V, Brown D, et al. (2003) Renal vacuolar H^+-ATPase. Physiol Rev 84: 1263-1314.

62. Potts WTW (1994) Kinetics of sodium uptake in freshwater animals - a comparison of ion exchange and proton pump hypotheses. Am J Physiol 266: R315-R320.

63. Fioroni P (1990) Our recent knowledge of the development of the cuttlefish (*Sepia officinalis*). Zool Anz 224: 1-25.

64. Bone Q, Brown E, Travers G (1994) On the respiratory flow in the cuttlefish *Sepia officinalis*. J Exp Biol 194: 153-165.

65. Nawata CM, Hirose S, Nakada T, Wood CM, Katoh A (2010) Rh glycoprotein expression is modulated in pufferfish (*Takifugu rubripes*) during high environmental ammonia exposure. J Exp Biol 213: 3150-3160.

66. Soupene E, King N, Field E, Liu P, Niyogi KK, et al. (2002) Rhesus expression in a green alga *Chlamydomonas reinhardtii* at high CO_2. Proc Nat Acad Sci USA 99: 7769-7773.

67. Soupene E, Inwood W, Kustu S (2004) Lack of the Rhesus protein Rh1 impairs growth of the green alga *Chlamydomonas reinhardtii* at high CO_2. Proc Nat Acad Sci USA 101: 7787-7792.

68. Lemaire J (1970) Table de développement embryonaire de *Sepia officinalis* L. (Mollusque Céphalopode). Bull Soc Zool Fr 95: 773-782.

Figure Legends

Figure 1. Ontogeny dependent relative activity of total ATPases and Na^+/K^+-ATPase in whole animal homogenates of *Sepia officinalis* plotted against the animal mass (g_{FM}) and stage (according to Lemaire (1970)) (A). The increase in maximum activity was fitted by sigmoidal curves for both, total ATPase (solid line; R = 0.8704) and Na^+/K^+-ATPase (dashed line; R = 0.9493). At stage 27 all the major vessels of the arterial and venous system become distinct and the auxiliary hearts are functionable. In earlier stages (20-25) only primitive vena cava vessels and hemal spaces are found in the yolk and head region. Cross sections of the cuttlefish gill at stages 24, 25, 27, 28, 29 and 30, (according to Lemaire (1970)) showing first occurrence of Na^+/K^+-ATPase in gill tissues at stage 26 and progressively increasing with the development of the gill epithelium (B). Cross sections of the cuttlefish pancreatic appendages (PA) at stages 24, 26, 27 and 30, showing first occurrence of Na^+/K^+-ATPase in the inner epithelium (ie) of PA tissues at stage 26 and progressively increasing with the differentiation of the PAs. Ductus hepatopancreas (dh); oesophagus (oes); outer epithelium (oe) (C).

Figure 2. Whole mount *in situ* hybridization of Na^+/K^+-ATPase (NKA) on *Sepia officinalis* embryos (A). In stage 27 embryos, single NKA expressing cells are scattered on the ventral side of the head. Additionally, cells of the oval shaped olfactory organ are rich in NKA mRNA. Dorsal view of the head of a *S. officinalis* embryo, showing sensory cells of the head line system and scattered cells below the eye with high NKA expression. Expression of NKA on the yolk epithelium. Note the “salt and pepper” pattern of these ionocytes. Some of the cells which are most likely ionocytes are marked with arrows. Immunohistological localization of Na^+/K^+-ATPase and NHE3-rich cells on the yolk sac epithelium of the squid *Sepioteuthis lessonianaand* cuttlefish *Sepia officinalis* (stage 27 embryo) (B). In both species ionocytes are scattered in a “salt and pepper” pattern over the entire yolk epithelium. Higher magnification images of several ionocytes with positive Na^+/K^+-ATPase (NKA) and Na^+/H^+-exchanger (NHE3) immunoreactivity on the ventral side of the yolk with densities of 40 – 60 cells per 100 μm^2. Na^+/K^+-ATPase-rich cells are approximately 10 µm in diameter and are co-localized with NHE-rich cells.

Figure 3. Na^+ accumulation in cells on the skin and yolk of *Sepioteuthis lessoniana* embryo showing the morphology of the animal divided in mantle, head and yolk (A). On the skin in the mantle and head region Sodium Green, a Na^+-dependent fluorescent reagent, predominantly stains round-to-oval shaped cells scattered on the skin surface of stage 28 embryos (B and C). Higher cell densities are found on the lateral side of the head region (C). High magnification of the yolk sac surface demonstrating the presence of Sodium Green signals equally distributed in epithelial cells (D). Note the grain like pattern of the fluorescence signal in these cells.

Figure 4. Localization of Na^+/K^+-ATPase (NKA), Na^+/H^+-exchanger (NHE3) and the glycoprotein Concavilin A (ConA) in epidermal cells on the skin of *Sepiteuthis lessoniana* embryos (stage 26-27). Epidermal cells which are positively labeled by Con A are not co localized with NaR cells (left panel). These NaR cells are not co localized with cells that exhibit positive NHE3 immunoreactivity and ConA labeling (right panel). Insertion: *S. lessoniana* embryo with a rectangle indicating the area observed for immuno and vital dye staining.

Concavalin A (ConA) labeled cells on the skin of embryos are rich in mitochondria and sodium. Stainings with the cell permeant Sodium Green vital dye demonstrates that ConA labeled cells accumulate sodium (left panel). In addition to epidermal ionocytes, sensory cells (sc) with belong to the head-line organ of cephalopods are also rich in mitochondria (indicated by arrows) (right panel). These sensory cells are not positively labeled by Con A. Insertion: *S. lessoniana* embryo with a rectangle indicating the area observed.

Figure 5. Scanning electron micrographs of the skin and yolk surface of a squid embryo (stage 27). Ciliated cells are scattered over the skin of the head and arms of the embryo. The entire yolk is covered with ciliated cells (A). In contrast to the body, different types of ciliated cells with long (indicated with dashed lines) and short cilia are found on the yolk sac epithelium covering the entire surface (B). A single ciliated cell located on the skin at higher magnification (C). Note the pore-like openings in between the cilia indicated by arrows. Furthermore, sodium green labeled cells merged with a phase contrast image demonstrate

the co localization of sodium rich cells (surrounded with dashed lines) with ciliated cells on the skin (cilia indicated by arrows). Insertion, enlarged picture of one single ciliated cell merged with the same sodium green labeled cell (D). High magnification of Con A labeled cells showing the scattered distribution of Con A labeling on the surface of cells which support the mesh-like openings of this type of ionocyte that are very similar to those observed in zebrafish (Horng et al. 2009) (E).

Figure 6. Measurement of proton gradients ([ΔH^+]) on the skin and yolk epithelium of *Sepioteuthis lessoniana* embryos (stage 28-29). Ion selective electrode technique measurements demonstrate that the entire animal including yolk, head and mantle shows positive $\Delta[H^+]$ values with highest levels detected in the head region (spot 6) indicating a secretion of protons. Lower H^+ secretion values were recorded for the entire yolk surface. Relative $[H^+]$ gradients (bars) ± SD and absolute values (dashed lines); n = 8.

Figure 7. Hypothetical model of two types of ciliated ionocytes located on the yolk epithelium and skin of cephalopod embryos. One type of ionocyte on the yolk epithelium is characterized by the occurrence of Na^+/K^+-ATPase (NKA), probably located in basolateral membranes and apical NHE. Furthermore the cells of this epithelium are characterized by high concentrations of Na^+ localized in intracellular vesicles. Electrophysiological measurements demonstrated that the yolk epithelium is characterized by only relatively low proton secretion.

The skin of cephalopod embryos exhibits at least one other type of ionocyte. These positively Con A labeled cells are rich in mitochondria (M) and show high intracellular sodium accumulation. Additionally, these cells show positive NHE3 immunoreactivity, but are not co localized with NKA rich cells. Electrophysiological data suggest that ionocytes located on the skin are involved in active acid (probably also CO_2) secretion.

Figure 1

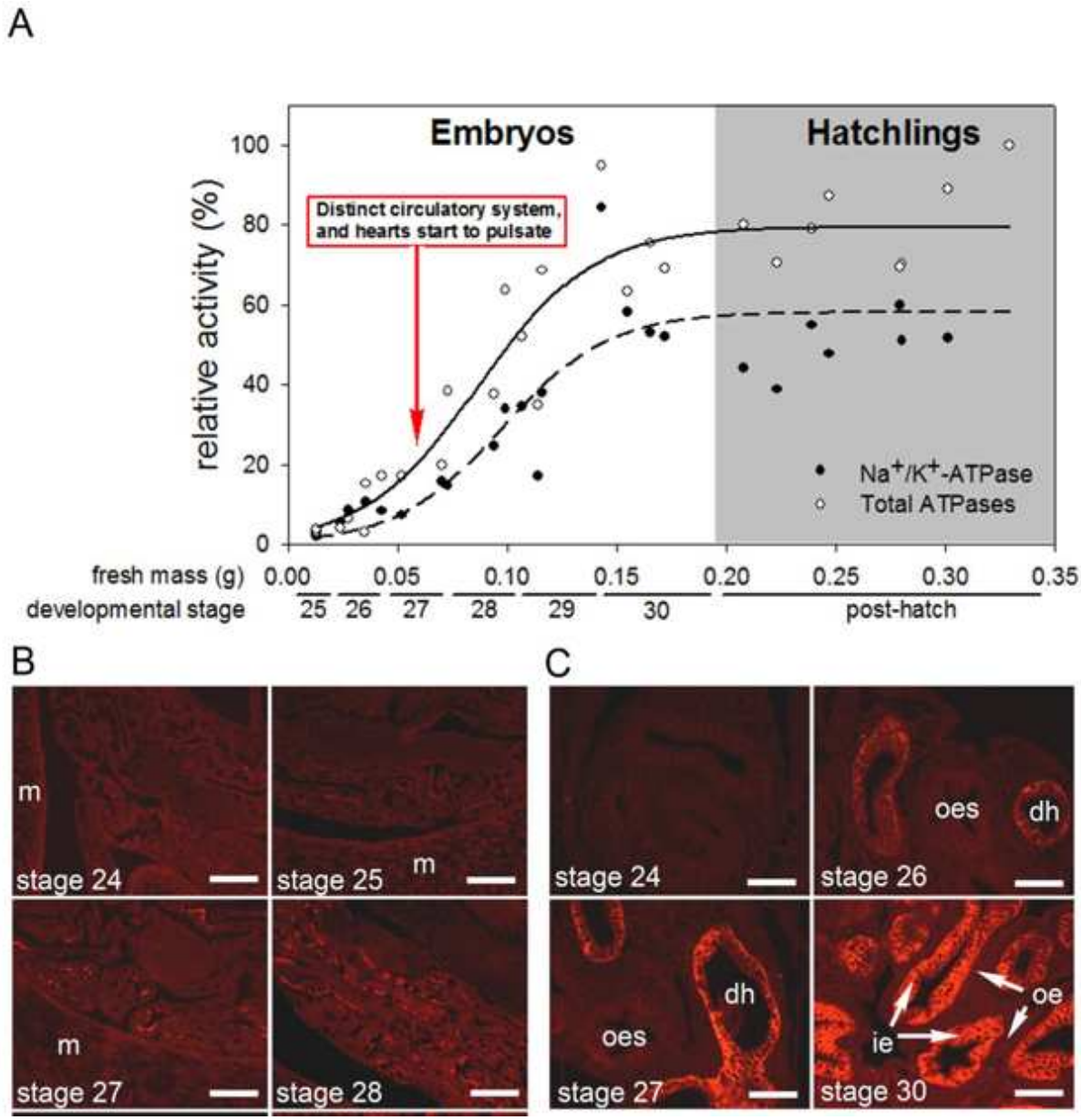
A
Embryos
Hatchlings
Distinct circulatory system, and hearts start to pulsate
relative activity (%)
100
80
60
40
20
0
Na+/K+-ATPase
Total ATPases
fresh mass (g)
0.00
0.05
0.10
0.15
0.20
0.25
0.30
0.35
developmental stage
25
26
27
28
29
30
post-hatch
B
m
stage 24
stage 25
m
m
stage 27
stage 28
C
stage 24
oes
dh
stage 26
dh
oes
stage 27
oe
ie
stage 30

Figure 2

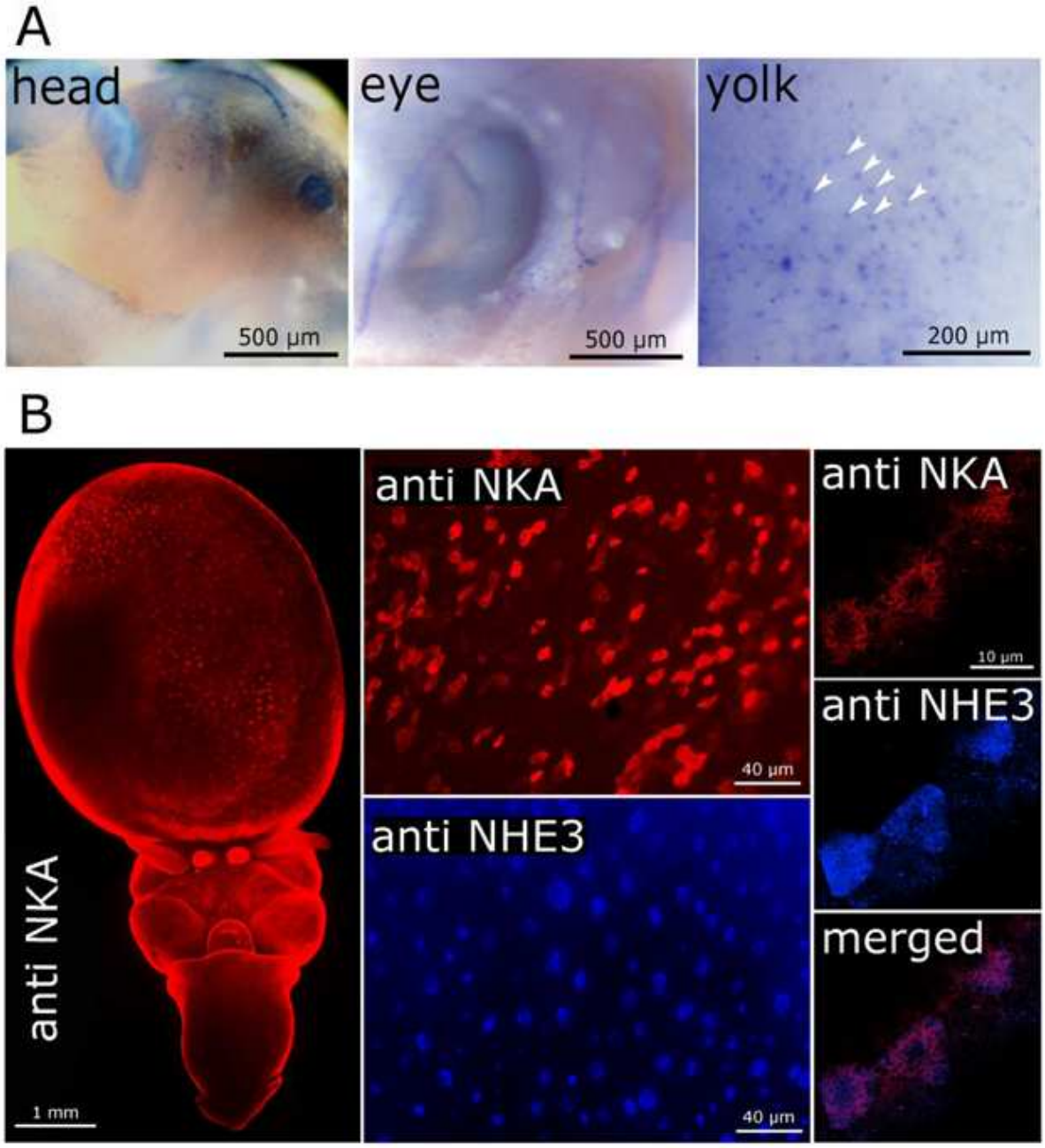
A
head
500 µm
eye
500 µm
yolk
200 µm
B
anti NKA
1 mm
anti NKA
40 µm
anti NKA
10 µm
anti NHE3
anti NHE3
40 µm
merged

Figure 3

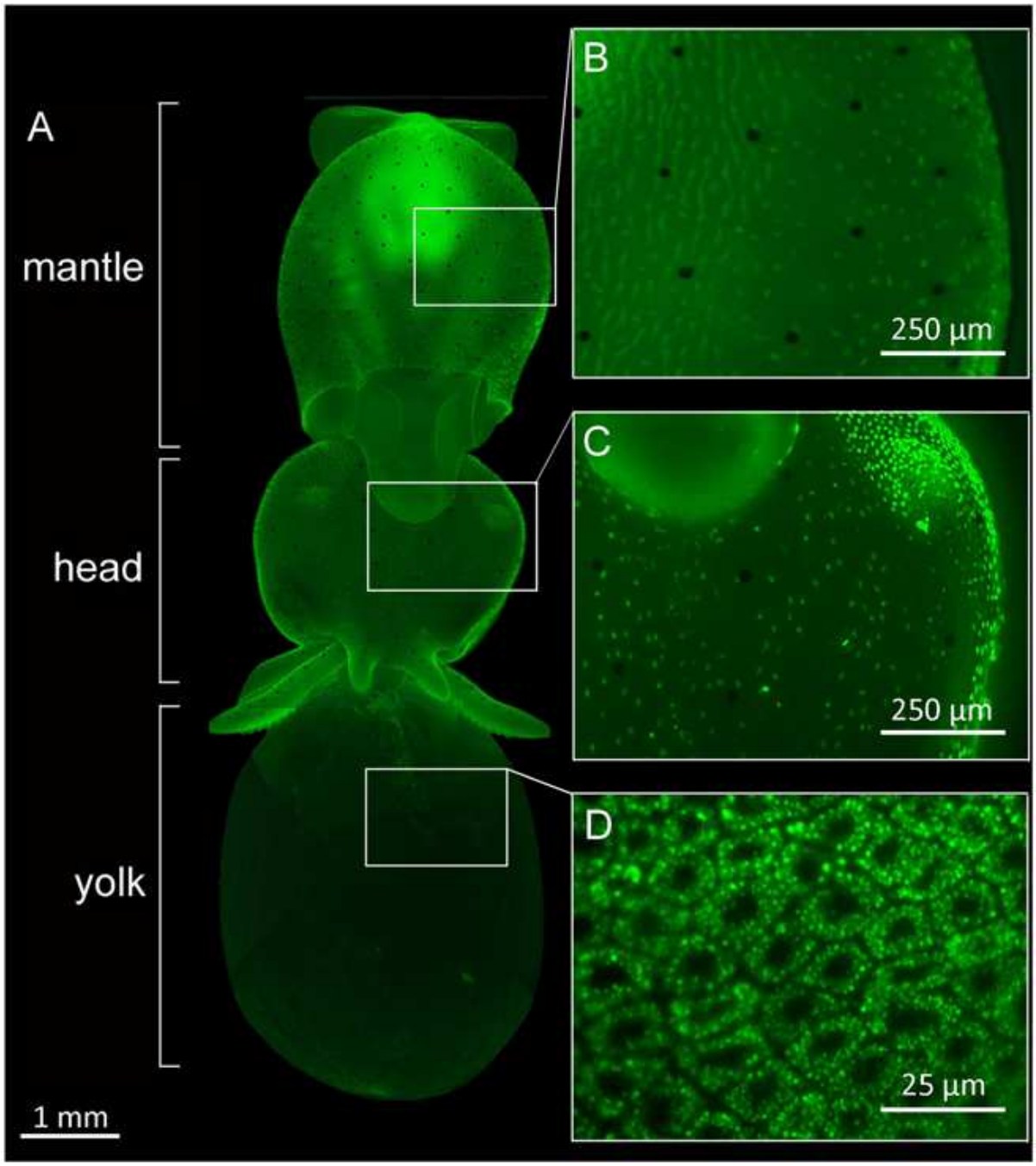

Figure 4

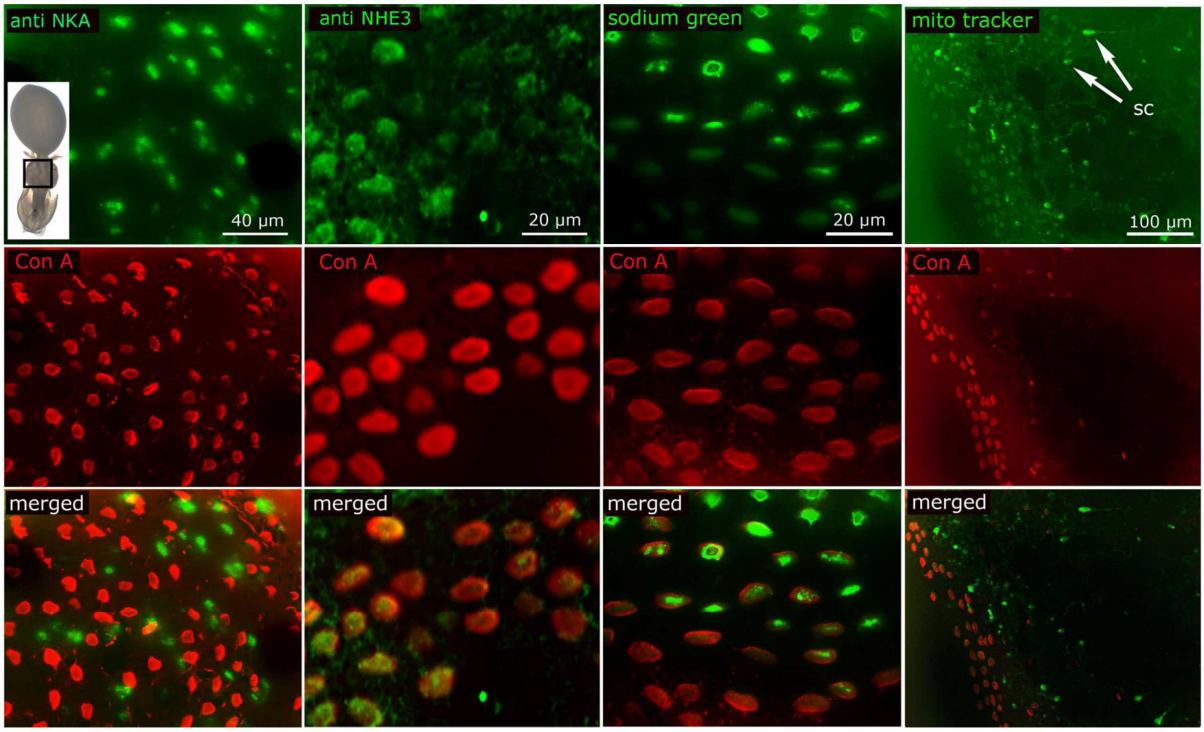
anti NKA
40 µm
anti NHE3
20 µm
sodium green
20 µm
mito tracker
sc
100 µm
Con A
Con A
Con A
Con A
merged
merged
merged
merged

Figure 5

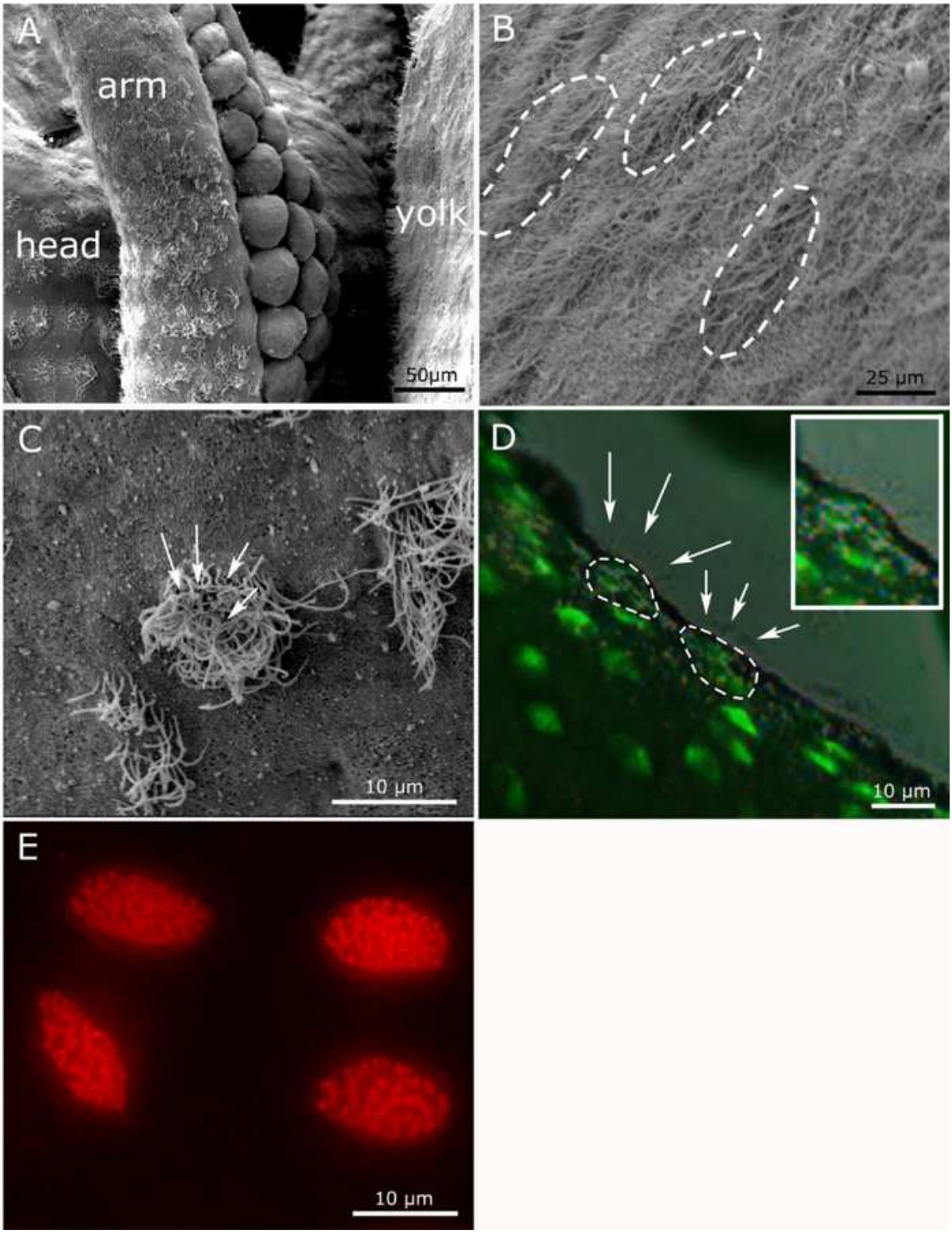

Figure 6

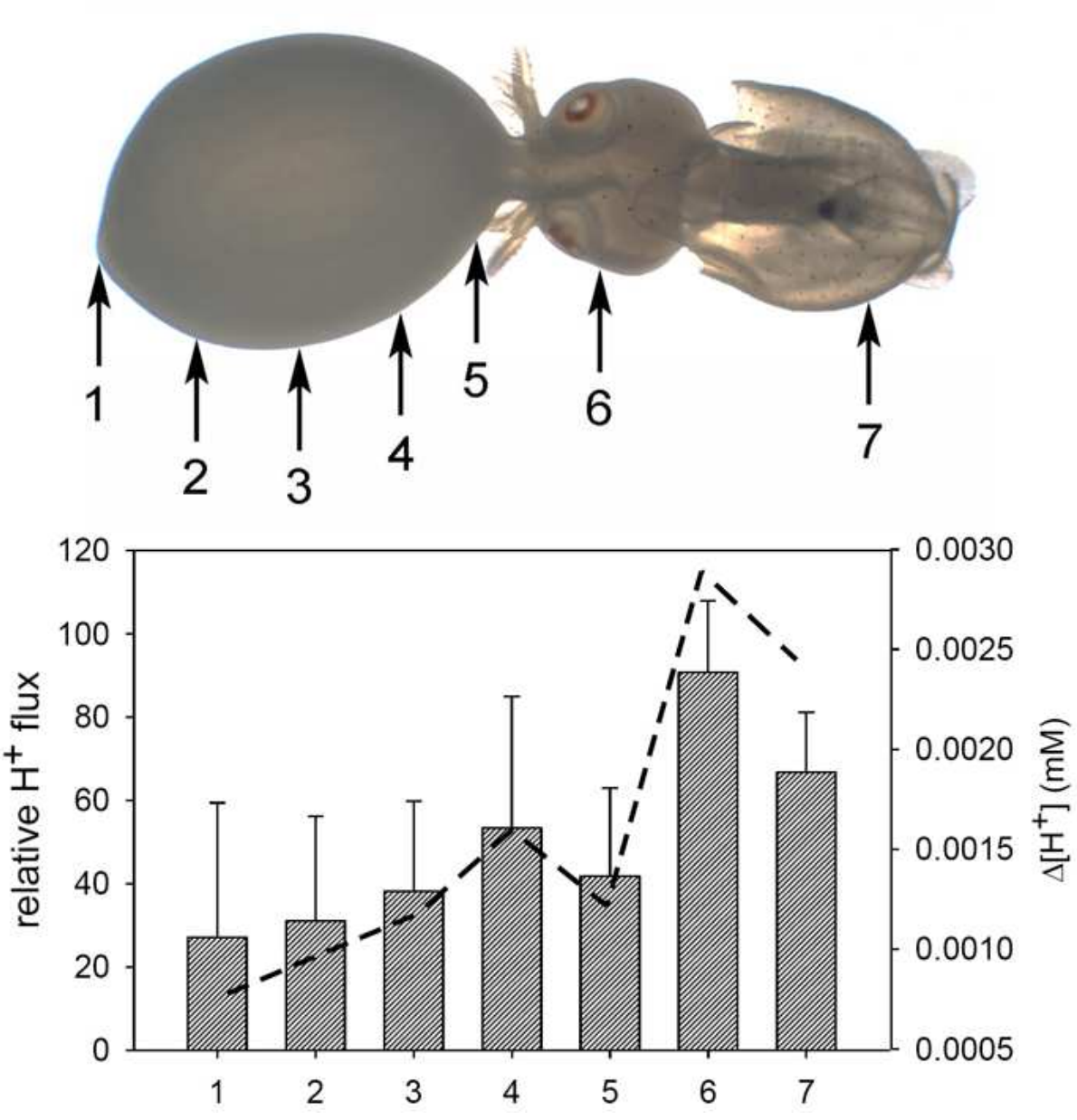
1
2
3
4
5
6
7
relative H+ flux
Δ[H+] (mM)
120
100
80
60
40
20
0
0.0030
0.0025
0.0020
0.0015
0.0010
0.0005
1
2
3
4
5
6
7

Figure 7

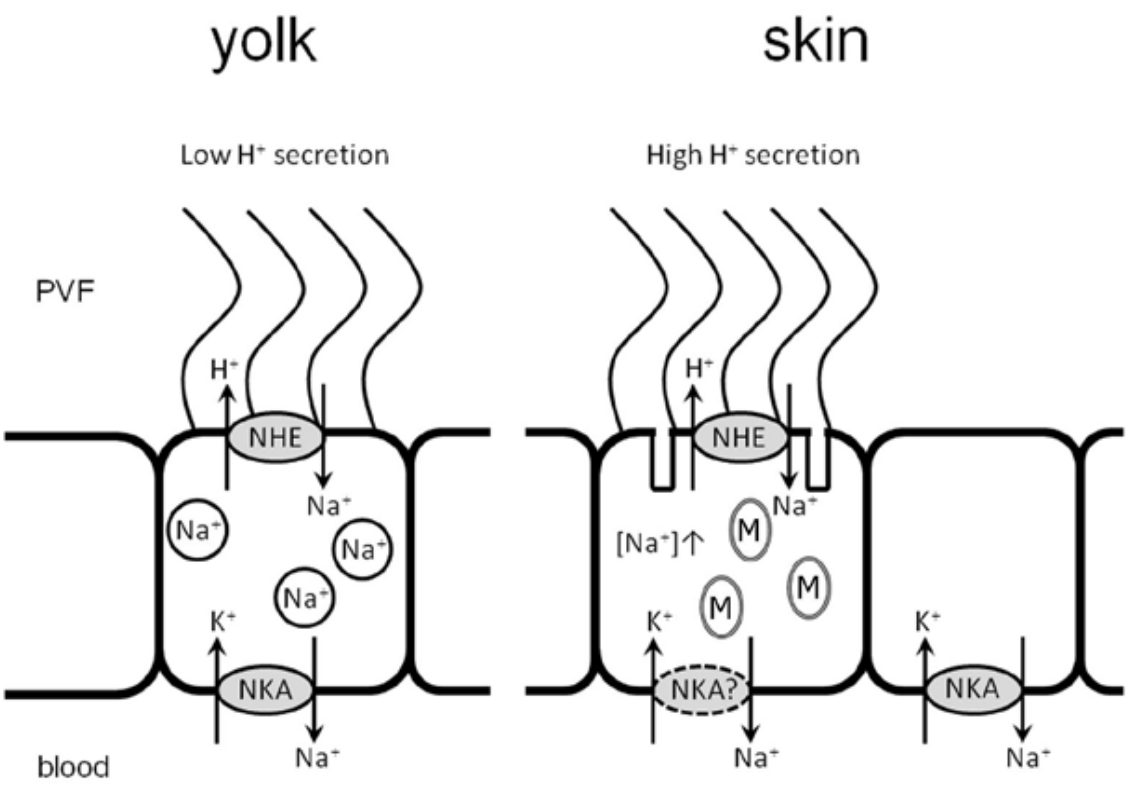
yolk
skin
Low H⁺ secretion
High H⁺ secretion
PVF
H⁺
NHE
Na⁺
Na⁺
Na⁺
Na⁺
K⁺
NKA
Na⁺
blood
H⁺
NHE
Na⁺
[Na⁺]↑
M
M
M
K⁺
NKA?
Na⁺
K⁺
NKA
Na⁺

Publication 3

Localization of ion-regulatory epithelia in embryos and hatchlings of two cephalopods

Localization of ion regulatory epithelia in embryos and hatchlings of two cephalopods

Marian Y. Hu[1*], Elliott Sucré[2], Mireille Charmantier-Daures[2], Guy Charmantier[2], Magnus Lucassen[3], Nina Himmerkus[4] and Frank Melzner[1]

[1] Leibniz-Institute of Marine Sciences (IFM-GEOMAR), Kiel 24105, Germany

[2]Equipe Adaptation Ecophysiologique et Ontogenèse, UMR 5119 Ecolag, Université Montpellier 2, F-34095 cedex 05, France

[3]Alfred Wegener Institute for Polar and Marine Research, Bremerhaven 27568, Germany

[4]Institute of Physiology, Christian-Albrechts-University, Kiel 24098, Germany

*To whom correspondence should be addressed:

e-Mail: mhu@ifm-geomar.de

tel: +49 (0)431-600 4275

fax: +49 (0)431-600 4446

Abstract

The tissue distribution and ontogeny of Na^+/K^+-ATPase was examined as an indicator for ion-regulatory epithelia in whole animal sections of embryos and hatchlings of two cephalopod species, the squid *Loligo vulgaris* and the cuttlefish *Sepia officinalis*. This is the first report that cephalopod Na^+/K^+-ATPase has been localized immuno-histochemically by using the polyclonal antibody α (H-300) raised against the human α1-subunit of the Na^+/K^+-ATPase. Na^+/K^+-ATPase immunoreactivity was observed in several tissues (gills, pancreatic appendages, nerves etc.), exclusively located in baso-lateral membranes lining blood sinuses. Furthermore, large single cells in the gill of adult *Loligo vulgaris* specimens have high similarity to NAR (Na^+/K^+-ATPase rich) cells described in fish. Immunohistochemical observations demonstrate that the amount and distribution of Na^+/K^+-ATPase in late cuttlefish embryos are already similar as in post embryonic stages and adults. The ion-regulatory epithelia (e.g. gills, excretory organs) of the squid embryos and paralarvae exhibited less differentiation when compared to adults. Na^+/K^+-ATPase activities for whole animals were higher in hatchlings of *S. officinalis* (157.0 ± 32.4 µmol g_{FM}^{-1} h^{-1}) than in those of *L. vulgaris* (31.8 ± 3.3 µmol g_{FM}^{-1} h^{-1}). *S. officinalis* gills and pancreatic appendages reached activities of 94.8 ± 18.5 and 421.8 ± 102.3 μmol_{ATP} g_{FM}^{-1} h^{-1}, respectively. High concentrations of Na^+/K^+-ATPase in late cephalopod embryos might be very important to cope with challenging abiotic conditions (low pH, high pCO_2) these organisms encounter inside their eggs. From our results, we also predict a higher sensitivity of squid vs. cuttlefish embryos to environmental acid-base disturbances.

Keywords: gill, ion-regulation, *Loligo vulgaris,* pancreatic appendages, *Sepia officinalis*

Introduction

Cephalopods are highly developed marine invertebrates that have a high degree of mobility, well developed neuronal systems and efficient sensory organs (Hanlon and Messenger 1996; Budelmann et al. 1997; Hu et al. 2009). It is believed that these features derived from the competition of cephalopods and fish (Packard 1972). In contrast to fish, most pelagic cephalopods evolved a less efficient swimming mode, jet propulsion, which demands high energetic costs leading to high metabolic rates (O`Dor 2002). In order to decrease these energetic costs, some cephalopods such as *Sepia* spp. decoupled swimming from ventilation by using undulatory movements of their fins for propulsion and specialized muscles for ventilation (Wells and Wells 1982; Wells 1990; Wells and O`Dor 1991). Furthermore, the utilization of protein as major energy source, high growth rates and a low oxygen binding capacity of the extracellular respiratory pigment hemocyanin are general factors leading to high energetic costs and metabolic rates (Houlihan et al. 1990; Melzner et al. 2007). The flip side of such high metabolic turnover rates is the increased accumulation of metabolic end products, such as NH_4^+ or CO_2 (Boucher-Rodoni and Mangold 1994; Pörtner and Zielinski 1998). Donaubauer (1981) proposed the NH_4^+ excretion to be achieved by an antiport of sodium via the Na^+/K^+-ATPase across gill epithelia in the cuttlefish *Sepia officinalis*. Furthermore, the accumulation of respiratory CO_2 and of protons during extensive exercise is known to cause an extracellular acidosis which is countered by an efficient acid-base regulating machinery (Pörtner 1994; Perry and Gilmour 2006). For instance, apical Na^+/H^+ exchangers (NHE) and Na^+ dependent Cl^-/HCO_3^- exchangers (NBCs) can extrude protons and import bicarbonate by utilizing the Na^+ gradient created by the sodium pump (Boron 2004; Romero et al. 2004). In the above mentioned processes the Na^+/K^+-ATPase is thought to be the main motor of ion exchange by creating ion- and electrochemical gradients that can be used by secondary active transporters (Evans et al. 2005; Perry and Gilmour 2006). Therefore, the Na^+/K^+-ATPase can be regarded as an excellent marker for the ion-regulatory capacity of a given tissue (Gibbs and Somero 1990).

The sodium potassium pump is an ubiquitous enzyme in the animal kingdom. The concept of this transporter was first proposed by Dean (1941) based on the antiport of K^+ ions into the cells and transport of Na^+ out of the cell. It is well established that the Na^+/K^+ ATPase is being involved in a variety of physiological processes such as, osmoregulation, acid-base regulation, transport of organic compounds and maintenance of membrane excitability. It

comprises a catalytic α subunit and a glycoprotein β subunit. This catalytic α subunit has a highly conserved amino acid sequence with a similarity of 80% among all vertebrates (Lebovitz et al. 1989; Fagan and Saier 1994) indicating that its structure and function is central for survival without allowing much sequence divergence. Recently the complete α and β subunits of *Loligo opalescens* and *L. pealei* were cloned and sequenced (Colina et al. 2007). Sequence alignments revealed that the primary structure of both subunits are similar to those found in mammalians with an approximate similarity of 75% to the human α 1-3 and a 30% similarity to human β 1-3. However, besides the presence of Na^+/K^+ ATPase in nerve fibres, this enzyme was additionally reported to be abundant in excretory organs such as pancreatic appendages, renal appendages and gills of the cuttlefish *S. officinalis* (Schipp et al. 1979; Donaubauer 1980; Donaubauer 1981).

Recent work demonstrated that not only adult specimens have to cope with high pCO_2 but also the late embryonic stages inside the protecting egg capsule (Gutowska and Melzner 2009). Late embryos of the cuttlefish *Sepia officinalis* are exposed to high respiratory CO_2 concentrations in the egg capsule due to their high metabolic activity and the egg capsule wall serving as a diffusion barrier. The consequence of elevated pCO_2 in the perivitelline fluid (PVF) and, thus, in body fluids, leads to a drop in pH that can constitute a major abiotic stressor. Towards hatching pO_2 declined from >12 kPa to less than 5 kPa, while pCO_2 increased from 0.13 to 0.41 kPa causing a pH drop in the PVF fom 7.7 to 7.2. Accordingly, advanced stages of cuttlefish embryos require an efficient acid-base regulating machinery which depends on the presence of transport active epithelia. While cuttlefish hatchlings are essentially isometric copies of adults, late embryos and hatchlings of squid are much smaller and termed “paralarvae” due to their incomplete development when compared to adults (Fioroni 1990). Although data regarding the abiotic conditions in *Loligo* eggs are not available yet, it is likely that late embryos of squid are challenged by less dramatic abiotic conditions when compared to cuttlefish mainly due to their less complete development within the egg.

In adult fish and crustaceans, it is well established that the gills are the predominant site of osmoregulation, acid-base regulation and excretion (Wheatly and Henry 1992; Lignot and Charmantier 2001; Claiborne and Edwards 2002; Evans et al. 2005; Hwang and Lee 2007). In this context specialized cells, so-called mitochondrion rich cells (MRCs) were identified as major sites of ionic regulation, characterized by high amounts of Na^+/K^+-ATPase, located in

basolateral membranes (for a review see Hwang and Lee 2007). In contrast to the adults fish early stages show alternative sites for ion-regulation that may change during ontogeny. For example, when gill epithelia are not yet fully developed, epidermal ionocytes are precociously scattered on the skin to mediate ion and acid-base balance (Hsiao et al. 2007; Hwang and Lee 2007). Recently, functional genomic and immunohistological studies revealed the embryonic yolk-sac membrane to be another major site for osmoregulation in euryhaline teleosts (Hiroi et al. 2005; Hiroi et al. 2008). Finally, the increase of basal mitochondria and Na^+/K^+-ATPase in the anterior and posterior part of the digestive tract of the euryhaline sea bass *Dicentrarchus labrax* was demonstrated to be the key to high osmo-tolerance in early stages of this species (Nebel et al. 2005; Giffard-Mena et al. 2006). Not only in vertebrates, but also in marine crustaceans such an ontogeny-dependent shift in ion-regulatory epithelia has been demonstrated (Charmantier and Charmantier-Daures 2001; Charmantier et al. 2001; Cieluch et al. 2005). For example, decapodit stages of the brown shrimp *Crangon crangon* exhibit Na^+/K^+-ATPase rich ionocytes in the branchiostegite epithelium, which disappear when they become juveniles. Instead, these juveniles exhibit positive Na^+/K^+-ATPase immunoreactivity in the cells of the gill shaft (Cieluch et al. 2005). In contrast, other crustaceans, mostly oceanic stenohaline species do not show a shift of osmoregulatory epithelia among developmental stages (Charmantier and Charmantier-Daures 2001).

We propose that, as in fish and crustaceans, the cephalopod gill may be the major site involved in ion regulation. Furthermore, the development of this organ might contribute significantly to the ability to osmoregulate, and to counter acid-base disturbances. In this context, immunohistological applications can be regarded a powerful tool to investigate functionality and ontogeny of ion-regulatory epithelia. Thus, in a first step, this work aimed at the establishment of an immunohistological protocol to localize the Na^+/K^+-ATPase as an indicator for tissues with high ion exchange capacities. An additional objective was to gain a first insight into the ontogeny of ion regulatory epithelia in late embryos and hatchlings / juveniles of the cuttlefish *S. officinalis* and of the squid *L. vulgaris*. The transition from embryo to hatchling can be seen as an event where biotic and abiotic environmental conditions change dramatically around the animal and, thus, may also trigger large changes in the organization and distribution of ion-regulatory epithelia.

1. Material and Methods

1.1. Animals

Egg masses of *Sepia officinalis* and *Loligo vulgaris* were obtained from Zeeland, Netherlands, in May 2008 by SCUBA diving, and transported alive to the IFM-GEOMAR, Kiel. 40 egg strands of *L. vulgaris* and 20-25 sepia eggs were kept at 15°C under a 12 h day and night regime in aerated 20 l plastic tanks. Filtered sea water from Kiel Fjord was adjusted to a salinity of 31 psu using artificial sea salt (Instant Ocean). Water was exchanged daily (40% of the tank volume). *Loligo vulgaris* embryos were collected several days before hatching (stage 28-29, (Arnold 1965), and hatchlings with mantle length (ML) of 1.8-2 mm were sampled 2-3 days after hatching. *Sepia officinalis* embryos were also collected at a similar stage (stage 28-29, (Lemaire 1970) and hatchlings were fed with live mysid shrimps and sampled 10-11 days after hatch (ML 10-12 mm). The embryos of both species showed a normal embryonic development and behaved normally after hatching. Gills of adult *L. vulgaris* specimens were obtained from local fishermen in southern France, Montpellier, and immediately fixed in Bouin's fixative. For immuno-blotting samples were immediately frozen in liquid nitrogen, and stored at -80°C.

1.2. Immuno localization of Na^+/K^+-ATPase

Whole animals were fixed by direct immersion for 24 h in Bouin's fixative followed by rinsing in 70% ethanol. Samples were fully dehydrated in graded ethanol series and embedded in Paraplast (Paraplast Plus, Sigma, P3683). Sections of 4 µm were cut on a Leitz Wetzlar microtome, collected on poly-l-lysine-coated slides, and stored at 37°C for 48 hours. One series was used for classical light microscopy using the Masson`s trichome method for tissular topography. The other series was used for immunohistology. The slides were deparafinized in Histochoice Tissue fixative (Sigma, H2904) for ten minutes, washed in Butanol and passed through a descending alcohol series (100%, 95%, 90%, 70% and 50 % for 5 min each). Slides were washed in PBS (pH 7.3) and exposed to a heat shock inside the PBS bath using a microwave (80% of power for 2x3 min) Afterwards samples were transferred to a PBS bath containing 150 mM NaCL and Tween 20 (conc. 0.2 µl/ml) for ten minutes, and a PBS bath containing 5% skimmed milk for 20 min to block non-specific bindings. The primary

antibody, a rabbit polyclonal antibody raised against an internal region of Na^+/K^+-ATPase α1 of human origin (Na^+/K^+-ATPase α (H-300), Santa Cruz Biotechnology, INC.) was diluted in PBS to 10 µg mL^{-1}, placed in small droplets of 100 µl on the sections, and incubated for 2 h at room temperature in a wet chamber. To remove unbound antibodies, the sections were then washed (3x5 min) in PBS and incubated for 1 h with small droplets (100 µl) of secondary antibody, tetramethyl rhodamine isothiocyanate -labeled goat anti rabbit IgG (Santa Cruz Biotechnology, INC.). After rinsing in PBS (3x5 min), sections were covered with a mounting medium and examined with a fluorescent microscope (Leitz Diaplan coupled to a Ploemopak 1-Lambda lamp) with an appropriate filter set (577 nm band-pass excitation filter) and a phase contrast device. For higher magnification, an Axiovert 200M microscope equipped with an ApoTome for optical sectioning using the Axio Vision 4.6 software (Carl Zeiss, Jena, Germany) was used. Negative controls were performed several times for every antibody and every species by omitting the primary antibody.

Another primary antibody (monoclonal antibody IgGα5, raised against the avian α subunit of the Na^+/K^+-ATPase. Developmental Studies Hybridoma Bank, University of Iowa) was tested. The primary antibody was diluted in PBS to 15 µg mL^{-1}, and stained with the secondary antibody, fluoresceinisothiocyanate (FITC)-labled goat anti-mouse IgG (Jackson Immunoresearch, West Baltimore, USA), which was applied with a concentration of 20 µg mL^{-1}. To observe the sections we used a filter set (450–490 nm band-pass excitation filter) and a phase contrast device.

For the localization of the Na^+/K^+-ATPase, five animals of each species and stage were examined except for adult *Loligo vulgaris* (n = 2).

1.3. Na^+/K^+-ATPase activity assay

Na^+/K^+-ATPase activity was measured in whole animal and tissue crude extracts in a coupled enzyme assay with pyruvate kinase (PK) and lactate dehydrogenase (LDH) using the method of Allen and Schwarz (1969) as described by Melzner et al. (2009a). Crude extracts were obtained by quickly homogenizing the tissue samples in a conical tissue grinder in 10 volumes of ice-cold buffer (50mM imidazole, pH 7.8, 250 mM sucrose, 1mMEDTA, 5 mM β-mercaptoethanol, 0.1% (w/v) deoxycholate, proteinase inhibitor cocktail from Sigma-Aldrich

(Taufkirchen, Germany, Cat. No. P8340) followed by Ultra Turrax treatment (3 x 5s) on ice. For *S. officinalis* whole animal homogenates the ink gland was quickly removed before homogenization, because is absorption of light during the photometric test. Cell debris was removed by centrifugation for 10 min at 1000 g and 4°C. The supernatant was used as crude extract. The reaction was started by adding 10 µl of the sample homogenate to the reaction buffer containing 100 mM imidazole, pH 7.8, 80 mM NaCl, 20 mM KCl, 5 mM MgCl2, 5 mM ATP, 0.24 mM Na-(NADH2), 2 mM phosphoenolpyruvate, about 12 U/ml PK and 17 U/ml LDH, using a PK/LDH enzyme mix (Sigma-Aldrich). The oxidation of NADH coupled to the hydrolysis of ATP was followed photometrically at 15°C in a DU 650 spectrophotometer. (Beckman Coulter, USA) over a period of 10 min, measuring the decrease of extinction at λ = 339 nm. The fraction of Na^+/K^+-ATPase activity in total ATPase (TA) activity was determined by the addition of 17 µl of 5 mM ouabain to the assay. Each sample was measured in sextuples. Enzyme activity was calculated using an extinction coefficient for NADH of ε = 6.31 $mM^{-1} \cdot cm^{-1}$ and given as micromoles ATP consumed per gram tissue fresh mass per hour.

1.4. Immunoblotting

For immunoblotting, 25 µl of crude extracts for Na^+/K^+-ATPase were used. Proteins were fractionated by SDS-PAGE on 10% polyacrylamide gels, according to Lämmli (1970), and transferred to PVDF membranes (Bio-Rad, Munich, Germany), using a tank blotting system (Bio-Rad). Blots were preincubated for 1 h at room temperature in TBS-Tween buffer (TBS-T, 50 mM Tris -HCl, pH 7.4, 0.9% (wt/vol) NaCl, 0.1% (vol/vol) Tween20) containing 5% (wt/vol) nonfat skimmed milk powder. The primary antibody for the Na^+/K^+-ATPase was the polyclonal antibody α (H-300). Blots were incubated with primary antibodies at 4°C overnight. After washing with TBS-T, blots were incubated for 1 h with horseradish conjugated goat anti-rabbit IgG antibody (Santa Cruz Biotechnology, INC.) diluted 1:2000 in TBS-T containing 5% non-fat skimmed milk powder. Protein signals were visualized by using the ECL Western Blotting Detection Reagents (GE Healthcare, Munich, Germany) and recorded by a LAS-1000 CCD camera (Fuji, Tokyo, Japan).

2. Results

2.1. Structure and immunolocalization

2.1.1. Pancreatic appendages, internal organs, skin

The pancreatic appendages (PA) in *Sepia* and *Loligo* are part of the digestive tract and consist of alveolar/tubular shaped protrusions of the ductus hepatopancreas within the dorsal renal sac. In embryos and hatchlings these protrusions had a diameter ranging from 15-25 µm for *L. vulgaris* (ML =2-3 mm) and 100-200 µm for *S. officinalis* (ML = 5-7 mm), respectively. These appendages consist of an inner and an outer epithelium. The cells of both epithelia line a blood sinus with their basal lamina. Generally, the cells of the inner epithelium are two to three-fold higher than those from the outer epithelium (Fig. 1d, e). The difference between the two epithelia is a very high density of Na^+/K^+-ATPase in cells of the inner epithelium for both species, whereas the outer epithelium shows little (indicated by arrows) immunoreactivity in its membranes at least for *S. officinalis*. Compared to the clearly visible (thickness: 20-30 µm, Fig. 1d, e) outer epithelium in PA of *S. officinalis*, this epithelium is not distinct in *Loligo* hatchlings and is characterized by large blood lacunae in between the tubulus system (Fig. 1a). No Na^+/K^+-ATPase immunoreactivity was observed in this outer part of the PA of *L. vulgaris* (Fig. 1c). The visual comparison of fluorescence intensities in PAs and gills suggests a rather similar intensity between both organs in *S. officinalis*, whereas in the late embryos and hatchlings of the squid the amount of Na^+/K^+-ATPase in the pancreatic appendages exceeds that of gill tissues by far (Fig. 1b, c). Another tissue that exhibited a positive staining in *Loligo vulgaris* was the funnel organ or funnel gland (Verill`s organ). Staining of the Na^+/K^+-ATPase in the funnel organ was only found in *L. vulgaris* embryos/hatchlings and immunoreaction was strongest in the basal layers of mucus cells and less intense on the apical surface of this organ (supplementary material Fig. 2b). The staining was filling the entire cells and can not be restricted to apical or basal membranes. Furthermore, small particles that are detached from the glandular structure were also stained (supplementary material Fig. 2b). Cells of the funnel gland of *S. officinalis* exhibited no immunoreactions (supplementary material Fig. 2a).We were not able to detect significant Na^+/K^+-ATPase immunoreactivity in other tissues, such as the midgut gland (pancreas), the renal appendages, branchial heart appendages branchial gland, oesophagus or skin.

2.1.2. Gills

The gills of decapod cephalopods are located inside the mantle cavity in lateral position to the renal sac with bilateral symmetry (Fig. 2a, 3a). In both species, *S. officinali*s and *L. vulgaris*, gill tissues displayed major sites for positive Na^+/K^+-ATPase immunoreactivity. In *L. vulgaris* embryos and hatchlings (ML = 2-3 mm), the gills were 160-200 µm in length and 60-80 µm in height. These gills consist of 6-8 lamellae which are not yet fully developed missing the 2nd and 3rd order lamellae (Fig. 2a). In these not fully differentiated gills the Na^+/K^+-ATPase was equally located along the lamellae with a tendency to be found in the posterior sections of the lamellae (Fig. 2c, d). In adults the gill becomes a highly folded epithelium (Fig. 2b) with Na^+/K^+-ATPase mainly located in the apical tips of the second order lamellae (Fig. 2e). The cells in this region of the transport active epithelium in adult *L. vulgaris* gills are voluminous, filling the entire lumen of the concave part of the second order lamellae which are approximately 0.8 mm thick (ML = 18-20 cm) (Fig. 2e). Additionally, high single cells surrounding the junction of third order vessels of the adult squid gill were also rich in Na^+/K^+-ATPase (Fig. 2f). In contrast to the squid, the gill of *S. officinalis* was almost fully differentiated in late stage embryos (ML = 5-6 mm) and comparable to that of adults, exhibiting 1st to 3rd order vessels and lamellae and a total length of approximately 900 µm (Fig. 3a). For both, embryos and juveniles the Na^+/K^+-ATPase was exclusively located in the concave part (3rd order lamellae) of the transport active epithelium of the entire 2nd order lamellae (Fig. 3c, e). The cells of this transport active epithelium are higher and more voluminous compared to those of the outer respiratory epithelium (Fig. 3b, d). Furthermore, the concentration of the enzyme was high in basolateral regions of the transport epithelium (close to the blood sinus) following the inversions of basolateral membranes deep into the cell body and fading to the apical side (Fig. 3d, f).

2.2. Na^+/K^+-ATPase-activity

Maximum enzyme activities determined for several tissues of juvenile *S. officinalis* and whole animal samples of *L. vulgaris* revealed highest activities in pancreatic appendages (PA) (Table 1). Na^+/K^+-ATPase activity in this tissue was as high as 421.8 ± 102.3 $\mu mol_{ATP}\ g_{FM}^{-1}\ h^{-1}$ and total ATPase activity reached 1083.4 ± 157.4 ($\mu mol_{ATP}\ g_{FM}^{-1}\ h^{-1}$). In the PA, 39% of total

ATPase activity was due to Na^+/K^+-ATPase. In cuttlefish gills, with maximal activities of 94.8 ± 18.5 $\mu mol_{ATP}\ g_{FM}^{-1}\ h^{-1}$, only 19% of total ATPases (499.6 ± 75.2 $\mu mol_{ATP}\ g_{FM}^{-1}\ h^{-1}$) was due to Na^+/K^+-ATPase. Finally, whole body preparations of squid paralarvae (mantle length approx. 2-3 mm) revealed Na^+/K^+-ATPase activities of 31.8 ± 3.3 and total ATPases activities of 373.8 ± 60.2 $\mu mol_{ATP}\ g_{FM}^{-1}\ h^{-1}$, respectively. In whole hatchlings the Na^+/K^+-ATPase comprised 9% to the total activity. The Na^+/K^+-ATPase activity of whole *S. officinalis* hatchlings reached 157.0 ± 32.4 $\mu mol_{ATP}\ g_{FM}^{-1}\ h^{-1}$ and accouted for 14% of total ATPases. On a comparative basis, highest concentrations of Na^+/K^+-ATPase occurred in pancreatic appendages followed by whole animal homogenates of *S. officialis* hatchlings, gills and finally those of whole *L. vulgaris* paralarvae.

2.3. Western-Blot

Westen blot analysis (Fig. 4) demonstrated the specificity of the primary antibody Na^+/K^+-ATPase α (H-300) towards a 100 kDa protein which is believed to be the Na^+/K^+-ATPase (MW 100 kDa) (Peterson and Hokin 1981). Using the monoclonal α5 antibody, a weak reaction product was obtained for *L. vulgaris* whole body homogenates, but not for *S. officinalis* gill tissues. Generally, western-blot signals were weaker for the monoclonal α5 antibody although the same concentrations were applied to the gel (100 mg FM ml^{-1}). Application of these antibodies for immunohistology showed almost no detectable fluorescence in gills of *L. vulgaris* hatchlings using the α5 (Fig. 4b) and a positive Na^+/K^+-ATPase immunoreactivity with the (H-300) (Fig. 4a). The specificity of the immunoreactivity using the Na^+/K^+-ATPase α (H-300) was proven by a negative control performed on gills of *S. officinali*s (Fig. 5a, b).

3. Discussion

Cephalopod hatchlings are essentially miniature models of their adults equipped with many necessary features for a predatory lifestyle, including nerves, functional sensory organs and ion regulatory epithelia (Schipp et al. 1979; Fioroni 1990; Mackie 2008). The proper functioning of these organs is highly dependent on the Na^+/K^+-ATPase that maintains high intracellular K^+ and low Na^+ concentrations (Colina et al. 2007). In the following, chief findings regarding the localization and capacity of Na^+/K^+-ATPase in late embryos and early juveniles of cephalopods with a pelagic and benthic type of development will be discussed.

3.1. Validity of methods & organs stained

The polyclonal Na^+/K^+-ATPase α (H-300) antibody, raised against the human α subunit of the Na^+/K^+-ATPase, showed positive and specific immunoreactivity towards the cephalopod Na^+/K^+-ATPase with high certainty. First, the localization of this enzyme in organs and transport active epithelia of the common cuttlefish is in accordance with earlier histochemical findings (Donaubauer 1980; Donaubauer 1981). Additionally, strong immunoreactivity of nerves and sensory cells in the cephalopod retina (see supplementary material) validate the specificity of this antibody because Na^+/K^+-ATPase is crucial in order to maintain the electrochemical gradient in these cells (Colina et al. 2007). Finally, western-blot analysis demonstrated the Na^+/K^+-ATPase α (H-300) to react with a 110 kDa protein from cuttlefish and squid. The molecular weight for the highly conserved α subunit of Na^+/K^+-ATPase was reported to be in the range of 100 kDa in various animal groups (Peterson and Hokin 1981).

Interestingly, a strong Na^+/K^+-ATPase immunoreactivity was observed in the funnel organ of *L. vulgaris* embryos and hatchlings but not in *S. officinalis*. Generally, the cephalopod funnel organ is located in the inner surface of the funnel, and is known to serve as a mucus gland (Fioroni 1962; Laurie 1983). The strong immunoreactivity in goblet cells of this epithelium is most probable due to an unspecific binding of the antibody to mucus. This assumption is supported by the fact that the binding sites of the antibody are not restricted to membranes, but filling the entire lumen of the glandular cells. Furthermore, particles inside the funnel which are probably mucus released from the gland are also stained.

In the two examined cephalopod species, tissues such as pancreatic appendages, gills or nerves (see supplementary material) exhibit high concentrations of this enzyme, indicating that these tissues are strongly involved in active transport processes. Other tissues such as skin and muscles exhibited low or no detectable immunoreactivity. Organs with positive staining for Na^+/K^+-ATPase are discussed below.

3.2. Pancreatic appendages

The pancreatic appendages (PA) of cephalopods are believed to be multifunctional organs, involved in the processes of nutrient absorption, osmoregulation, water balance and excretion (Potts 1965; Schipp and von Boletzky 1976; Wells and Wells 1989). In both species, the PAs consist of two epithelial layers which are separated by a blood sinus. The inner epithelium is highly Na^+/K^+-ATPase immunoreactive in both species. This corresponds to earlier findings that demonstrated reaction precipitates of a sodium potassium-dependent ATPase in inner epithelial cells and to a lesser extent in the outer epithelium of the PA in *S. officinalis* (Donaubauer 1981). In comparison to *S. officinalis*, the squids` (embryos and hatchlings) Na^+/K^+-ATPase was exclusively present in high concentrations in the inner epithelium of the PA, but not in the outer epithelium which exhibited large blood lacunae. This outer epithelium is supposed to be involved in active secretion and re-absorption of low-molecular compounds such as sugars, amino acids and ions (Potts 1965; Donaubauer 1981). It is generally believed that this epithelium is involved in urine formation and, thus, osmoregulation (Potts 1965; Schipp and von Boletzky 1976). The inner epithelium of the PA is mainly involved in processes of nutrient absorption from the chyme (Schipp and von Boletzky 1976; Boucher-Rodoni and Mangold 1977). Generally, the uptake of carbohydrates such as glucose from intestinal brush border membranes is believed to be a symport of two sodium ions and one glucose molecule into the cell, and an uptake of the glucose to the blood by a glucose uniporter (GluT2). The driving force for this coupled transport depends on a sodium gradient created by basolateral Na^+/K^+-ATPase (Murer and Hopfer 1974). This general mechanism would also apply to the inner epithelium of cephalopod PAs. In the Pas, a high capacity for active nutrient uptake from the chyme can be considered very important in order to support the high growth rates of cephalopods (von Boletzky 1983).

Together with the renal appendages and branchial heart appendages, the outer epithelium of the PA is proposed to be mainly involved in urine formation (Schipp and von Boletzky 1976; Donaubauer 1981). The urine of most cephalopods was described to be acidic (5-6 pH) and rich in ammonia ($NH4^+$), whereas other nitrogenic compounds like nitrate or nitrite were absent (Emanuel and Martin 1956). Regarding the urine formation in terms of excretion of metabolic end products, e.g. NH_4^+, the location of Na^+/K^+-ATPase in basolateral membranes in the outer epithelium of the PA (only observed for *S. officinalis*) offers plausible possibilities. It was demonstrated that the transport of NH_4^+ into epithelial cells of excretory organs of vertebrates can be achieved by a direct link to the Na^+/K^+-ATPase (Garvin et al. 1985; Kurtz and Balaban 1986; Wall et al. 1999). In a first step, NH_4^+ is transported baso-laterally into the cell via the Na^+/K^+-ATPase instead of K^+, and in a second step NH_3 and H^+ is transported out of the cell on the apical side into the renal sac lumen (Boucher-Rodoni and Mangold 1994; Knepper 2008). In fish, the transport of nitrogen-buffer compounds across excretory epithelia was shown to be coupled to acid-base regulation (Wood et al. 1999; Bolner and Baldisserotto 2007). As cephalopods produce acidic urine, it can be assumed that similar to fish, ammonia excretion is connected to pH regulation. It remains to be elucidated in quantitative terms how much the excretory organs and especially the PA are involved in acid-base regulation.

3.3. Gills

In both *S. officinalis and L. vulgaris*, the gill belonged to the predominant sites of Na^+/K^+-ATPase immunoreactivity. Immunohistochemical localization of the Na^+/K^+-ATPase in baso-lateral membranes of the transport active epithelium of the cuttlefish gill confirms earlier findings by Donaubauer (1981), who demonstrated Na^+ and K^+ dependent ATPase activity in the same regions of the cuttlefish gill using a histochemical approach. The maximum Na^+/K^+-ATPase activity measured in the gills homogenates from juvenile *S. officinalis* were as high as 94.8 ± 18.5 ($\mu mol_{ATP}\ g_{FM}^{-1}\ h^{-1}$) which is comparable to activities described for shallow water teleost fish and crustaceans (Siebers et al. 1982; Siebers et al. 1983; Gibbs and Somero 1990). Thus, localization and activity level of Na^+/K^+-ATPase in cephalopod gills suggests that this organ has similar ion-regulatory capacities as fish or decapod crustacean gills (Perry and

Gilmour 2006; Melzner et al. 2009b). Although cephalopods are known to be weak osmoregulators, their high metabolic rate and increased energetic costs due to their less efficient mode of locomotion, jet propulsion, leads to an accumulation of respiratory CO_2 (O`Dor and Webber 1991). As the hydration of CO_2 causes an acidosis by the titration of non-bicarbonate buffers in body fluids, these animals require an efficient acid-base regulating machinery, depending on a driving force, which is provided by the Na^+/K^+-ATPase (Pörtner 1994; Perry and Gilmour 2006).

The gills of adult specimens of the common squid show similar general features regarding the gill structure and localization of Na^+/K^+-ATPase compared to *S. officinalis*. Additionally, large single cells with a strong staining located around the junction of 3rd order vessels and large cells in the outer region of the 1st order lamellae reminded of NaR (Na^+/K^+ ATPase-rich) cells which are specialized cells involved in ion- and acid-base regulation localized in gills and the skin of fish (Perry and Gilmour 2006; Hwang and Lee 2007).

The comparison of squid and cuttlefish hatchlings and late embryos reveal general differences regarding the morphology and Na^+/K^+-ATPase organization in gills. The general structure of the adult cephalopod gill exhibiting 1st -3rd order vessels and lamellae is already present in late embryos and hatchlings of the cuttlefish, whereas these features were not observed in the squid`s embryo and hatchlings, respectively. Instead, these gills consist only of rudimentary 1st -2nd order vessels and lamellae. Generally, the hatchlings of squid are often referred as paralarvae with a planktonic development whereas hatchlings of *S. officinalis* are miniature models of adults (Fioroni 1990; Nixon and Mangold 1998).

In crustaceans, different types of ion regulation ontogeny were described: (1) adult type of ion regulation established in first post-embryonic stage (2) shift from larval to adult type of ion regulation during the post-embryonic development (Charmantier and Charmantier-Daures 2001). Similar ion-regulatory types may also apply for the ontogeny of the squid paralarvae compared to the cuttlefish hatchling. Although the gills of *L. vulgaris* paralarvae exhibit Na^+/K^+-ATPase staining, it is not clearly restricted to a defined region of the epithelium as it is the case for adult specimens of this species or in cuttlefish gills. These observations suggest a rudimentary range of gill functions in terms of ion regulation for the squid`s paralarvae compared to adults. Late embryos and hatchlings of *S. officinalis* may regulate acid-base disturbances as do adults. It has been shown that adult cephalopods can efficiently compensate blood pH when exposed to elevated environmental pCO_2 by

increasing blood [HCO_3^-] levels through active ion regulatory processes (Gutowska et al. 2009). This is important in order to protect blood oxygen transport via the pH-sensitive respiratory pigment hemocyanin. As late stage embryonic cephalopods rely on hemocyanin driven oxygen transport as well, adult-like acid-base regulatory capacities can be considered essential in order to cope with the high pCO_2 and low pH in their egg fluids (Gutowska and Melzner 2009).

For late embryos and hatchlings of *L. vulgaris*, which do not show fully differentiated adult-type gills, two possibilities can be proposed: (1) rudimentary gills cover ion regulatory needs of the organism (2) another organ which has not yet been identified replaces gill functionality until gills become functional. In fish, it has been demonstrated that other tissues such as skin, yolk-sac membrane or the urinary system cover the functions of the gills as long as they are not fully functional (Nebel et al. 2005; Giffard-Mena et al. 2006; Hwang and Lee 2007; Hiroi et al. 2008). Nevertheless, immunohistological observations were not able to identify such alternative epithelia. Additionally the five fold higher Na^+/K^+-ATPase activity in whole *S. officinalis* hatchlings compared to those determined for *L. vulgaris* hatchlings suggests a higher demand of Na^+/K^+-ATPase-rich epithelia for the cuttlefish.

Further investigations will address the expression and localization of Na^+/K^+-ATPase in whole mount preparations of cephalopod embryos using in-situ hybridisation and immunostaining methods in order to investigate other possible sites of ion regulation such as yolk sac membrane or the skin.

3.4. Conclusion

This work described the location and aspects of the ontogeny of ion regulatory epithelia on a comparative basis for the cephalopods *Sepia officinalis* and *Loligo vlgaris*, respectively. The highly differentiated hatchling of *S. officinalis*, with extreme adult-like morphology, is typical of the benthonic type of development among cephalopods. This feature goes along with well developed adult-like ion-regulatory epithelia, for both late embryos and hatchlings. In contrast, late embryos and hatchlings of *L. vulgaris*, which are usually termed paralarvae, belong to the planctonic type and differ morphologically from adults. In these paralarvae, ion regulatory epithelia (e.g. gills) are not completely developed. Most probably, the gills of

the squids` paralarvae exhibit relatively lower capacities compared to adults. These differences between the two examined cephalopods are also supported by higher Na^+/K^+-ATPase activity levels in the cuttlefish. Nevertheless, the ability to regulate ion fluxes to a certain degree can be regarded as a very important feature with respect to challenging acid-base disturbances in eggs. The ontogeny of these epithelia in earlier developmental stages will provide further knowledge regarding a possible “bottleneck” in terms of ion and acid-base regulation in early cephalopod stages. Further investigations will address the ion-regulatory capacity and the response of these epithelia in cephalopod embryos towards additional stressors such as elevated environmental CO_2.

Acknowledgements

The authors would like to thank Prof. Dr. P. Saftig for providing the confocal microscope (Axiovert 200M) at the Unit of Molecular Cell Biology and Transgenic Research, Kiel and E. Grousset for valuable assistance with classical histology. We are grateful for the valuable suggestions of three anonymous reviewers that improved the manuscript.

These investigations comply with the German animal welfare principles No. V 31 and the animal use protocols were approved by the animal care committee of the Christian-Albrechts-University, Kiel.

References

Arnold JM (1965) Normal embryonic stages of the squid, *Loligo pealii* (Lesueur). Biol Bull 128:24-32

Bolner KCS, Baldisserotto B (2007) Water pH and urinary excretion in silver catfish *Rhamdia quelen*. J Fish Biol 70:50-64

Boron WF (2004) Regulation of intracellular pH. Adv Physiol Educ 28:160-179

Boucher-Rodoni R, Mangold K (1977) Experimental study of digestion in *Octopus vulgaris* (Cephalopoda, Octopoda). J Zool Lond 183:505-515

Boucher-Rodoni R, Mangold K (1994) Ammonia production in cephalopods, physiological and evolutionary aspects. Mar Fresh Behaw Physiol 25:53-60

Budelmann BU, Schipp R, von Boletzky S (1997) Cephalopoda. In: Harrison FW, Kohn AJ (eds) Microscopic anatomy of invertebrates, Vol 6A. Wiley-Liss, New-York

Charmantier G, Charmantier-Daures M (2001) Ontogeny of osmoregulation in crustaceans: The embryonic phase. Amer Zool 41:1078-1089

Charmantier G, Haond C, Lignot J-H, Charmantier-Daures M (2001) Ecophysiological adaptation to salinity throughout a life cycle: A review in homarid lobsters. J Exp Biol 204:967-977

Cieluch U, Charmantier G, Grousset E, Charmantier-Daures M, Anger K (2005) Osmoregulation, immunolocalization of Na^+/K^+-ATPase, and ultrastructure of branchial epithelia in the developing brown shrimp, *Crangon crangon* (Decapoda, Caridea). Physiol Biochem Zool 78(6):1017-1025

Claiborne JB, Edwards SL (2002) Acid-base regulation in fishes: Cellular and molecular mechanisms. J Exp Zool 293:302-319

Colina C, Rosenthal JJC, DeGiorgis JA, Srikumar D, Iruku N, Holmgren M (2007) Structural basis of Na^+/K^+-ATPase adaptation to marine environments. Nat Struc Mol Biol 14:427 431

Dean RB (1941) Theories of electrolyte equilibrium in muscle. Biol Symposia 3:331-348

Donaubauer HH (1980) Adenosine triphosphatase localization in the branchial heart of *Sepia officinalis* L. (Cephalopoda). Histochemistry 69:27-37

Donaubauer HH (1981) Sodium- and potassium-activated adenosine triphosphatase in the excretory organs of *Sepia officinalis* (Cephalopoda). Mar Biol 63:143-150

Emanuel CF, Martin AW (1956) The composition of octopus renal fluid. J Comp Physiol 39:226-234

Evans DH, Piermarini PM, Choe KP (2005) The multifunctional fish gill: Dominant site of gas exchange, osmoregulation, acid-base regulation, and excretion of nitrogenous waste. Physiol Rev 85:97-177

Fagan MJ, Saier MH (1994) P-type ATPases of eukaryotes and bacteria: sequence analyses and construction of phylogenetic trees. J Mol Evol 38:57-99

Fioroni P (1962) Die embryonale Entwicklung der Hautdrüsen und des Trichterorganes von *Octopus vulgaris* Lam. Acta annat 50:264-295

Fioroni P (1990) Our recent knowledge of the development of the cuttlefish (*Sepia officinalis*). Zool Anz 224:1-25

Garvin JL, Burg MB, Knepper MA (1985) Ammonium replaces potassium in supporting sodium transport by the Na-K-ATPase of renal proximal straight tubules. Am J Physiol Renal Physiol 249:F785-F788

Gibbs A, Somero GN (1990) Na^+-K^+-adenosine triphosphatase activities in gills of marine teleost fishes: changes with depth, size and locomotory activity level. Mar Biol 106:315-321

Giffard-Mena I, Charmantier G, Grousset E, Aujoulat F, Castille R (2006) Digestive tract ontogeny of *Dicentrarchus labrax*: Implication in osmoregulation. Development Growth Diff 48:139-151

Gutowska MA, Melzner F (2009) Abiotic conditions in cephalopod (*Sepia officinalis*) eggs: embryonic development at low pH and high pCO_2. Mar Biol 156:515-519

Gutowska MA, Melzner F, Langenbuch M, Bock C, Claireaux G, Pörtner H-O (2009) Acid-base regulatory ability of the cephalopod (*Sepia officinalis*) in response to environmental hypercapnia. J Comp Physiol B in Press

Hanlon RT, Messenger JB (1996) Cephalopod behaviour, Vol. Cambridge University Press, Cambribge

Hiroi J, McCormick SD, Ohtani-Kaneko R, Kaneko T (2005) Functional classification of mitochondrion-rich cells in euryhaline Mozambique tilapia (*Oreochromis mossambicus*) embryos, by means of triple immunofluorescence staining for Na^+/K^+-ATPase, $Na^+/K^+/2Cl^-$ cotransporter and CFTR anion channel. J Exp Biol 208:2023-2036

Hiroi J, Yasumasu S, McCormick SD, Hwang PP, Kaneko T (2008) Evidence for an apical Na-Cl cotransporter involved in ion uptake in a teleost fish. J Exp Biol 211:2584-2599

Houlihan DF, McMillan DN, Agnisola C, Trara Genoino I, Foti L (1990) Protein synthesis and growth in *Octopus vulgaris*. Mar Biol 106:251-259

Hsiao CD, You MS, Guh YJ, Ma M, Jiang YJ, Hwang PP (2007) A positive regulatory loop between *foxi3a* and *foxi3b* is essential for specification and differentiation of zebrafish epidermal ionocytes. PLoS ONE 2:e302

Hu MY, Yan HY, Chung WS, Shiao YC, Hwang PP (2009) Acoustically evoked potential in two cephalopods infered using the auditory brainstem response (ABR) approach. Comp Biochem Physiol 153:278-283

Hwang PP, Lee TH (2007) New insights into fish ion regulation and mitochondrion-rich cells. Comp Biochem Physiol A 148:479-497

Knepper MA (2008) Physiology: Courier service for ammonia. Nature 456:336-337

Kurtz I, Balaban RS (1986) Ammonium as a substrate for Na^+-K^+-ATPase in rabbit proximal tubules. AM J Physiol Renal Physiol 250:F497-F502

Lämmli UK (1970) Cleavage of structural proteins during the assembly of the head of Bacteriophage T4. Nature 227:680-685

Laurie M (1983) The organ of verrill in Loligo. Q J Micr Sci 29:97-100

Lebovitz RM, Takeyasu K, Fambrough DM (1989) Molecular characterization and expression of the (Na^++K^+)-ATPase α-subunit in *Drosophila melanogaster*. EMBO J 8:193-202

Lemaire J (1970) Table de développement embryonaire de *Sepia officinalis* L. (Mollusque Céphalopode). Bull Soc Zool Fr 95:773-782

Lignot J-H, Charmantier G (2001) Immunolocalization of Na^+/K^+-ATPase in the branchial cavity during the early development of the european lobster *Homarus gammarus* (Crustacea, Decapoda). J Histochem Cytochem 49(8):1013-1023

Mackie GO (2008) Immunostaining of peripheral nerves and other tissues in whole mount preparations from hatchling cephalopods. Cell Tiss Res 40:21-29

Melzner F, Göbel S, Langenbuch M, Gutowska MA, Pörtner H-O, Lucassen M (2009a) Swimming performance in atlantic cod (*Gadus morhua*) following long-term (4-12 month) acclimation to elevated seawater pCO_2. Aqua Toxicol 92:30-37

Melzner F, Gutowska MA, Langenbuch M, Dupont S, Lucassen M, Thorndyke MC, Bleich M, Pörtner H-O (2009b) Physiological basis for high CO_2 tolerance in marine ectothermic animals: pre-adaptation through lifestyle and ontogeny? Biogeosci Discuss 6:4693-4738

Melzner F, Mark FC, Pörtner H-O (2007) Role of blood-oxygen transport in thermal tolerance of the cuttlefish, *Sepia officinalis*. Integr Comp Biol 47:645-655

Murer H, Hopfer U (1974) Demonstration of electrogenic Na+-dependent D-glucose transport in intestinal brush border membranes. Proc Nat Acad Sci 71:484-488

Nebel C, Negre-Sadargues G, Blasco C, Charmantier G (2005) Morphofunctional ontogeny of the urinary system of the European sea bass *Dicentrarchus labrax*. Anat Embryol 209:193-206

Nixon M, Mangold K (1998) The early life of *Sepia officinalis*, and the contrast with that of *Octopus vulgaris* (Cephalopoda). J Zool Lond 245:407-421

O`Dor RK (2002) Telemetered cephalopod energetics: Swimming, soaring, and blimping. Integr Comp Biol 42:1065-1070

O`Dor RK, Webber DM (1991) Invertebrate athletes: Trade-offs between transport efficiency and power density in cephalopod evolution. J exp Biol 160:93-112

Packard A (1972) Cephalopods and fish: the limits of convergence. Biol Rev 47:241-307

Perry SF, Gilmour KM (2006) Acid–base balance and CO_2 excretion in fish: Unanswered questions and emerging models. Resp Physiol Neurobiol 154:199-215

Peterson GL, Hokin LE (1981) Molecular weight and stoichiometry of the sodium- and potassium-activated adenosine triphosphatase subunits. J Biol Chem 256:3751-3761

Pörtner H-O, Zielinski S (1998) Environmental constraints and the physiology of performance in squids. S Afr J mar sci 20:207-221

Pörtner HO (1994) Coordination of metabolism, acid-base regulation and haemocyanin function in cephalopods. Mar Fresh Behav Physiol 25:131-148

Potts WTW (1965) Ammonia excretion in *Octopus dolfeini*. Comp Biochem Physiol 14:339-355

Romero MF, Fulton CM, Boron WF (2004) The SLC4 family of HCO_3^- transporters. Eur J Physiol 447:495-509

Schipp R, Mollenhauer S, Boletzky S (1979) Electron microscopical and histochemical studies of differentiation and function of the cephalopod gill (*Sepia officinalis* L.). Zoomorph 93:193-207

Schipp R, von Boletzky S (1976) The pancreatic appendages of dibranchiate cephalopods. Zoomorph 86:81-98

Schwartz AA, Allen JC, Harigaya S (1969) Possible involvement of cardiac Na^+/K^+-adenosine triphosphatase in the mechanism of action of cardiac glycosides. J Pharmacol Exp Ther 168:31-41

Siebers D, Leweck K, Markus H, Winkler A (1982) Sodium regulation in the shore crab *Carcinus maenas* as related to ambient salinity. Mar Biol 69:37-43

Siebers D, Winkler A, Leweck K, Madian A (1983) Regulation of sodium in the shore crab *Carcinus maenas*, adapted to environments of constant and changing salinities. Helgoländer Meeresunters 36:303-312

von Boletzky S (1983) *Sepia officinalis*. In: Boyle PR (ed) Cephalopod Life Cycles, Vol I. Academic Press, London

Wall SM, Davis BS, Hassell KA, Mehta P, Park SJ (1999) In rat tiMCD, NH_4^+ uptake by Na^+/K^+-ATPase is critical to net acid secretion during chronic hypokalemia Am J Physiol, p F866-F847

Wells JM, O`Dor RK (1991) Jet propulsion and the evolution of the cephalopods. Bull Mar Sci 49:419-432

Wells JM, Wells J (1989) Water uptake in a cephalopod and the function of the so-called "pancreas". J Exp Biol 145:215-226

Wells MJ (1990) Oxygen extraction and jet propulsion in cephalopods. Can J Zool 68:815-824

Wells MJ, Wells J (1982) Ventilatory currents in the mantle of cephalopods. J Exp Biol 99:315-330

Wheatly MG, Henry RP (1992) Extracellular and intracellular acid-base regulation in crustaceans. J Exp Zool 263:127-142

Wood CM, Milligan LC, Walsh PJ (1999) Renal responses of trout to chronic respiratory and metabolic acidosis and metabolic alkalosis. Am J Physiol Regul Integr Comp Physiol 277:482-492

Figure legends

Fig. 1 Pancreatic appendages of a *Loligo vulgaris* hatchling (Masson`s stain) showing the inner epithelium that consists of high cells exhibiting an apical microvillous border and the outer epithelium that is characterized by large blood lacunae (**a**). Na^+/K^+-ATPase immuno staining transverse section through pancreatic appendages of *Loligo vulgaris* hatchling (**b, c**) and *Sepia officinalis* embryos (**d, e**) In both species, the inner epithelium is characterized by an extraordinary amount of Na^+/K^+-ATPase. Only in *S. officinalis* the outer epithelium Na^+/K^+-ATPase occurs in basolateral membranes close to the blood sinus (**d**) as indicated by arrowheads. Indications used: blood sinus (bs); branchial gland (bg); blood lacunae (bl); ductus hepatopancreas (dh); gill lamellae (gl); inner epithelium (ie); mantle cavity (mc); microvillous (mv); outer epithelium (oe); midgut gland (mg); oesophagus (oes); pancreatic appendages (pa).

Fig. 2 Gill morphology and Na^+/K^+-ATPase localization in *Loligo vulgaris*. Masson`s staining of a longitudinal section through a *L. vulgaris* hatchling (ML = 2 mm) (**a)** and the gill lamellae of an adult specimen (ML = 15 cm) (**b)**. Localization of the enzyme in the coronal section through the gill of a late embryo (**c)** and sagittal section through the gill of a 2 day hatchling (**d**). 1^{st} order gill lamellae of an adult showing Na^+/K^+-ATPase location in the convex part of the transport epithelium of 3^{rd} order lamellae (3°gl) (only at the tip of 2^{nd} order lamellae (2°gl)) (**e**). Na^+/K^+-ATPase rich cells surrounding a junction of a 3^{rd} order efferent vessel (**f**). For better contrast at high magnification, blue auto-fluorescence by UV excitation was used to indicate the non-stained areas. Indications used: branchial heart (bh); blood vessel (bv); epithelium (e); gill (g); gill lamellae (gl); intestines (I); lumen (lu); mantle (m); mantle cavity (mc); nucleus (n).

Fig. 3 Mantle cavity overview, gill morphology and Na^+/K^+-ATPase localization in *Sepia officinalis* juveniles and embryos. Overview of the mantle cavity of a juvenile *Sepia officinalis* (coronal section) showing major internal organs (**a**). Na^+/K^+-ATPase immuno stainings of *Sepia officinalis* gills from juveniles (**b, c, d**) and embryos (**e, f**). 2^{nd} order gill lamellae of a 6 day old juvenile showing Na^+/K^+-ATPase located exclusively in the convex part of the transport epithelium in the 3^{rd} order gill lamellae (3°gl) (**c**). For a better demonstration of cell-organization in the gill epithelium a phase contrast and a fluorescent image of the same area were superimposed (**b**). High concentrations of Na^+/K^+-ATPase in basolateral regions close to the blood sinus (blue auto-fluorescence) (**d**). Localization of the enzyme in the sagittal section through the gill of a late embryo (**e, f**). Indications used: auricle (au); branchial heart (bh); blood sinus (bs); blood vessel (bv); caecum (ca); gill (g); gill lamellae (gl); inner epithelium (ie); ink gland (ig); mantle (m); mantle cavity (mc); outer epithelium (oe);

pancreatic appendages (pa); pericardial coelom (pc); stomach (st); ventricle (ven).

Fig. 4 Western blot analysis of Na^+/K^+-ATPase α expression for *Loligo vulgaris* (LV) and *Sepia officinalis* (SO) homogenates (100 mg FM ml^{-1}) (B) using the primary antibodies Na^+/K^+-ATPase α (H-300) (**a**) and α5 (**b**). Transverse sections through the gill of *L. vulgaris* hatchlings stained with the primary antibody (H-300) (**a**) and the α5 (**b**).

Fig. 5 Specificity control of the anti bodies performed on gills of *Sepia officinalis* hatchlings. A negative control was performed by omitting the primary antibody Na^+/K^+-ATPase α (H-300) (**a**). Positive immuno-reactivity was achieved only with both, primary and secondary antibodies (**b**)

Table legends

Table 1 Na^+/K^+-ATPase and total ATPase activities of *Loligo vulgaris* hatchlings (4-4.5 mg_{FM}) and *Sepia officinalis* hatchlings (140-180 mg_{FM}) measured in whole animal homogenates given in ($\mu mol_{ATP}\ g_{FM}^{-1}\ h^{-1}$). Additionally, activities were determined for gills and pancreatic appendages of *S. officinalis* juveniles (10-15 g_{FM}). Activities presented as mean and standard deviation; (n) Number of specimens tested.

Figure 1

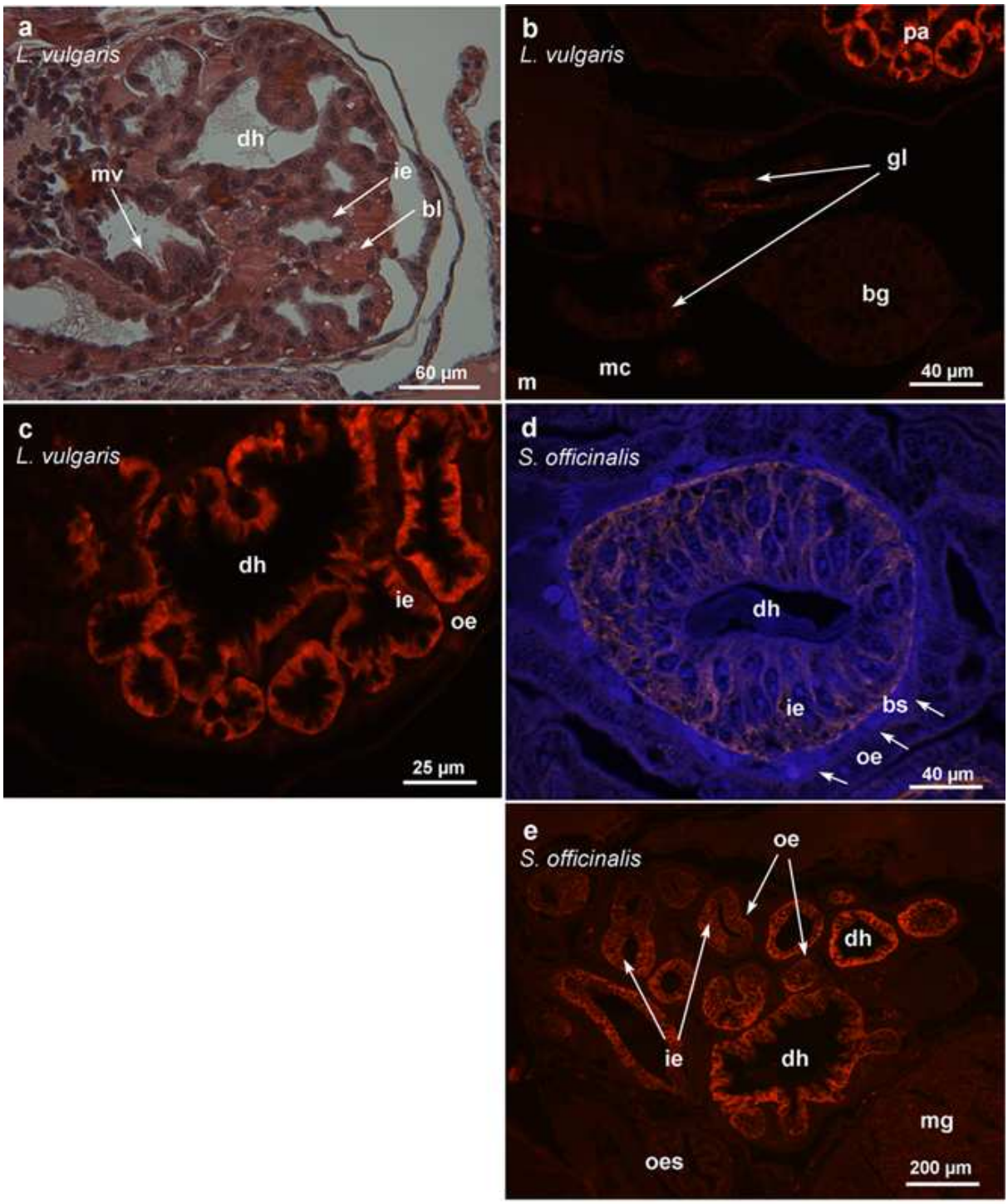
a
L. vulgaris
dh
mv
ie
bl
60 µm
b
L. vulgaris
pa
gl
bg
mc
m
40 µm
c
L. vulgaris
dh
ie
oe
25 µm
d
S. officinalis
dh
ie
bs
oe
40 µm
e
S. officinalis
oe
dh
ie
dh
mg
oes
200 µm

Figure 2

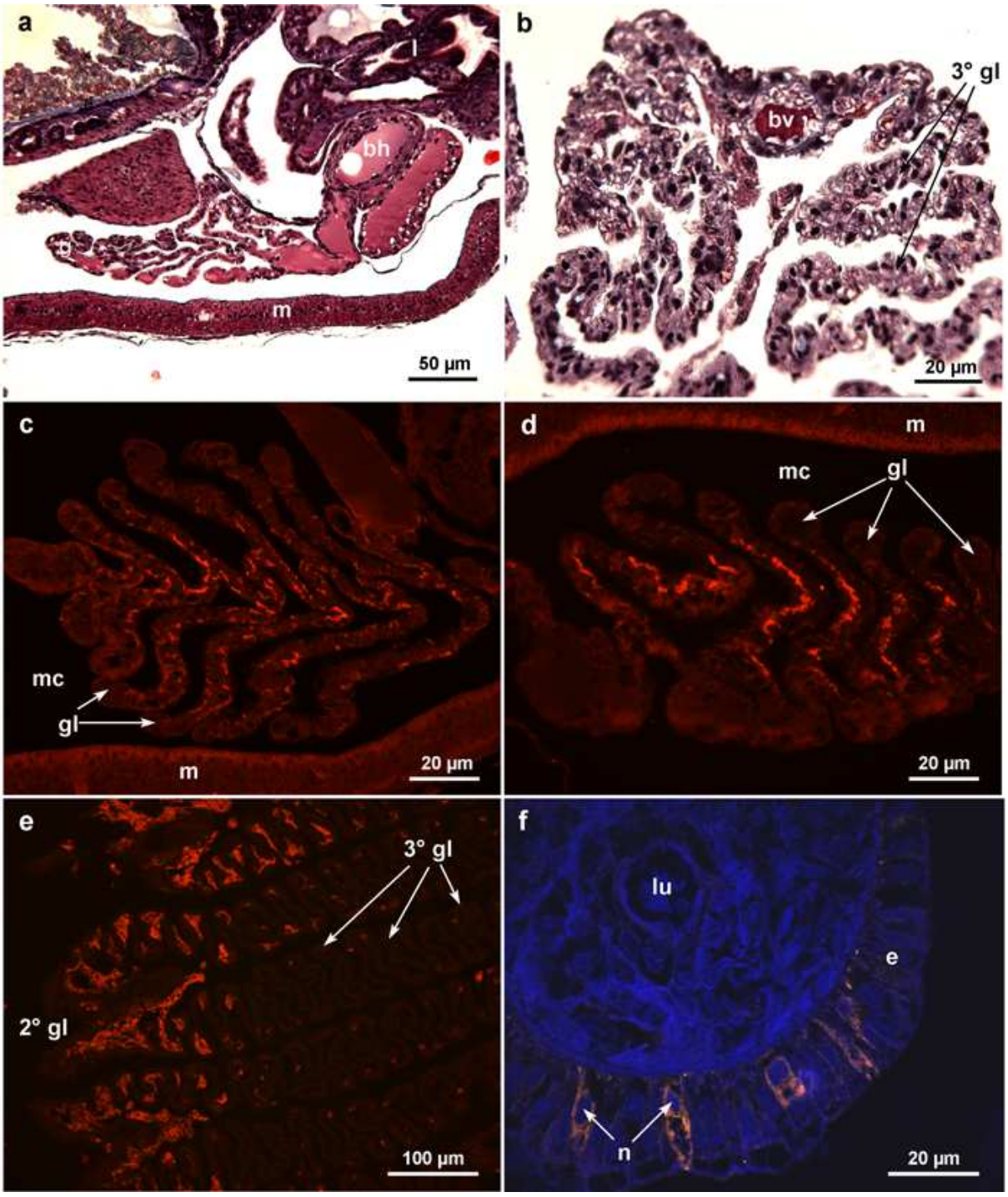
a
bh
m
50 µm
b
3° gl
bv
20 µm
c
mc
gl
m
20 µm
d
m
mc
gl
20 µm
e
3° gl
2° gl
100 µm
f
lu
e
n
20 µm

Figure 3

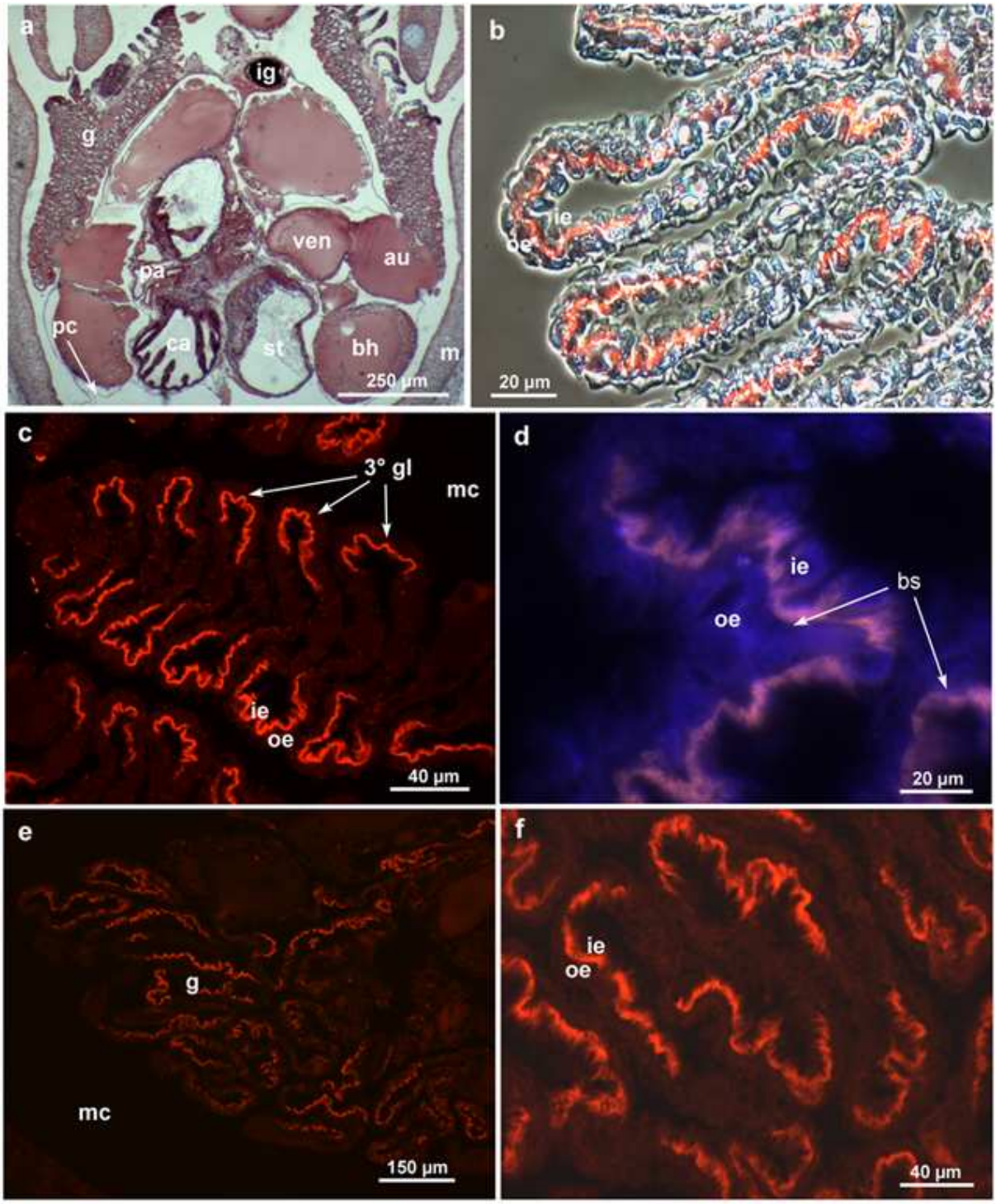
a
ig
g
ven
au
pa
pc
ca
st
bh
m
250 µm
b
ie
oe
20 µm
c
3° gl
mc
ie
oe
40 µm
d
ie
bs
oe
20 µm
e
g
mc
150 µm
f
ie
oe
40 µm

Figure 4

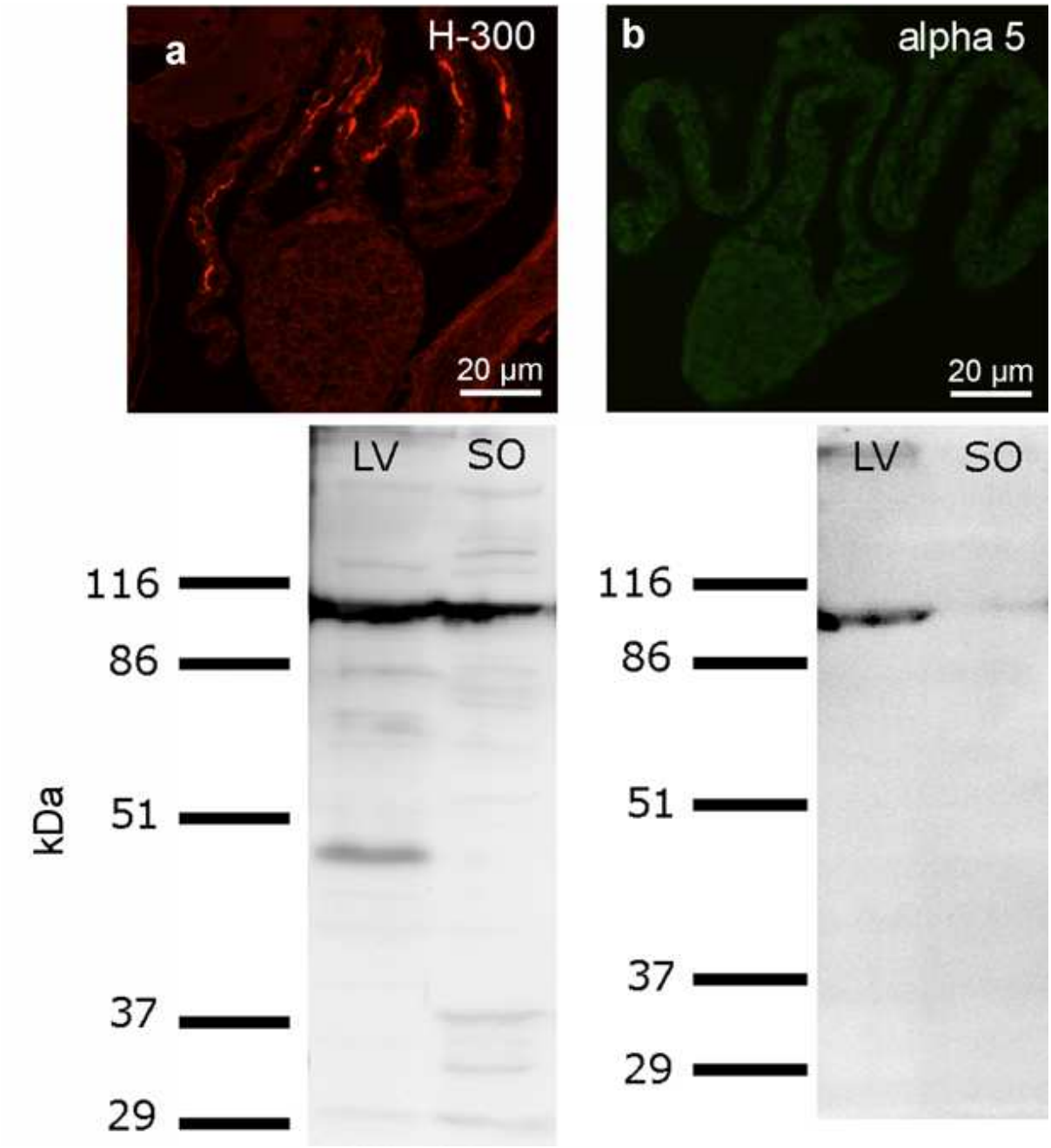
a
H-300
20 µm
b
alpha 5
20 µm
LV
SO
LV
SO
kDa
116
86
51
37
29
116
86
51
37
29

Figure 5

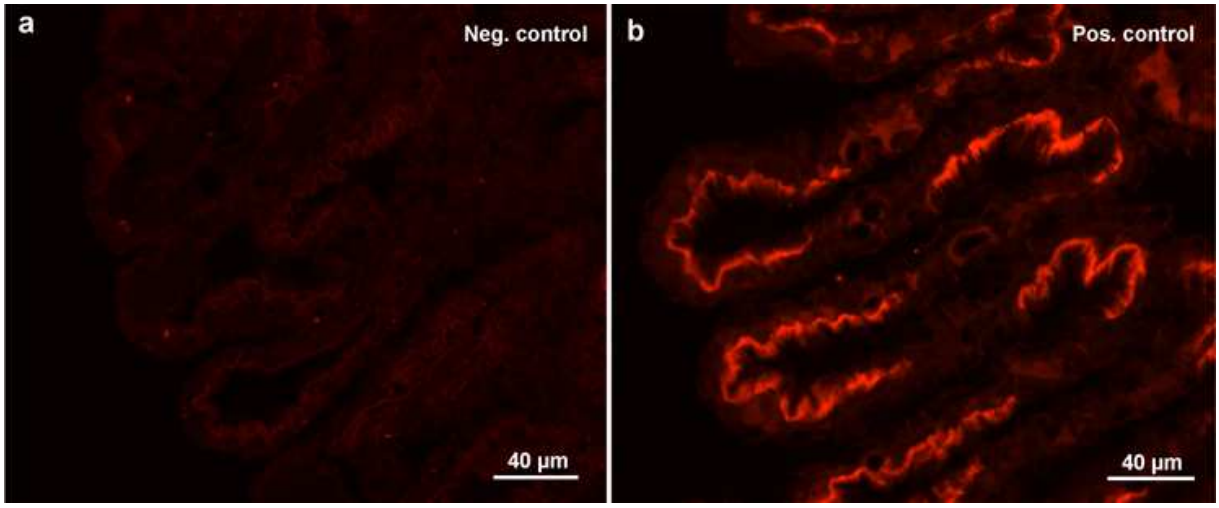

Table 1

	Loligo vulgaris	*Sepia officinalis*		
	whole animals (5)	whole animals (6)	gill (8)	pancreatic appendages (8)
Na^+/K^+-ATPase	31.83 ± 3.28	156.97 ± 32.35	94.83 ± 18.49	421.75 ± 102.25
Other ATPases	341.94 ± 59.57	928.74 ± 125.62	404.81 ± 66.76	661.69 ± 66.51
Total ATPases	373.77 ± 60.21	1106.02 ± 132.65	499.64 ± 75.15	1083.44 ± 157.37
Na^+/K^+-ATPase (% of total ATPases)	8.52	14.19	18.98	38.92

4. Discussion

The overall question of the present study addresses the physiological response of cephalopods towards elevated environmental pCO_2. This is an important research question in the frame of the previously described phenomenon of ocean acidification, as cephalopods, especially cuttlefish and squid, are of high commercial value and key species in marine food webs (Piatkowski et al. 2001; Nottage et al. 2006). Generally, marine invertebrates such as echinoderms, crustaceans and molluscs have been shown to alter growth rates, oxygen consumption and gene expression in response to hypercapnia (Kurihara et al. 2007; Dupont et al. 2010; Lanning et al. 2010; Walther et al. 2010; Stumpp et al. submitted). The reasons why elevated seawater pCO_2 affects marine organisms are complex. In a first step towards understanding hypercapnia sensitivity, it has proven useful to separate between direct and indirect effects of ocean acidification. Earlier studies concluded that marine calcifying organisms, especially those with an external $CaCO_3$ shell or skeleton have been shown to be particularly sensitive to ocean acidification due to a negative effect on the calcification rate or the direct dissolution of their $CaCO_3$ structures (Riebesell et al. 2000; Orr et al. 2005; Comeau et al. 2009; Lischka et al. 2010; Nienhuis et al. 2010). For example, the marine snail *Nucella lamellosa* decreased its shell weight gain per day linearly with increasing CO_2 levels. Due to the fact that this effect was paralleled by shell weight loss per day in empty shells, the authors suggested that these declines in shell weight gain were due to increased dissolution of existing shell material (Nienhuis et al. 2010). Moreover, observations made for the mussel *Mytilus edulis* and the oyster *Crassostrea gigas* suggested that calcification rates decrease linearly with increasing water pCO_2 during short-term exposure (Gazeau et al. 2007). However, long-term exposure experiments of *M. edulis* to elevated water pCO_2 have drawn different conclusions (Thomsen et al. 2010) which are discussed in greater detail in the following paragraph. Decreased calcification rates indicated by significantly lower incorporation of ^{45}Ca under CO_2 treatment were also described for the pteropod *Limacina helicina* at two temperatures (Comeau et al. 2010). Calcification in larval stages of marine bivalves (*C. gigas* and *M. galloprovincialis*) was shown to be particularly impacted by elevated water pCO_2 indicated by complete inhibition of shell mineralization in 45% of CO_2 (>0.2 kPa) treated larvae (Kurihara et al. 2007; Kurihara et al. 2008).

More recent studies suggested that reductions in growth, calcification and development can be explained from an energetic point of view. This approach can be more complex but probably represents a more exhaustive approach to explain decrased growth and

calcification levels in response to elevated seawater pCO_2. In this case somatic growth and development are not affected by the direct external dissolution of $CaCO_3$ structures but rather by rearrangement of energy budgets towards compensatory processes such as increased calcification or acid-base regulation (Findley et al. 2009; Cummings et al. 2010; Lanning et al. 2010; Thomsen and Melzner 2010; Stumpp et al. submitted). For example, higher metabolic activity is believed to compensate for internal shell dissolution in the polar pteropod *Limacina helicina* and thus may represent a severe energetic challenge for periods of food scarcity (e.g. winter season) and reproduction phases (Lischka et al. 2010). Another example demonstrated that elevated seawater pCO_2 levels (0.4 kPa) significantly reduced shell length and mass of the blue mussel *Mytilus edulis*. These calcification reductions were accompanied by an increased energy expenditure of up to 58% and linearly increased NH_4^+ excretion rates (Thomsen and Melzner 2010). These observations suggest that negative effects on growth and calcification may also result from a shift of the energy budgets towards compensatory processes such as metabolism and acid-base regulation.

Active organisms like fish and cephalopods are believed to have a higher ability to tolerate hypercapnia induced acid-base disturbances due to their high metabolic/respiratory rate and rate fluctuations, leading to naturally large pCO_2 variations, of 0.2 kPa or more in extracellular fluids of these organisms (Larsen et al. 1997; Gutowska et al. 2009). During excessive exercise pCO_2 in body fluids increases, causing an extracellular acidosis with maximum pCO_2 values between 0.4 kPa (cephalopods) and up to 1.0 kPa (teleost fish) (Pörtner et al. 1991; Brauner et al. 2000). Furthermore, these “tolerant” organisms can be characterized by high NKA activity levels in their gill tissues which can be regarded an essential feature in order to counter for acid-base disturbances caused by a respiratory acidosis (Seidelin et al. 2001; Choe and Evans 2004). Based on this knowledge, Melzner et al. (2009b) suggested that these features can be regarded a pre-adaptation of active organisms in order to cope with elevated environmental hypercapnia, at least during short-term exposure. In my PhD thesis, I have investigated to what degree cephalopods can be regarded pre-adapted to cope with elevated environmental pCO_2, and to which degree this relative tolerance is a function of the ontogenetic stages studied.

4.1. Differential response of ontogenetic stages

Like adult fish (Fivelstad et al. 2003; Foss et al. 2003), juvenile/adult cephalopods can tolerate high seawater pCO_2 of up to 0.6 kPa over long exposure times without suffering from decreased growth and calcification (Gutowska et al. 2008). However, the present work demonstrated that even if juvenile or adult cuttlefish can tolerate high pCO_2, early life stages are more susceptible towards environmental hypercapnia. This sensitivity is indicated by a reduction of somatic growth by approximately 20-30% (BM) at an ambient water pCO_2 of 0.37 kPa in *S. officinalis* late embryos (publication 1 and figure 4.1.A). This retarded growth is likely linked to a developmental delay as well as indicated by a delay in hatching, and a reduced consumption of yolk (figure 4.1.B and figure 4.2.). In order to determine hypercapnia sensitivity thresholds of cuttlefish early developmental stages two different CO_2 concentrations, one medium (0.14 kPa) and one high (0.37 kPa) were applied. By comparing the effects of these two concentrations on cuttlefish embryonic development it can be concluded that the high CO_2 concentration significantly depresses somatic growth and development, whereas the intermediate level seems not to have a significant effect on these parameters. Accordingly, it can be concluded that increases in water pCO_2 as projected for the coming 300 years will probably not significantly affect the early development of cuttlefish. However, if water pCO_2 increase beyond these levels, especially in naturally hypoxic/hypercapnic coastal habitats, this may lead to slowed embryonic development and a smaller hatching size.

Hypercapnia induced reductions in larval and embryonic growth/development have also been observed in several other invertebrate species such as crustaceans, echinoderms, and bivalves (Kurihara et al. 2004; Kurihara et al. 2007; Dupont et al. 2008; Kurihara 2008; Dupont and Thorndyke 2009; Walther et al. 2010). All marine fish species studied so far have been described as very tolerant towards ocean acidification relevant pCO_2 levels, indicated by maintained growth metabolic rates and swimming speeds (Melzner et al. 2009a; Munday et al. 2009a; Ishimatsu and Dissanayake 2010). Only few studies described distinct adverse CO_2 effects on fish early life stages which can be proposed to react more sensitively towards hypercapnia than adults. Some studies demonstrated that embryonic development of marine teleosts is unaffected by exposure to CO_2 concentrations of up to 0.16 kPa. Therefore fish larvae are apparently more tolerant than larval stages of most invertebrates (Munday et al. 2009a; Tseng et al. in prep.). However, two further studies demonstrated that elevated sea water pCO_2 (0.1 kPa and 0.25 kPa) leads to increased growth of otoliths in larval white sea

bass *Atractoscion nobilis* (Checkley et al. 2009) and that olfactory discrimination is disrupted in the clownfish *Amphiprion percula*. Recent investigations tested the effects of moderate hypercapnia (0.16 kPa and 0.58 kPa) on seawater acclimated medaka (*Oryzias latipes*) (Tseng et al. in prep.). The results suggest that during embryogenesis, just before epidermal ionocytes occur (4-6 days post fertilization), a sensitivity bottleneck exists, indicated by a reduced somatic growth and development. After hatching, 0.58 kPa treated animals exhibit a slightly reduced length whereas 0.16 kPa treated fish show the tendency of being longer compared to control animals. The high hypercapnia tolerance in these fish early life stages is probably / might be linked to the presence of an efficient acid-base regulating machinery, localized in epidermal ionocytes (Tseng et al. in prep.).

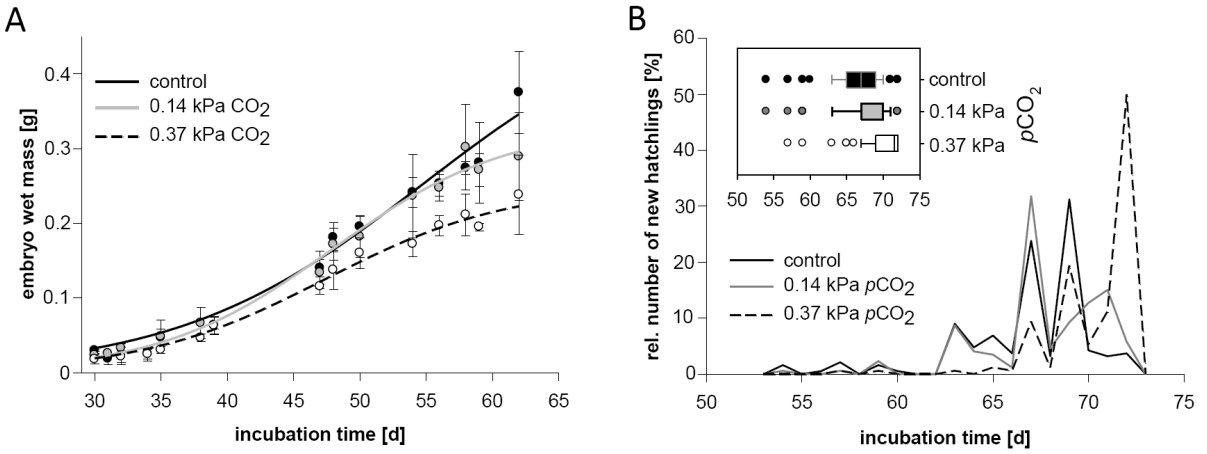

Figure 4.1. *Sepia officinalis* embryo wet mass as a function of time for embryos reared under different pCO_2 (A). Circles and error bars represent mean ± SD (n = 3-15). Regression lines represent sigmoid regressions for the control group (EWM[g]=0.503/(1+e$^{(-(t[d]-54.699)/9.254)}$, R^2=0.936), the 0.14 kPa CO_2 group (EWM[g]=0.331/(1+e$^{(-(it[d]-47.951)/6.565))}$, R^2=0.873) and the 0.37 kPa CO_2 group (EWM[g]=0.250/(1+e$^{(-(it[d]-47.373)/6.968))}$, R^2=0.909). Effects of pCO_2 on the relative number of new hatchlings during incubation time (B). Box plot representation of the effect of different pCO_2 on the absolute numbers of new hatchlings over incubation time (insert in B). Box plots show 25th and 75th percentiles, median, 10th and 90th percentiles (bars) and outliers (circles).

It has been demonstrated in earlier studies that hypercapnic conditions can lead to an uncompensated acidosis, which is believed to induce metabolic depression (Pörtner et al. 2000; Pörtner et al. 2004). Metabolic depression is a major strategy in most invertebrate phyla and all vertebrate classes to survive environmental stress (Dezwaan and M 1976; Guppy 2004; Ramnanan and Storey 2006). Although the biochemical mechanisms remain unclear, several studies suggested that reduction in intracellular pH (pH_i) (Guppy et al. 1994; Guppy 2004) or extracellular pH (pH_e) (Reipschläger and Pörtner 1996b) may be the trigger that elicits metabolic depression. Furthermore, it has been demonstrated, that during aestivation of

the snail, *Helix aspersa*, at least 75% of the depression of oxygen consumption is derived from a metabolic control of the producing processes (e.g. glycolysis, citric acid cycle and the electron transport chain) whereas only 25% of the reduction is due to metabolic control of the consuming processes including ATP synthesis and all processes involved in ATP consumption (Bishop et al. 2002). Such a primary effect on the energy providing processes suggests an upstream control of metabolic depression (Bishop et al. 2002).

In marine invertebrates like the worm *Sipunculus nudus*, hypercapnia induced reductions in pH_e (and not in pH_i) were demonstrated to elicit metabolic depression as indicated by reduced oxygen consumption rates in isolated muscle tissues (Reipschläger and Pörtner 1996a). Such a metabolic depression due to an uncompensated acidosis may also present a parsimonious explanation for retarded development and growth under acidified conditions. However, recent studies demonstrated that in response to moderate hypercapnia several marine organisms decrease their growth and developmental rates dispite an maintained or even increased metabolic rate (Comeau et al. 2010; Thomsen and Melzner 2010; Stumpp et al. submitted).

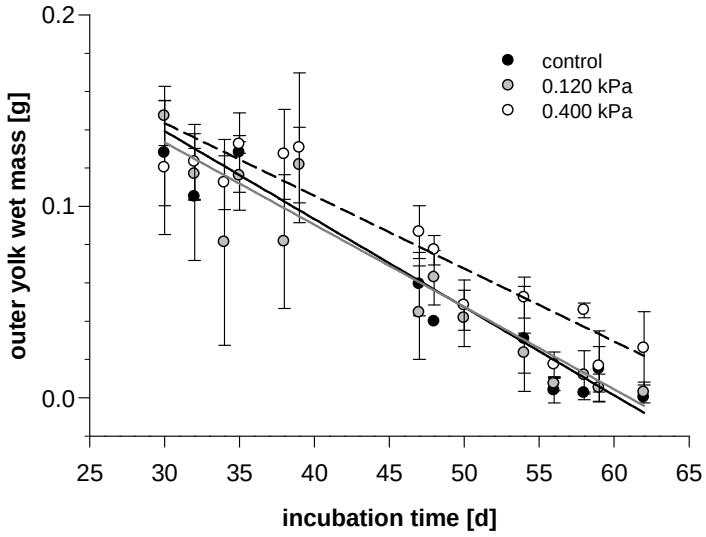

Figure 4.2. Relationship between yolk mass [g] and incubation time [d] for embryos reared under different pCO_2. Regression lines represent exponential regressions of raw data for the control group (OYM [g] = $1.5144*e^{(0.0770*it[d])}$, R^2=0.7668; black line), the 0.14 kPa CO_2 group (OYM[g] = $1.1018*e^{(0.0668*it[d])}$, R^2=0.7368; grey line) and the 0.37 kPa CO_2 group (OYM[g] = $0.5365*e^{(0.0428*it[d])}$, R^2=0.6718; dashed line). Circles and error bars represent mean ± SD.

These observations gave rise to new hypotheses regarding the reasons for reductions in growth and development in response to moderate seawater hypercapnia. For example cuttlefish accumulate millimolar concentrations of HCO_3^- in their blood in response to hypercapnia in order to stabilize pH_e (Gutowska et al. 2010a), and thus, high blood pCO_2 values might also represent a severe energetic challenge to the developing embryo and could result in a higher fraction of aerobic scope spent on acid-base regulation. This energy allocation could in turn have negative repercussions on embryonic growth. The latter is

supported by determinations of metabolic and yolk consumption rates of cuttlefish embryos reared under different pCO_2 concentrations. The metabolic rates of control and 0.14 kPa pCO_2 treated embryos at stage 28-29 were similar to those values reported for *Sepia officinalis* stage 29 embryos (Wolf et al. 1985). However, cuttlefish embryos reared under 0.37 kPa pCO_2 exhibited a lower aerobic metabolism when compared to control animals at the same time point. The lower respiration rates are in agreement with the delayed development of these animals under elevated environmental pCO_2 (figure 4.3.A). However, when oxygen consumption rates were corrected for wet mass, embryos treated with elevated pCO_2 did not have higher metabolic rates (figure 4.3.B). Although high pCO_2 embryos tended to have a lower metabolic rate, regression analysis did not provide significant results probably due to the low statistical power of the data. These observations indicated that metabolic depression is not an important response towards environmental hypercapnia in cephalopod embryonic stages. Nevertheless, more sensitive respiration measurements in combination with enzyme activities and expression studies will be fruitful further research targets in order to provide a definitive answer.

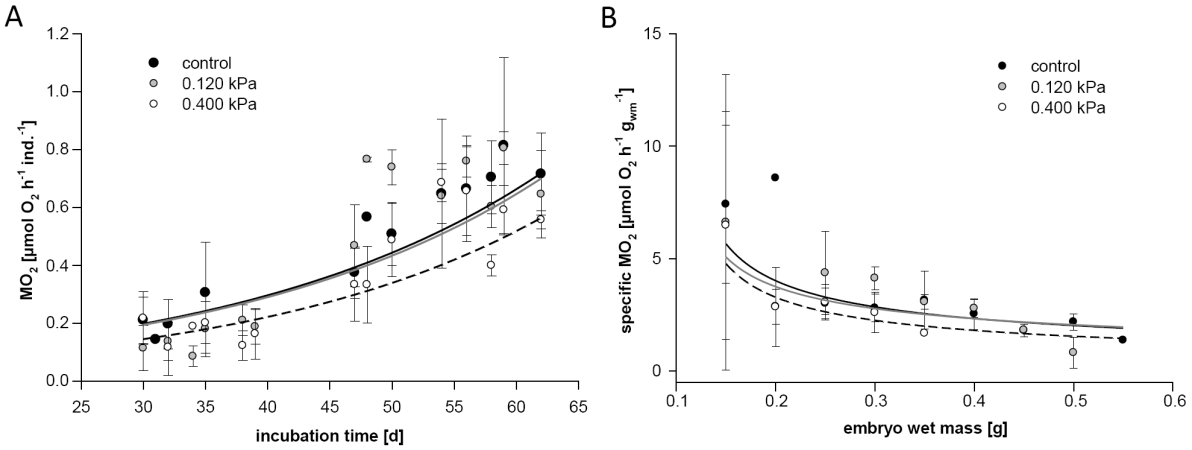

Figure 4.3. Respiration rate as a function of time for embryos reared under different pCO_2 concentrations fitted by exponential regression lines (A): control group (MO_2 [µmol O_2 h^{-1} ind^{-1}]=0.0594*$e^{(0.0402*it[d])}$, R^2=0.6593), the 0.14 kPa CO_2 group (MO_2 [µmol O_2 h^{-1} ind^{-1}]=0.0586*$e^{(0.0400*it[d])}$, R^2=0.5315) and the 0.37 kPa CO_2 group (MO_2 [µmol O_2 h^{-1} ind^{-1}]=0.0407*$e^{(0.0424*it[d])}$, R^2=0.5869) Circles and error bars represent mean ± SD. Specific MO_2 as a function of embryo wet mass for embryos reared under different pCO_2 (B). Regression lines represent power regressions of raw data for the control group (spec. MO_2 [µmol O_2 h^{-1} g^{-1}] = 12.868*EWM[g]$^{-0.4942}$, R^2=0.6565), the 0.14 kPa CO_2 group (spec. MO_2 [µmol O_2 h^{-1} g^{-1}] = 13.821*EWM[g]$^{-0.4335}$, R^2=0.1811) and the 0.37 kPa CO_2 group (spec. MO_2 [µmol O_2 h^{-1} g^{-1}] = 0.9398*EWM[g]$^{-0.5424}$, R^2=0.3240). Circles and error bars represent mean ± SD.

Interestingly, beside effects on the organismic level, also gene expression profiles determined for gill tissues revealed strong differences in terms of CO_2 sensitivity between early developmental stages (late embryos and hatchlings) compared to juveniles and adults (figure

4.4.). While no significant changes were detected in juveniles during short and long-term exposure, strong changes in gene expression were measured in early developmental stages. In late embryos and hatchlings exposed to 0.37 kPa CO_2 for 5 weeks, reduced somatic growth is accompanied by changes in the expression of several genes which are involved in ion regulatory (e.g. so*NKA*, so*NBCe*, soc*CAII*) and metabolic (e.g. *ATP-synthas*e, *COX*, *CYP450*) processes. Intriguingly, mRNA of all acid-base regulatory gene candidates (so*NKA*, so*NBCe* and soc*CAII*), were down regulated by up to 80% in response to elevated seawater pCO_2.

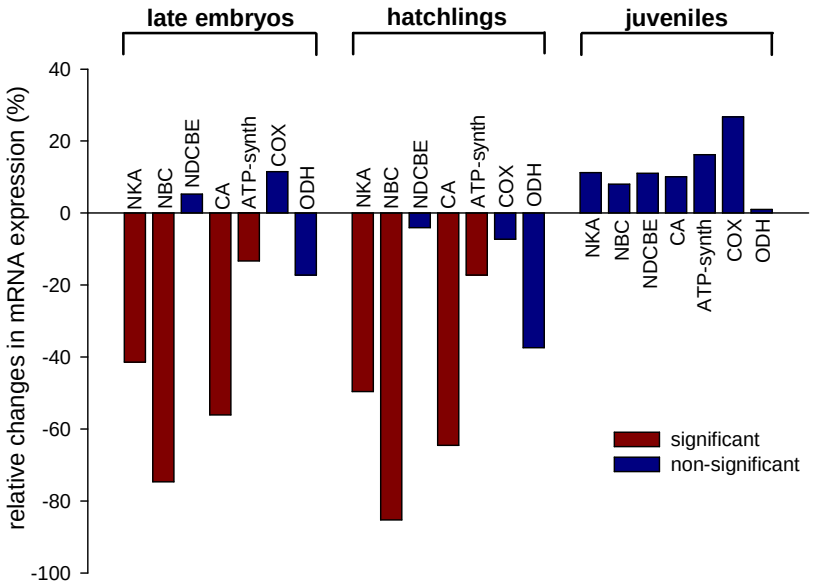

Figure 4.4. Expression profiles from selected ion-regulatory and metabolic genes determined for gill tissues of different ontogenetic stages of *Sepia officinalis*. Embryos and hatchlings were incubated at different pCO_2 values (contol and 0.37 kPa) for four weeks until hatching whereas juveniles (C) were incubated for six weeks at a pCO_2 of 0.32 kPa. Expression of the gene candidates are normalized to the geometric mean of so*CPSF* and so*UBC* (n = 8-10). See publication 1.

The significant down regulation of the ion regulatory gene candidates is also likely causally linked to the developmental delay of the embryonic gill. Large differences in mRNA expression profiles have been attributed to a hypercapnia induced developmental delay in sea urchin larvae (Stumpp et al. submitted). Thus, strong differences in mRNA expression could be indirect hypercapnia effects. For example, in larvae of *Strongylocentrotus purpuratus NKA*, mRNA levels peak during gastrulation (25 h post - fertilization) followed by an almost 100% decline to trace levels at 60 h post-fertilization (Marsh et al. 2000). Thus, a slight difference in developmental rate would cause large changes in *NKA* mRNA expression. Bearing this hypercapnia induced developmental delay in mind, it becomes crucial for future studies to avoid ontogenetic shifts in the sampling procedure in order to provide a more conclusive basis for a mechanistic understanding of acid-base regulation in cephalopod early stages.

4.2. Why are early stages more sensitive?

4.2.1. The cephalopod egg: a naturally hypercapnic environment

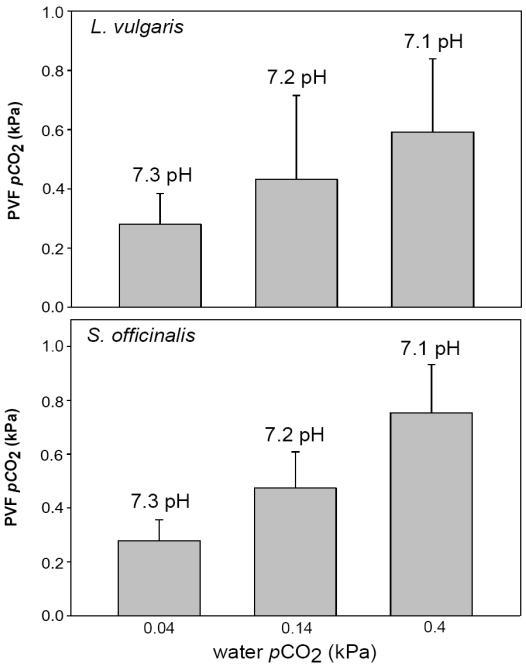

Figure 4.5. pH and calculated CO_2 concentrations in the PVF of squid *Loligo vulgaris* and cuttlefish *Sepia officinalis* at different ambient pCO_2 concentrations (0.04 kPa, 0.14 kPa and 0.4 kPa). Bars indicate mean ± SD.

With respect to the egg microenvironment, environmental fluctuations in pCO_2 can be regarded as an additional stressor for the developing embryo as the abiotic conditions in the PVF are directly influenced by the pCO_2 of the surrounding seawater (publication 1). Cephalopod embryos are exposed to very low pO_2 values (<6 kPa, ca. 28% air saturation) during the final phase of embryonic development. This is due to increasing metabolic rates and the egg casing acting as a diffusion barrier for dissolved gases (Cronin and Seymour 2000). This diffusion limitation not only decreases pO_2 inside the egg, but also results in PVF pCO_2 values >0.3 kPa and pH values <7.5 under control conditions (Gutowska and Melzner 2009). The present work demonstrates that environmental pCO_2 is additive to the natural accumulation of CO_2 in the PVF leading to very high PVF pCO_2 of up to 0.5 and 0.7 kPa inside the egg at a seawater pCO_2 of 0.16 or 0.37 kPa, respectively (publication 1; figure 4.5.). This almost linear increase of PVF pCO_2 is necessary in order to conserve the CO_2 diffusion gradient across the egg capsule that drives excretion of metabolic CO_2 to the seawater. Similar pCO_2 values and linear increases of PVF pCO_2 in response to increasing environmental pCO_2 were also observed for squids (*Loligo vulgaris*) (figure 4.5.) which have much smaller eggs (0.5. to 1 cm in diameter), packed in dense egg masses.

Thus, alterations in environmental pCO_2 create a greater challenge to the developing embryo in comparison to juveniles or adults, which are directly exposed to seawater. This is particularly striking, as cephalopod blood pCO_2 typically is 0.2-0.3 kPa higher than that of the surrounding medium (Pörtner et al. 1991; Gutowska et al. 2009). It is therefore reasonable to expect a blood pCO_2 in the 0.7-1.0 kPa range in the hypercapnic embryos when exposed to 0.4 kPa CO_2, which can be regarded a severe stressor in terms of acid-base disturbances to the developing embryo. As low PVF pO_2 and is coupled to high PVF pCO_2 and low pH values

(hypercapnia) (Gutowska and Melzner 2009; Melzner et al. submitted-a), it can be expected that these effects also hold true for embryonic stages of other oviparous taxa. For example low oxygen partial pressures within the egg were reported for molluscs (Cronin and Seymour 2000; Brante 2006), crustaceans (Fernandez et al. 2000) and fish (Diez and Davenport 1987; Ciuhandu et al. 2007) suggesting that the egg environment of these organisms has a high pCO_2 and comparatively low pH, too. It can be proposed that increases of environmental pCO_2 directly influence the diffusion gradient of CO_2 across the egg capsule, representing a more severe stressor for organisms with an oviparous mode of reproduction.

4.2.2. Ontogeny of ion-regulatory epithelia in early stages

Besides the afore hand mentioned extreme abiotic conditions in the cephalopod egg, increased sensitivity of cephalopod early life stages could be related to gill development: similar to the situation in fish and decapod crustaceans, the cephalopod gill is also one of the most important site for ion-regulatory processes in juveniles and adults (Schipp et al. 1979; publication 1; publication 3). During larval development, rudimentary gill structures occur at stage 20, and significantly differentiate over the course of embryonic development as well as after hatching (Arnold 1965; publication 2; Schipp et al. 1979). Schipp et al. (1979) demonstrated that the cephalopod gill changes morphogenetically within several days after hatching to become a highly folded epithelium with a high density of vesicles, mitochondria and a high concentration of cCA and NKA. Furthermore, enzyme activity measurements and immunohistology demonstrate that NKA expression and activity steeply increase towards hatching in late stage (29-30) embryos (publication 2). This differentiation indicates that gas exchange and ion regulatory capacity might be fully activated only after leaving the protective egg capsule. This incomplete differentiation and functionality of the gill could partially explain the higher susceptibility of embryonic stages to environmental hypercapnia.

Moreover, the comparison of cuttlefish (*Sepia officinalis*) and squid (*Loligo vulgaris*) demonstrates that even in the group of coleoid cephalopods, different sensitivities towards acid-base disturbances can be expected for early stages due to different modes of embryonic development. While the hatchlings of squid are often referred to as paralarvae with a planktonic development, hatchlings of *S. officinalis* are nearly isometric copies of adults (Fioroni 1990; Nixon and Mangold 1998). These different types of development are also reflected in the development of ion regulatory epithelia. For example, the general structure of the adult cephalopod gill exhibiting 1° -3° vessels and lamellae is already present in late embryos and hatchlings of the cuttlefish, whereas these features were not observed in squid

embryos and hatchlings, respectively. Instead, their gills consist only of rudimentary 1° to 2° order vessels and lamellae. Additionally the present work shows that the gills of *L. vulgaris* paralarvae exhibit low NKA immunoreactivity, which is not clearly restricted to a defined region of the epithelium as it is the case for adult specimens of this species. These observations suggest a rudimentary range of gill functions in terms of ion regulation for squid paralarvae in comparison to adults. However, late embryos and hatchlings of *S. officinalis* may regulate acid-base disturbances similar to adults indicated by a distinct NKA immunoreactivity in basolateral membranes and comparatively high NKA activity in gill tissues. The present work shows that cephalopod embryonic stages exhibit alternative sites of ionic regulation such as their integument or yolk epithelium before gills become fully functional (see publication 2). Besides gill epithelia, it can be hypothesized that other organs such as branchial heart- or renal-appendages may also play an important role in acid-base regulation in adult cephalopods. In cephalopods the branchial heart appendages are involved in urine formation via ultrafiltration, whereas active reabsorption and secretion takes place in the renal appendages (Schipp et al. 1975; Schipp and Hevert 1981). As the urine of cephalopods is known to be rich in NH_4^+ (approximately 150 mM l^{-1}) and has a particularly low pH (pH 5), this may represent another potential mechanism to secrete proton equivalents from body fluids (Robertson 1949; Schipp et al. 1975; Schipp and Hevert 1981). However, the first anlage of branchial hearts and renal appendages occurs in stage 22 (Lemaire 1970) embryos (Fioroni 1990), to become functional only in later stages (25 -28), as indicated by the differentiation of transport active cells (Schipp et al. 1975). Thus, acid-base regulation between extracellular fluids and the environment via these organs may not be the major pathway in embryonic stages. Nevertheless, embryonic acid-base regulation can be considered very important in order to protect basic blood oxygen transport via the pH-sensitive respiratory pigment hemocyanin (Pörtner 1994).

4.3. The cephalopod gill: site of acid-base regulation

4.3.1. Role of the gill Na^+/K^+-ATPase in acid-base regulation

In adult fish and crustaceans, it is well established that organs such as the gill, kidneys and gut are predominant sites of acid-base relevant ion transport by active transport of acid-equivalents (e.g. H^+ or NH_4^+) and bicarbonate ions from the blood space to the environment/luminal space (Wheatly and Henry 1992; Claiborne and Edwards 2002; Evans et

al. 2005; Grosell 2006; Grosell et al. 2009b; Hwang and Perry 2010; Wu et al. 2010). The current model denotes that the NKA is present in high concentrations in these ion regulatory epithelia located mainly in basolateral membranes, providing an electrochemical gradient that can be used by secondary active transporters which are involved in maintaining pH homeostasis in body fluids. The acid-base regulatory machinery has been extensively investigated for various species of marine teleost fish (Seidelin et al. 2001; Evans et al. 2005; Horng et al. 2007; Deigweiher et al. 2008; Hwang 2009; Melzner et al. 2009a). These studies proposed models of acid-base regulation in specialized, mitochondria-rich cells (MRC) localized in skin or gill epithelia (see introduction 1.3.). In these models the carbonic anhydrase (CA) catalyzes the reversible hydration/dehydration reactions of CO_2 and the acid-base equivalents H^+ and HCO_3^- and therefore plays key roles in both CO_2 excretion and acid–base regulation (Henry and Swenson 2000; Perry and Gilmour 2006; Gilmour and Perry 2009; Gilmour et al. 2009). The central role of CA in regulating acid-base balance was recently demonstrated by Georgalis et al. (2006). Their work provided direct evidence for a role of the gill CA in regulating acid–base balance during exposure to 0.8 kPa CO_2 by demonstrating a reduction of 20% in branchial acid efflux in trout subjected to CA inhibition.

In several cephalopods, including cuttlefish (*Sepia officinalis*), squid (*Loligo vulgaris*) and octopus (*Octopus vulgaris*), the gill belongs to the predominant sites of NKA immunoreactivity as well (figure 4.6.). The gills of squid, cuttlefish and octopus show similar general features regarding the gill structure and localization of NKA with NKA-rich cells located exclusively in the inner transport active epithelium of the 3º gill lamellae. Immunohistochemical localization of the NKA in baso-lateral membranes of the transport active epithelium of the cuttlefish gill confirms earlier findings by Donaubauer (1981), who demonstrated Na^+ and K^+ dependent ATPase activity in the same regions of the cuttlefish gill using a histochemical approach. Furthermore, the maximum NKA activity measured in gill homogenates from juvenile *S. officinalis* were as high as 94.8 ± 18.5 ($\mu mol_{ATP}\ g_{FM}^{-1}\ h^{-1}$) which compares in magnitude to those determined for telost fish or decapods crustaceans. Thus, localization and activity level of NKA in cephalopod gills suggests that this organ has similar ion-regulatory capacities as described for fish or decapod crustacean gills (Siebers et al. 1982; Gibbs and Somero 1990; Melzner et al. 2009b). Although cephalopods are known to be weak osmoregulators (Robertson 1949; Hendrix et al. 1981), their high metabolic rate lead to large blood pCO_2 and pH variations if not actively compensated. Especially during extreme exercise, large blood pCO_2 and pH variations occur, which need to be tightly regulated in order to protect the pH sensitive respiratory pigment hemocyanin (Pörtner et al. 1991). In

order to compensate for such a respiratory acidosis these animals require an efficient acid-base regulating machinery, depending on a driving force, which is provided by the NKA (Perry and Gilmour 2006).

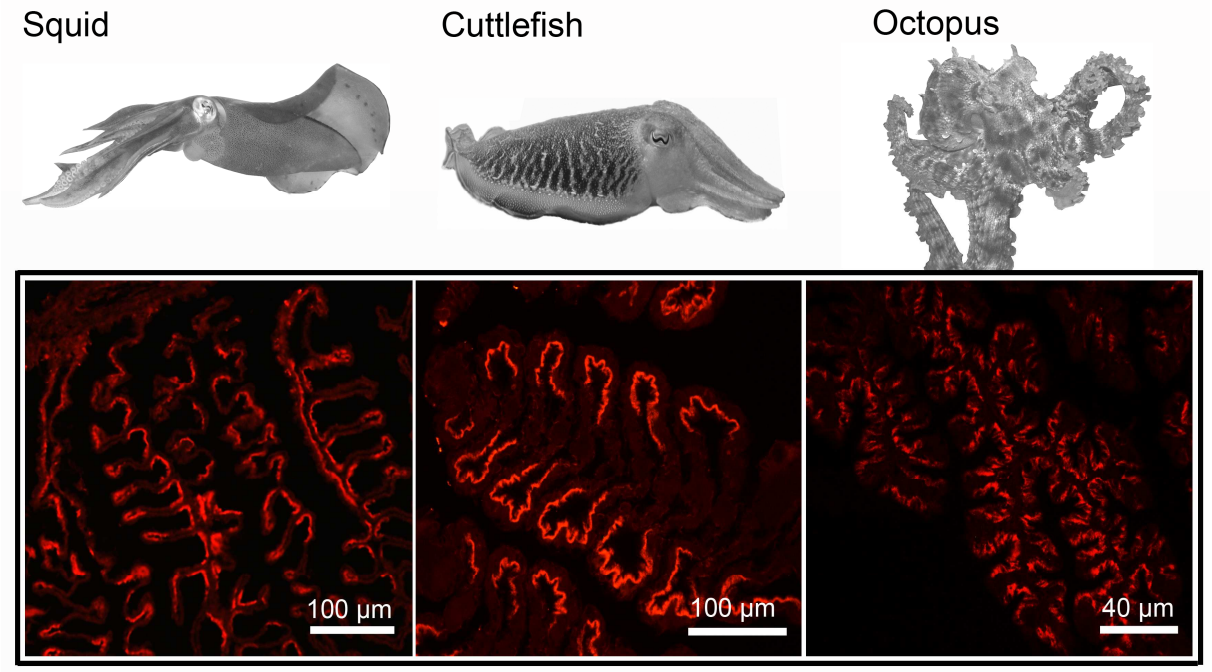

Figure 4.6. Immunohistological detection of Na^+/K^+-ATPase (NKA) in gill tissues of squid (*Sepioteuthis lessoniana)*, cuttlefish (*Sepia officinalis*) and octopus (*Octopus vulgaris*). Note the homology of NKA occurrence in concave inner epithelia of the third order lamellae. For an overview of gill morphology see figure 1.7. and figure 4.10.

4.3.2. Response of gill Na^+/K^+-ATPase to CO_2 stress

Two generally different response phases of gill NKA activity, protein concentration and mRNA expression were observed for juvenile cuttlefish in response to elevated (0.35 kPa) sea water pCO_2 (figure 4.7.). The first phase is a short-term response up to 11 days, and the second is a long-term acclimation phase up to 42 days of exposure to environmental hypercapnia. During short-term exposure to elevated water pCO_2 the determination of NKA maximum activity revealed a CO_2 induced 15% increase in activity after 48 h and 10 days, which was also reflected in the increase of NKA protein concentration (figure 4.7.A, B). This increase indicates a higher demand of the electrochemical gradient and, thus, higher acid-base regulatory capacities in response to elevated water pCO_2. These results corroborate with earlier findings by Gutowska et al. (2010a) who described an increase of blood bicarbonate concentration from 3.4 to 10.4 mmol in *S. officinalis* juveniles in response to acute hypercapnia (0.6 kPa CO_2). In the study by Gutowska et al. it was concluded that

accumulation of blood bicarbonate is most probably achieved by active transport mechanisms. NKA can be regarded as the main driving force for other secondary active transporters such as NBC and NHE that may help to secrete protons and increase blood [HCO_3^-] and, thus control pH_e homeostasis. Similar observations were made for Atlantic cod *Gadus morhua* and eelpout *Zoarces viviparus* exposed to 0.3 kPa and 0.6 kPa CO_2, respectively. In these teleosts NKA activity almost doubled in response to 0.6 kPa CO_2 (Deigweiher et al. 2008; Melzner et al. 2009a).

However, during 11 days of hypercapnia exposure an increase of NKA protein concentrations and activity levels in gill tissues was recorded but no response was observed on the mRNA expression level (figure 4.7.C). A first explanation for this phenomenon may be offered by the temporal separation between gene expression response and translation. It was reported that the expression of ion regulatory and stress response genes induced by environmental stressors such as temperature and salinity usually responds within several hours (Wang et al. 2003; Hiroi et al. 2008; Colinet et al. 2009). Besides this initial high expression and the *de novo* synthesis of protein, mRNA levels were reported to rapidly decline to initial levels within hours but the protein concentration remains unchanged (Yang and Somero 1996; Marsh et al. 2000). For example, Marsh et al. (2000) demonstrated that sea urchin larvae greatly increase NKA mRNA concentration/expression by 70%, producing a large increase in this enzyme when the embryo approaches gastrulation. Once NKA has been synthesized, mRNA transcripts rapidly returned to 0-10% of the relative gene expression, but enzyme activities maintained at high levels. Also in teleost fish (zebrafish *Danio rerio*) strong ontogeny dependent expression patterns of carbonic anhydrase isoforms were measured during embryogenesis. Expression of carbonic anhydrase isoforms increased steadily after fertilization with maximum expression after 96 h and declined by approximately 70% after 120 h (Gilmour et al. 2009).

The possibility of having such temporal pattern of regulation during development indicates the difficulty of using functional genomics as an unambiguous indicator of physiological state at a certain time point. In this context the control mechanisms at the mRNA and protein level can be considered even more complex when addressing multiple enzymes in metabolic pathways (Hockachka et al. 1998).

On the other hand, long-term acclimation of 42 days revealed a decrease of elevated NKA activity and protein concentration in cuttlefish gills back to control levels (figure 4.7.A,B). One possible explanation for this effect would be the reorganization of physiological processes to a certain degree in order to cope with this relatively moderate environmental stressor without investigating high energetic costs. From a physiological point of view the long-term maintenance of elevated NKA activity is an energetically very expensive way to counter moderate disturbances in ionic homeostasis (Febry and Lutz 1987; Gibbs and Somero 1990). For example, Febry and Lutz (1987) estimated that as much as 12-16% of the total metabolic rate may be expended in osmoregulation, and, thus, NKA activity during salinity transfer in tilapia *Oreochromis mossambicus.*

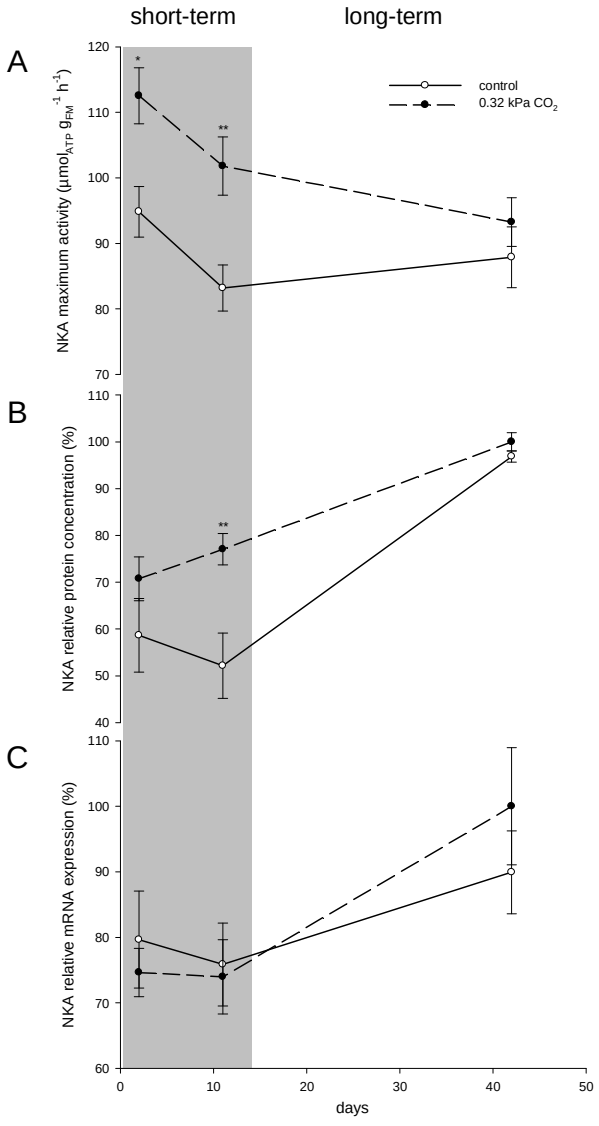

Figure 4.7. Specific gill Na^+/K^+-ATPase activity (A), relative protein concentration (B) and relative mRNA expression (C) in control (0.04 kPa) and CO_2 treated (0.3 kPa) animals (adults) at the three time points 48 h, 11 d and 42 d. Activity is given in micromoles ATP per gram fresh mass (FM) per hour. Expression of the Na^+/K^+-ATPase is normalized to the geometric mean of so*CPSF* and so*UCP* and given in % of the maximum expression determined. Significant differences compared to the control group ($P < 0.05$*; $P < 0.02$**) are indicated by asterisks (t-test). Values are means ± SE (n = 6-8).

4.3.3. Candidate genes for acid-base regulation in the cephalopod gill

The expression of genes that are most likely involved in acid-base regulation (e.g. *NKA*, *NBC*, *NDCBE*, *CAII* and VHA) represents only a minor relative proportion to the highly expressed genes such as haemocyanin (isoform 1 and 2), superoxide dismutase (SOD) and tubulin (figure 4.8.). Nevertheless, these genes are believed to contribute significantly to blood pH homeostasis and, thus, deserve special attention in this work. Semi-quantitative

tissue scan demonstrated that the sodium pump, which is believed to be the main driving force for secondary active transport processes, is highly expressed in gill tissues when compared to other tissues such as optic lobes or intestines (figure 4.9.).

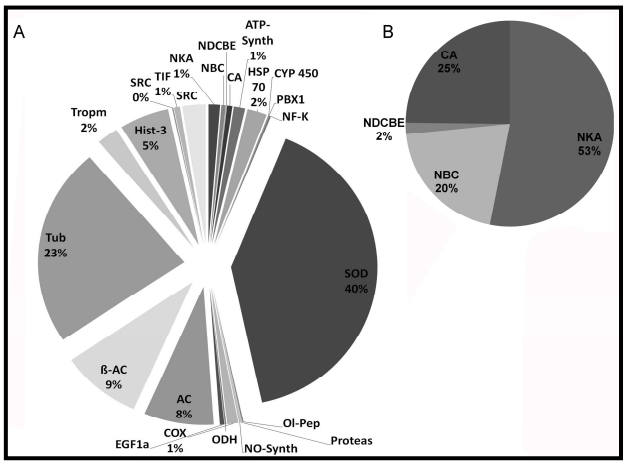

Figure 4.8. Expression profiles of 25 genes (normalized to the geometric mean of *soCPSF* and *soUBC*) revealed that under control conditions, superoxide dismutase (SOD) (21%) exhibited highest transcription levels (21%) in the gill of S*epia officinalis*, followed by genes coding for tubulin (12%), ß-actin (5%), actin (4%) and tropomyosin (1%). All remaining candidates contribute to less than 10% of the genes tested. Ion regulatory genes (e.g. *soNKA*, *soNBC*, *soNDCBE* and *socCA*) contributed to a small relative proportion of the studied gene transcripts (A). Within these four genes that are potentially involved in acid-base regulation *soNKA* exhibits highest expression level (50%) followed by *socCA* (25%), *soNBC* (22%) and *soNDCBE* (2%) (B).

For the two bicarbonate transporters belonging to the SLC4 solute carrier family, sequence alignments show a maximum identity of 83% (*NBCe*) and 100% (*NDCBE*) when compared to the respective sequences from the squid *Loligo pealei*. Electrophysiological studies demonstrated that base equivalent transport by squid *NBCe* is electrogenic with a 1:2 stochiometry whereas *NDCBE* is electroneutral, achieving the exchange of one external Na^+ for one internal Cl^- and the inward flux of two base equivalents (Virkki et al. 2002; Piermarini et al. 2006). The relative expression of these two bicarbonate transporters in *S. officinalis* gill tissues revealed that *soNBCe* is expressed at least one order of magnitude higher than *soNDCBE* in cuttlefish gill (figure 4.8 and 4.9). This finding corresponds to studies that cloned and characterized *NBCe* and *NDCBE* orthologues in the squid *Loligo pealei* (Virkki et al. 2002; Piermarini et al. 2006). These studies demonstrated the presence of the transporters in giant fiber lobes, olfactory lobes, heart and gills. On one hand, Northern blots revealed strong signals for *NDCBE* in olfactory and giant fibre lobes but only weak signals in gills and heart. Expression of *NDCBE* in *Xenopus* oocytes added evidence to earlier studies that pH_i homeostasis in squid axons is achieved via the transport of base equivalents, most likely in the form of HCO_3^-, CO_3^{2-} or the $NaCO_3^-$ ion pair (Boron 1985; Boron and Knakal 1989a; Boron and Knakal 1989b; Virkki et al. 2002). However on the other hand, high expression of squid electrogenic *NBCe* was detected in gills and heart, but not in olfactory and giant fiber lobes (Piermarini et al. 2006). In that study it was suggested that *NBCe* in gills of squid could be involved in HCO_3^- uptake similar to the situation in the vertebrate kidney, and thus, acid-base regulation.

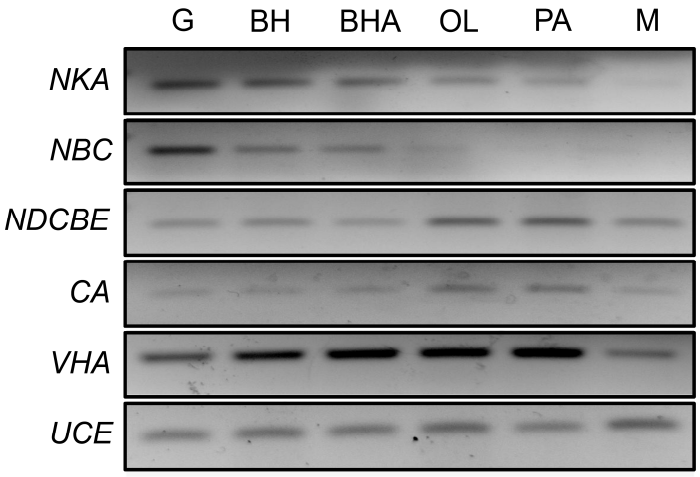

Figure 4.9. cDNA tissue panel for gills (g), branchial hearts (BH), branchial heart appendages (BHA), optic lobes (OL), pancreatic appendages (PA) and mantle (M) of *Sepia officinalis* demonstrating the expression of various potential acid-base regulatory genes: *Na^+-K^+-ATPase* (*soNKA*), *Na^+/HCO_3^- cotransporter* (*soNBC*), *Na^+-dependent Cl^-/HCO_3^- exchanger* (*soNDCBE*), *cytosolic carbonic anhydrase* (*socCA*), *V-type-H^+-ATPase* (*soVHA*) and ubiquitin conjugated enzyme (*UCE*) as reference gene.

Furthermore, the central role of cytosolic carbonic anhydrase in acid-base regulation of fish and crustaceans (Henry and Cameron 1983; Henry 1988; Henry and Swenson 2000; Perry and Gilmour 2006; Gilmour and Perry 2009; Gilmour et al. 2009) prompted us to formulate the hypothesis, that also in cephalopods this enzyme is involved in the compensation process during hypercapnia induced acidosis. Earlier work by Schipp et al. (1979) already demonstrated a high concentration of cCA in the transport active cells of the inner epithelium but only low concentrations in the outer, respiratory epithelium.

Finally, we cloned a V-type-H^+-ATPase from cuttlefish gills as this enzyme is believed to promote direct apical H^+ secretion in several vertebrate models. For example, although there is still some debate, H^+-ATPase has been demonstrated to be the major player in the apical acid secretion pathway in freshwater fish gill ionocytes (Hwang and Perry 2010). Moreover, acidification of the lumen of the vertebrate kidney proximal tubule was demonstrated to be sensitive to bafilomycin, indicating the central role of H^+-ATPase in this process (Wagner et al. 2003).

Besides the direct ATP consuming extrusion of protons via V-type-H^+-ATPases secondary active transporters of the NHE family were identified to play an important role in processes of sodium dependent acid secretion in the vertebrate kidney proximal tubule (Wang et al. 1999) and fish ionocytes, respectively (Edwards et al. 2005; Esaki et al. 2007). Especially NHE3 was identified as a major player of acid-base regulation in teleosts, especially in marine species (Wu et al. 2010). The involvement of NHE in order secrete acid equivalents in the marine environment can be regarded thermodynamically favorable due to high external [Na^+] compared to low intracellular [Na^+] which provides a natural driving force to secrete protons. We have strong evidence that NHE proteins are also expressed in the cephalopod gill. We succeeded to obtain the sequence information of a cuttlefish NHE via a

454-sequencing run of a *S. offocinalis* branchial gland cDNA library (F. Mark, AWI Bremerhaven, personal communication). Moreover, sequence information is available for different NHE isoforms in the Hawaiian bobtail squid (*Euprymna scolopes*, N. Kremer University of Wisconsin-Madison, personal communication), including NHE isoforms 1, 3, 6, 7 and 8. This suggest, that also in cephalopods NHE proteins may play an important role in regulating cellular and extracellular pH homeostasis. Further PCR and cloning will be conducted in order to receive more NHE sequence information for various tissues of the cephalopod *S. officinalis*.

4.4. Acid-base regulation in gill epithelia: juveniles and adults

The sophisticated ion regulatory machinery is beneficial in coping with acid-base disturbances caused by respiratory acidosis (Seidelin et al. 2001; Choe and Evans 2004), and might pre-adapt species to cope with future environmental hypercapnia through ocean acidification (Melzner et al. 2009b). The present work demonstrates for the first time that gene transcripts essential for acid-base regulation in teleost fish are also found in the gill of the cephalopod mollusc *S. officinalis*. The cephalopod gill is a highly folded epithelium equipped with NKA-rich cells exclusively located in basolateral membranes of the transport active inner epithelium (Schipp et al. 1979; publication 3). In contrast to fish ionocytes (Tseng et al. 2006; Hwang and Lee 2007; Hwang 2009), ionocytes (NAK-rich cells) in the cephalopod gill are not separated from each other, but form a dense conglomerate in the concave part of the third order lamellae. Furthermore, acid-base relevant proteins such as *soNBC* and *soVHA* are co-expressed in these NKA-rich cells representing a set of enzymes that have been shown to be fundamental for pH_e homeostasis in gills of teleosts or the vertebrate kidney. (see publication 1).

In the renal proximal tubule of the mammalian kidney, HCO_3^- reabsorption is achieved via electrogenic NBCe1-A, which is located basolaterally. The basolateral HCO_3^- efflux is also accompanied by a decrease in intracellular [Na^+], which may also enhance proton excretion via Na^+-dependent H^+-exchangers (NHE) across both, apical and basolateral membranes (Boron and Boulpaep 1983; Boron 2006). The majority of protons are excreted into the lumen of the tubule via different NHE isoforms, including NHE2, NHE3 and NHE8 located in the brush-border membrane of the proximal tubule (Wang et al. 1999; Goyal et al. 2003). Genetic knock-out demonstrated that among these NHE isoforms, NHE3 mediates up to 50% of the total NHE activity in this epithelium (Wang et al. 1999). Moreover, up to 40%

of the proximal tubule HCO_3^- reabsorption is Na^+-independent and is sensitive to bafilomycin inhibition, which supports the involvement of V-type-H^+-ATPase (VHA), also located in the brush-border membrane (Wagner et al. 2003). Following acidification of the lumen, secreted H^+ and filtered HCO_3^- form H_2O and CO_2 catalyzed by extracellular membrane-bound CAIV. CO_2 diffuses into the tubule cells, where it reacts with H_2O to form HCO_3^- mediated by cCAII. The generated HCO_3^- is reabsorbed into the blood via basolateral electrogenic Na^+/HCO_3^- cotransportes (Wagner et al. 2003; Boron 2006).

We hypothesize that active HCO_3^- accumulation in body fluids and, thus, pH_e regulation in cephalopods is potentially achieved according to the hypothetical model depicted in figure 4.10.B. In this model HCO_3^- is formed via CO_2 hydration in the cytosol by cCAII. The central role of cytosolic CAII in regulating acid-base balance was studied in great detail for both, fish and crustaceans (Henry and Cameron 1983; Henry 1988; Henry and Swenson 2000; Perry and Gilmour 2006; Gilmour and Perry 2009; Gilmour et al. 2009). For example Georgalis et al. (2006) provided direct evidence for a role of gill cCAII in regulating acid–base balance during exposure to 0.8 kPa CO_2 by demonstrating a 20% reduction in branchial acid efflux in trout subjected to CA inhibition. Subsequently, the increased intracellular [HCO_3^-] and negative membrane potential created by the sodium pump could drive electrogenic efflux of Na^+ and HCO_3^- across the basolateral membrane through NBCe. The ability to actively elevate blood [HCO_3^-] during hypercapnic exposure guarantees extracellular pH values suitable for protein mediated gas transport (Larsen et al. 1997; Gutowska et al. 2010a). However, maintenance of blood acid-base status requires continuous net H^+ excretion, thus, ion regulatory effort. In this respect, VHA and via NHE can be regarded potential candidates for the apical secretion of protons in the cephalopod gill. Expression of *VHA* in the transport active epithelium of cuttlefish gill was detected via *in situ* hybridization technique (Publication 1). Preliminary studies using a NHE3 specific antibody (see publication 2) demonstrated the presence of single NHE-rich cells in the same epithelium (figure 4.10.D).

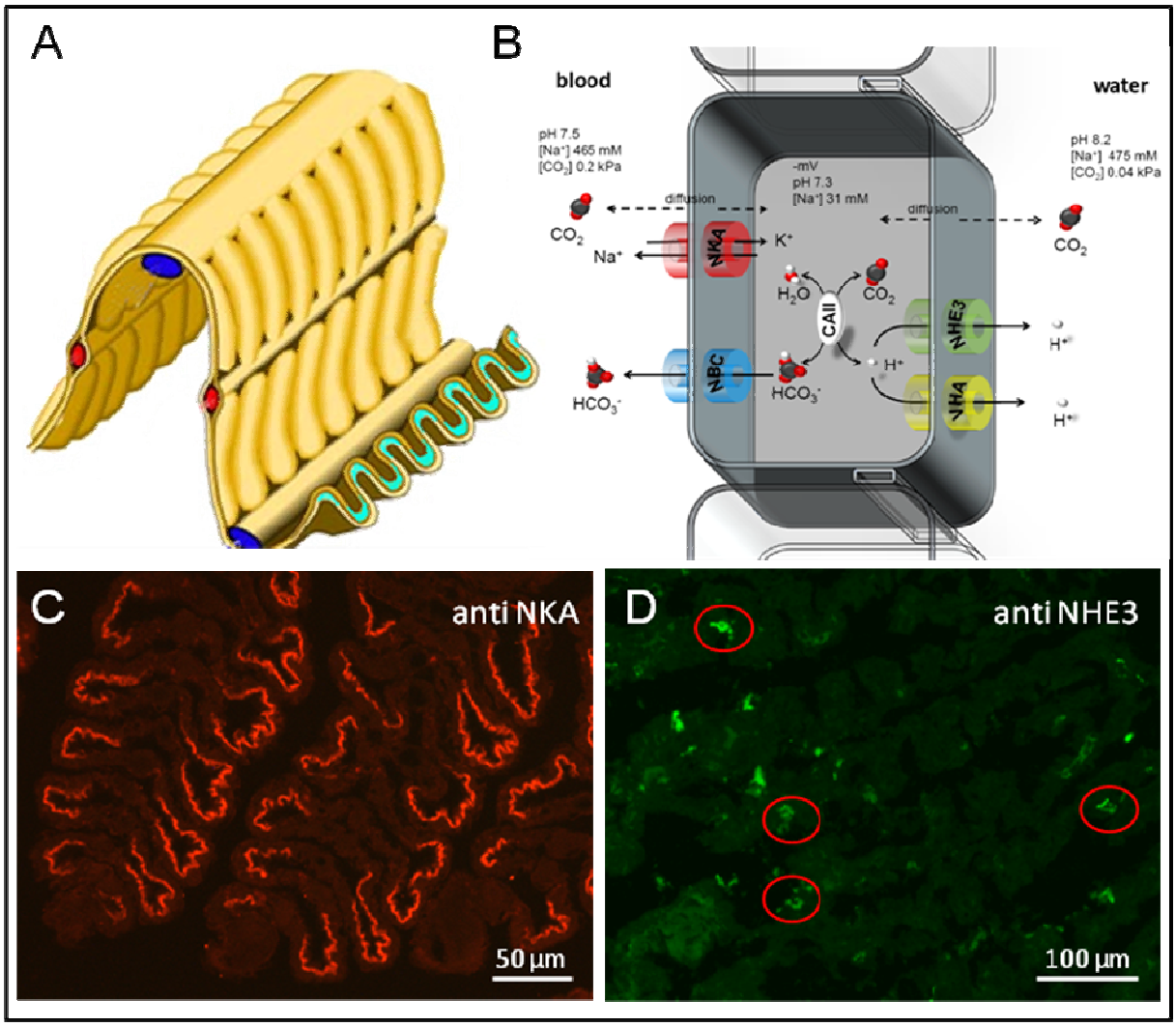

Figure 4.10. Diagram of the gill morphology of *Sepia officinalis* (A), showing the folded lamellae of the gill of *S. officinalis*. The concave inner epithelium (green) of the third order gill lamellae belongs to the transport active epithelium, whereas the outer epithelium (yellow) is exclusively involved in respiratory processes. Drawings adopted and modified from Young and Vecchione (2004). Hypothetical model of a cell in the transport active inner epithelium (rectangular sector in A) equipped with various transporters, which are involved in acid-base regulatory processes (B). CO_2 is hydrated by carbonic anhydrase (CA) after diffusive entry resulting in HCO_3^- and H^+ formation. Net accumulation of extracellular HCO_3^- is supported by basolateral NBC. Net proton extrusion is possibly achieved by apical NHE powered by elevated Na^+/K^+-ATPase activity in the basolateral membrane of single specialized NHE rich cells within the transport active epithelium. Immunohistochemical staning of gill lamella, demonstrating NKA rich cells filling the entire inner part of the transport active epithelium (C) and single NHE3-rich cells to be exclusively located in the inner epithelium of the third order lamellae (D).

4.5. Acid-base regulation: embryonic stages

Marine animals that exhibit an oviparous mode of development such as most fish and cephalopods are exposed to very high pCO_2 values during their embryonic development (see section 5.2.). This is primairly due to the fact that egg capsules have been shown to act as a diffusion barrier for respiratory O_2 and CO_2 (Diez and Davenport 1987; Cohen and

Strathmann 1996; Cronin and Seymour 2000; Fernandez et al. 2000; Gutowska and Melzner 2009). The present study demonstrated, that increases in environmental pCO_2 are additive to those of the PVF of cephalopod eggs, leading to pCO_2 values as high as 0.6 kPa at an environmental pCO_2 of 0.35 kPa (publication 1). Such high environmental pCO_2 values can be encountered by cephalopod and fish egg masses in seasonally hypoxic coastal habitats (Thomsen et al. 2010). Hypoxic hypercapnic conditions constitute a major abiotic stress to the developing embryo in terms of acid-base disturbances as they also lead to an increased pCO_2 of body fluids in order to maintain the diffusive flux of CO_2 out of the animal (Melzner et al. 2009b). As late stage embryonic fish and cephalopods rely on haemoglobin/haemocyanin driven oxygen transport as well, it can be assumed that these embryonic stages require an efficient acid-base regulatory machinery in order to protect their pH sensitive respiratory pigments from hypercapnia induced pH reductions.

During larval development of fish and cephalopods, rudimentary gill structures progressively occur and become completed when the organism has reached an adult-type morphology (Arnold 1965; Schipp et al. 1979; Evans et al. 2005; Pan et al. 2005). However, this work shows for the first time that before gills and intestines are developed to full functionality the skin and yolk sac epithelium of cephalopod molluscs is a major site of ionic exchange in the developing embryo (publication 2). This is similar to the situation described for teleost fish (Hiroi et al. 2005; Nebel et al. 2005; Giffard-Mena et al. 2006; Hwang and Lee 2007; Hiroi et al. 2008). In cephalopod embryos epidermal ionocytes are predominantly located on the skin in the head region (figure 4.11.). Further characterization demonstrated that one group of cells which were recognized by Con A (a lectin protein capable of selectively binding α-mannopyranosyl and α-glucopyranosyl residues) and MitoTracker also express NHE3. These NHE3-rich cells in the head epithelium are apparently responsible for sodium uptake. Besides the uptake of sodium, the functionality of these cells in term of acid-base regulation via NHE3 is further supported by electrophysiological data demonstrating that the surface of the head region is actively secreting protons from the animal to the perivitelline fluid. Here it needs to be noted that the gradient of protons from the animal to the environment may also derive from CO_2 that is diffusing out of the animal to be hydrated to HCO_3^- and protons. Another group of epithelial cells are exclusively labeled by NKA. In zebrafish (*Danio rerio*) embryos, there are at least three types of epidermal ionocytes which were identified and divided into Na^+/Cl^--cotransporter (NCC), Na^+/K^+-ATPase (NaR) and proton pump (HR) rich cells, covering different functions. It is believed that NCC cells are involved in the uptake of Cl^- and Na^+ from the environment where as NaR cells are

responsible for the active transport of Ca^{+}. The third subtype of ionocyte has been characterized as proton pump-rich cells which are equipped with apical H^{+}-ATPase, NHE3 and ammonia transporters such as Rhcg (for a review see Hwang and Lee 2007). Convergent evolution of diverse ionocytes' differention from progenitor cells may occur in both, cephalopods and fish. The molecular mechanisms behind the differentiation and ontogenesis of ionocytes were recently described in great detail (Hsiao et al. 2007). In zebra fish larvae, two forkhead transcription factors, *foxi3a* and *foxi3b*, were identified as the key factors for specification and differentiation of epidermal ionocytes, indicating that the fate of ionocyte progenitor cells is mediated by the Delta-Notch lateral inhibition mechanism. Moreover, this differentiation of epidermal ion regulatory organs/cells (e.g. localized in kidney, gill and skin) from the non-neural ectoderm is highly conserved among vertebrates. However, in cephalopods the relationship between skin ionocyte progenitor cells' differentiation, specification and ion regulation during development is an issue for further investigations.

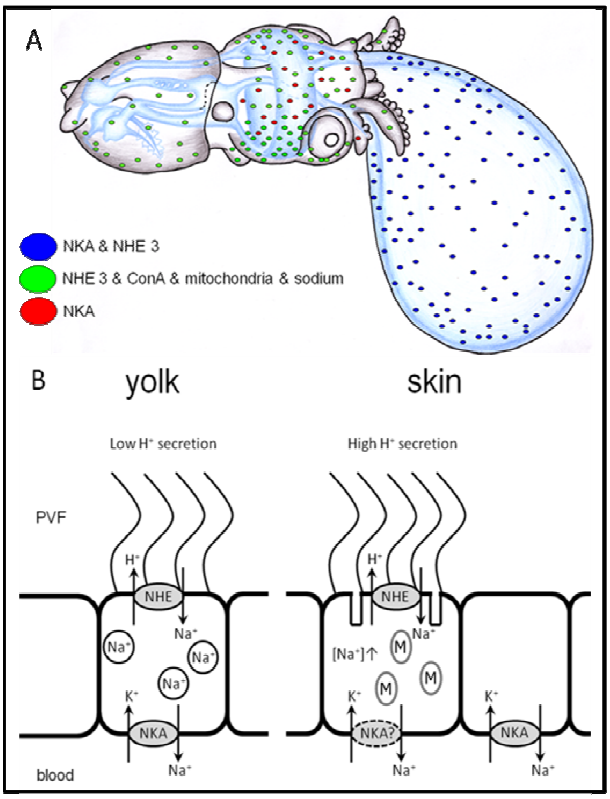

Figure 4.11. There are at least three types of epidermal ionocytes in cephalopod embryos, located on skin and yolk epithelium. Highest densities of ionocytes are found in areas with large sub-cutaneous blood spaces such as head and yolk (A). Hypothetical model of two types of ciliated ionocytes located on the yolk epithelium and skin of cephalopod embryos (B). One type of ionocyte on the yolk epithelium is characterized by the occurrence of NKA, probably located in basolateral membranes and apical NHE. Furthermore the cells of this epithelium are characterized by high concentrations of Na^{+} localized in intracellular vesicles. Electrophysiological measurements demonstrated that the yolk epithelium is characterized by only relatively low proton secretion. The skin of cephalopod embryos exhibits at least one other type of ionocyte. These positively Con A labeled cells are rich in mitochondria (M) and show high intracellular sodium accumulation. Additionally, these cells show positive NHE3 immunoreactivity, but are not co-localized with NKA rich cells. Electrophysiological data suggest that ionocytes located on the skin are involved in active acid (probably also CO_2) secretion.

Electrophysiological data of the present study suggest that yolk and skin represent major sites of acid equivalent secretion. These data demonstrate that the skin, especially in the head and tentacle region, is characterized by a strong outward directed proton flux. Here we identified one type of ionocytes localized on the yolk epithelium, which are rich in NKA and NHE3. Another group of Con A- positive cells which are similar to accessory cells can surprisingly absorb sodium from ambient environment (types of ionocytes summarized in figure 4.11.A).

Although a detailed cellular characterization of ionic regulation on cephalopod yolk epithelium needs further studies, new mechanistic concepts of acid-base regulation in teleosts are recently emerging for the marine environment (Nawata et al. 2010). In this context it has been described that epithelial ionocytes of *Oryzias latipes* larvae, which are rich in NHE3 and Rhcg are actively involved in the secretion of protons (Wu et al. 2010). Furthermore, it was demonstrated for pufferfish *(Takifugu rubripes)* that in the seawater environment NHE3 in combination with apical Rhcg located in gill tissues are key players in the active secretion of ammonia and protons in response to 1 kPa CO_2 induced hypercapnia (Nawata et al. 2010). This involvement of NHE-like proteins in the secretion of protons and thus acid-base regulation shows many parallel features to another prominent example, the renal proximal tubule of the mammalian kidney. Here, the majority of protons are excreted into the lumen of the tubule via different NHE isoforms located in the brush-border microvilli of the proximal tubule (see section 5.4.) (Wang et al. 1999; Goyal et al. 2003; Wagner et al. 2003).

We hypothesize that active proton secretion from body fluids to the environment and, thus, pH_e regulation in cephalopod embryos is potentially achieved according to the hypothetical model depicted in figure 4.11.B. In this model mitochondria-rich cells located on the skin in the head region of the embryo, which is well perfused by large blood spaces, exhibit positive NHE3 immunoreactivity and high cytosolic sodium accumulation. Furthermore, the micro-environment in this area is characterized by increased proton secretion. These findings are in accordance for those obtained for fish HR cells (e.g. Lin et al. 2006) and suggest that also in cephalopod embryos, NHE proteins may be a major player of proton secretion in exchange for environmental sodium. In contrast to adults the role of NBC proteins from the SLC4 transporter family in epidermal ionocytes needs further functional and morphological characterization in order to answer the question, whether embryonic stages are capable of active HCO_3^- accumulation in body fluids as do adults.

Intriguingly, the present work demonstrates that epidermal ionocytes of cephalopod embryos bare cilia on their surface. Earlier studies discribed that these ciliated cells on the surface of the animal create a polarized circulatory current inside the perivitelline fluid in order to prevent the formation of pO_2 gradients within the egg fluid (Arnold and Williams-Arnold 1980; Fioroni 1990). This convective current is an important feature in order to remove metabolic end products such as NH_4^+ and CO_2 from the animal and deliver oxygen from the egg capsule to the developing embryo. These observations suggest that ciliated epidermal cells are involved in creating a conveyor current inside the fluid filled egg capsule, but at the same time are capable of ionic exchange.

4.6. Conclusions and future directions

The present work provides molecular evidence that juveniles of the cuttlefish *Sepia officinalis* can tolerate elevated seawater pCO_2 (0.3 kPa CO_2) over long exposure times without significantly altering mRNA expression profiles of potential key acid-base regulatory and metabolic proteins. These observations corroborate with earlier findings (Gutowska et al. 2008) that juveniles of this species can tolerate elevated seawater pCO_2 (0.3 kPa CO_2) over long exposure times without altering their growth rates.

Although transient and moderate responses were found on the NKA protein level, routine expression of genes coding for important ion-regulatory proteins seem to be sufficient to cope with a CO_2 induced acidosis up to 0.3 kPa CO_2. These observations further support the hypothesis that active organisms like adult teleost fish and cephalopods can tolerate long-term exposure to elevated seawater pCO_2 comparatively well. Nevertheless, several studies have demonstrated that a hypercapnia induced acid-base disturbance, which is compensated via HCO_3^- accumulation in body fluids may lead to a hypercalcification of $CaCO_3$ structures, such as fish otoliths, crustacean carapaces and cephalopod cuttlebones (Checkley et al. 2009; Ries et al. 2009; Gutowska et al. 2010b). In the long run, hypercalcification of structures responsible for buoyancy and balance control may negatively influence swimming behavior, active metabolism and prey capture.

Although adult cephalopods seem to be relatively tolerant, embryos respond more sensitive to environmental acid-base disturbances. This is indicated by a delayed development and hatching in cuttlefish embryonic stages associated with a smaller hatchling size. It has been hypothesized that smaller cephalopod hatchlings would need more time to escape from the "window of vulnerability" (Pecl et al. 2004), and thus, elevated pCO_2 may negatively influence their survival with respect to predation. As a consequence, even if elevated CO_2 levels are tolerable for juveniles or adults, cephalopod populations may still be affected due to the decreased survival of embryos and hatchlings. The higher sensitivity in early life stages is most probably due to extreme hypercapnic conditions (pCO_2 up to 0.7 kPa) inside the egg. Moreover, an increased sensitivity may also be explained by the incomplete development and functionality of high capacity ion-regulatory epithelia such as gills and kidneys in early developmental stages. The shift from epidermal ionocytes to adult type ion regulatory epithelia (e.g. gills and kidneys) may represent a "bottleneck" phase with increased sensitivity towards acid-base disturbances. The highly differentiated hatchling of *S. officinalis*, with extreme adult-like morphology, is typical of the benthonic type of development among cephalopods and has well developed ion-regulatory epithelia. In contrast, late embryos and

hatchlings of *L. vulgaris*, which are usually termed paralarvae, belong to the planktonic type and differ morphologically from adults. In these paralarvae, ion regulatory epithelia (e.g. gills) are not completely developed and probably not fully functional. These observations lead to the assumption that cephalopods with a planktonic "paralarvae" (e.g. squid and most octopods) which can be classified as "R-strategists" among cephalopods are probably more susceptible towards abiotic stressors than cephalopods with a lower number of offspring but adult-like hatchlings (e.g. cuttlefish).

Nevertheless, the ability to regulate ion fluxes to a certain degree can be regarded a very important feature for cephalopod embryos with respect to challenging acid-base disturbances in eggs. The present work demonstrates for the first time that lecithotrophic larvae of cephalopods and fish share a convergent evolution of ion-regulatory mechanisms: epidermal ionocytes located on the skin and the yolk sac epithelium are major sites of acid-base relevant ion transport in early life stages before adult-type ion regulatory epithelia cover these functions. The gill of adult cephalopods can be characterized by NKA rich cells, equipped with proteins such as NBCe, cCAII, VHA and probably also NHE3, which shows a convergent evolutionary pattern to that of decapod crustaceans and teleost fish. The key players of an acid-base regulatory machinery seem to follow very conserved patterns among invertebrates and vertebrates. These conserved general features of acid-base regulatory systems may be explained by the same physiological demands of organisms and thus, long-term selection pressures exerted on them. In this context hypercapnia can be considered an ubiquitous factor in all biological systems that shaped the functional requirements of an ion-regulatory machinery.

Future work should be dedicated to the question, why marine organisms react with reduced growth and development in response to moderate environmental hypercapnia although metabolic depression does not seem to be the major reason for this developmental retardation. Energy partitioning and allocation has proven to be a more suitable explanation for a higher fraction of energy spent on acid-base regulation than on growth and development. Thus, future experiments will investigate metabolic and excretion rates of embryonic stages in response to hypercapnic conditions. Special attention will be dedicated to the excretion of NH_4^+ as this metabolic end product may also play a major role in the maintenance of pH homeostasis of an organism. In this context, future research effort should be directed to the identification and characterization of proteins such as NHE isoforms and Rh proteins in cephalopods. The latter were proposed to have dual NH_3/CO_2 transport function (Soupene et al. 2002; Soupene et al. 2004; Nawata et al. 2010), and, thus, may represent another key

player of acid-base regulation and gas exchange. Further investigations should apply molecular, histological and electrophysiological tools in order to clarify the mechanistic basis for acid-base regulation in marine high-power taxa like fish, crustaceans and cephalopods. Comparative studies on key acid-base regulatory proteins in a variety of marine ectothermic animals would contribute towards a general understanding of the evolution and common principles of extracellular pH regulation mechanisms.

5. References

Arnold JM (1965) Normal embryonic stages of the squid, *Loligo pealii* (Lesueur). Biol Bull 128: 24-32

Arnold JM, Williams-Arnold LD (1980) Development of the ciliature pattern on the embryo of the squid *Loligo pealei*: a scanning electron microscope study. Biol Bull 159: 102-116

Bertorello AM, Katz AI (1995) Regulation of Na^+-K^+-pump activity: Pathways between Receptors and effectors. News Physiol Sci 10: 253-259

Bishop T, St-Pierre J, Brand MD (2002) Primary causes of decreased mitochondrial oxygen consumption during metabolic dpression in snail cells. Am J Physiol Regul Integr Comp Physiol 282: 372-382

Bolner KCS, Baldisserotto B (2007) Water pH and urinary excretion in silver catfish *Rhamdia quelen*. J Fish Biol 70: 50-64

Bone Q, Brown E, Travers G (1994) On the respiratory flow in the cuttlefish *Sepia officinalis*. J Exp Biol 194: 153-165

Boron WF (1985) Intracellular pH-regulating mechanism of the squid axon. Relation between the external Na^+ and HCO_3^- dependeces. J Gen Physiol 85: 325-345

Boron WF (2004) Regulation of intracellular pH. Adv Physiol Educ 28: 160-179

Boron WF (2006) Acid-base transport by the renal proximal tubule. J Am Soc Nephrol 17: 2368-2382

Boron WF, Boulpaep EL (1983) Intracellular pH regulation in the renal proximal tubule of the salamander: basolateral HCO_3^- transport. J Gen Physiol 81: 53-94

Boron WF, Knakal RC (1989a) Intracellular pH-regulating mechanism of the squid axon: interaction between DNDS and extracellular Na^+ and HCO_3^-. J Gen Physiol 93: 123-150

Boron WF, Knakal RC (1989b) Na^+-dependent Cl-HCO_3 exchange in the squid axon. J Gen Physiol 99: 817-837

Boucher-Rodoni R, Mangold K (1977) Experimental study of digestion in *Octopus vulgaris* (Cephalopoda, Octopoda). J Zool Lond 183: 505-515

Boucher-Rodoni R, Mangold K (1994) Ammonia production in cephalopods, physiological and evolutionary aspects. Mar Fresh Behaw Physiol 25: 53-60

Brante A (2006) An alternative mechanism to reduce intracapsular hypoxia in ovicapsules of *Fusitriton oregonensis* (Gastropoda). Mar Biol 149: 269-274

Brauner CJ, Thorarsen H, Gallaugher P, Farrel AP, Randall DJ (2000) CO_2 transport and excretion in raibow trout (*Oncorhynchus mykiss*) during graded sustained exercise. Resp Physiol 119: 69-82

Brix O, Bardgard A, Cau A, Colosimo SGC, Giardina B (1989) Oxygen-binding properties of cephalopod blood with special reference to environmental temperatures and ecological distribution. J Exp Zool 252: 34-42

Budelmann BU, Schipp R, von Boletzky S (1997) Cephalopoda. In: Harrison FW, Kohn AJ (eds) Microscopic anatomy of invertebrates. Wiley-Liss, New-York

Caldeira K, Wickett ME (2003) Anthropogenic carbon and ocean pH. Nature 425: 365

Caldeira K, Wickett ME (2005) Ocean model predictions of chemistry changes from carbon dioxide emissions to the atmosphere and ocean. J Geophys Res 110

Cameron JN, Iwama GK (1987) Compensation of progressive hypercapnia in channel catfish and blue crabs. J Exp Biol 133: 183-197

Cao L, Caldeira K (2008) Atmospheric CO_2 stabilization and ocean acidification. Geophys Res Lett 35: doi: 10.1029/2008GL035072

Chapelle S, Dandrifosse G, Zwingelstein G (1976) Metabolism of phospholipids of anterior or posterior gills of the crab *Eriocheir sinensis* during the adaptation of this animal to media of various salinities. J Biochem 7: 343-351

Charmantier G, Charmantier-Daures M (2001) Ontogeny of osmoregulation in crustaceans: The embryonic phase. Amer Zool 41: 1078-1089

Charmantier G, Haond C, Lignot J-H, Charmantier-Daures M (2001) Ecophysiological adaptation to salinity throughout a life cycle: A review in homarid lobsters. J Exp Biol 204: 967-977

Checkley J, David M, Dickson AG, Takahashi M, Radich JA, Eisenkolb N, Asch R (2009) Elevated CO_2 enhances otolith growth in young fish. Science 324: 1683

Chibalin AV, Ogimoto G, Pedemonte CH, Pressley TA, Katz AI, Féraille E, Berggren P-O, Bertorello AM (1999) Dopamine-induced endocytosis of Na^+/K^+-ATPase is initiated by phosphorylation of Ser-18 in the rat α subunit and is responsible for the decreased activity in epithelial cells. J Biol Chem 274: 1920-1927

Choe KP, Evans DH (2004) Compensation for hypercapnia by a euryhaline elasmobranch: Effect of salinity and roles of gills and kidneys in fresh water. J Exp Zool A 297A: 52-63

Cieluch U, Charmantier G, Grousset E, Charmantier-Daures M, Anger K (2005) Osmoregulation, immunolocalization of Na^+/K^+-ATPase, and ultrastructure of branchial epithelia in the developing brown shrimp, *Crangon crangon* (Decapoda, Caridea). Physiol Biochem Zool 78(6): 1017-1025

Ciuhandu CS, Wright PA, Goldberg JI, Stevens ED (2007) Parameters influencing the dissolved oxygen in the boundary layer of rainbow trout (*Oncorhynchus mykiss*) embryo and larvae. J Exp Biol 210: 1435-1445

Claiborne JB, Edwards SL (2002) Acid-base regulation in fishes: Cellular and molecular mechanisms. J Exp Zool 293: 302-319

Claiborne JB, Evans DH (1992) Acid-base balance and ion transfers in the spiny dogfish (*Squalus acanthias*) during hypercapnia - a role for ammonia excretion. J Exp Zool 261: 9-17

Claiborne JB, Heisler N (1984) Acid-base regulation and ion transfers in the carp (*Cyprinus carpio*) during and after exposure to environmental hypercapnia. J Exp Biol 108: 25-43

Cohen CS, Strathmann RR (1996) Embryos at the edge of tolerance: Effects of environment and structure of egg masses on supply of oxygen to embryos. Biol Bull 190: 8-15

Colina C, Rosenthal JJC, DeGiorgis JA, Srikumar D, Iruku N, Holmgren M (2007) Structural basis of Na^+/K^+-ATPase adaptation to marine environments. Nat Struc Mol Biol 14: 427 431

Colinet H, Lee SF, Hoffmann A (2009) Temporal expression of heat shock genes during cold stress and recovery from chill coma in adult *Drosophila melanogaster*. FEBS J 277: 174-185

Comeau S, Gorsky J, Jeffree J, Teyssié J-L, Gattuso JP (2009) Impact of ocean acidification on a key Arctic pelagic mollusc (Limacina helicina). Biogeosci 6: 1877-1882

Comeau S, Jeffree J, Teyssie L, Gattuso JP (2010) Response of the Arctic pteropod Limacina helicina to projected future environmental conditions. PLoS ONE 5: e11362

Cronin ER, Seymour RS (2000) Respiration of the eggs of the giant cuttlefish *Sepia apama*. Mar Biol 136: 863-870

Cummings V, Hewitt J, Van Rooyen A, Currie K, Beard S, Thrush S, Norkko J, Barr N, Heath P, Halliday NJ, Sedcole R, Gomez A, McGaw C, Metcalf V (2010) Ocean acidification at high latitudes: potential effects on functioning of the antarctic bivalve *Laternula elliptica*. PLoS ONE 6: doi: 10.1371/journal.pone.0016069

Dean RB (1941) Theories of electrolyte equilibrium in muscle. Biol. Symposia 3: 331-348

Deigweiher K, Koschnick N, Pörtner H-O, Lucassen M (2008) Acclimation of ion regulatory capacities in gills of marine fish under environmental hypercapnia. Am J Physiol 295: R1660–R1670

Dezwaan A, M WTC (1976) Anaerobic metabolism in bivalvia (mollusca) - characteristics of anaerobic metabolism. Comp Biochem Physiol B 54: 313-323

Dickson A, Millero F (1987) A comparison of the equilibrium constants for the dissociation of carbonic acid in seawater media. Deep Sea Res A 34: 1733-1743

Dickson AG, Afghan JD, Anderson GC (2003) Reference materials for oceanic CO_2 analysis: a method for the certification of total alkalinity. Mar Chem 80: 185-197

Dickson AG, L SC, R CJ (2007) Guide to best practices for ocean CO_2 measurements. PICES Special Publication 3: 1-191

Diez JM, Davenport J (1987) Embryonic respiration in the spiny dogfish (*Scyliorhinus canicula* L.). J Mar Biol Ass UK 67: 249-261

Donaubauer HH (1980) Adenosine triphosphatase localization in the branchial heart of *Sepia officinalis* L. (Cephalopoda). Histochemistry 69: 27-37

Donaubauer HH (1981) Sodium- and potassium-activated adenosine triphosphatase in the excretory organs of *Sepia officinalis* (Cephalopoda). Mar Biol 63: 143-150

Donini A, O´Donnell MJ (2005) Analysis of Na^+, Cl^-, K^+, H^+, and NH_4^+ concentration gradients adjacent to the surface of anal papillae of the mosquito *Aedes aegypti*: application of self-referencing ion-selective microelectrodes. J Exp Biol 208: 603-610

Dupont S, Havenhand J, Thorndyke W, Peck L, Thorndyke MC (2008) CO_2-driven ocean acidification radically affect larval survival and development in the brittlestar *Ophiothrix fragilis*. Mar Ecol Prog Ser 373: 285-294

Dupont S, Ortega-Martinez O, Thorndyke MC (2010) Impact of near-future ocean acidification on echinoderms. Ecotoxycology 19: 449-462

Dupont S, Thorndyke MC (2009) Impact of CO_2-driven ocean acidification on invertebrates early life-history–what we know, what we need to know and what we can do. Biogeosciences 6: 3109-3131

Edwards SL, Wall BP, Morrison-Shetlar A, Sligh S, Weakley JC, Claiborne JB (2005) The effect of environmental hypercapnia and salinity on the expression of NHE-like isoforms in the gills of a euryhaline fish (*Fundulus heteroctilus*). J Exp Zool 303: 464-475

Emanuel CF, Martin AW (1956) The composition of octopus renal fluid. J Comp Physiol 39: 226-234

Esaki M, Hoshijima K, Kobayashi S, Fukuda H, Kawakami K, Hirose S (2007) Visualization in zebrafish larvae of Na^+ uptake in mitochondria-rich cells whose differentiation is dependent on *foxi3a*. Am J Physiol Regul Integr Comp Physiol 292: R470-R480

Evans DH, Piermarini PM, Choe KP (2005) The multifunctional fish gill: Dominant site of gas exchange, osmoregulation, acid-base regulation, and excretion of nitrogenous waste. Physiol Rev 85: 97-177

Fabry VJ, Seibel BA, Feely RA, Orr JC (2008) Impacts of ocean acidification on marine fauna and ecosystem processes. J Mar Sci 65: 414-432

Fagan MJ, Saier MH (1994) P-type ATPases of eukaryotes and bacteria: sequence analyses and construction of phylogenetic trees. J Mol Evol 38: 57-99

Faszewski EE, Kunkel JG (2001) Covariance of ion flux measurements allows new interpretation of *Xenopus laevis* oocyte physiology. J Exp Zool 290: 652-661

Febry R, Lutz P (1987) Energy partitioning in fish: the activity-related cost of osmoregulation in a euryhaline cichlid. J Exp Biol 128: 63-85

Feder ME, Walser J-C (2005) The biological limitations of transcriptomics in elucidating stress and stress responses. J Evol Biol 18: 901-910

Feely RA, Sabine CL, Hernandez-Ayon JM, Ianson D, Hales B (2008) Evidence for upwelling of corrosive "acidified" water onto the continental shelf. Science 320: 1490-1492

Feely RA, Sabine CL, Lee K, Berelson W, Kleypas J, Fabry VJ, Millero F (2004) Impact of anthropogenic CO_2 on the $CaCO_3$ system in the oceans. Science 305: 362-366

Fernandez M, Bock C, Pörtner H-O (2000) The cost of being a caring mother: the ignored factor in the reproduction of marine invertebrates. Ecol Lett 3: 487-494

Findley HS, Wood HL, Kendall MA, Spicer I, Twitchett RJ, Widdicombe S (2009) Calcification, a physiological process to be considered in the context of the whole organism. Biogeosciemces 6: 2267-2284

Fioroni P (1962) Die embryonale Entwicklung der Hautdrüsen und des Trichterorganes von *Octopus vulgaris* Lam. Acta annat 50: 264-295

Fioroni P (1990) Our recent knowledge of the development of the cuttlefish (*Sepia officinalis*). Zool Anz 224: 1-25

Fivelstad S, Olsen AB, Asgard T, Baeverfjord G, Rasmussen T, Vindheim T, Staffanson S (2003) Long-term sublethal effects on carbon dioxide on Atlantic salmon smolts (*Salmo solar* L.): ion regulation, haematology, element composition, nephrocalcinosis and growth parameters. Aquaculture 215: 301-319

Forsythe J, Lee P, Walsh L, Clark T (2002) The effects of crowding on growth of the European cuttlefish, *Sepia officinalis* Linnaeus, 1758 reared at two temperatures J Exp Mar Biol Ecol 269: 173-185

Foss A, Rosnes BA, Oiestad V (2003) Graded environmental hypercapnia in juvenile spotted wolffish (*Anarhichas minor* Olafson): effects on growth, food conversion efficiency and nephrocalcinosis. Aquaculture 220: 607-617

Garvin JL, Burg MB, Knepper MA (1985) Ammonium replaces potassium in supporting sodium transport by the Na-K-ATPase of renal proximal straight tubules. Am J Physiol Renal Physiol 249: F785-F788

Gazeau F, Quiblier C, Jansen JM, Gattuso J-P, Middelburg JJ, Heip CHR (2007) Impact of elevated CO_2 on shellfish calcification. Geophys Res Let 34

Georgalis T, Perry SF, Gilmour KM (2006) The role of branchial carbonic anhydrase in acid–base regulation in rainbow trout (*Oncorhynchus mykiss*). J Exp Biol 209: 518-530

Gibbs A, Somero GN (1990) Na^+-K^+-adenosine triphosphatase activities in gills of marine teleost fishes: changes with depth, size and locomotory activity level. Mar Biol 106: 315-321

Giffard-Mena I, Charmantier G, Grousset E, Aujoulat F, Castille R (2006) Digestive tract ontogeny of *Dicentrarchus labrax*: Implication in osmoregulation. Development Growth Diff 48: 139-151

Gilmour KM, Perry SF (2009) Carbonic anhydrase and acid-base regulation in fish. J Exp Biol 212: 1647-1661

Gilmour KM, Thomas K, Esbaugh AJ, Perry SF (2009) Carbonic anhydrase expression and CO_2 excretion during early development in zebrafish *Danio rerio*. J Exp Biol 212: 3837-3845

Goyal S, Vanden Heuvel G, Aronson PS (2003) Renal expression of novel Na/H exchanger isoform NHE8. Am J Physiol Renal Physiol 284: F467–F473

Grigoriou P, Richardson CA (2004) Aspects of the growth of cultured cuttlefish *Sepia officinalis* (Linnaeus 1758). Aquacult Res 35: 1141-1148

Grigoriou P, Richardson CA (2008) The effect of ration size, temperature and body weight on specific dynamic action of the common cuttlefish *Sepia officinalis*. Mar Biol 154: 1085-1095

Grosell M (2006) Intestinal anion exchange in marine fish osmoregulation J Exp Biol 209: 2813-2817

Grosell M, Genz J, Taylor JR, Perry SF, Gilmour KM (2009a) The involvement of H^+-ATPase and cerbonic anhydrase in intestinal HCO_3^- secretion in seawater-acclimated rainbow trout. J Exp Biol 212: 1940-1948

Grosell M, Mager EM, Williams C, Taylor JR (2009b) High rates of HCO_3^- secretion and Cl^- absorption against adverse gradients in the marine teleost intestine: the involvement of an electrogenic anion exchanger and H^+-pump metabolon? J Exp Biol 212: 1684-1696

Guggino WBT (1980) Salt balance in embryos of *Fundulus heteroclitus* and *F. bermudae* adapted to sea water. Am J Physiol 238R: 42-49

Guppy M (2004) The biochemistry of metabolic depression: a history of perceptions. Comp Biochem Physiol B 139: 435-442

Guppy M, Fuery CJ, Flanigan JE (1994) Biochemical principles of metabolic depression. Comp Biochem Physiol B 109: 175-189

Gutowska MA, Melzner F (2009) Abiotic conditions in cephalopod (*Sepia officinalis*) eggs: embryonic development at low pH and high pCO_2. Mar Biol 156: 515-519

Gutowska MA, Melzner F, Langenbuch M, Bock C, Claireaux G, Pörtner H-O (2009) Acid-base regulatory ability of the cephalopod (*Sepia officinalis*) in response to environmental hypercapnia. J Comp Physiol B 180: 323-335

Gutowska MA, Melzner F, Langenbuch M, Bock C, Claireaux G, Pörtner H-O (2010a) Acid-base regulatory ability of the cephalopod (*Sepia officinalis*) in response to environmental hypercapnia. J Comp Physiol B 180: 323-335

Gutowska MA, Melzner F, Pörtner H-O, Meier S (2010b) Cuttlebone calcification increases during exposure to elevated seawater pCO_2 in the cephalopod *Sepia officinalis*. Mar Biol 157: 1653-1663

Gutowska MA, Pörtner H-O, Melzner F (2008) Growth and calcification in the cephalopod *Sepia officinalis* under elevated seawater pCO_2. Mar Ecol Prog Ser 373: 303-309

Hall-Spencer J, Rodolfo-Metapla R, Martin S, Ransome E, Fine M, Turner S, Rowley S, Tedesco D, Buia M (2008) Volcanic carbon dioxide vents show ecosystem effects of ocean acidification. Nature 454: 96-99

Hanlon RT, Messenger JB (1996) Cephalopod behaviour. Cambridge University Press, Cambribge

Heisler N (1984) Acid-base regulation in fishes. Academic Press, New York

Heisler N (1986) Acid-base regulation in animals. Elsevier Biomedical Press, Amsterdam

Heisler N (1989) Interactions between gas exchange, metabolism and ion transport in animals: an overview. Can. J. Zool. 67: 2923-2935

Hendrix JR, Hulet WH, Greeberg MJ (1981) Salinity tolerance and the responses to hypoosmotic stress of the bay squid *Lolliguncula brevis*, a euryhaline cephalopod mollusc. Comp Biochem Physiol A 69: 641-648

Henry RP (1988) Multiple functions of carbonic anhydrase in the crustacean gill. J Exp Zool 248: 19-24

Henry RP, Cameron JN (1983) The role of carbonic anhydrase in respiration, ion regulation and acid-base balance in the aquatic crab *Callinectes sapidus* and the terrestrial crab *Gecarcinus lateralis*. J Exp Biol 103: 205-223

Henry RP, Swenson ER (2000) The distribution and physiological significance on carbonic anhydrase in vertebrate gas exchange organs. Resp Physiol 121: 1-12

Hiroi J, McCormick SD, Ohtani-Kaneko R, Kaneko T (2005) Functional classification of mitochondrion-rich cells in euryhaline Mozambique tilapia (*Oreochromis mossambicus*) embryos, by means of triple immunofluorescence staining for Na^+/K^+-ATPase, $Na^+/K^+/2Cl^-$ cotransporter and CFTR anion channel. J Exp Biol 208: 2023-2036

Hiroi J, Yasumasu S, McCormick SD, Hwang PP, Kaneko T (2008) Evidence for an apical Na-Cl cotransporter involved in ion uptake in a teleost fish. J Exp Biol 211: 2584-2599

Hockachka PW, McClelland GB, Burness GP, Staples JF (1998) Integrating metabolic pathway fluxes with gene-to-enzyme expression rates. Comp Biochem Physiol B 120: 14-26

Hoppema JMJ (1993) Carbon dioxide and oxygen disequilibrium in a tidal basin (Dutch wadden sea). Neth J Sea Res 31: 221-229

Horng JL, Lin LY, Huang JC, Katoh F, Kaneko T, Hwang PP (2007) Knockdown of V-ATPase subunit A (atp6v1a) impairs acid secretion and ion balance in zebrafish (*Danio rerio*). Am J Physiol Regul Integr Comp Physiol 292: R2068-R2076

Horng JL, Lin LY, Hwang PP (2009) Functional regulation of H^+-ATPase-rich cells in zebrafish embryos acclimated to an acidic environment. Am J Physiol Cell Physiol 296: c682-692

Houlihan DF, McMillan DN, Agnisola C, Trara Genoino I, Foti L (1990) Protein synthesis and growth in *Octopus vulgaris*. Mar Biol 106: 251-259

Hsiao CD, You MS, Guh YJ, Ma M, Jiang YJ, Hwang PP (2007) A positive regulatory loop between *foxi3a* and *foxi3b* is essential for specification and differentiation of zebrafish epidermal ionocytes. PLoS ONE 2: e302

Hu MY, Yan HY, Chung WS, Shiao YC, Hwang PP (2009) Acoustically evoked potential in two cephalopods infered using the auditory brainstem response (ABR) approach. Comp Biochem Physiol 153: 278-283

Hwang PP (1990) Salinity effects on development of chloride cells in the larvae of ayu *Plecoglossus altivelis*. Mar Biol 107: 1-7

Hwang PP (2009) Ion uptake and acid secretion in zebrafish (*Danio rerio*). J Exp Biol 212: 1745-1752

Hwang PP, Lee TH (2007) New insights into fish ion regulation and mitochondrion-rich cells. Comp Biochem Physiol A 148: 479-497

Hwang PP, Perry SF (2010) Ionic and acid-base regulation. In: Perry SF, Ekker M, Farrel AP, Brauner CJ (eds) Zebrafish. Elsevier, London, pp 311-344

Hwang PP, Tsai YN, Tung YC (1994) Calcium balance in embryos and larvae of the freshwater-adapted teleost, *Oreochromis mossambicus*. Fish Physiol Biochem 13: 325-333

Hyashi M, Kita J, Ishimatsu A (2004) Comparison of the acid-base responses to CO_2 and acidification in Japanese flounder (*Paralichthys olivaceus*). Mar Poll Bull 49: 1062-1065

IPCC (2001) The third assessment report of the Intergovernmental Panel on Climate Change (IPCC). Cambridge University Press, Cambridge, UK, and New York, USA

Ishimatsu A, Dissanayake A (2010) Life threatened in acidic coastal waters. In: Ishimatsu A, Lie H-J (eds) Coastal environmental and ecosystem issues of the East China Sea. TERRAPUB, Nagasaki, pp 283-303

Ishimatsu A, Hayashi M, Lee K-S (2005) Physiological effects on fishes in a high-CO_2 world. J Geophys Res 110: 1-8

Kimelberg HK, Papahadjopoulus D (1972) Phospholipid requirements for (Na^++K^+)ATPase activity: head-group specificity and fatty acid fluidity. Biochim Biophys Acta 282: 277-292

King AJ, Henderson SM, Schmidt MH, Cole AG, Adamo SA (2005) Using ultrasound to understand vascular and mantle contributions to venous return in the cephalopod *Sepia officinalis* L. J Exp Biol 208: 2071-2082

Knepper MA (2008) Physiology: Courier service for ammonia. Nature 456: 336-337

Kurihara H (2008) Effects of CO_2-driven ocean acidification on the early developmental stages of invertebrates. Mar Ecol Prog Ser 373: 275-284

Kurihara H, Asai SK, Ishimatsu A (2008) Effects of elevated pCO2 on early development in the mussel *Mytilus galloprovincialis*. Aquatic Biol 4: 225-233

Kurihara H, Kato S, Ishimatsu A (2007) Effects of increased seawater pCO_2 on early development of the oyster *Crassostrea gigas*. Aquat Biol 1: 91-98

Kurihara H, Shimode S, Shirayama Y (2004) Effects of raised CO_2 concentration on the egg production rate and early development of two marine copepods (*Acartia steueri* and *Acartia erythraea*). Mar Poll Bull 49: 721-727

Kurihara H, Shirayama Y (2004) Effects of increased atmospheric CO_2 on sea urchin early development. Mar Ecol Prog Ser 274: 161-169

Kurtz I, Balaban RS (1986) Ammonium as a substrate for Na^+-K^+-ATPase in rabbit proximal tubules. AM J Physiol Renal Physiol 250: F497-F502

Lalli CM, Parsons TM (2004) Biological oceanography an introduction. Elsevier, Oxford

Lämmli UK (1970) Cleavage of structural proteins during the assembly of the head of Bacteriophage T4. Nature 227: 680-685

Lanning G, Eilers S, Pörtner H-O, Sokolova M, Bock C (2010) Impact of ocean acidification on energy metabolism of oyster, *Crassostrea gigas*- Changes in metabolic pathways and thermal response. Mar Drugs 8: 2318-2339

Larsen BK, Pörtner H-O, Jensen FB (1997) Extra- and intracellular acid-base balance and ionic regulation in cod (*Gadus morhua*) during combined and isolated exposures to hypercapnia and copper. Mar Biol 128: 337-346

Laurie M (1983) The organ of verrill in Loligo. Q J Micr Sci 29: 97-100

Lebovitz RM, Takeyasu K, Fambrough DM (1989) Molecular characterization and expression of the (Na^++K^+)-ATPase α-subunit in *Drosophila melanogaster*. EMBO J 8: 193-202

Lemaire J (1970) Table de développement embryonaire de *Sepia officinalis* L. (Mollusque Céphalopode). Bull Soc Zool Fr 95: 773-782

Lewis E, Wallace DWR (1998) Program developed for CO2 system calculations. Oak Ridge, Oak Ridge National Laboratory ORNL/CDIAC-105

Lignot J-H, Charmantier G (2001) Immunolocalization of Na^+/K^+-ATPase in the branchial cavity during the early development of the european lobster *Homarus gammarus* (Crustacea, Decapoda). J Histochem Cytochem 49(8): 1013-1023

Lin LY, Horng JL, Kunkel JG, Hwang PP (2006) Proton pump-rich cell secretes acid in skin of zebrafish larvae. Am J Physiol Cell Physiol 290: C371-378

Lischka S, Büdenbender J, Boxhammer T, Riebesell U (2010) Impact of ocean acidification and elevated temperatures on early juveniles of the polar shelled pteropod *Limacina helicina*: mortality, shell degradation, and shell growth. Biogeosciences 7: 8177-8214

Lloyd R, White WR (1967) Effects of high concentrations of carbon dioxide on the ionic composition of rainbow trout blood. Nature 216: 1341-1342

Lucu C, Towle DW (2003) Na^++K^+-ATPase in gills of aquatic crustacea. Comp Biochem Physiol A 135: 195-214

Mackie GO (2008) Immunostaining of peripheral nerves and other tissues in whole mount preparations from hatchling cephalopods. Cell Tiss Res 40: 21-29

Madan JJ, Wells MJ (1996) Cutaneous respiration in *Octopus vulgaris*. J Exp Biol 199: 2477-2483

Marsh AG, Leong PKK, Manahan DT (2000) Gene expression and enzyme activities of the sodium pump during sea urchin development: implications for indices of physiological state. Biol Bull 199: 100-107

Mehrbach C, Culberso C, Hawley J, Pytkowic R (1973) Measurement of apparent dissociation constants of carbonic acid in seawter at atmospheric pressure. Limnol Oceanogr 18: 897-907

Melzner F, Göbel S, Langenbuch M, Gutowska MA, Pörtner H-O, Lucassen M (2009a) Swimming performance in atlantic cod (*Gadus morhua*) following long-term (4-12 month) acclimation to elevated seawater pCO_2. Aqua Toxicol 92: 30-37

Melzner F, Gutowska MA, Langenbuch M, Dupont S, Lucassen M, Thorndyke MC, Bleich M, Pörtner H-O (2009b) Physiological basis for high CO_2 tolerance in marine ectothermic animals: pre-adaptation through lifestyle and ontogeny? Biogeosciences 6: 2313-2331

Melzner F, Hu MY, Lacoue-Labarthe T, Gutowska MA (submitted-a) Metabolic depression in squid embryos is linked to egg abiotic conditions. PloS ONE

Melzner F, Körtzinger A, Koeve W, Oschlies A, Gutowska MA, Bange H, Hansen HP (submitted-b) Future ocean acidification will be amplified by hypoxia in coastal habitats.

Melzner F, Mark FC, Pörtner H-O (2007) Role of blood-oxygen transport in thermal tolerance of the cuttlefish, *Sepia officinalis*. Integr Comp Biol 47: 645-655

Messenger JB, Nixon M, Ryan KP (1985) Magnesium chloride as an anaesthetic for cephalopods. Comp. Biochem. Physiol. 82: 203-205

Meunier B, De Visser SP, Shaik S (2004) Mechanism of oxidation reactions catalyzed by cytochrome P450 enzymes. Chem Rev 104: 3947-3980

Michaelidis B, Spring A, Pörtner H-O (2005) Effects of long-term moderate hypercapnia on acid-base balance and growth rate in marine mussels *Mytilus galloprovincialis*. Mar Ecol Prog Ser 293: 109-118

Miles H, Widdicombe S, Spicer IJ, Hall-Spencer J (2007) Effects of anthropogenic seawater acidification onacid-base balance in the sea urchin *Psammechinus miliaris*. Mar Poll Bull 54: 89-96

Mo JL, Devos P, Trausch G (1998) Dopamine as a modulator of ionic transport and Na^+/K^+-ATPase activity in the gills of the Chinese crab *Eriocheir sinensis*. J Crust Biol 18: 442-448

Moyes CD, LeMoine CMR (2005) Control of muscle bioenergetic gene expression: implications for allometric scaling relationships of glycolytic and oxidative enzymes. J Exp Biol 208: 1601-1610

Munday PL, Crawley NE, Nilsson GE (2009a) Interacting effects of elevated temperature and ocean acidification on the aerobic performance of coral reef fishes. Mar Ecol Prog Ser 388: 235-242

Munday PL, Dixson DL, Donelson JM, Jones GP, Pratchett MS, Devitsina GV, Doving KB (2009b) Ocean acidification impairs olfactory discrimination and homing ability of marine fish. Proc Nat Acad Sci 106: 1848-1852

Munday PL, Donelson JM, Dixson DL, Endo GGK (2009c) Effects of ocean acidification on the early life history of a tropical marine fish. Proc Roy Soc B doi: 10.1098/rspb.2009.0784

Murer H, Hopfer U (1974) Demonstration of electrogenic Na+-dependent D-glucose transport in intestinal brush border membranes. Proc Nat Acad Sci 71: 484-488

Nawata CM, Hirose S, Nakada T, Wood CM, Katoh A (2010) Rh glycoprotein expression is modulated in pufferfish (*Takifugu rubripes*) during high environmental ammonia exposure. J Exp Biol 213: 3150-3160

Nebel C, Negre-Sadargues G, Blasco C, Charmantier G (2005) Morphofunctional ontogeny of the urinary system of the European sea bass *Dicentrarchus labrax*. Anat Embryol 209: 193-206

Nienhuis S, Palmer AR, Harley CDG (2010) Elevated CO2 affects shell dissolution rate but not calcification rate in a marine snail. Proc R Soc B doi: 10.1098/rspb.2010.0206

Nixon M, Mangold K (1998) The early life of *Sepia officinalis*, and the contrast with that of *Octopus vulgaris* (Cephalopoda). J Zool Lond 245: 407-421

Nottage JD, West JR, Montgomery SS, Graham K (2006) Cephalopod diversity in commercial fisheries landings of New South Wales, Australia. Rev Fish Biol Fisheries 17: 271-281

O`Dor RK (2002) Telemetered cephalopod energetics: Swimming, soaring, and blimping. Integr Comp Biol 42: 1065-1070

O`Dor RK, Webber DM (1986) The constraints on cephalopods: why squid aren´t fish. Can J Zool 64: 1591-1605

O`Dor RK, Webber DM (1991) Invertebrate athletes: Trade-offs between transport efficiency and power density in cephalopod evolution. J exp Biol 160: 93-112

Orr JC, Caldeira K, Fabry VJ, Gattuso JP, Haugan P, Lehodey P, Pantoja S, Pörtner H-O, Riebesell U, Trull T, Urban E, Hood M, Broadgate W (2009) Research priorities for understanding ocean acidification- Summary from the second symposium on the oceans in a high-CO_2 world. Oceanogaphy 22: 182-189

Orr JC, Fabry VJ, Aumont O, Bopp L, Doney SC, Feely RA, Gnanadesikan A, Gruber N, Ishida A, Joos F, Key RM, Lindsay K, Maier-Reimer E, Matear R, Monfray P, Mouchet A, Najjar RG, Plattner G-K, Rodgers KB, Sabine CL, Sarmiento JL, Schlitzer R, Slater RD, Totterdell IJ, Weirig M-F, Yamanaka Y, Yool A (2005) Anthropogenic ocean acidification over the twenty-first century and its impact on calcifying organisms. Nature 437: 681-686

Packard A (1972) Cephalopods and fish: the limits of convergence. Biol Rev 47: 241-307

Palacios E, Racotta IS (2007) Salinity stress test and its relation to future performance and different physiological responses in shrimp postlarvae. Aquaculture 268: 123-135

Pan TC, Liao BK, Huang CJ, Lin LY, Hwang PP (2005) Epithelial Ca(2+) channel expression and Ca(2+) uptake in developing zebrafish. Am J Physiol Regul Integr Comp Physiol 289: R1202-1211

Pane EF, Barry JP (2007) Extracellular acid-base regulation during short-term hypercapnia is effective in a shallow-water crab, but ineffective in a deep-sea crab. Mar Ecol Prog Ser 334: 1-9

Pecl GT, Steer MA, Hodgson KE (2004) The role of hatchling size in generating the intrinsic size-at-age variability of cephalopods: extending the Forsythe hypothesis. Mar Freshw Res 55: 387-394

Perry SF, Braun MH, Genz J, Vulesevic B, Taylor J, Grosell M, Gilmour KM (2010) Acid-base regulation in the plainfin midshipman (*Porichthys notatus*): an aglomerular marine teleost. J Comp Physiol B 180: 1213-1225

Perry SF, Gilmour KM (2006) Acid–base balance and CO_2 excretion in fish: Unanswered questions and emerging models. Resp Physiol Neurobiol 154: 199-215

Peterson GL, Hokin LE (1981) Molecular weight and stoichiometry of the sodium- and potassium-activated adenosine triphosphatase subunits. J Biol Chem 256: 3751-3761

Petit J, Jouzel J, Raynaud D, Barkov N, Barnola J, Basile I, Bender M, Chappellaz J, Davis M, Delaygue G, Delmotte M, Kotlyakov V, Legrand M, Lipenkov V, Lorius C, Pepin L, Ritz C, Saltzman E, Stivenard M (1999) Climate and atmospheric history of the past 420,000 years from the Vostok ice core, Antarctica. Nature 399: 429-436

Piatkowski U, Pierce GJ, Morais da Cunha M (2001) Impact of cephalopods in the food chain and their interaction with the environment and fisheries: an overview. Fish Res 52: 5-10

Piermarini PM, Choi I, Boron WF (2006) Cloning and characterization of an electrogenic Na/HCO_3^- cotransporter from the squid giant fiber lobe. Am J Physiol Cell Physiol 292: C2023-C2045

Pisam M, Rambourg A (1991) Mitochondria-rich cells in the gill epithelium of teleost fishes: an ultrastructural approach. Int Rev Cytol 130: 191-232

Pörtner H-O (1990) An analysis of the effects of pH on oxygen binding by squid (*Illex illecebrosus*, *Loligo pealei*) haemocyanin. J Exp Biol 150: 407-424

Pörtner H-O, Bock C, Reipschläger A (2000) Modulation of the costs of pHi during metabolic depression: a (31)P-NMR study in invertebrate (*Sipunculus nudus*) isolated muscle. J Exp Biol 203: 2417-2428

Pörtner H-O, Webber DM, Boutilier RG, O`Dor RK (1991) Acid-base regulation in exercising squid (*Illex illecebrosus, Loligo pealei*). Am J Physiol Regul Integr Comp Physiol 261: R239-R246

Pörtner H-O, Zielinski S (1998) Environmental constraints and the physiology of performance in squids. S Afr J Mar Sci 20: 207-221

Pörtner HO (1994) Coordination of metabolism, acid-base regulation and haemocyanin function in cephalopods. Mar Fresh Behav Physiol 25: 131-148

Pörtner HO, Langenbuch M, Reipschläger A (2004) Biological impact of elevated ocean CO_2 concentrations: Lessons from animal physiology and earth history. J Oceanograph 60: 705-718

Potts WTW (1965) Ammonia excretion in *Octopus dolfeini*. Comp Biochem Physiol 14: 339-355

Potts WTW (1994) Kinetics of sodium uptake in freshwater animals - a comparison of ion exchange and proton pump hypotheses. Am J Physiol 266: R315-R320

Ramnanan CJ, Storey KB (2006) Suppression of Na^+/K^+-ATPase activity during estivation in the land snail *Otala lactea*. J Exp Biol 209: 677-688

Raven J, Caldeira K, Elderfield H, Hoegh-Guldberg O, Liss P, Riebesell U, Shepherd J, Turley C, Watson A (2005) Ocean acidification due to increasing atmospheric carbon dioxide, Cardiff

Reipschläger A, Pörtner H-O (1996a) Metabolic depression during environmental stress: the role of extra- versus intracellular pH in *Sipunculus nududs*. J Exp Biol 199: 1801-1807

Reipschläger A, Pörtner H-O (1996b) Metabolic depression during environmental stress: the role of extracellular versus intracellular pH in *Sipunculus nudus*. J Exp Biol 199: 1801-1807

Riebesell U, Zondervan I, Rost B, Tortell PD, Zeebe RE, Morel FMM (2000) Reduced calcification of marine plankton in response to increased atmospheric CO_2. Nature 407: 364-467

Ries JB, Cohen AI, McCorkle DC (2009) Marine calcifiers exhibit mixed responses to CO_2-induced ocean acidificaton. Geol Soc Am 37: 1131-1134

Robertson JD (1949) Ionic regulation in some marine invertebrates. J Exp Biol 26: 182-200

Romero MF, Fulton CM, Boron WF (2004) The SLC4 family of HCO_3^- transporters. Eur J Physiol 447: 495-509

Sabine CL, Feely RA, Gruber N, Key RM, Lee K, Bullister JL, Wanninkhof R, Wong CS, Wallace DWR, Tilbrook B, Millero FJ, Peng T-H, Kozyr A, Ono T, Rios AF (2004) The oceanic sink for anthropogenic CO_2. Science 305: 367-371

Schipp R, Hevert F (1980) Ultrafiltration in the branchial heart appendage of dibranchiate cephalopods: a comparative ultrastructural and physiological study. J Exp Biol 92: 23-35

Schipp R, Hevert F (1981) Ultrafiltration in the branchial heart appendage of dibranchiate cephalopods: a comparative ultrastructural and physiological study. J Exp Biol 92: 23-35

Schipp R, Mollenhauer S, Boletzky S (1979) Electron microscopical and histochemical studies of differentiation and function of the cephalopod gill (*Sepia officinalis* L.). Zoomorph 93: 193-207

Schipp R, Von Boletzky S, Doell G (1975) Ultrastructural and cytochemical investigations on the renal appendages and their concrements in dibranchiate cephalopods (Mollusca, Cephalopoda). Z Morph Tiere 81: 279-304

Schipp R, von Boletzky S (1976) The pancreatic appendages of dibranchiate cephalopods. Zoomorph 86: 81-98

Schwartz AA, Allen JC, Harigaya S (1969) Possible involvement of cardiac Na^+/K^+-adenosine triphosphatase in the mechanism of action of cardiac glycosides. J Pharmacol Exp Ther 168: 31-41

Seibel BA, Drazen JC (2007) The rate of metabolism in marine animals: environmental constraints, ecological demands and energetic opportunities. Phil Trans R Soc B doi: 10.1098/rstb2007.2101

Seidelin M, Brauner CJ, Jensen FB, Madsen SS (2001) Vacuolar-Type H^+-ATPase and Na^+,K^+-ATPase expression in gills of atlantic salmon (*Salmo salar*) during isolated and combined exposure to hypoxia and hypercapnia in fresh water. Zool Sci 18: 1199-1205

Seymour RS, Bradford DF (1994) Gas exchange through the jelly capsule of the terrestrial eggs of the frog, *Pseudophryne bibroni*. J Comp Physiol B 157: 477-481

Shih TH, Horng JL, Hwang PP, Lin LY (2008) Ammonia excetion by the skin of zebrafish (*Danio rerio*) larvae. Am J Physiol Cell Physiol 295: C1625-C1632

Siebers D, Leweck K, Markus H, Winkler A (1982) Sodium regulation in the shore crab *Carcinus maenas* as related to ambient salinity. Mar Biol 69: 37-43

Siebers D, Winkler A, Leweck K, Madian A (1983) Regulation of sodium in the shore crab *Carcinus maenas*, adapted to environments of constant and changing salinities. Helgoländer Meeresunters 36: 303-312

Small D, Calosi D, White J, Spicer I, Widdicombe S (2010) Impact of medium-term exposure to CO_2 enriched seawater on the physiological functions of the velvet swimming crab *Necora puber*. Aquatic Biol 10: 11.21

Smith MR, Caron J-B (2010) Primitive soft-bodied cephalopods from the Cambrian. Nature 465: 469-472

Smith PJ, Hammar K, Porterfield DM, Sanger RH, Trimarchi JR (1999) Self-referencing, non-invasive, ion selective electrode for single cell detection of trans-plasma membrane calcium flux. Microsc Res Tech 46: 398-417

Somero GN, Childress JJ (1980) A violation of the metabolism-size scaling paradigm: activities of glycolytic enzymes in muscle increase in larger fish. Physiol Zool 53: 322-337

Soupene E, Inwood W, Kustu S (2004) Lack of the Rhesus protein Rh1 impairs growth of the green alga *Chlamydomonas reinhardtii* at high CO_2. Proc Nat Acad Sci USA 101: 7787-7792

Soupene E, King N, Field E, Liu P, Niyogi KK, Huang C-H, Kustu S (2002) Rhesus expression in a green alga *Chlamydomonas reinhardtii* at high CO_2. Proc Nat Acad Sci USA 99: 7769-7773

Spicer JI, Raffo A, Widdicombe S (2007) Influence of CO_2-related seawater acidification on extracellular acid-base balance in the velvet swimming crab *Necora puber*. Mar Biol 151: 1117-1125

Thisse B, Heyer V, Lux A, Alunni V, Degrave A, Seiliez I, Kirchner, Jasinska E, Parkhill JP, Thisse C (2004) Spatial and temporal expression of the zebrafish genome by large-scale in situ hybridization screening Methods Cell Biol 77: 505-519

Thomsen J, Gutowska MA, Saphörster J, Heinemann A, Trübenbach K, Fietzke J, Hiebenthal C, Eisenhauer A, Körtzinger A, Wahl M, Melzner F (2010) Calcifying invertebrates succeed in a naturally CO_2 enriched coastal habitat but are threatened by high levels of future acidification. Biogeosciences 7: 5119-5156

Thomsen J, Melzner F (2010) Moderate seawater acidification does not elicit long-term metabolic depression in the blue mussel *Mytilus edulis*. Mar Biol 157: 2667-2676

Toews DP, Holeton GF, Heisler N (1983) Regulation of the acid-base status during environmental hypercapnia in the marine teleost fish *Conger conger*. J Exp Biol 107: 9-20

Towle DW (1977) Sodium pump sites in teleost gill: unmasking by detergent. Am Zool 177: 877

Truchot JP (1984) Water carbonate alkalinity as a determinant of hemolymph acid-base balance in the shore crab, *Carcinus maenas* - a study at two different ambient pCO_2 and O_2 levels. J Comp Physiol 154: 601-606

Tseng Y-C, Huang C-J, Chang JC-H, Wen-Yuan Teng W-Y, Baba O, Fann M-J, Hwang PP (2006) Glycogen phosphorylase in glycogen-rich cells is involved in the energy supply for ion regulation in fish gill epithelia. Am J Physiol Regul Integr Comp Physiol 293: R482-R491

Tseng YC, Lee JR, Lee SJ, Hwang PP Functional analysis of the glucose transporters-1, -6, and -13.1 expressed by zebrafish epithelial cells. Am J Physiol Regul Integr Comp Physiol (in press)

Tunnicliffe V, Davies KTA, Butterfield DA, Embley RW, Rose JM, Chadwick WW (2009) Survival of mussels in extremely acidic waters on a submarine vocano. Nature Geosci 2: 344-348

Turner N, Hulbert AJ, Else PL (2004) Sodium pump molecular activity and membrane lipid composition in two disparate ectotherms, and comparison with endotherms. J Comp Physiol B 175: 77-85

Virkki LV, Choi I, Davis BA, Boron WF (2002) Cloning of a Na^+-driven Cl/HCO_3^- exchanger from squid giant fiber lobe. Am J Physiol Cell Physiol 285: C771-C780

von Boletzky S (1983) *Sepia officinalis*. In: Boyle PR (ed) Cephalopod Life Cycles. Academic Press, London

von Boletzky S (1987a) Embryonic phase. In: Boyle RP (ed) Cephalopod lifecycles. Academic Press, London, pp 5-31

von Boletzky S (1987b) Ontogenetic and phylogenetic aspects of the cephalopod circulatory system. Experientia 43: 478-483

Wagner CA, Finberg KE, Breton S, Marshanski V, Brown D, Geibel JP (2003) Renal vacuolar H^+-ATPase. Physiol Rev 84: 1263-1314

Wall SM, Davis BS, Hassell KA, Mehta P, Park SJ (1999) In rat tiMCD, NH_4^+ uptake by Na^+/K^+-ATPase is critical to net acid secretion during chronic hypokalemia Am J Physiol 277: F866-F847

Walther K, Anger K, Pörtner H-O (2010) Effects of ocean acidification and warming on the larval development of the spider crab *Hyas araneus* from different latitudes (54° vs. 79°N). Mar Ecol Prog Ser 417: 159-170

Wang H, Miyazaki S, Kawai K, Deyholos M, Galbraith DW, Bohnert HJ (2003) Temporal progression of gene expression responses to salt shock in maize roots. Plant Mol Biol 52: 873-891

Wang T, Yang CL, Abbiati T, Schultheis PJ, Shull GE, Giebisch G, Aronson PS (1999) Mechanism of proximal tubule bicarbonate absorption in NHE3 null mice. Am J Physiol Renal Physiol 277: F298–F302

Wells JM, O`Dor RK (1991) Jet propulsion and the evolution of the cephalopods. Bull Mar Sci 49: 419-432

Wells JM, Wells J (1989) Water uptake in a cephalopod and the function of the so-called "pancreas". J Exp Biol 145: 215-226

Wells MJ (1990) Oxygen extraction and jet propulsion in cephalopods. Can. J. Zool. 68: 815-824

Wells MJ, Wells J (1982) Ventilatory currents in the mantle of cephalopods. J Exp Biol 99: 315-330

Wells PR, Pinder AW (1996) The respiratory development of atlantic salmon. J Exp Biol 199: 2737-2744

West GB, Brown JH, Enquist BJ (1997) A general model for the origin of allometric scaling laws in biology. Science 276: 122-126

Wheatly MG, Henry RP (1992) Extracellular and intracellular acid-base regulation in crustaceans. J Exp Zool 263: 127-142

Whiteley NM, Scott JL, Breeze SJ, McCann L (2001) Effects of water salinity on acid-base balance in decapod crustaceans. J Exp Biol 204: 1003-1011

Winslow JL, Cooper RL, Atwood HL (2002) Intracellular ionic concentration by calibration from fluorescence indicator emission spectra, its relationship to the K_d, F_{min}, F_{max} formula, and use with Na-Green for presynaptic sodium. J Neurosci Methods 118: 163-175

Wolf G, Verheyen E, Vlaeminck A, Lemaire J, Decleir W (1985) Respiration of *Sepia officinalis* during embryonic and early juvenile life. Mar Biol 90: 35-39

Wood CM, Milligan LC, Walsh PJ (1999) Renal responses of trout to chronic respiratory and metabolic acidosis and metabolic alkalosis. Am J Physiol Regul Integr Comp Physiol 277: 482-492

Wu S-C, Horng J-L, Liu S-T, Hwang PP, Wen Z-H, Lin C-S, Lin LY (2010) Ammonium-dependent sodium uptake in mitochondrion-rich cells of medaka (*Oryzias latipes*) larvae. Am J Physiol Cell Physiol 298: C2237-2250

Yang T-H, Somero G (1996) Activity of lactate dehydrogenase but not its concentration of messenger RNA increases with body size in barred sand bass, *Paralabrax nebulifer* (Teleostei). Biol Bull 191: 155-158

Young RE, Vecchione M (2004) Cephalopod gills- Tree of Life Web Project: http://to/web.org

Marian Hu
Holtenauerstr. 340
24106 Kiel

Kiel, den 28. März 2011

Erklärung gem. § 9 PromO

Ich erkläre hiermit,

1. dass die Abhandlung - abgesehen von der Beratung durch die Betreuerin oder den Betreuer - nach Inhalt und Form die eigene Arbeit ist,

2. dass diese Arbeit vor dem jetzigen Promotionsverfahren keinem anderen Promotionsverfahren unterzogen wurde

   und

3. dass die Arbeit unter Einhaltung der Regeln guter wissenschaftlicher Praxis der Deutschen Forschungsgemeinschaft entstanden ist;

(Marian Yong-An Hu)